



**HAL**  
open science

# The role of the histone chaperone ASF1 in recycling parental histones during DNA replication

Camille Clement

► **To cite this version:**

Camille Clement. The role of the histone chaperone ASF1 in recycling parental histones during DNA replication. Cellular Biology. Université Paris sciences et lettres, 2018. English. NNT : 2018PSLET005 . tel-02518693

**HAL Id: tel-02518693**

**<https://theses.hal.science/tel-02518693>**

Submitted on 25 Mar 2020

**HAL** is a multi-disciplinary open access archive for the deposit and dissemination of scientific research documents, whether they are published or not. The documents may come from teaching and research institutions in France or abroad, or from public or private research centers.

L'archive ouverte pluridisciplinaire **HAL**, est destinée au dépôt et à la diffusion de documents scientifiques de niveau recherche, publiés ou non, émanant des établissements d'enseignement et de recherche français ou étrangers, des laboratoires publics ou privés.

# THÈSE DE DOCTORAT

de l'Université de recherche Paris Sciences et Lettres  
PSL Research University

Préparée à l'Institut Curie

## The role of the histone chaperone ASF1 in recycling parental histones during DNA replication

Ecole doctorale n°515

COMPLEXITÉ DU VIVANT

**Spécialité** BIOLOGIE CELLULAIRE

Soutenue par Camille **CLÉMENT**  
le 22 mai 2018

Dirigée par Geneviève **ALMOUZNI**

### COMPOSITION DU JURY :

Mme ALABERT Constance  
University of Dundee  
Rapporteur

M. CAVALLI Giacomo  
Institut de Génétique Humaine  
Rapporteur

Mme CORPET Armelle  
Université Claude Bernard  
Membre du jury

M. DAHAN Maxime  
Institut Curie  
Président du jury

M. SALE Julian  
MRC Laboratory of Molecular Biology  
Membre du jury



## Acknowledgements

First, I am grateful to Geneviève Almouzni for having given me the opportunity to join her team as a student. I thank her for her support and supervision. She has entrusted me with the writing of several publications and, most importantly, with the development of a new cutting-edge technology for my PhD project. I thank her for her critical thinking, for sharing her scientific knowledge and for placing her trust in me as my project progressed.

I thank Constance Alabert and Giacomo Cavalli for their critical reading and evaluation of this manuscript, as well as Armelle Corpet, Maxime Dahan, and Julian Sale for kindly agreeing to take part in the jury of my PhD defense. I also appreciate the contribution of the UMR3664 team leaders Antoine Coulon, Nathalie Dostatni, Ines Drinnenberg and Angela Taddei, as well as Françoise Ochsenbein and Eric Allemand, to my yearly thesis committees – their outside view was of great help throughout my project. I thank the PIC3i "UNDERSTAND DYNAMIC ARC" consortium of the Institut Curie and all its members for our helpful meetings.

I am grateful to the Ecole Doctorale Complexité du Vivant and to Paris Sciences et Lettres for having given me the training and the access to funding that have enabled me to pursue a PhD. The Ligue Contre le Cancer provided additional funding for my 4<sup>th</sup> year, for which I am equally grateful. I thank the Training Unit of the Institut Curie for a fruitful collaboration over the years in organizing the Epigenetics Course.

I want to thank past and present members of the Almouzni team and UMR3664 for these four years spent together. In particular, in the team, I thank Dominique, Christèle, Audrey and Iva for our discussions. I am very grateful to Dominique, Elena and Marion for help with dealing with the administration and for the dance classes. I thank Isabelle, Isabelle, and Caroline for their kindness, as well as their support during the great FACS/liquid Nitrogen crises of 2017. I thank the entire lunch crew, past and present, including Delphine, Hatem, François, Monica, Laurence, Dan, for the many laughs at the canteen and at happy hour.

Special thanks to Alberto for the endless debates, and for teaching me the date of the Epiphany. To Shweta and Tejas for being so understanding and for the amazing restaurant recommendations. To DJ and Katrina, for always thinking out of the box. To Antoine, for our time together in the little office. To Anaïs, our awesome newest addition, for achieving the impossible and replacing Yann, the irreplaceable.

Additional special thanks go to those who, to quote Eric Clapton, still knew me when I was down and out. To Zack, an inspiring mentor and friend who gave me the tools to survive. To Yann, the heart of the lab, the shoulder to cry on, the friend you can count on (*merci à toi d'avoir canalisé David pendant si longtemps*). To Katia, who teaches me strength and wisdom, who listens and understands. To Julia and David, my co-PhD students, who supported me, made me laugh, drove me crazy (David), and made me think, endlessly and with tireless energy, over these past four years. The bro of the bros and the sis of the sises. And of course... to Guille, to whom I owe this PhD. A genius scientist, an exceptional mentor, a rare friend. *De ceux qu'on compte sur les doigts d'une main.*

Enfin, je remercie bien sûr ma famille et mes proches. Merci à mes parents qui me soutiennent, me consolent et me motivent depuis toujours. Merci à mon frère et ma sœur adorés qui m'inspirent, que ce soit devant un caviar d'aubergine, une rediffusion du Seigneur des Anneaux (version longue), ou un concert de chant. Merci à Siam, Scarlette et Maïa, dont la philosophie de vie me rend humble. Merci à mes amis, source d'évasion, pour les dîners, les verres de vin, les séances Game of Thrones.

But above all... I am grateful to Craig, who crossed an ocean to be by my side.



## Table of Contents

---

|   |           |
|---|-----------|
| <b>Introduction</b> .....   | <b>7</b>  |
| <b>1. Chromatin at different scales</b> .....                                     | <b>9</b>  |
| 1.1. The basic unit of chromatin .....  | 9         |
| 1.1.1. The nucleosome .....   | 9         |
| 1.1.2. Chromatin: a signaling module or a carrier of epigenetic information ..... | 11        |
| 1.1.2.1. DNA methylation .....  | 12        |
| 1.1.2.2. Histone variants .....   | 13        |
| 1.1.2.2.1. The replicative variants H3.1 and H3.2 .....                           | 15        |
| 1.1.2.2.2. The replacement variant H3.3 .....                                     | 16        |
| 1.1.2.2.3. The centromeric variant CenH3 .....                                    | 18        |
| 1.1.2.2.4. Other H3 variants.....   | 19        |
| 1.1.2.3. Histone post-translational modifications .....                           | 19        |
| 1.2. Spatial organization of chromatin in the nucleus.....                        | 22        |
| 1.2.1. Chromatin fiber.....   | 22        |
| 1.2.2. Topologically associated domains .....                                     | 23        |
| 1.2.3. Heterochromatin and euchromatin .....                                      | 26        |
| <b>2. The challenge of replicating chromatin</b> .....                            | <b>28</b> |
| 2.1. The replication machinery .....  | 28        |
| 2.2. Inheritance of DNA methylation .....   | 30        |
| 2.3. Inheritance of histones.....   | 31        |
| 2.3.1. Theoretical framework.....   | 31        |
| 2.3.2. Histone segregation on daughter strands .....                              | 33        |
| 2.3.3. Histone dynamics during DNA replication .....                              | 34        |
| 2.3.3.1. Histone chaperones .....   | 34        |
| 2.3.3.2. Dynamics of new histones in vivo .....                                   | 36        |
| 2.3.3.3. The histone chaperone Anti-Silencing Function 1 .....                    | 38        |
| 2.3.3.3.1. ASF1 sequence and conservation .....                                   | 38        |
| 2.3.3.3.2. The two paralogs ASF1 and ASF1b.....                                   | 40        |
| 2.3.3.3.3. Role of ASF1 in histone import and storage .....                       | 41        |
| 2.3.3.3.4. Histone recycling during replication and ASF1 .....                    | 42        |
| 2.3.3.3.5. Role of ASF1 in gene expression.....                                   | 46        |
| 2.3.3.3.6. ASF1 and DNA repair.....   | 48        |
| 2.3.4. Restoring chromatin after the replication fork.....                        | 49        |
| 2.3.5. Barriers to replication.....   | 51        |
| 2.3.5.1. DNA secondary structures.....  | 51        |
| 2.3.5.2. Replication stress .....   | 51        |
| 2.3.5.3. Telomeric regions.....   | 52        |

|  |            |
|--|------------|
| <b>3. Implications of histone inheritance or loss during replication .....</b> | <b>53</b>  |
| 3.1. Epigenetic memory of transcriptional states .....                         | 53         |
| 3.2. Nuclear organization.....   | 56         |
| 3.3. Cell fate.....  | 58         |
| 3.3.1. Asymmetric division .....   | 58         |
| 3.3.2. Histone chaperones as a safeguard of cell identity? .....               | 59         |
| <b>Question .....</b>  | <b>61</b>  |
| <b>Results .....</b>   | <b>65</b>  |
| 1. Strategy and methodology.....   | 67         |
| 2. Publication.....  | 72         |
| <b>Discussion.....</b>   | <b>157</b> |
| <b>Conclusion .....</b>  | <b>169</b> |
| <b>Annexes .....</b>   | <b>173</b> |
| <b>References.....</b>   | <b>199</b> |

# Introduction

---



# 1. Chromatin at different scales

In eukaryotic cells, genetic information in the form of DNA is organized in chromatin and compartmentalized in the nucleus. This is where all DNA processes take place. Chromatin was discovered and named due to its ability to bind coloring dyes (Flemming 1882). Electron microscopy visualization of chromatin in the nucleus led to the observation of two distinct types of chromatin: the lightly stained, less condensed euchromatin localized in the nuclear interior, and the densely stained, more condensed heterochromatin, mostly located at the periphery of the nucleus and around nucleoli in the observed cells (Heitz 1928). Following this discovery, and based on general correlations, the view emerged that euchromatin contained mostly active parts of the genome and heterochromatin silent regions.

Because of the existence of these distinct domains, the 3D organization of the genome within the nucleus was attributed a central role in defining genome function. In this section, I will present how genetic information is organized at different scales, from its molecular components to the 3D compartmentalization in the nuclear space.

## 1.1. The basic unit of chromatin

### 1.1.1. The nucleosome

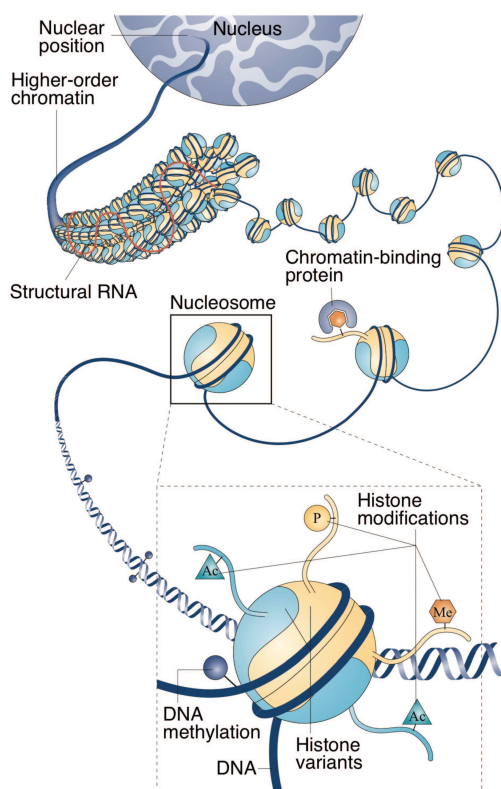


**Figure 1: Chromatin organization.**

DNA wraps around histones to form the nucleosome, the basic unit of chromatin. Histones can exist in the form of different variants, and can present histone post-translational modifications (for example, by (P) phosphorylation, (Ac) acetylation, (Me) methylation).

DNA can be covalently modified by methylation of cytosine residues.

Families of methyl- or histone-binding proteins can recognize these modifications and impact genome regulation.

Adapted from Probst et al. 2009.

At the molecular level, the genome is packaged into a nucleoprotein structure termed chromatin. The basic unit of chromatin is the nucleosome, comprised of about 146 base pairs of DNA wrapped around an octamer of proteins called histones, a 50 base pair linker DNA and a linker histone (Figure 1). The length of the linker DNA and the linker histone can vary between different cell types.

The first evidence of the existence of a repeating unit of chromatin came from an experiment in rat liver nuclei, where digestion of chromatin with a nuclease resulted in DNA fragments of 180-200 base pairs (Hewish and Burgoyne 1973). Electron microscopy enabled the visualization of this repeating unit as chromatin resembled beads on a string (Olins and Olins 1974, Oudet, Gross-Bellard et al. 1975) (Figure 2).

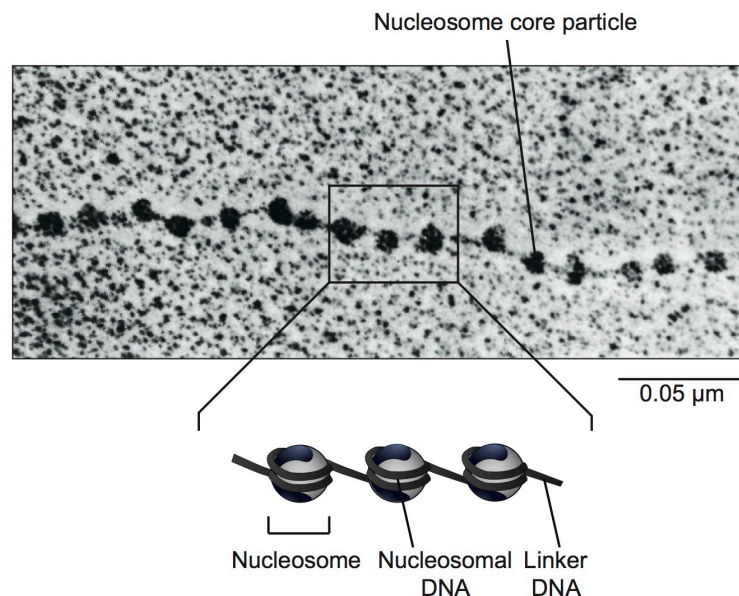


**Figure 2: The basic unit of chromatin, the nucleosome.**

(Top) Electron microscopy image shows that chromatin resembles beads on a string. Adapted from Olins & Olins 1974. (Bottom) Schematic representation of nucleosomes.

The composition of the nucleosome was determined in biochemical experiments and X ray diffraction (Kornberg 1974), following the discovery that histone proteins blocked DNA accessibility (Billing and Bonner 1972, Mirsky, Silverman et al. 1972, Pederson 1972). Eight histones are present in the nucleosome core particle: two copies of histone H2A, H2B, H3 and H4, which assemble into an octamer composed of a core tetramer (H3-H4)<sub>2</sub> flanked by two H2A-H2B dimers. In addition, the linker histone H1 binds linker DNA between two nucleosome

cores. Histones are small basic proteins (20 kDa), which contain a histone fold domain - implicated in histone dimerization - and have a less-structured N-terminal end (Arents and Moudrianakis 1995). As illustrated in the structure of the nucleosome core particle, the DNA helix wraps twice around the histone octamer, and histone N- and C-terminal tails extend outside the nucleosome and are not visible in the structure (Richmond, Searles et al. 1988, Arents, Burlingame et al. 1991, Luger, Mader et al. 1997, Davey and Richmond 2002, Davey, Sargent et al. 2002)(Figure 3).

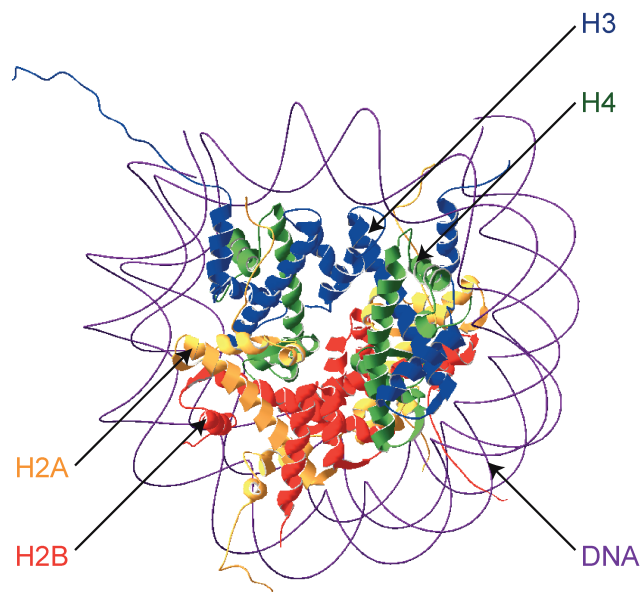


**Figure 3: Crystal structure of the nucleosome.**

Nucleosome core particle: ribbon traces for the 146-bp DNA phosphodiester backbones (purple) and eight histone protein main chains (blue: H3; green: H4; yellow: H2A; red: H2B). The views are down the DNA superhelix axis for the left particle and perpendicular to it for the right particle. For both particles, the pseudo-twofold axis is aligned vertically with the DNA centre at the top. From Luger et al. 1997.

This organization allows a first level of packaging for DNA. Notably, the nucleosome represents a versatile module that can be modulated to regulate genome function.

### **1.1.2. Chromatin: a signaling module or a carrier of epigenetic information**

Both DNA and histones can convey information, either through chemical modification or via the nature of the histone itself. This provides an additional

layer of information to the genome, beyond the genetic code itself. These features are often referred to as “epigenetic” when simply considering that the meaning of the prefix “epi” is “above genetics”. However, the term epigenetics has had evolving definitions. It was first coined by Waddington in a broad manner to define how to link the genotype to the phenotype. Later, based on methylation studies, it was defined as the study of heritable phenotype changes that do not involve alterations of the DNA sequence, and can, in turn, influence genome function (Holliday 1994). The heritability can be mitotic or even meiotic when transmitted across generations. While short-term variations in the nucleosome module can rather be involved in signaling, long-term changes can be considered as truly epigenetics. A more recent view is proposed by Adrian Bird, defining epigenetic events as the structural adaptation of chromosomal regions so as to register, signal or perpetuate altered activity states (Bird 2007).

#### ***1.1.2.1. DNA methylation***

DNA, through addition of a methyl group by dedicated enzymes, can carry information beyond the genetic code, which can possibly be stably transmitted through cell division. The most famous modification is DNA methylation, which is the addition of a methyl group by dedicated enzymes (reviewed in (Li and Zhang 2014)). In mammals, this occurs mostly at cytosines preceding a guanine (the pair is termed CpG) and on both strands of DNA (Bird 1986) and is mediated by DNA methyltransferases (DNMTs). A fraction of CpG is concentrated in GC-rich genomic regions called CpG islands (Bird, Taggart et al. 1985). CpG islands locate at the transcriptional start site of genes and are either predominantly methylated or unmethylated, impacting the transcriptional status of the underlying region. Indeed, hypermethylation is associated with gene repression in several contexts, including silencing of genes (Boyes and Bird 1991), DNA repeats (Lehnertz, Ueda et al. 2003), or inactivation of the X chromosome in female cells (Mohandas, Sparkes et al. 1981). Consistently, lack of methylation has been associated with transcription of housekeeping genes (Zhu, Liu et al. 2008). DNA methylation influences genome function by recruiting repressing factors (Boyes and Bird 1991, Hendrich and Bird 1998), or on the contrary by impeding binding of transcription factors (Watt and Molloy 1988). DNA can be

demethylated passively by dilution through cell division if no methylation is imposed on newly synthesized DNA, or actively (reviewed in (Wu and Zhang 2010)). Indeed, Tet proteins can convert methylated cytosines into hydroxymethylcytosine, formylcytosine and carboxylcytosine (Kriaucionis and Heintz 2009, Tahiliani, Koh et al. 2009, Ito, D'Alessio et al. 2010, He, Li et al. 2011, Ito, Shen et al. 2011). These products could be further cleaved by additional pathways, resulting in demethylation, such as Base Excision Repair (BER) mechanisms, but they can also serve as modifications conveying information themselves.

### **1.1.2.2. Histone variants**

Histones exist under different forms called histone variants encoded by separate genes (Franklin and Zweidler 1977) (Table). Some eukaryotic histone variants, such as centromeric histone variant H3 (CenH3), H3.3, H2A.Z and H2A.X, are found in the earliest known diversifications of eukaryotic lineages (Talbert 2002, Malik and Henikoff 2003). Distinct histone variants sometimes differ by only a few amino acids, yet they are not always functionally equivalent. In mammals, histone H3 has eight variants known to date: H3.1, H3.2, H3.3, H3.4 (H3.1t), H3.5, CenH3, as well as the primate-specific H3.X and H3.Y. All variants are escorted by histone chaperones: proteins that bind histones and are involved in their transfer (De Koning, Corpet et al. 2007)(Figure 9). Chaperones can show some degree of specificity either for a variant (dedicated chaperones), or for a particular function. At the level of chromatin, distinct histone chaperones deposit histones to form the nucleosome. Biochemical isolation of tagged versions of H3 variants helped determine which histone chaperone was dedicated for each variant, involving them in distinct deposition pathways (Tagami, Ray-Gallet et al. 2004)(see section 2).

| Histone family | Histone variant             | Conservation                                    | Genomic distribution | Dedicated chaperones |
|----------------|-----------------------------|---|----------------------|----------------------|
| H3             | H3.1 and H3.2 (replicative) | Metazoan<br>Dm, Xl: H3.2<br>Mm, Hs: H3.1 & H3.2 | Global               | CAF-1 complex        |

|     |                              |   |  |                                   |
|-----|------------------------------|---|--|-----------------------------------|
|     | H3.3                         | Ubiquitous<br>Sc, Sp: H3<br>Dm, Xl, Mm,<br>Hs: H3.3   | Promoters and active gene bodies,<br>gene regulatory elements, other<br>regions with high turnover<br>Hs: Nucleosome-depleted regions<br>Mm: telomeres, meiotic XY body<br>Mm, Hs: Centromeres<br>Dm, Mm: Paternal chromatin at<br>fertilization | HIRA<br>complex<br><br>DAXX/ATRX  |
|     | CenH3                        | Ubiquitous<br>Sc: Cse4<br>Sp: Cnp1<br>Dm: CID<br>Xl, Mm, Hs:<br>CENP-A                                | Centromeres<br>Sc: Regions with high histone<br>turnover, tRNA genes   | HJURP                             |
|     | H3.4                         | Mammals<br>Mm, Hs: H3.t   | ND (sperm)   | ND                                |
|     | H3.5                         | Hominids<br>Hs: H3.5  | Euchromatin (sperm)  | ND                                |
|     | H3.X                         | Primates  | ND   | ND                                |
|     | H3.Y                         | Primates  | Euchromatin  | ND                                |
| H4  | H4<br>(no known<br>variants) | Ubiquitous  | Global   | All H3<br>chaperones              |
| H2A | H2A<br>(replicative)         | Ubiquitous  | Global   | FACT (Spt16)<br>Nap1<br>Nucleolin |
|     | H2A.X                        | Metazoan<br>Dm: H2Av<br>Xl, Mm, Hs:<br>H2A.X  | Global,<br>$\gamma$ H2A.X at DSB sites   | ND                                |
|     | H2A.Z                        | Ubiquitous<br>Sc: Htz1,<br>Sp: Pht1<br>Dm: H2Av<br>Xl: H2A.Zl<br>Mm, Hs:<br>H2A.Z.1,<br>H2A.Z.2 & 2.2 | Promoters and the body of active<br>and inducible genes, gene<br>regulatory elements, nucleolus.<br>Sc, Sp: subtelomeric regions.<br>Sp, Dm Mm, Hs: centromeres<br>Mm: meiotic XY body   | SRCAP,<br>p400                    |
|     | macroH2A                     | Amniotes  | Inactive X-chromosome,   | ND                                |

|     |                      |  |  |                       |
|-----|----------------------|--|--|-----------------------|
|     |                      | Gg: mH2A.1 & mH2A.2<br>Mm, Hs:<br>mH2A.1.1, 1.2 & mH2A.2         | promoters of imprinted genes,<br>promoters of inducible<br>developmental genes, telomeres,<br>centromeres, nucleolus, meiotic XY<br>body |                       |
|     | H2A.B                | Mammals<br>Mm:<br>H2A.Bbd1-5,<br>H2A.Lap1-4<br>Hs:<br>H2A.Bbd1&2 | Euchromatin and pericentric<br>heterochromatin (sperm)   | ND                    |
| H2B | H2B<br>(replicative) | Ubiquitous   | Global   | All H2A<br>chaperones |
|     | H2B.1                | Mammals<br>Mm, Hs:<br>TSH2B                                      | Global (sperm)<br>Telomeres (somatic cells)  | ND                    |
|     | H2B.W                | Mammals<br>Ms: H2BL1<br>Hs: H2BWT                                | Telomeres (sperm)  | ND                    |

**Table - List of histone variants.** ND, not determined; Sc, *Saccharomyces cerevisiae*; Sp, *Schizosaccharomyces pombe*; Dm, *Drosophila melanogaster*; Xl, *Xenopus laevis*; Gg, *Gallus gallus*; Mm, *Mus musculus*; Hs, human. Adapted from Szenker et al. 2013.

#### ***1.1.2.2.1. The replicative variants H3.1 and H3.2***

In mammals, the H3 variants H3.1 and H3.2, also referred to as replicative variants, provide the main supply of histones during DNA replication. Genes encoding for H3.1/2 are organized in tandem, multicopy clusters (Elgin and Weintraub 1975). This allows a massive H3.1/2 expression at the end of G1 and beginning of S phase in preparation for DNA replication (Prescott 1966, Robbins and Borun 1967, Takai, Borun et al. 1968, Sadgopal and Bonner 1969). Indeed, H3.1 is deposited genome-wide in S phase, when a supply of histones is needed to assemble newly synthesized DNA into chromatin (Ahmad and Henikoff 2002, Ray-Gallet, Woolfe et al. 2011). Throughout the cell cycle, but also coupled to DNA synthesis, H3.1 can be deposited at sites corresponding to nucleotide excision repair (Polo, Roche et al. 2006). H3.2 is less well characterized. It was

found to interact with H3.1-binding partners – namely Chromatin Assembly Factor 1 (CAF-1), Anti-Silencing Function 1 (ASF1), and one of the subunits of the Mini Chromosome Maintenance helicase (MCM2), see section 2 -, suggesting common deposition pathways (Latreille, Bluy et al. 2014). Considering that H3.2 differs from H3.1 by only one amino acid, the two variants may be redundant, yet they carry different post-translational modifications (Hake, Garcia et al. 2006), which might give rise to specific functions, and they feature different deposition patterns after oocyte fertilization of oocytes (Goldberg, Banaszynski et al. 2010, Santenard, Ziegler-Birling et al. 2010, Akiyama, Suzuki et al. 2011). Future work will help determine the specificity of H3.2.

#### **1.1.2.2.2. The replacement variant H3.3**

Independently of DNA synthesis, any DNA process that disrupts the chromatin structure may require new histone deposition. The replacement variant H3.3, encoded by two genes, is expressed throughout the whole cell cycle, with the exception of mitosis, and deposited in a DNA synthesis-independent manner (Wu and Bonner 1981). H3.3 is one of the most conserved proteins in all eukaryotes (Malik and Henikoff 2003). It differs from H3.1/H3.2 by five/four amino acids. As described below, several studies indicate that H3.3 is more than simply a replacement for H3.1 and has specific functions.

#### **H3.3 and transcription**

Chromatin immunoprecipitation and immunofluorescence experiments revealed that H3.3 is enriched at gene bodies and regulatory elements such as promoters and enhancers (Ahmad and Henikoff 2002, Mito, Henikoff et al. 2005, Goldberg, Banaszynski et al. 2010, Ray-Gallet, Woolfe et al. 2011), suggesting an association of this variant with active transcription. A few studies proposed that H3.3 might have an active role in transcription. H3.3 nucleosomes are unstable relative to H3.1 nucleosomes when treated with high ionic strength buffers, and presence of the H2A variant H2A.Z further destabilizes H3.3 nucleosomes, suggesting that H3.3 might confer specific properties to nucleosomes to facilitate chromatin accessibility (Jin and Felsenfeld 2007). Furthermore, in *Xenopus laevis*, H3.3 was shown to be necessary for the epigenetic memory of the active state of a gene upon nuclear transplantation of somatic nuclei in embryos (Ng

and Gurdon 2008). Yet, in *Drosophila*, absence of H3.3 led to transcriptional defects but could be compensated by increased expression of H3.1, suggesting that transcription was affected due to lack of histone replacement rather than the nature of H3.3 itself (Sakai, Schwartz et al. 2009). Therefore, it is still unclear whether H3.3 has a passive role in replacing H3.1 throughout the cell cycle, or an active one in maintaining chromatin accessible for transcriptional activity. Yet, H3.3 was also found associated with repressed regions, suggesting that its link with transcription is more complex.

### **H3.3 and silent regions**

Interestingly, H3.3 was also found enriched at silent regions, including telomeres and Polycomb-repressed genes in mouse ES cells, as well as pericentric heterochromatin in mouse embryonic fibroblasts and HeLa cells (Hake, Garcia et al. 2005, Wong, Ren et al. 2009, Drane, Ouararhni et al. 2010, Goldberg, Banaszynski et al. 2010, Santenard, Ziegler-Birling et al. 2010, Banaszynski, Wen et al. 2013), suggesting other possible functions of this variant at specific genomic loci. Intriguingly, H3.3 is needed at telomeres to silence telomeric repeats (Goldberg, Banaszynski et al. 2010). At centromeres, it was found to serve as a placeholder for the centromeric variant CenH3 in S phase until CenH3 incorporation in late mitosis (Dunleavy, Almouzni et al. 2011). Overall, the exact role of H3.3, in particular compared to H3.1, at specific genomic loci remains unclear.

### **H3.3 during development**

Several developmental studies provide evidence of the functional role of H3.3. In *Drosophila*, males and females depleted for H3.3 are viable but sterile (Hodl and Basler 2009, Sakai, Schwartz et al. 2009), yet fertility is rescued by H3.2 overexpression (Hodl and Basler 2012). Conversely, mutants without H3.2 and with concomitant S phase-expression of H3.3 survive and show no obvious defects (Hodl and Basler 2012), suggesting that replicative and replacement variants can compensate for each other in *Drosophila*. In vertebrates, however, the two variants do not seem to be able to replace each other. During *Xenopus laevis* development, H3.3-depleted embryos do not develop past gastrulation, and this phenotype cannot be rescued by H3.2 overexpression (Szenker, Lacoste et al. 2012). In mouse development, lack of H3.3 is lethal (Couldrey, Carlton et al.

1999, Bush, Yuen et al. 2013). Loss of H3.1 and H3.2 caused by depletion of their depositing factor leads to an increased incorporation of H3.3, but this compensation is insufficient to rescue viability (Akiyama, Suzuki et al. 2011).

Furthermore, during spermatogenesis, in *Drosophila*, humans, and mice, histones are replaced with smaller proteins termed protamins, enabling sperm genome condensation (Balhorn 2007), yet this is not the case in *X. laevis* or *C. elegans* (Orsi, Couble et al. 2009). Upon entry into the oocyte, the sperm genome undergoes a number of changes including chromatin decondensation; protamins are then removed and H3.3 is incorporated genome-wide as a replacement (Loppin, Bonnefoy et al. 2005, van der Heijden, Dieker et al. 2005, Torres-Padilla, Bannister et al. 2006).

Taken together, these findings highlight the functional importance and specific requirement of H3.3 in the context of fertilization and development.

#### **1.1.2.2.3. The centromeric variant CenH3**

CenH3 is the centromeric H3 variant. Centromeric histone proteins are less conserved than histone H3 and may have multiple phylogenetic origins (Malik and Henikoff 2003, Dawson, Sagolla et al. 2007). As a consequence, although the first identified version was termed CENPA in mammals (Earnshaw and Rothfield 1985), they have often been referred to as CenH3 (Talbert 2002). Centromeric DNA sequence is not sufficient for centromere formation and chromosome segregation, which require additional epigenetic features (reviewed in (Allshire and Karpen 2008)). This includes the presence of the histone variant CenH3. CenH3 shares 50-60% identity with H3.1 at the histone fold domain and a divergent N-terminal tail, making it the most divergent H3 variant. Its expression and deposition dynamics vary between species (reviewed in (Boyarchuk, Montes de Oca et al. 2011)). In humans, CenH3 is expressed in late G2 and deposited during telophase and early G1 at centromeres (Jansen, Black et al. 2007). Therefore, during S phase, parental CenH3 is temporarily diluted until the next telophase. Meanwhile, the resulting nucleosome gaps at centromeric regions are likely filled with H3.3 - serving as a placeholder (Dunleavy, Almouzni et al. 2011). Whether there are hemisomes is still debated (Dimitriadis, Weber et al. 2010). During mitosis, CenH3 serves as a foundation to recruit a network of proteins

essential for kinetochore formation (reviewed in (Allshire and Karpen 2008, Black and Bassett 2008)). (CenH3-H4)<sub>2</sub> tetramers were proposed to be more rigid compared to (H3.1-H4)<sub>2</sub>, possibly to resist forces during mitosis (Black, Foltz et al. 2004). CenH3-containing nucleosomes were also shown to wrap DNA in a distinct manner, possibly allowing the formation of a platform for the assembly of kinetochore proteins (Dalal, Furuyama et al. 2007, Furuyama and Henikoff 2009). Overall, CenH3 provides a clear example of a specific function of a histone variant to define a chromosomal domain.

#### ***1.1.2.2.4. Other H3 variants***

Other H3 variants are less characterized, yet they also seem to display specific features relative to H3.1. H3.1t differs from H3.1 by four amino acids and is only found in testis (Witt, Albig et al. 1996, Govin, Caron et al. 2005). H3.5 is highly expressed in testis and localizes to euchromatin (Urahama, Harada et al. 2016). The tissue-specific expression suggests a potential role in development, possibly to provide more histones during proliferation. In primates, H3.X and H3.Y have also been identified, but their function remains to be elucidated (Wiedemann, Mildner et al. 2010).

#### ***1.1.2.3. Histone post-translational modifications***

The presence of distinct histone variants in chromatin provides the first layer of histone-based information allowing the definition of chromatin domains. Another essential source of information comes from post-translational modifications of histones (PTMs). Histone modifications have been extensively characterized in the literature, in particular acetylation, methylation, phosphorylation, ubiquitination - corresponding to the covalent addition of, respectively, an acetyl, methyl, phosphate group or ubiquitin protein (reviewed in (Kouzarides 2007)). They are found on all histones, and mostly on histone N- and C-terminal tails. Importantly, because histone variants differ in their amino acid sequence, some histone post-translational modifications are specific to certain histone variants (Hake, Garcia et al. 2006, Loyola, Bonaldi et al. 2006). Histone modifications may influence chromatin in two non-exclusive ways: first, by directly impacting contacts between histones or between histones and DNA, and, second, by recruiting other proteins that will, in turn, alter the chromatin

configuration. The first hypothesis is exemplified by the fact that acetylation neutralizes the basic charge of a lysine, which might loosen the electrostatic interactions between histones and DNA and, as a consequence, chromatin structure (Bode, Gomez-Lira et al. 1983, Garcia-Ramirez, Dong et al. 1992, Garcia-Ramirez, Rocchini et al. 1995, Tse, Sera et al. 1998, Shogren-Knaak, Ishii et al. 2006). However, there are more examples of the second mechanism. Given that histone tails locate outside the nucleosomes, modifications are accessible to a number of histone-binding factors, including histone-modifying enzymes, readers, and writers. Therefore, the presence of a certain modification or combination of modifications can recruit other factors to a specific function in processes such as transcription or DNA repair. This possibility to translate PTMs into DNA activity is referred to as the “histone code”, yet its exact extent and functional impact remains incompletely elucidated (Jenuwein and Allis 2001). Importantly, histone modifications are reversible, which provides plasticity to chromatin by allowing dynamic changes, for example during differentiation.

Acetylation, methylation and phosphorylation were the first modifications discovered on histones, giving a hint of their great variety (Allfrey, Faulkner et al. 1964, Allfrey and Mirsky 1964, Murray 1964, Stevely and Stocken 1966). The finding that hyperacetylated histones correlated with gene expression provided the first clue that histone modifications may be linked to transcription (Allfrey, Faulkner et al. 1964, Allfrey and Mirsky 1964). In yeast, mutations in histone tails affected gene expression (Johnson, Kayne et al. 1990), further supporting the connection, while, in *Drosophila*, acetylated forms of H4 distributed distinctly in euchromatin and heterochromatin (Turner, Birley et al. 1992). Lysine acetylation is recognized by bromodomain modules, which are found in many different proteins including histone modifying enzymes and transcription regulators (Dhalluin, Carlson et al. 1999, Winston and Allis 1999, Owen, Ornaghi et al. 2000). Extensive work has enabled the characterization of transcription-associated histone PTMs, as well as the enzymes that deposit them (reviewed in (Rivera and Ren 2013)). For example, in terms of H3 modifications, the H3K4me3 mark is enriched at promoters (Bernstein, Kamal et al. 2005, Pokholok, Harbison et al. 2005), H3K36me3 at transcribed gene bodies (Barski,

Cuddapah et al. 2007), H3K4me1 and H3K27ac at active enhancers (Heintzman, Hon et al. 2009, Creyghton, Cheng et al. 2010, Rada-Iglesias, Bajpai et al. 2011). Conversely, other PTMs are associated with heterochromatin. In particular, two methylation marks are well characterized: H3K27me3, which marks polycomb-repressed regions (Bernstein, Duncan et al. 2006, Lee, Jenner et al. 2006), and H3K9me3 at constitutive heterochromatin (Peters, O'Carroll et al. 2001, Peters, Kubicek et al. 2003, Mikkelsen, Ku et al. 2007). H3K9me3 provides a good example of how a histone mark is maintained and influences chromatin compaction (reviewed in (Maison and Almouzni 2004, Mozzetta, Boyarchuk et al. 2015)). The methyltransferases G9a, SetDB1 and Suv39H1 collaborate to mono-, di- and tri-methylate H3K9 (Loyola, Tagami et al. 2009). Importantly, heterochromatin Protein 1 (HP1) recognizes and binds H3K9me3, then recruits more Suv39H1 in order to spread the mark on neighboring nucleosomes (Platero, Hartnett et al. 1995, Melcher, Schmid et al. 2000, Bannister, Zegerman et al. 2001, Lachner, O'Carroll et al. 2001, Machida, Takizawa et al. 2018). This reader-writer model enables the maintenance of H3K9me3-HP1 domains over large heterochromatic regions. However, other mechanisms mediate de novo establishment of these domains (reviewed in (Probst and Almouzni 2011)). For example, in mouse cells, long noncoding RNAs at pericentric heterochromatin associate with SUMO-modified HP1 (Maison, Bailly et al. 2011). This modification is required for de novo targeting of HP1 to pericentric regions. Importantly, evidence shows that this organization impacts chromatin status. The capacity of HP1 to dimerize may enable heterochromatin compaction by assembly of neighboring HP1 proteins (reviewed in (Eissenberg and Elgin 2000)). Furthermore, HP1 also interacts with several factors associated with the nuclear membrane (Poleshko, Mansfield et al. 2013, Camozzi, Capanni et al. 2014). This is consistent with a long line of electron microscopy studies showing that heterochromatin locates at the nuclear periphery, and is further supported by more recent DamID experiments showing that genomic regions associated with the nuclear envelope (Lamin-Associated Domains, LADs) are enriched for H3K9me3 (Towbin, Gonzalez-Aguilera et al. 2012, Kind, Pagie et al. 2013). Considering the importance of the nuclear periphery in many genomic processes, including gene expression and DNA replication, the role of H3K9me3 in nuclear

localization is particularly interesting. Furthermore, H3K9me3 can recruit the linker histone H1, which may contribute to chromatin compaction (Daujat, Zeissler et al. 2005).

Notably, modifications found in soluble pools of histones compared to histones incorporated into chromatin are different. For example, in humans, new dimers of H3.1-H4 are diacetylated at lysines 5 and 12 of H4 (Sobel, Cook et al. 1995, Loyola, Bonaldi et al. 2006), while, in yeast, the modification H3K56ac is systematically found on new H3 (Masumoto, Hawke et al. 2005). New histones H3 are overall not methylated, with the exception of H3K9me1 (Loyola, Bonaldi et al. 2006). This distinction between modifications typical of new or incorporated histones is likely important to handle histones during their de novo deposition or recycling, respectively.

In summary, the first scale of chromatin is an array of nucleosomes. Nucleosomes can contain different histone variants and histone post-translational modifications, which influence chromatin structure and function. This organization varies depending on nuclear localization.

## **1.2. Spatial organization of chromatin in the nucleus**

### **1.2.1. Chromatin fiber**

How is chromatin organized at the next scale? The initial model proposed that nucleosomes were packed into a compact 30 nm fiber (Finch and Klug 1976, Thoma, Koller et al. 1979) (Figure 4). In line with this hypothesis, many studies proposed different models for the internal organization of this compact structure, exploiting a vast array of technologies, such as X ray crystallography (Dorigo, Schalch et al. 2004, Schalch, Duda et al. 2005), electron microscopy (Robinson, Fairall et al. 2006), or CryoEM (Song, Chen et al. 2014). Importantly however, all these findings emerged from in vitro reconstituted fibers, therefore the relevance of this model in vivo remained to be established.

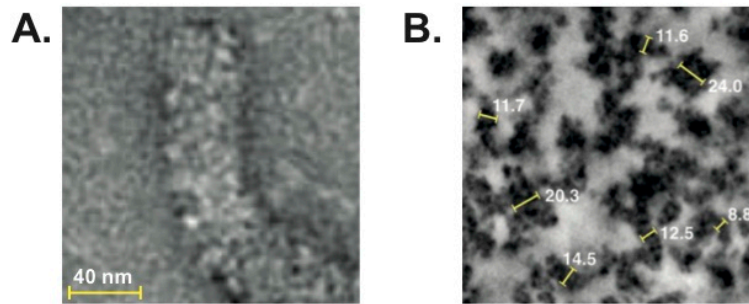


**Figure 4: Higher order chromatin organization.**

(A) Image of a chromatin fiber from an *in vitro* reconstitution system that generates regularly spaced nucleosome arrays from purified histones and tandem arrays of a strong nucleosome positioning sequence. From Robinson et al. 2006. (B) ChromEMT images showing chromatin as a disordered chain that has diameters between 5 and 24 nm and is packed together at different concentration densities in interphase nuclei of human small-airway epithelial cells. From Ou et al. 2017.

Several studies challenged the 30 nm fiber model of chromatin organization. Indeed, techniques including X ray scattering (Nishino, Eltsov et al. 2012), CryoEM (McDowall, Smith et al. 1986, Eltsov, Maclellan et al. 2008), electron spectroscopy imaging (Fussner, Strauss et al. 2012) and electron microscopy (Ou, Phan et al. 2017) failed to detect it *in vivo*. Based on these findings, the current view is that chromatin forms irregularly folded nucleosome fibres. The density of these fibers can vary depending on the nuclear localization (Ou, Phan et al. 2017), yet nucleosomes never seem to pack in a highly compact and organized manner as observed *in vitro*. In mitotic chromosomes, this disorganized fiber is also observed, although more dense (Nishino, Eltsov et al. 2012, Ou, Phan et al. 2017). Overall, while the existence of a highly compact fiber is not theoretically impossible, this second model is more compatible with many DNA processes that occur *in vivo* and require rapid access to DNA, such as transcription and repair.

### **1.2.2. Topologically associated domains**

Genomic loci located at great genomic distances, or even on different chromosomes, can be found very close in the nuclear space. This is for example the case for promoters and distal enhancers, which are in contact in the nucleus. In the past decade, the development of chromosome conformation capture

techniques (such as 4C, 5C, or Hi-C) - which combine proximity ligation with sequencing and allow the establishment of maps of contacts between different genomic regions (Lieberman-Aiden, van Berkum et al. 2009, Dixon, Selvaraj et al. 2012) - led to propose the existence of megabase-sized topologically associated domains (TADs). At a larger scale, these Hi-C maps also detected two compartments, with less contact with each other than within each of them. This showed that chromatin regions clustered together based on their transcriptional status. Existing chromatin-looping models seemed compatible with the existence of TADs (Schleif 1992). Although the exact mechanism and nature of loop formation and dynamics is debated, it appears that chromatin loops involves the role of cohesin; in absence of cohesin, TADs seem to disappear from contact maps (Rao, Huang et al. 2017). Notably, TAD establishment coincides with establishment of the replication-timing program, further supporting the interconnections between this structural compartmentalization and genome function (Dileep, Ay et al. 2015).

Although the development of C techniques provided great insight into genome organization, further work is required to understand how TADs and compartments organize in single cells in the nuclear space. Indeed, contact maps are often obtained from population of cells and, as a consequence, can only detect events that occur in a sufficient number of cells. Furthermore, they describe relative frequency of interactions between genomic loci, which does not indicate that these genomic loci are always physically together in the nucleus. Imaging approaches provide the means to visualize physical proximity in the nuclear space. The use of Fluorescence In Situ Hybridization (FISH) to monitor localization of regions from certain TADs in the nuclear space has been informative, sometimes recapitulating data from C techniques, but also sometimes highlighting discrepancies between contact maps and microscopy images (Bantignies, Roure et al. 2011, Sexton, Yaffe et al. 2012, Williamson, Berlivet et al. 2014, Wang, Su et al. 2016, Cattoni, Cardozo Gizzi et al. 2017, Szabo, Jost et al. 2018). For example, a study in mouse comparing C approaches and FISH data identified regions that did feature spatial proximity as predicted by 5C, and others that did not, showing that contact maps do not always reflect physical proximity in the nucleus (Williamson, Berlivet et al. 2014). Overall, it is

clear that the combination of Hi-C and microscopy is required to bridge the gap and give us the global view of how the genome is organized in the nucleus of individual cells.

More generally, imaging approaches enabled the visualization of DNA corresponding to each chromosome and showed that they occupied distinct territories in the nuclear space (Bolzer, Kreth et al. 2005) (Figure 5), while induction of DNA damage in a specific area of the nucleus led to damage in only a few chromosomes (Zorn, Cremer et al. 1979), in line with the existence of chromosome territories. The use of oligonucleotide-based probes (Oligopaint) combined with super-resolution microscopy approaches allowed the targeting of specific DNA sequences as well as entire chromosomes while improving the resolution and distinguishing maternal and paternal homologous chromosomes (Beliveau, Joyce et al. 2012, Beliveau, Boettiger et al. 2015).

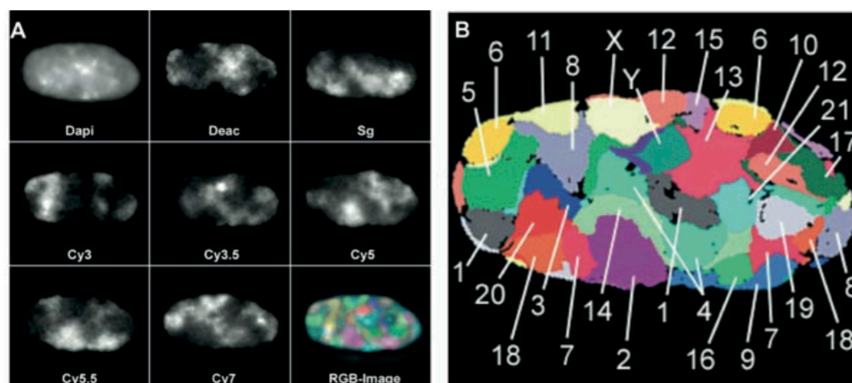


**Figure 5: Chromosome territories.**

24-Color 3D FISH Representation and Classification of Chromosomes in a Human G0 Fibroblast Nucleus. (A) A deconvoluted mid-plane nuclear section recorded by wide-field microscopy in eight channels: one channel for DAPI (DNA counterstain) and seven channels for the following fluorophores: diethylaminocoumarin (Deac), Spectrum Green (SG), and the cyanine dyes Cy3, Cy3.5, Cy5, Cy5.5, and Cy7. Each channel represents the painting of a chromosome territory subset with the respective fluorophore. (B) False color representation of all chromosome territories visible in this mid-section. From Bolzer et al. 2005.

Taken together, these findings show that chromatin undergoes some form of compartmentalization in the nucleus.

### 1.2.3. Heterochromatin and euchromatin

As mentioned previously, chromatin is divided into two categories based on electron microscopy observations: euchromatin (the “real” chromatin) and heterochromatin (the “other” chromatin). Heterochromatin is more stained and condensed, and locates at the nuclear periphery and around nucleoli (Heitz 1928) (Figure 6). Euchromatin, on the other hand, is unstained and decondensed and localizes in the nuclear interior. This discovery led to the proposal that heterochromatin contained silenced regions of the genome, while euchromatin was composed of active genes. This general rule has since been extensively tested and characterized in the literature and, today, the terms euchromatin and heterochromatin are used to refer to transcriptionally active and silent regions. As mentioned above, Hi-C maps feature such a division of the genome into two compartments, likely corresponding to euchromatin and heterochromatin. Interestingly, another characteristic feature that distinguishes euchromatin and heterochromatin is that they replicate at distinct times in S phase. In multicellular organisms, early replication correlates with transcriptional activity and varies during development, while this is not always the case in unicellular organisms (Hiratani and Gilbert 2009, Hiratani, Takebayashi et al. 2009). A general rule in human cells is that euchromatin replicates early in S phase, while heterochromatin replicates late in S phase (reviewed in (Rhind and Gilbert 2013)).

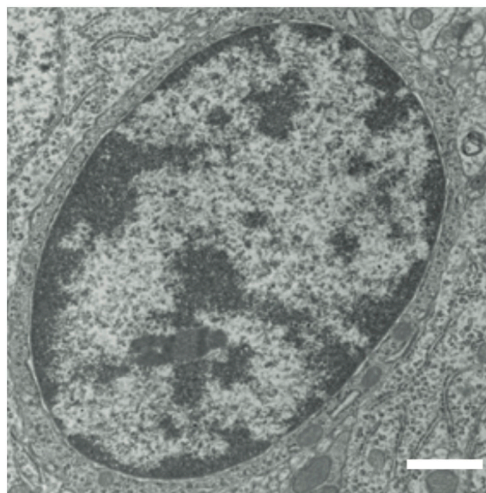


**Figure 6: Heterochromatin and euchromatin.**

Electron micrographs of a rat glial cell nucleus. Darkly stained material is heterochromatin; lightly stained regions are euchromatin. Scale bars: 1  $\mu$ m. From Pueschel et al. 2016.

Within heterochromatin, two main categories have been described: facultative and constitutive heterochromatin. Constitutive heterochromatin is always compact, independently of the cell type. It is present in regions such as centromeres or telomeres, composed of gene-poor and repeated DNA sequences. For example, in pericentric heterochromatin regions in mouse cells, DNA is more compact and can clearly be observed when staining DNA with DAPI (Probst and Almouzni 2011). Many studies suggest that constitutive heterochromatin has special physical properties accounting for its specific dynamics and compaction (reviewed in (Pueschel, Coraggio et al. 2016)) (Larson, Elnatan et al. 2017, Strom, Emelyanov et al. 2017). At the histone level, constitutive heterochromatin is marked by the modification H3K9me3, which recruits HP1 as previously mentioned. Facultative heterochromatin, on the other hand, varies between cell types. Indeed, facultative heterochromatin regions can change between a transcriptionally active and inactive state depending on the cell stage, as exemplified by genes that get inactivated during differentiation in a given lineage, or inactivation of the X chromosome in female cells during development. A well-characterized feature of facultative heterochromatin is the presence of the modification H3K27me3, which mediates gene inactivation through the recruitment of Polycomb proteins (reviewed in (Trojer and Reinberg 2007)). Additionally, mapping of certain proteins, including chromatin factors, in *Drosophila* enabled the definition of five chromatin domains featuring distinct protein configurations: three types of heterochromatin - constitutive, facultative, and a third and prevalent kind -, and two types of euchromatin (Filion, van Bommel et al. 2010). In summary, chromatin in the nucleus is divided into compartments, which share functional properties, such as transcriptional state and replication timing. How chromatin is replicated is depicted in the next section.

## **2. The challenge of replicating chromatin**

Chromatin is highly organized in the nucleus at all scales. It serves as a means to compact the DNA and has to be considered for all DNA transactions impacting genome function and regulation. How chromatin states, once established, can be transmitted or changed through cell division has received a lot of attention. In particular, how this fundamental organization contributes to the concept of epigenetic memory depends on the capacity to maintain features that can survive cellular division. Here, we describe how chromatin is challenged by and copes with DNA replication.

### **2.1. The replication machinery**

In order to duplicate the genetic material during DNA replication, the sequential assembly of a number of factors is necessary (Figure 7). First, unwinding of the DNA double helix is required. In mammals, this is achieved through the assembly of the Origin Recognition Complex (ORC), Cdc6, Cdt1, and the Minichromosome Maintenance (MCM) helicase, composed of the subunits MCM2-7 at origins of replication in late mitosis and early G1, forming the pre-RC complex in a step called origin licensing (reviewed in (Masai, Matsumoto et al. 2010, Fragkos, Ganier et al. 2015)). At the frontier between G1 and S, phosphorylation mediated by the DDK and CDK kinases is essential for the activation of the pre-RC complex and to prevent relicensing. In the beginning of S phase, a subset of origins initiates replication. The two loaded MCM helicases can translocate to bind single stranded DNA. The two complexes bind different strands to progress on the leading strands in opposite directions, creating two replication forks. To allow DNA replication, additional factors are required including GINS and Cdc45 (forming, with the MCM, the CMG complex) as well as replisome progression complexes (RPCs), which include fork-stabilizing factors. DNA polymerases are then positioned on their respective DNA strands (Pol $\epsilon$  for the leading strand and Pol $\delta$  for the lagging strand), in complex with the ring-shaped factor Proliferating Cell Nuclear Antigen (PCNA) present on both the leading and lagging strands. Interestingly, in *S. cerevisiae*, length of Okazaki fragments correlates with nucleosomal DNA length, linking lagging strand synthesis to chromatin assembly (Smith and Whitehouse 2012).

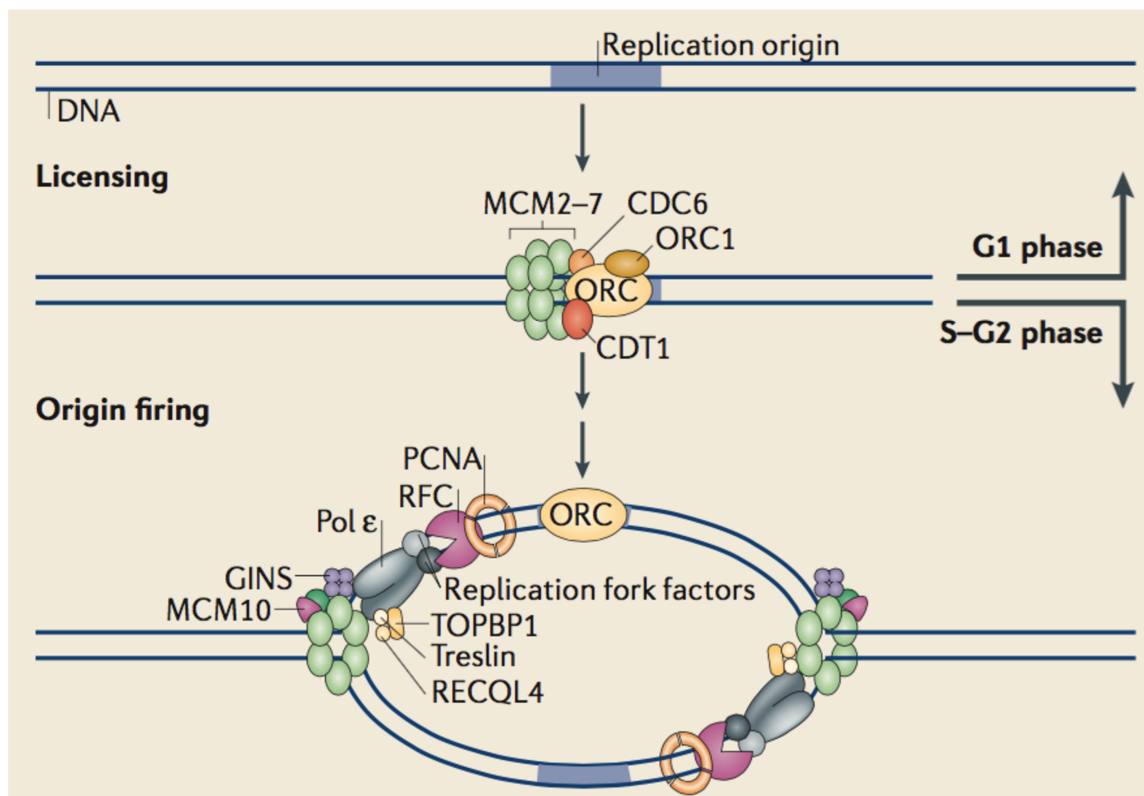


**Figure 7: Formation and activation of DNA replication origins.**

Licensing of replication origins is restricted to the G1 phase of the cell cycle and results from the sequential loading of pre-replication complex (pre-RC) proteins on all potential origins in the genome. First, the origin recognition complex (ORC), which has ATPase activity, is recruited to replication origins. This is followed by the binding of CDC6 and CDC10-dependent transcript 1 (CDT1). Loading of the mini-chromosome maintenance (MCM) helicase complex, which contains the six subunits MCM2–7, is the last step of the licensing reaction and can take place only if ORC, CDC6 and CDT1 are already bound to origins. Origin activation involves the formation of a pre-initiation complex (pre-IC) and activation of the MCM helicase complex. Assembly of the pre-IC is triggered by DBF4-dependent kinase (DDK) and cyclin-dependent kinases (CDKs) at the G1/S phase transition, and its activation into a functional replisome occurs in the S phase. DDK and CDKs phosphorylate several replication factors (including MCM10, CDC45, ATP-dependent DNA helicase Q4 (RECQL4), treslin, GINS, DNA topoisomerase 2-binding protein 1 (TOPBP1) and DNA polymerase  $\epsilon$  (Pol $\epsilon$ )) to promote their loading on origins, as well as several residues within the MCM2–7 complex, resulting in helicase activation and DNA unwinding. During helicase activation, the MCM2–7 double hexamer divides into two hexamers that function at the two replication forks emanating from the replication origin. Helicase activation induces the recruitment of other proteins (such as replication factor C (RFC), proliferating cell nuclear antigen (PCNA), replication protein A (RPA) and other DNA polymerases) that convert the pre-IC into two functional replication forks that move in opposite directions from the activated origin, with the replisome at each replication fork. From Fragkos et al. 2015.

The choice of the subset of initiating origins is not fully understood. At the level of the whole genome, the study of the replication program has reached two major conclusions: (i) origin activation is a stochastic event, and (ii) nuclear territories replicate in a defined order leading to clear replication patterns. Reconciling both models, the current view is that origin activation is indeed stochastic but within a chromatin region: origins in open euchromatin fire first, allowing the replication of transcribed regions, until replication forks reach heterochromatin, thereby firing origins in these regions as a domino effect (Guilbaud, Rappailles et al. 2011).

Importantly, the replisome replicates DNA assembled into chromatin, and therefore encounters nucleosomes. In this context, an additional network of proteins intervenes to handle histones, including histone chaperones and chromatin remodelers.

## **2.2. Inheritance of DNA methylation**

As previously described, DNA methylation provides a layer of information that influences genome function. How DNA methylation is transmitted through cell division, guaranteeing the transmission of information, is well characterized. For a detailed review of inheritance of DNA methylation, see (Almouzni and Cedar 2016). In brief, CpG dinucleotides are symmetric on the DNA strand, and methylated sites are mostly methylated on both DNA strands. During replication, DNA synthesis creates hemi-methylated strands and therefore, although diluted, the DNA methylation pattern is transmitted in a semi-conservative manner. Restoration of the original pattern involves methylating the other side of hemi-methylated dinucleotides. Very schematically, a simple view is that DNA methyltransferase I (Dnmt1) recognizes the methylated sequence and methylates the complementary strand (Li et al. 1992, Li et al. 2014). This is facilitated by other factors at the replication fork, such as the factor UHRF1, which can bind both methylated DNA and histone H3 (Cheng et al. 2014). While this semi-conservative transmission of DNA methylation can guarantee the maintenance of DNA methylation patterns, inheritance of histones is less well understood.

## 2.3. Inheritance of histones

### 2.3.1. Theoretical framework

During replication elongation, the replication machinery needs to disrupt parental nucleosomes ahead of the replication fork (reviewed in (Corpet and Almouzni 2009, Probst, Dunleavy et al. 2009) (Figure 8).

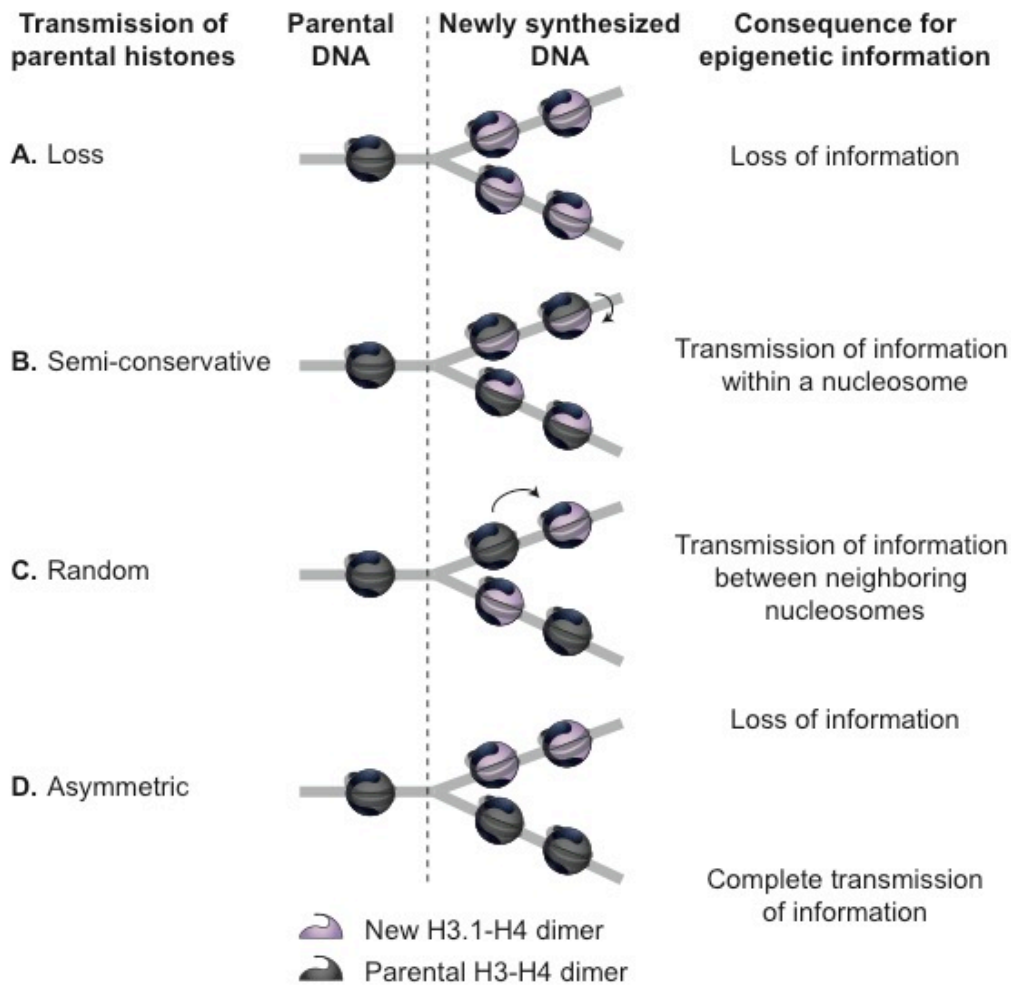


**Figure 8: Histone inheritance at the replication fork.**

Four theoretical models are possible for distribution of parental (grey) and new (purple) histones at the replication fork. (A) Parental histones are not recycled and only new histones are used to assemble nucleosomes on nascent DNA. (B) Parental (H3-H4)<sub>2</sub> tetramers are split at the fork. The resulting H3-H4 dimers are then distributed between the leading and lagging strand, and new H3.1-H4 dimers are used to complete the nucleosomes. Parental histone post-translational modifications can, in turn, be copied to new histones within a nucleosome (arrow). (C) Parental (H3-H4)<sub>2</sub> tetramers are recycled as such either on the leading or on the lagging strand (randomly distributed). New histones are used to form nucleosomes to maintain nucleosomal density. Parental histone post-translational modifications can, in turn, be copied to new histones from

one nucleosome to its neighbor (arrow). (D) Parental (H3-H4)<sub>2</sub> tetramers are recycled asymmetrically on one strand. New histones are used to form nucleosomes on the other strand. Based on Corpet et al. 2009, Probst et al. 2009.

Two opposite outcomes can be considered: (i) newly synthesized DNA is assembled into chromatin from scratch using a supply of new histones (Figure 8A), or (ii) histones present on the parental strand of DNA are recycled on newly synthesized DNA and chromatin is restored as before.

In the first model, all histone-based information is lost. This can be useful in some contexts where a cell needs to change its identity, for example during differentiation or reprogramming. However, this is not optimal if the daughter cell is meant to be identical to its parent. The second option provides means to transfer histone-based information as well, thereby supporting inheritance of genome expression programs.

In this second scenario, however, three models for parental histone recycling are possible. As nucleosomes contain two copies of each histone, an attractive hypothesis is that one copy of each histone transfers to each daughter DNA strand, complemented with new histones to form a nucleosome (Figure 8B). As a consequence, half of each new nucleosome would contain parental material and therefore parental information. Copy of this information to the second half would ensure restoration of the original status. An alternative hypothesis is that all histones within a parental nucleosome transfer together to a new nucleosome, located randomly on one of the two daughter strands (Figure 8C). In this case, on each daughter strand, half the nucleosomes would contain only parental material, and the other half only new material. Restoration of the original chromatin would then require copy of the information from the parental nucleosome to its new neighbor. These first two models ensure an equal distribution of parental histones between the two daughter strands. However, a third model introducing imbalances is also conceivable, proposing that all parental histones transfer to the same daughter strand, creating an identical chromatin landscape on one strand, but a reset one on the other (Figure 8D). In the context of differentiation for example, this could provide means for a stem cell to produce an identical stem cell and a differentiated cell.

In summary, histone segregation can theoretically be modulated to duplicate or change parental chromatin.

### **2.3.2. Histone segregation on daughter strands**

In mammals, upon passage of the replication fork, chromatin is rapidly reassembled (reviewed in (Corpet and Almouzni 2009, Probst, Dunleavy et al. 2009). This was first shown using in vitro replication of simian virus 40 and electron microscopy approaches (Sogo, Stahl et al. 1986) (McKnight and Miller 1977). Visualization of psoralen cross-linked chromatin at replication forks with electron microscopy showed that two nucleosomes were destabilized before the fork and that nucleosomes reassembled about 250 bp after the fork (Sogo, Stahl et al. 1986, Gasser, Koller et al. 1996). The use of the SV40 system also provided evidence that parental histones redistributed randomly between the leading and lagging strand (Cusick, DePamphilis et al. 1984, Krude and Knippers 1991, Sugawara, Ishimi et al. 1992). Although some in vitro studies suggested that nucleosomes may stay associated with DNA during passage of the replication fork (Bonne-Andrea, Wong et al. 1990, Krude and Knippers 1991, Randall and Kelly 1992, Sugawara, Ishimi et al. 1992, Krude and Knippers 1993, Vestner, Waldmann et al. 2000), it then became clear that histones dissociated from DNA: the two H2A-H2B dimers, which have a more labile association to the nucleosome, would dissociate, followed by the H3-H4 tetramer, which would then transfer to newly synthesized DNA (Jackson and Chalkley 1985, Gruss, Wu et al. 1993). On nascent DNA, histones would reassemble in a stepwise manner: the H3-H4 tetramer would reassemble first, then H2A and H2B would complete the nucleosome, and finally histone H1 would bind (Klempnauer, Fanning et al. 1980, Galili, Levy et al. 1981, Jackson and Chalkley 1981, Cusick, DePamphilis et al. 1984). Overall, these earlier studies provided the first insight into histone recycling at the replication fork, hinting towards the model where parental histones randomly distribute between daughter DNA strands (Figure 8B or 8C). In order to distinguish between the models from Figure 8B and 8C, the important aspect to consider is whether parental H3-H4 tetramers split into dimers, and, if they do, whether they mix with new H3-H4 dimers when forming a new nucleosome (Ray-Gallet and Almouzni 2010). In a mass spectrometry assay

combining the use of inducible tagged histones and heavy isotope lysine labeling to distinguish parental and new histones, Xu et al. detected almost no mixing of parental and new H3.1-H4 dimers (Xu, Long et al. 2010). Interestingly, they detected 10% of mixing of H3.3-H4 dimers (Xu, Long et al. 2010), and these events are enriched at active genes and enhancers (Huang, Zhang et al. 2013). Overall, this data suggests that parental H3-H4 dimers rarely mix with new during DNA replication, favoring the model depicted in Figure 8C. Yet, the biological context likely dictates these mechanisms: given that DNA replication offers an opportunity for cell fate change, other mechanisms for histone inheritance may be at play during specific steps of differentiation (see section 3). In the next section, however, we focus on the mechanisms by which parental histones randomly distribute between the two daughter strands.

### **2.3.3. Histone dynamics during DNA replication**

#### **2.3.3.1. *Histone chaperones***

Not long after the discovery of nucleosomes, *in vitro* experiments showed the importance of external factors to assemble chromatin. Indeed, while incubation of DNA and histones alone failed to give rise to regular arrays of nucleosomes (Stein, Whitlock et al. 1979, Stein 1989), addition of cell-free extracts from *X. laevis* eggs provided the additional proteins required for chromatin assembly, including histone chaperones. As mentioned, histone chaperones are proteins that bind histones and are involved in their transfer without necessarily being part of chromatin (De Koning, Corpet et al. 2007) (Figure 9).

Using *X. laevis* oocytes, the first histone chaperone identified was purified in 1978 and named nucleoplasmin (Laskey, Mills et al. 1977, Laskey, Honda et al. 1978, Earnshaw, Honda et al. 1980). *In vitro* chromatin assembly assays also using *X. laevis* extracts further enabled the identification of two pathways for histone deposition: DNA synthesis-coupled and DNA synthesis-independent (Gaillard, Martini et al. 1996, Ray-Gallet and Almouzni 2004).

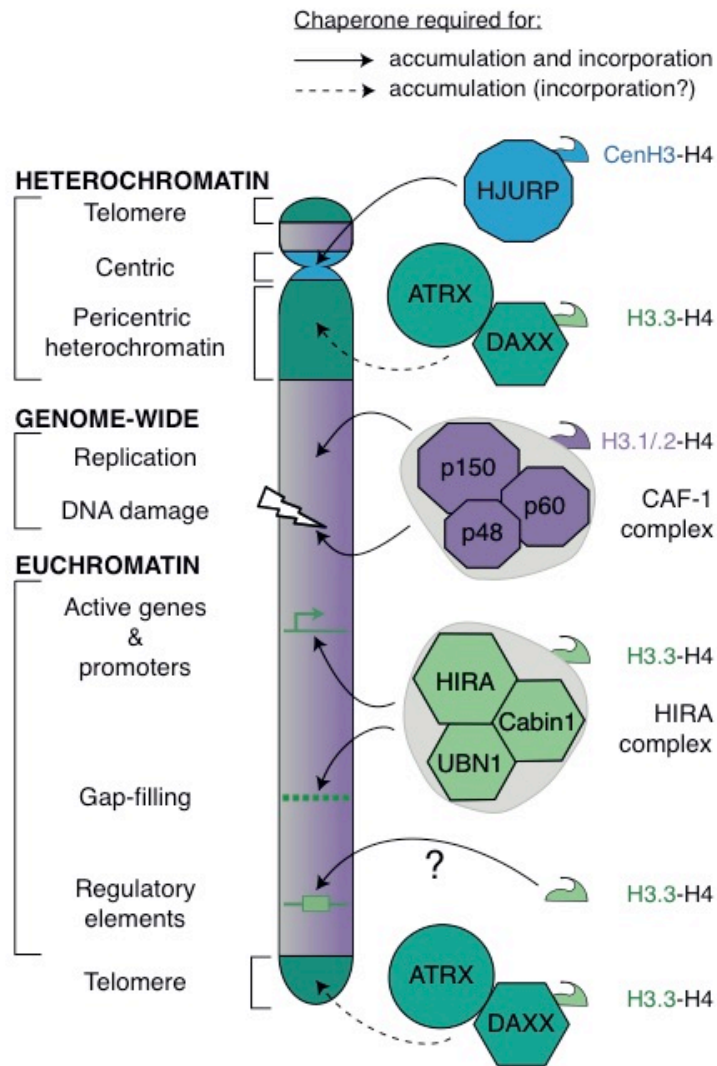


**Figure 9: Histone chaperones.**

Incorporation of H3.1 and H3.2 (purple) occurs genome-wide during DNA replication and at sites of damage during DNA repair. These DNA synthesis-coupled (DSC) events are promoted by the CAF-1 chaperone complex, which comprises three subunits referred to in humans as p150, p60, and p48. In mouse somatic and embryonic cells, H3.3 (light green) is enriched in coding regions and at specific chromatin landmarks. In heterochromatin, DAXX cooperates with the chromatin remodeler ATRX to give rise to the accumulation of H3.3 at pericentric satellite repeats and telomeres. In euchromatin, the HIRA complex (comprising HIRA, Cabin1 and UBN1 proteins) is responsible for H3.3 enrichment in the body of transcribed genes and at promoters of transcribed or non-transcribed genes. In addition, the HIRA complex can broadly incorporate H3.3 presumably by binding to transiently accessible non-nucleosomal DNA (gap-filling mechanism). The chaperone HJURP is involved in the deposition of CenH3 (blue) specifically at centromeres. From Filipescu et al. 2013.

Replication of the SV40 virus in presence of human cell extracts allowed the identification of the histone chaperone Chromatin Assembly Factor-1 (CAF-1) as

responsible for histone deposition coupled to DNA synthesis (Stillman 1986, Smith and Stillman 1989). CAF-1 has three subunits, p48, p60 and p150, and localizes at the replication fork through its interaction with PCNA (Shibahara and Stillman 1999, Shibahara, Verreault et al. 2000). The capacity of CAF-1 to dimerize may enable the assembly of two H3-H4 dimers into a tetramer for nucleosome assembly (Quivy, Grandi et al. 2001, Mattioli, Gu et al. 2017). The histone chaperone Histone Regulator A (HIRA) in turn showed DNA synthesis-independent histone deposition activity *in vitro* (Lamour, Lecluse et al. 1995, Lorain, Quivy et al. 1998, Ray-Gallet, Quivy et al. 2002). Importantly, biochemical isolation of factors interacting with specific histone variants provided evidence that CAF-1 was dedicated to the histone variant H3.1, and HIRA to the variant H3.3 (Tagami, Ray-Gallet et al. 2004). The chaperone complex DAXX-ATRAX (death domain-associated protein and  $\alpha$ -thalassemia/mental retardation syndrome protein) was later identified as dedicated to H3.3 as well, and was associated with deposition of H3.3 at telomeres and pericentric heterochromatic (Drane, Ouararhni et al. 2010, Goldberg, Banaszynski et al. 2010). The factor Holliday Junction-Recognizing Protein (HJURP) was found to be the histone chaperone responsible for CenH3 deposition (Dunleavy, Roche et al. 2009, Foltz, Jansen et al. 2009). While CAF-1, HIRA, DAXX-ATRAX and HJURP are chaperones dedicated to specific variants, other chaperones are less dedicated. For example, the H3-H4 histone chaperones Nuclear Autoantigenic Sperm Protein (NASP) and Anti-Silencing Function 1 (ASF1) can handle both the H3.1 and H3.3 variants (Tagami, Ray-Gallet et al. 2004, Cook, Gurard-Levin et al. 2011). ASF1 was first discovered in yeast where its overexpression inhibited silencing (Le, Davis et al. 1997). It was later found to have histone chaperone activity and is now known to intervene at many different steps of histone management (see section 2.3.3.3).

### **2.3.3.2. Dynamics of new histones *in vivo***

Studies exploiting the SNAP system confirmed, in somatic cells, the implication of CAF-1, HIRA and HJURP in the *de novo* deposition of H3.1, H3.3 and CenH3 respectively (Jansen, Black et al. 2007, Ray-Gallet, Woolfe et al. 2011) (Figure 10).

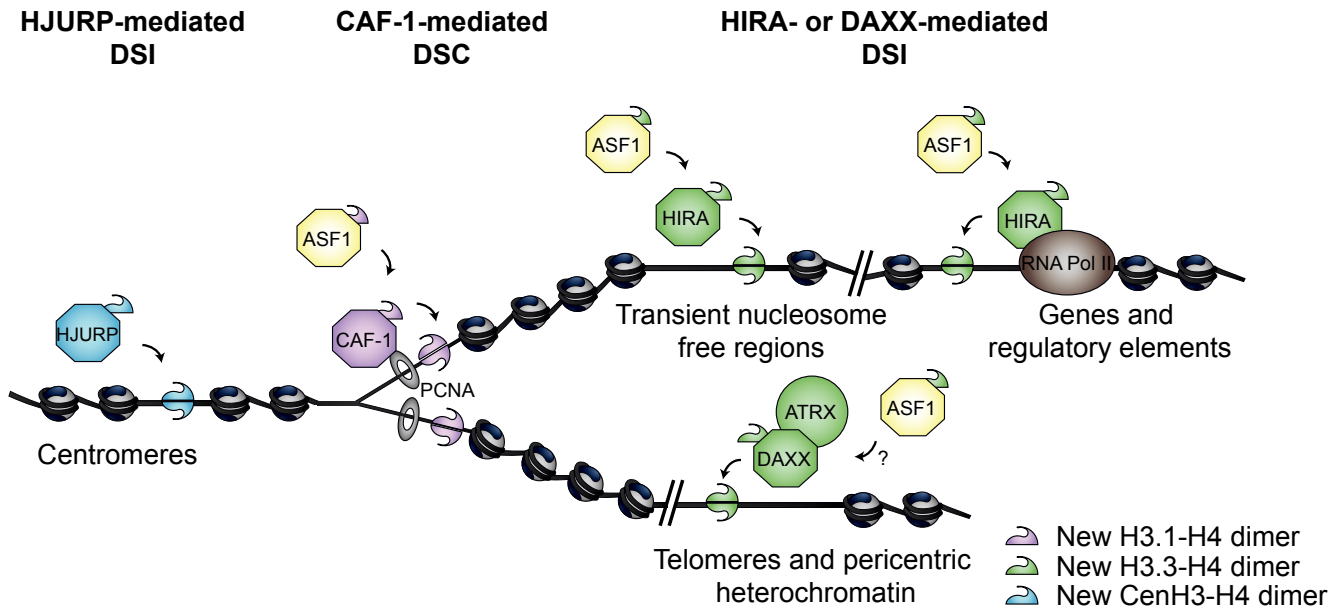


**Figure 10: DNA synthesis-coupled (DSC) and -independent (DSI) histone deposition pathways.**

CAF-1 mediates H3.1 deposition through its interaction with PCNA during replication (and DNA repair) while the HIRA complex mediates H3.3 deposition broadly through binding to transient accessible non-nucleosomal DNA during postreplication, sperm reprogramming, and any event generating transient naked DNA. In regions associated with RNA pol II (promoters, coding regions, and a subset of cis-regulatory elements), the interaction between the HIRA complex and RNA pol II facilitates H3.3 deposition. The DAXX-ATRX complex mediates H3.3 deposition at telomeres and pericentric heterochromatin. HJURP deposits CenH3 at centromeres. Adapted from Ray-Gallet et al. 2011.

The SNAP-tag is a mutant of the human DNA repair protein O<sub>6</sub>-alkylguanine-DNA alkyltransferase. It can specifically, covalently, and irreversibly bind to a benzylguanine (Keppler, Gendreizig et al. 2003) (Figure 16, Results section). Therefore, when fused to a protein of interest and expressed in cells, it can react with fluorescent or non-fluorescent dyes (derivatives of benzylguanine), allowing the specific visualization of either new or parental proteins. Combined with labeling of replication sites (with EdU incorporation), the use of SNAP-tagged histones showed that, in cells, deposition of new H3.1 occurred specifically in S phase at sites of DNA synthesis in a pathway mediated by CAF-1 (Ray-Gallet, Woolfe et al. 2011), in line with *in vitro* studies and with *in vivo* work in *Drosophila* (Ahmad and Henikoff 2002, Ahmad and Henikoff 2002, Loppin,

Bonnefoy et al. 2005, Schwartz and Ahmad 2005). Conversely, de novo deposition of H3.3 occurs independently of DNA synthesis throughout the cell cycle and is impaired by depletion of HIRA. Interestingly, upon CAF-1 depletion, HIRA can fill nucleosome gaps and deposit new H3.3 at sites of DNA synthesis. Finally, de novo deposition of CenH3 by HJURP is achieved in late mitosis/early G1 (Jansen, Black et al. 2007).

In summary, CAF-1, HIRA, DAXX-ATRX and HJURP mediate histone variant de novo deposition, while other histone chaperones can have broader roles. NASP and ASF1 can handle other aspects of histone management, including histone storage in the nucleus (Groth, Ray-Gallet et al. 2005, Cook, Gurard-Levin et al. 2011). Importantly, histone chaperones also interact with each other, forming a network of partners that collaborate to orient histone in distinct pathways.

### ***2.3.3.3. The histone chaperone Anti-Silencing Function 1***

#### ***2.3.3.3.1. ASF1 sequence and conservation***

ASF1 is a highly conserved protein (60% homology between yeast and human). All organisms possess a conserved N-terminal domain of 155 base pairs and a divergent C-terminal region. While yeast only has one ASF1, in many other organisms, including mammals, *X. laevis*, *C. elegans*, and *A. thaliana*, ASF1 exists as two paralogs, termed ASF1a and ASF1b in mammals, coded by two different genes (Abascal, Corpet et al. 2013) (to simplify, when referring to both paralogs, we will use the term “ASF1”). ASF1a and ASF1b share a 71% homology, but the C-terminal region is mostly responsible for their differences with only 29% homology. ASF1 can be phosphorylated by Tousled-like kinase (Tlk1/2), which may regulate its activity and interactions (Sillje and Nigg 2001). The ASF1 N-terminal domain organizes into an immunoglobulin-like fold with beta sheets organized as a sandwich (Figure 11). This region mediates the interaction with a dimer of H3-H4 and with other ASF1 binding partners (Daganzo, Erzberger et al. 2003, Mousson, Lautrette et al. 2005). Importantly, ASF1 binds the C-terminal helix of histone H3, which mediates the tetramerization of H3-H4, and the C-terminal domain of H4 (Munakata, Adachi et al. 2000, Mousson, Lautrette et al. 2005, Antczak, Tsubota et al. 2006, English, Adkins et al. 2006, Agez, Chen et al.

2007, Natsume, Eitoku et al. 2007). *In vitro*, addition of ASF1 to (H3-H4)<sub>2</sub> tetramers splits the tetramers into dimers, forming the ASF1-H3-H4 complex (Natsume, Eitoku et al. 2007). This is achieved by a strand-capture mechanism, where ASF1 uses the C-terminus of H4 as a handle to disrupt the (H3-H4)<sub>2</sub> tetramer (English, Adkins et al. 2006).

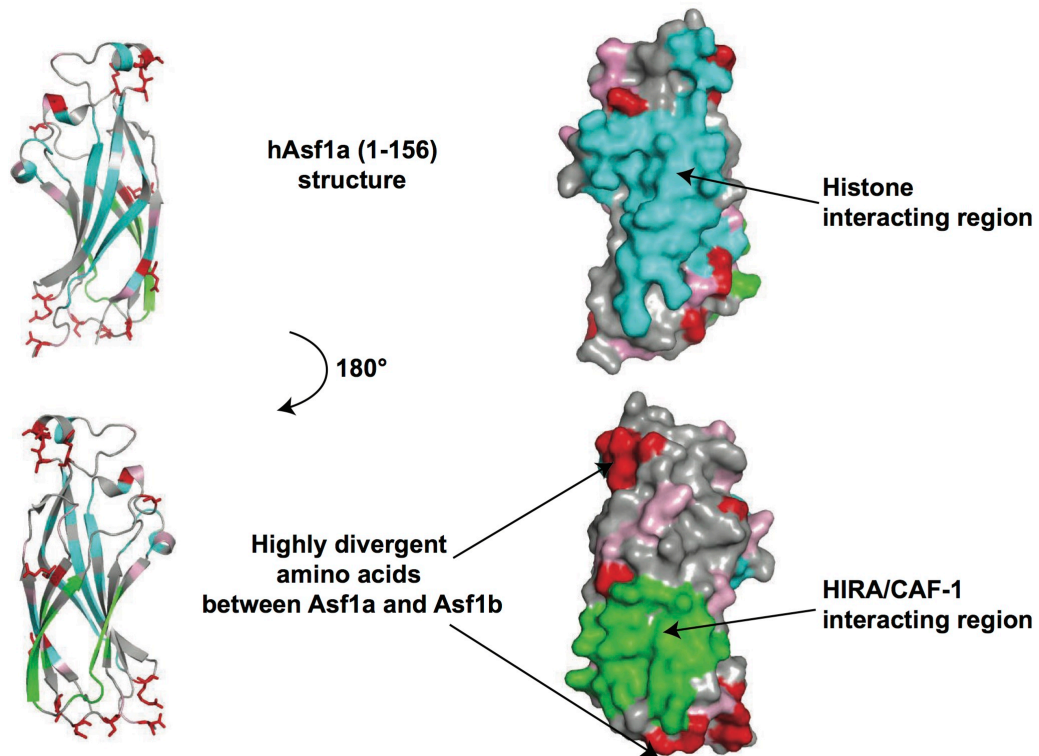


**Figure 11: ASF1 structure.**

The NMR structure of human ASF1a with indicated conserved binding domains. Adapted from Abascal et al. 2013.

Opposite the histone-binding region, ASF1 (both a and b) contains a domain, the AIP box, which mediates its interaction with other histone chaperones. Indeed, this region of the ASF1 N-terminal domain interacts with the B-domain of HIRA (Daganzo, Erzberger et al. 2003, Zhang, Poustovoitov et al. 2005, Tang, Poustovoitov et al. 2006). Via the AIP box, ASF1 also binds the p60 subunit of CAF-1, which contains motifs similar to the HIRA B-domain (Tyler, Adams et al. 1999, Tyler, Collins et al. 2001, Mello, Sillje et al. 2002, Sanematsu, Takami et al. 2006). ASF1 binds HIRA or p60 in a manner that is mutually exclusive (Tang, Poustovoitov et al. 2006, Malay, Umehara et al. 2008), but compatible with the

presence of histones. This enables the formation of either a ASF1-H3-H4-HIRA or a ASF1-H3-H4-CAF-1 complex for different histone deposition pathways. Considering that ASF1 (both a and b) binds equally H3.1 and H3.3 (Tagami, Ray-Gallet et al. 2004, Abascal, Corpet et al. 2013), it is unclear how it delivers the proper H3 variant to HIRA or CAF-1. Furthermore, although the region involved in the interaction with HIRA or CAF-1 is conserved in ASF1a and ASF1b, the two paralogs actually have preferential binding partners: ASF1a interacts preferentially with HIRA (Tang, Poustovoitov et al. 2006) and ASF1b with CAF-1 (Abascal, Corpet et al. 2013). Therefore, differences in other regions of the N-terminal core must account for the paralog-specific interactions. Another possible explanation relies in the divergent unstructured flexible C-terminal region of ASF1a and b, which might fine-tune the specific interactions of the two paralogs. In turn, the ASF1a-HIRA complex would likely preferentially handle H3.3, while the ASF1b-CAF-1 complex would handle H3.1, due to the variant specificity of HIRA and CAF-1 respectively.

#### ***2.3.3.3.2. The two paralogs ASF1 and ASF1b***

Although highly similar in sequence, ASF1a and ASF1b are not entirely functionally equivalent. First, the two paralogs have different expression patterns, with ASF1a ubiquitously expressed, and ASF1b expressed in proliferating tissues (Umehara and Horikoshi 2003). Given its overexpression in cancer, ASF1b is thought to have a more specific role during replication (Corpet, De Koning et al. 2011) (see below). Second, as previously mentioned, ASF1a and ASF1b have preferential binding partners – HIRA and CAF-1 respectively -, which orient them in distinct pathways. In yeast, in ASF1 knockout strains, reintroduction of either ASF1a or ASF1b restores distinct functions: ASF1a rescues defects in the DNA damage response, while ASF1b rescues growth defects (Tamburini, Carson et al. 2005). Furthermore, ASF1a knockout mice are lethal, while ASF1b knockouts are viable but sterile (Hartford, Luo et al. 2011, Messiaen, Guiard et al. 2016). Biochemical, structural, and evolutionary biology approaches suggest that, to optimize distinct functions, ancestral ASF1 functions were distributed between two gene duplicates, a process known as subfunctionalization (Abascal, Corpet et al. 2013). Yet, whether the paralogs can

compensate for each other to some extent or in particular contexts cannot be excluded.

#### ***2.3.3.3.3. Role of ASF1 in histone import and storage***

ASF1 is a key factor in the network of histone chaperones and is implicated in many steps of histone management, from their transport to their deposition in chromatin (reviewed in (Mousson, Ochsenbein et al. 2007)). First, ASF1 binds nuclear import factors - Importin 4 - as well as histones (Blackwell, Wilkinson et al. 2007, Jasencakova, Scharf et al. 2010), suggesting that it may be involved in importing histones in the nucleus. ASF1 also binds Codanin 1 (Ask, Jasencakova et al. 2012), which can retain ASF1 in the cytoplasm and, in turn, control histone supply in the nucleus. Thus, Codanin 1 can be considered a regulator of the amount of ASF1 in the nucleus. In the nucleus, ASF1 is essential for histone storage (Groth, Ray-Gallet et al. 2005). Indeed, ASF1 and histones form a complex with the histone chaperones NASP and RbAp48 (Cook, Gurard-Levin et al. 2011). This multichaperone complex buffers soluble histones in the nucleus and protects them from degradation via the chaperone-mediated autophagy pathway. This mechanism guarantees a supply of new histones for subsequent deposition in chromatin in different contexts, including replication, transcription or repair, by other chaperones such as CAF-1, HIRA or DAXX. Importantly, ASF1 interacts with these chaperones to hand off histones for their de novo deposition. Although it is not required *in vitro* for assembly of new nucleosomes (Ray-Gallet, Quivy et al. 2007), ASF1 interactions with other chaperones *in vivo* facilitates histones deposition in chromatin. Indeed, ASF1a participates in the DNA synthesis-independent de novo deposition of H3.3 in partnership with HIRA (Daganzo, Erzberger et al. 2003, Green, Antczak et al. 2005, Tang, Poustovoitov et al. 2006), while ASF1b interacts with CAF-1 for the DNA synthesis-dependent de novo deposition of H3.1 (Tyler, Adams et al. 1999, Mello, Sillje et al. 2002) (Figure 10). Recently, work in *Drosophila* also suggested that ASF1 and DAXX collaborate for the DNA synthesis-independent de novo deposition of H3.3 (Fromental-Ramain, Ramain et al. 2017). The current model is that ASF1a and ASF1b act as histone donors and acceptors, handing off histones to other chaperones for their subsequent deposition.

#### 2.3.3.3.4. Histone recycling during replication and ASF1

Several lines of evidence indicate that ASF1 plays a critical role during DNA replication and it is important to determine how it relates to its function in handling histones. Depletion of ASF1 using RNA interference in human (both ASF1a and b) and *Drosophila* cells, and inactivation of the gene in DT40 chicken cells leads to an accumulation of cells in S phase (Groth, Ray-Gallet et al. 2005, Sanematsu, Takami et al. 2006, Schulz and Tyler 2006, Groth, Corpet et al. 2007), suggesting the importance of ASF1 for S phase progression. ASF1b, which is expressed specifically in proliferating tissues, is required for proliferation of human cultured cells (Corpet, De Koning et al. 2011). Its expression level can serve as a marker of cycling or non-cycling cells (Umehara and Horikoshi 2003) and carries prognostic value in different tumor types (Corpet, De Koning et al. 2011, Montes de Oca, Gurard-Levin et al. 2015). We describe here the molecular mechanisms involving ASF1 during replication (Figure 12).

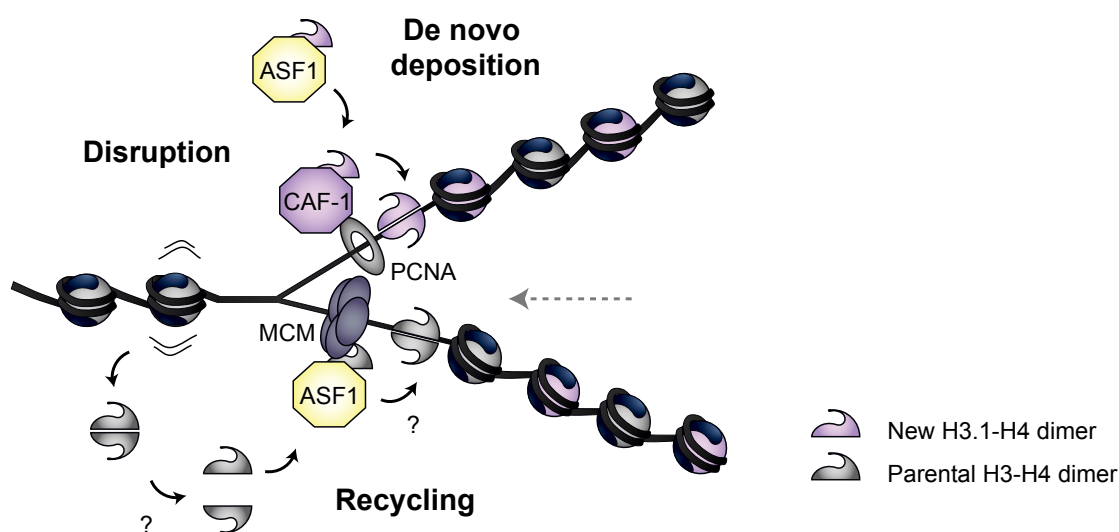


**Figure 12: Dynamics of histones at the replication fork.**

(1) For each parental nucleosome disrupted by replication fork passage (indicated by the gray arrow), an H3-H4 tetramer or two H3-H4 dimers are made available. (2) The histones are in turn recycled on newly synthesized DNA either directly as a tetramer or as two dimers. MCM2 and ASF1 may cochaperone H3-H4 for this recycling. (3) New histones are deposited by CAF-1 on nascent DNA to ensure a full complement of nucleosomes on the nascent DNA. Recycling of parental histones and de novo deposition are thought to occur randomly on both the leading and the lagging strands. Here, for clarity, de novo deposition is depicted on the bottom strand. Adapted from Corpet et al. 2009, Clément et al. 2015, and earlier schemes from the lab.

During DNA replication, parental nucleosomes have to be evicted from the parental strand of DNA to allow passage of the replication machinery. The force of the replicative helicase may be enough to disrupt nucleosomes, as suggested by *in vitro* experiments using optical tweezers showing that helicase progression can disrupt a histone octamer (Hall, Shundrovsky et al. 2009). However, further studies exploiting *in vitro* replication of SV40 or rDNA replication in yeast indicated that histones are destabilized but not evicted from DNA (Sogo, Stahl et al. 1986, Gruss, Wu et al. 1993, Lucchini and Sogo 1995, Gasser, Koller et al. 1996). Therefore, additional factors are likely required to evict parental histones, such as chromatin remodelers.

While histone eviction allows progression of the replication fork, histone incorporation occurs immediately after the fork - to ensure proper packaging of newly synthesized DNA - via two pathways: histone de novo deposition and histone recycling. As mentioned previously, ASF1 (preferentially ASF1b) hands off new histones H3.1-H4 to CAF-1 for their de novo deposition during DNA replication. In humans, CAF-1 localizes at the replication fork via the interaction of one of its subunit with PCNA (Shibahara and Stillman 1999), while, in yeast, ASF1 was also found to bind RFC (Majka and Burgers 2004). Extensive evidence in yeast shows that ASF1 participates in the deposition of the mark H3K56ac through its interaction with the acetylase Rtt109 (Recht, Tsubota et al. 2006). In turn, this mark, predominantly found on newly synthesized histones, facilitates histone de novo deposition and, therefore, chromatin assembly during replication. In humans, however, as this modification is found on less than 1.5% of histones, it is unlikely to play the same role as in yeast (Jasencakova, Scharf et al. 2010). Yet, other modifications are typical of new histones in human cells and found in complex with ASF1, such as H4K5K12diAc (Groth, Ray-Gallet et al. 2005, Jasencakova, Scharf et al. 2010), consistent with the importance of ASF1 for controlling histone supply during replication and facilitating histone de novo deposition at the replication fork.

Importantly, however, work from our laboratory provided evidence that ASF1 may also be involved in the recycling of parental histones at the replication fork (Figure 12). Indeed, ASF1 forms a complex with the MCM2 subunit of the MCM

helicase, via a H3-H4 histone bridge (Groth, Corpet et al. 2007). During the first year of my PhD, several groups determined the structure of MCM2 in complex with either a H3-H4 tetramer, or a dimer of H3-H4 and ASF1 (Huang, Strømme et al. 2015, Richet, Liu et al. 2015). Induction of replication stress with hydroxyurea provided further evidence for ASF1 role at the fork. Hydroxyurea suppresses the nucleotide pool, which would cause an uncoupling of helicase and polymerase progression. Due to this physical uncoupling, hydroxyurea treatment usually leads to the appearance of single-stranded DNA (Groth, Corpet et al. 2007, Jasencakova and Groth 2010), yet no single stranded DNA was detected upon ASF1 depletion in presence of hydroxyurea, suggesting defects in DNA unwinding. Furthermore, upon hydroxyurea treatment, ASF1 and MCM2 accumulate with histones carrying parental post-translational modifications (modifications typically found on histones incorporated into chromatin, not new histones). Proximity ligation assays enabled the visualization of ASF1 at active replisomes in human cells (Huang, Strømme et al. 2015), and, in *Drosophila*, ASF1 localizes at replication forks (Schulz and Tyler 2006). However, given that a mass spectrometry study could not detect ASF1 with the active replisome (Campos, Smits et al. 2015), it is likely that ASF1 only binds transiently to unload the MCM. Importantly, as mentioned above, parental H3-H4 rarely mix with new H3-H4 (Xu, Long et al. 2010). Whether H3-H4 tetramers split - even temporarily - during their recycling remains unknown. Although it would seem simpler to transfer intact tetramers, the finding that the main histone chaperones CAF-1, HIRA and DAXX use H3-H4 dimers to form nucleosomes *in vivo*, and that ASF1 also handles dimers, suggests that a temporary splitting may still occur before reassembly of the original tetramer.

Importantly, crosstalk with other factors of the replication machinery, as well as other histone chaperones and chromatin remodelers, requires further investigation in order to be incorporated into the picture. One immediate candidate to collaborate with ASF1 for parental histone redeposition is CAF-1. However, work in yeast shows that CAF-1 preferentially interacts with new histones rather than parental (Kaufman, Kobayashi et al. 1995, Verreault, Kaufman et al. 1996). Furthermore, as CAF-1 is dedicated to H3.1, it is not an ideal candidate to recycle parental H3.3 (Tagami, Ray-Gallet et al. 2004).

Importantly, however, the p150 subunit of CAF-1 binds HP1, and is thought to participate in its recycling during replication (Murzina, Verreault et al. 1999, Quivy, Roche et al. 2004). CAF-1 also forms a complex with MBD1 (methyl-CpG-binding protein 1) and SETDB1, a H3K9 methyltransferase (Maison and Almouzni 2004). Therefore, in heterochromatin, CAF-1 likely participates in recycling factors of the parental chromatin environment. It is possible that it also handles parental histones in this specific context. Another interesting histone chaperone to consider is the H2A-H2B chaperone Facilitates Chromatin Transcription (FACT) (Orphanides, Wu et al. 1999). Indeed, FACT also localizes to replication forks and interacts with the MCM helicase (Tan, Chien et al. 2006). While FACT has mainly been proposed to recycle parental H2A-H2B, it can also bind H3-H4 and could be involved in their recycling (Belotserkovskaya, Oh et al. 2003, VanDemark, Blanksma et al. 2006, Kemble, Whitby et al. 2013, Yang, Zhang et al. 2016). Two recent studies investigated the role of the Replication Protein A (RPA) in histone handling (Liu, Xu et al. 2017, Zhang, Gan et al. 2017). Through its single-stranded DNA binding property, RPA is recruited to replicating DNA, regulatory elements and actively transcribing genes. In HeLa cells, RPA interacts with HIRA, forming a RPA-HIRA-H3.3 complex. RPA colocalizes with HIRA and H3.3 at regulatory elements, and its depletion impairs HIRA localization and H3.3 de novo deposition at these regions as well as defects in gene transcription (Zhang, Gan et al. 2017). In yeast, RPA interacts with H3-H4 at the replication fork and could participate in replication-coupled histone deposition (Liu, Xu et al. 2017). Furthermore, several other factors of the replication machinery have histone binding domains, such as DNA polymerase epsilon (Pol $\epsilon$ ) (Li, Pursell et al. 2000). Therefore, several components of the replication machinery could serve as a platform for the transfer of parental histones to the other side of the replication fork.

In summary, when I started my PhD, the model was that ASF1 and MCM may co-chaperone parental histones for their recycling during DNA replication. However, a direct monitoring of the histones themselves at replication sites had not documented the fate of parental histones at the time. Since then, work from our lab exploiting the SNAP labeling technique increased our ability to monitor specific subpopulations of histones, such as new or parental histones. Therefore,

I decided to use this system to directly follow parental histones and test in cells the role of ASF1 in recycling parental histones during DNA replication. During the first year of my PhD, determination of the structure of the MCM2 complexes refined the model: a parental H3-H4 tetramer, once disrupted, would transfer to MCM2 at the replication fork. This parental tetramer could then either (i) remain intact and transfer directly to the daughter DNA strand, or (ii) be split into dimers by ASF1, which would unload the MCM and transfer H3-H4 dimers to the daughter DNA strand.

### 2.3.3.3.5. Role of ASF1 in gene expression

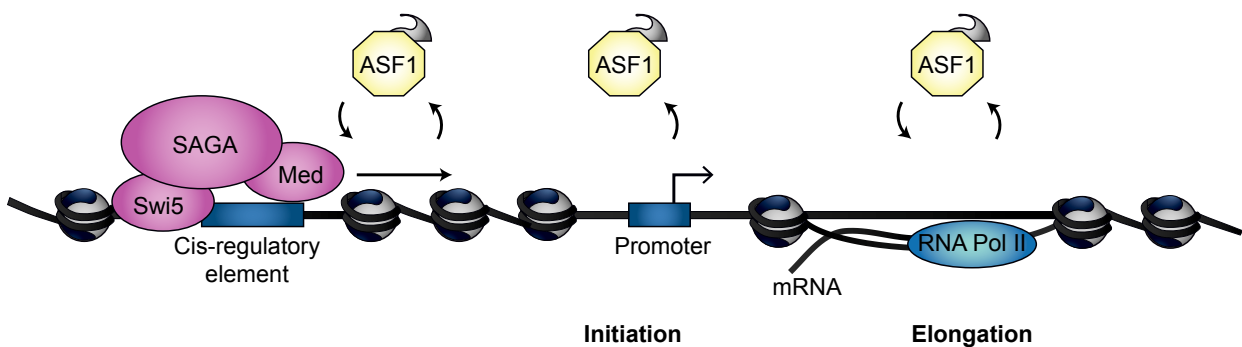


**Figure 13: ASF1 and transcription in yeast.**

ASF1 is involved in histone eviction/reassembly at regulatory elements of the HO gene and promoters. During RNA PolII progression, ASF1 is involved in both histone eviction and reassembly. Adapted from De Koning et al. 2007.

Most of the work concerning ASF1 and gene expression comes from yeast (reviewed in (Mousson, Ochsenbein et al. 2007)) (Figure 13). At the promoter of PHO5 - a useful inducible system -, ASF1 is necessary for the disruption of nucleosomes, which is required for gene expression (Adkins, Howar et al. 2004, Adkins and Tyler 2004), although this is dependent on induction conditions (Korber, Barbaric et al. 2006). CHIP experiments showed that ASF1 localizes to the promoter of transcriptionally active genes and is required both for disassembly and reassembly of nucleosomes during elongation by PolII (Schwabish and Struhl 2006). Several other studies highlight the role of ASF1 in nucleosome reassembly upon transcription, while others find ASF1 and the Hir proteins (yeast homolog of the HIRA complex) to be dispensable for reassembly

due to compensation by other factors including Spt6 (Kaplan, Laprade et al. 2003, Adkins, Howar et al. 2004, Adkins and Tyler 2004, Adkins and Tyler 2006). This suggests redundant roles for ASF1, Hir and Spt6, yet overall it is clear that, in yeast, ASF1 is important for the dynamics of histone exchange at gene promoters and bodies. At regulatory elements, the presence of ASF1, as well as the H2A-H2B histone chaperone Facilitates Chromatin Transcription (FACT) and the chromatin remodeler complex Swi/snf, is needed for nucleosome removal, which allows access to transcriptional coactivators (Takahata, Yu et al. 2009). Although there are divergent reports of the effect of ASF1 loss on overall chromatin compaction (Robinson and Schultz 2003, Adkins and Tyler 2004, Prado, Cortes-Ledesma et al. 2004), gene expression is globally affected (Zabaronick and Tyler 2005). Recruitment of ASF1 to promoters and regulatory elements may be mediated by its interaction with transcription factor Bdf1 (interaction between hASF1a and hTAFII250 in humans) (Chimura, Kuzuhara et al. 2002). Addition of a H3-H4 tetramer to the complex hASF1a- hTAFII250 leads to complex disruption and creation of the complex ASF1-H3-H4, which provides insight into how ASF1 may facilitate nucleosome disassembly (Akai, Adachi et al. 2010). Interestingly, a recent study in yeast highlighted the importance of ASF1 for gene expression specifically in S phase (Voichek, Bar-Ziv et al. 2016). Indeed, in eukaryotes, mRNA production remains overall stable as S phase progresses, despite the duplication of the genetic material (Killander and Zetterberg 1965, Pfeiffer 1968, Elliott and McLaughlin 1978). Strikingly, this regulatory process, termed expression homeostasis, disappears when ASF1 is lost (Voichek, Bar-Ziv et al. 2016). This may in part be due to decreased H3K56Ac, or more generally defects in chromatin assembly upon passage of the replication fork. Whether this remains true in humans is unknown.

In yeast, ASF1 is also implicated in gene repression. While ASF1 was originally discovered because its overexpression led to derepression of the MAT locus, telomeric loci and rDNA (Le, Davis et al. 1997, Singer, Kahana et al. 1998), several other studies suggest that ASF1 loss leads to defects in gene silencing, in particular in double mutants where Cac1 (yeast homolog of a CAF-1 subunit) is also mutated (Singer, Kahana et al. 1998, Tyler, Adams et al. 1999, Osada, Sutton et al. 2001, Sharp, Fouts et al. 2001, Sutton, Bucaria et al. 2001, Krawitz, Kama et

al. 2002, Tamburini, Carson et al. 2005). A recent study showed that H2Bub and ASF1 collaborate to mediate silencing at telomeres and mating loci (Wu, Lin et al. 2017). In *Drosophila*, ASF1 has been implicated in silencing of pericentric heterochromatin (Moshkin, Armstrong et al. 2002) and of the NOTCH signaling pathway (Goodfellow, Krejci et al. 2007, Moshkin, Kan et al. 2009). In mammals, ASF1 has also been linked to gene silencing, as ASF1a is required for the formation of SAHF (Senescence-Associated Heterochromatin Foci) involved in repressing proliferating genes when entering senescence (Zhang, Poustovoitov et al. 2005) (reviewed in (Adams 2009)), and ASF1 was found in a screen searching for epigenetic silencing factors in mice (Gazin, Wajapeyee et al. 2007). Interestingly, ASF1 and the Hir proteins have been implicated in repression of histone genes in yeast (Sherwood and Osley 1991, Sutton, Bucaria et al. 2001, Fillingham, Kainth et al. 2009). In *Drosophila*, ASF1 localizes at histone gene clusters on polytene chromosomes (Moshkin, Armstrong et al. 2002). How ASF1 participates in histone gene regulation in mammals will be a fascinating issue to explore further with arising new technologies.

#### ***2.3.3.3.6. ASF1 and DNA repair***

In yeast, ASF1 has been implicated in the response to DNA damage. ASF1 mutants are sensitive to a number of genotoxic agents, including hydroxyurea, methyl-methane-sulfonate (MMS), cisplatin, camptothecin, bleomycin (Le, Davis et al. 1997, Tyler, Adams et al. 1999, Emili, Schieltz et al. 2001, Hu, Alcasabas et al. 2001, Ramey, Howar et al. 2004, Mousson, Lautrette et al. 2005, Tamburini, Carson et al. 2005). ASF1 forms a complex with the DNA damage checkpoint kinase Rad53 and this complex can dissociate upon induction of certain forms of genotoxic stress, such as hydroxyurea treatment (Emili, Schieltz et al. 2001, Hu, Alcasabas et al. 2001, Jiao, Seeger et al. 2012). Disassociation of the complex was not observed for all genotoxic agents (Jiao, Seeger et al. 2012), suggesting a differential regulation of the complex in response to distinct forms of stress. Rad53 competes with histones and chaperones for binding to ASF1 (Jiao, Seeger et al. 2012). The ASF1-Rad53 could for example enable the recruitment of ASF1 at DNA damage sites to mediate chromatin accessibility and reassembly, or on the other hand keep Rad53 inactive in absence of stress. Studies introducing

mutations of H3K56 also suggested that the role of ASF1 in DNA repair might be linked to H3K56Ac (Masumoto, Hawke et al. 2005, Recht, Tsubota et al. 2006). In humans, however, an equivalent interaction with DNA damage checkpoint proteins has not been identified.

In a study exploiting the SNAP system to monitor de novo deposition of histones after UV damage, depletion of ASF1 did not affect H3.3 accumulation at damaged site while HIRA depletion did, suggesting that ASF1 is not essential for chromatin assembly in this context (Adam, Polo et al. 2013). Interestingly, however, ASF1 forms a complex with the TONSL-MMS22L complex and MCM2 in the soluble pool (Saredi, Huang et al. 2016). TONSL is required for repair of DNA damage caused by replication (Duro, Lundin et al. 2010, O'Connell, Adamson et al. 2010, O'Donnell, Panier et al. 2010, Piwko, Olma et al. 2010). TONSL recognizes the H4K20me0 modification present specifically on new histones, thereby associating with post-replicative chromatin to facilitate subsequent repair if required (Saredi, Huang et al. 2016). Its interaction with ASF1 and MCM2 may provide means to recruit TONSL to replicated chromatin.

#### **2.3.4. Restoring chromatin after the replication fork**

While coordination of de novo deposition and recycling pathways is needed to ensure reassembly of nucleosomes on newly synthesized DNA with a density that compares to the preexisting one, this can be unbalanced and additional steps are required to reestablish the epigenetic landscape in terms of histone modifications and associated factors. Recent studies have provided valuable insight into the maturation of nucleosome positioning and restoration of histone post-translational modifications.

Combination of purification of newly synthesized DNA exploiting biotin-dUTP, siLac labeling (stable isotope labeling with amino acids in cell culture) to distinguish parental from new histones, and mass spectrometry allowed the monitoring of the presence of histone post-translational modifications on newly synthesized DNA (Alabert, Bukowski-Wills et al. 2014, Alabert, Barth et al. 2015). First, histone modifications are transferred on nascent DNA with parental histones and therefore diluted by two. Then, they are progressively reestablished on new histones until reaching the original state within one cell

cycle. This can occur in two modes: gradual modifications of new histones over 2 to 24 hours for most histone marks, or modification of both parental and new histones over several cell generations in the case of H3K9me3 and H3K27me3. In *Drosophila* S2 cells, newly synthesized DNA was purified upon incorporation and biotinylation of the modified nucleotide ethynyldeoxyuridine (EdU), then digested with Micrococcal nuclease (MNase) and sequenced, allowing mapping of nucleosome positioning on nascent DNA (Ramachandran and Henikoff 2016). Interestingly, the authors found that nucleosome positioning at enhancers and promoters immediately following DNA synthesis was blurred compared to steady state. One hour later, however, this positioning was almost fully recovered. This indicates that nucleosome positioning after passage of the replication fork is not completely identical to positioning before passage of the fork, but is restored within one hour of chromatin maturation. Strikingly, upon depletion of CAF-1, while the overall number of nucleosomes is decreased, their positioning is more clearly defined, similarly as in steady state, than when the major subunit of CAF-1 is present. This suggests that blurred nucleosome positioning is due to the deposition of new histones. The nucleosome profile upon CAF-1 depletion is likely representative of nucleosomes formed using recycled parental histones, suggesting that histone recycling would occur precisely at the original position, unlike de novo deposition. Furthermore, in light of these results in addition to previous arguments, it seems unlikely that CAF-1 is solely involved in parental histone recycling, or at least that CAF-1-independent pathways exist to recycle parental histones. Chromatin remodelers can slide nucleosomes and are essential factors for nucleosome positioning (Ramachandran, Ahmad et al. 2017). In yeast, nucleosome positioning is also transiently affected upon passage of the replication fork, although it is reestablished much faster (Vasseur et al. 2016). This reestablishment is dependent on transcription and the Hir complex. In yeast, human and *Drosophila*, the remodelers ISW1, CHD1, INO80 and BRM have been implicated in reshaping chromatin after the replication fork (Poot, Bozhenok et al. 2004, Cairns 2009, Alabert, Bukowski-Wills et al. 2014, Ramachandran and Henikoff 2016, Yadav and Whitehouse 2016).

## **2.3.5. Barriers to replication**

### ***2.3.5.1. DNA secondary structures***

Progression of the replication fork can be impaired by a number of factors, either in normal or stress conditions (reviewed in (Svikovic and Sale 2017)). Single-stranded DNA can form secondary structures such as G-quadruplexes (G4) in G-rich genomic regions (Gellert, Lipsett et al. 1962). Such structures can potentially block DNA polymerases. In chicken DT40 cells, DNA polymerase REV1 is important for replication of DNA damage sites, suggesting a role for this protein in DNA damage tolerance at the replication fork (Edmunds, Simpson et al. 2008, Jansen, Tsaalbi-Shtylik et al. 2009). Interestingly, in absence of REV1, the presence of a G4 on the DNA template leads to loss of parental histones downstream of the G4 location (Sarkies, Reams et al. 2010, Sarkies, Murat et al. 2012, Schiavone, Guilbaud et al. 2014). This could be due to a physical uncoupling of helicase and polymerase progression caused by polymerase block at the G4 site. Parental histones evicted by the helicase would no longer directly transfer to newly synthesized DNA due to the loss of proximity. This, in turn, can have implications for local histone modifications and transcriptional state.

### ***2.3.5.2. Replication stress***

Perturbations at the replication fork also occur when inducing replication stress. Replication stress is a general expression used to refer to impediments to DNA replication. This includes the use of drugs that impair the replication machinery. For example, hydroxyurea (HU) or aphidicolin impair DNA polymerase progression by suppressing the nucleotide pool or inhibiting polymerases. Similarly as for G4 replication, this can lead to an uncoupling of the helicase and the polymerase and, therefore, can impact histone management at the replication fork. Upon treatment with HU, histones carrying parental modifications accumulate with ASF1 in the nucleus (Groth, Corpet et al. 2007, Jasencakova and Groth 2010). After removal of HU, this pool disappears, suggesting that parental histones are redeposited randomly in chromatin. Increasing studies have started considering replication stress as a hallmark of cancer (Halazonetis, Gorgoulis et al. 2008), proposing that replication stress is

one of the main causes of genome instability in cancer (reviewed in (Macheret and Halazonetis 2015)). In tissue culture, overexpression of oncogenes can activate replication stress checkpoints (Bartkova, Rezaei et al. 2006, Di Micco, Fumagalli et al. 2006), and, in nontransformed cells, leads to the appearance of single-stranded DNA, suggesting uncoupling of helicase and polymerase (Cimprich and Cortez 2008). DNA combing approaches provided further insight into the effect of oncogene overexpression at replication forks, as replication fork speed, symmetry and termination, as well as interorigin distance were impaired (Bensimon, Simon et al. 1994, Bartkova, Rezaei et al. 2006, Di Micco, Fumagalli et al. 2006, Bester, Roniger et al. 2011, Jones, Mortusewicz et al. 2013, Srinivasan, Dominguez-Sola et al. 2013, Costantino, Sotiriou et al. 2014). In this context, electron microscopy allowed detection of aberrant DNA structures (Neelsen, Zanini et al. 2013). Some fragile genomic regions are particularly sensitive to replication stress. Oncogene overexpression leads to deletions or loss of heterozygosity in such regions, similarly as treatment with HU or aphidicolin (Di Micco, Fumagalli et al. 2006, Arlt, Mülle et al. 2009, Arlt, Ozdemir et al. 2011). Strikingly, these fragile regions are often targeted in precancerous lesions and cancers (Bartkova, Horejsi et al. 2005, Gorgoulis, Vassiliou et al. 2005, Tsantoulis and Gorgoulis 2005, Di Micco, Fumagalli et al. 2006). How oncogenes induce replication stress is unclear, but could involve origin licensing and firing deregulation, or replication-transcription interference. Interestingly, a recent study showed that oncogenes could activate dormant origins (Macheret and Halazonetis 2018). These origins locate in transcribed genes, where active transcription usually hinders origin activation, and are prone to fork collapse and DNA double-strand breaks as a consequence of replication-transcription collisions.

### **2.3.5.3. *Telomeric regions***

Telomeres are considered as fragile sites and are a challenge for replication (O'Sullivan and Almouzni 2014). Due to their G-rich composition, they are prone to DNA secondary structure formation including G4, forming a first obstacle to replication. As a consequence, replication forks frequently collapse at telomeres and feature increased DNA damage. Specialized factors are involved in resolving

G-quadruplexes at telomeres, including ATRX, binding factor of the histone chaperone DAXX. The ATRX-DAXX complex is recruited to telomeric repeats and can resolve G-quadruplexes, while DAXX can mediate chromatin assembly (O'Sullivan and Almouzni 2014). Importantly, ATRX and DAXX mutations are associated with cancers that use the Alternative Lengthening of Telomeres (ALT) pathway. 5-15% of cancers feature the ALT pathway, an alternative pathway to telomerase. Strikingly, depletion of ASF1 (both ASF1 and ASF1b) can lead to the induction of ALT in several cell lines with long telomeres (O'Sullivan, Arnoult et al. 2014). This finding provided means to artificially trigger ALT for the first time – enabling more detailed study of its specific features -, but also highlighted the importance of proper histone management at fragile genomic sites. A possible explanation is that absence of ASF1 impairs replication fork progression, favoring the formation of DNA secondary structures and DNA damage. When this occurs over long enough genomic regions, for example at long telomeres, this may trigger the ALT pathway as a response to DNA damage.

### **3. Implications of histone inheritance or loss during replication**

Complex mechanisms involving the replication machinery, histone chaperones and chromatin remodelers can transfer parental histones to newly synthesized DNA and, in turn, daughter cells. This mechanism for the transmission of parental histone variants and their post-translational modifications is central to understand how to reestablish the parental epigenetic state. Here, we describe the implications of histone recycling for cell function, cell fate and disease.

#### **3.1. Epigenetic memory of transcriptional states**

Loss of parental histones at replication sites leads to local loss of both histone variant and histone modification distribution. However, whether this actually impairs the reestablishment of the epigenetic landscape, or more generally whether this impairs epigenetic memory, is debated. Are parental histones a vector of epigenetic memory? Indeed, while the transmission of histone variants and their marks would be a convenient way to maintain chromatin information

during replication and, as a consequence, the transcriptional status of genes, one could imagine other pathways to reestablish variants and marks at the right place in the genome even on a bare template, such as histone modifying enzymes and histone chaperones recruited and/or maintained at specific genomic loci. Overall, this does not seem to be the case in most eukaryotic organisms, although it was suggested in *Drosophila*, where a group observed the loss of methylated histones during DNA replication, reestablished later, thereby bypassing the need for parental histone or parental histone modification maintenance (Petruk, Sedkov et al. 2012, Petruk, Black et al. 2013). However, this finding is controversial and may reflect issues of detection. On the contrary, another study in *Drosophila* showed that introduction of a H3K27 mutation led to a progressive phenotype due to progressive loss of the mark, and not a drastic one as would be expected if the mark was erased or lost at each round of replication (Pengelly, Copur et al. 2013). In humans - as well as in yeast (Radman-Livaja, Verzijlbergen et al. 2011)-, parental histones are recycled on newly synthesized DNA and mechanisms exist to propagate modifications on new histones based on parental histones (Alabert, Bukowski-Wills et al. 2014, Alabert, Barth et al. 2015), suggesting that maintenance of the epigenetic landscape during cell division relies, at least in part, on parental histone recycling.

Experiments in various organisms monitoring histone modifications or histone variants over several cell generations are in line with this model that parental histones are a vector of epigenetic memory and that interfering with the recycling of histone variants and modifications can impact gene expression. First, treating cells with trichostatin A (TSA) or valproic acid, which inhibit deacetylase activity, leads to hyperacetylation of histones during several cell divisions, even after removal of the drug, indicating the memory of histone-based information (Ekwall, Olsson et al. 1997, VerMilyea, O'Neill et al. 2009). In *X. laevis*, as previously mentioned, H3.3 is required for the epigenetic memory, over 24 cell generations, of the active state of the MyoD gene upon nuclear transplantation of somatic nuclei in embryos, and this relies on the K4me3 modification of H3.3 (Ng and Gurdon 2008). Overall, while it may not be the case for all transcription-associated histone modifications, transmission of H3K4me3 and the H3.3 variant could participate in the transmission of the transcriptional status of specific loci,

and loss or gain of this information could shut down or activate gene expression over several generations.

Recycling parental histones is also important for epigenetic memory of heterochromatin and gene repression. The case of H3K27me3 and H3K9me3 is informative. As mentioned previously, the pathways that propagate these marks both rely on a “reader-writer” model: histone-modifying enzymes (mainly EZH2 and Suv39h respectively) are recruited to target sites via preexisting marks (or via proteins bound to preexisting marks, such as HP1 for H3K9me3) and then impose the marks on neighboring histones. This provides a strong framework for preexisting marks to serve as a template to propagate heterochromatic regions over cell generations. Although de novo establishment can also occur, parental histone recycling can provide the means to perpetuate heterochromatic regions over cell generations. In mouse cells, targeting HP1 to a reporter locus established an artificial H3K9me3 domain de novo (Hathaway, Bell et al. 2012). This domain was inherited through several cell divisions. Importantly, histone turnover competed with this maintenance mechanism to determine the boundaries of the domain, suggesting the dependence on parental histone recycling for inheritance of the heterochromatic status. A similar model was proposed for the maintenance of H3K27me3 domains (reviewed in (Margueron and Reinberg 2010), (Margueron, Justin et al. 2009)). However, de novo establishment of the mark could be achieved in embryonic stem cells: depletion of PRC2 first led to loss of the modification, but could then be rescued by reintroducing the factor, bypassing the need of a parental histone template (Hojfeldt, Laugesen et al. 2018). This may be due to residual factors or RNAs localized in these regions, or possibly other histone marks. Importantly, this was observed in embryonic stem cells, therefore it remains possible that inheritance of H3K27me3 is required during a differentiation process. In *C. elegans*, H3K27me3 and PRC2 are important to transmit repressive memory across generations of cells and even individuals (Gaydos, Wang et al. 2014). In *Drosophila*, H3K27me3 can similarly contribute to propagating the OFF state of Hox genes (Coleman and Struhl 2017), while in this system the repressive DNA regulatory elements are perpetually required, indicating that H3K27me3 is not sufficient to maintain repression (Laprell, Finkl et al. 2017).

Taken together, these data show that parental histone recycling is essential for the memory of epigenetic states. Yet, to what extent recycling is required for domain maintenance is an interesting question. Indeed, cells can likely tolerate some loss of histone-based information while still being able to reestablish proper domains. How robust a domain is likely relies in part on its size, and large domains can be maintained without full recycling of histone-based information (Dodd, Micheelsen et al. 2007, Ramachandran and Henikoff 2015). However, small domains, such as promoters where histone marks are sometimes present on only a few nucleosomes, may not be able to afford any parental histone loss and may even use alternative recycling methods, such as H3-H4 tetramer splitting as detected for H3.3 (Xu, Long et al. 2010, Huang, Zhang et al. 2013), to maintain information on both daughter strands.

### **3.2. Nuclear organization**

Large-scale recycling of histones can in turn potentially impact major nuclear domains, including centromeric and pericentromeric regions, telomeres, nucleoli or the nuclear periphery. Indeed, extensive work suggests a link between chromatin and nuclear organization. The nuclear membrane is a good example. Lamins are filament proteins that form the inner nuclear membrane (reviewed in (Dittmer and Misteli 2011)). Direct or indirect interactions between several types of lamins (B, C, Dm0) and chromatin have been identified, including histones H3, H4 and HP1alpha and beta, suggesting interplay between the two entities (Montes de Oca, Andreassen et al. 2011, Hirano, Hizume et al. 2012, Camozzi, Capanni et al. 2014). Importantly, lamins also tether DNA damage response factors and transcription factors to the nuclear periphery, suggesting that the nuclear membrane can serve as a platform to regulate chromatin dynamics and gene activity. Importantly, heterochromatin locates at the nuclear periphery, likely through redundant tethering mechanisms. First, the factor PRR14 associates with the nuclear lamina and with HP1 (Poleshko, Mansfield et al. 2013). Furthermore, Lamin B Receptor (LBR) – a lamin B binding partner – interacts with HP1, providing additional means to connect heterochromatin to the nuclear periphery (Olins, Rhodes et al. 2010). Connections have also been found between prelamin A - precursor protein of lamin A -, HP1, LAP2alpha and

BAF, two lamin-associated factors (Camozzi, Capanni et al. 2014). Mutations or misregulation of lamins or lamin-associated factors give rise to a class of disease termed laminopathies (reviewed in (Camozzi, Capanni et al. 2014)). As a consequence of their lamin-related defects, cells of laminopathy patients feature aberrant nuclear shapes as well as heterochromatin defects. In cells that do not express LBR or lamin A/C, heterochromatin locates in the nuclear interior, highlighting the importance of the nuclear envelope to tether heterochromatin at the periphery (Solovei, Wang et al. 2013). This illustrates how defects in factors essential for the nuclear structure and organization deeply impact the state of chromatin.

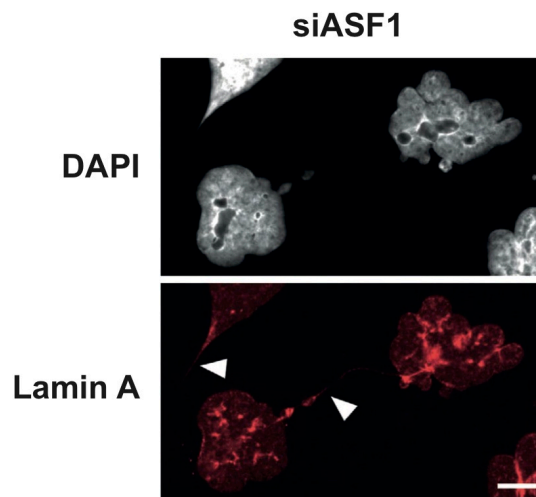


**Figure 14: ASF1 depletion leads to abnormal nuclear shape.**

Immunofluorescence analysis of DAPI and Lamin A staining in Hs578T cells treated for 48h by RNA interference against ASF1a and ASF1b. Arrowheads mark DNA bridges. Scale bar is 10 mm. From Corpet et al. 2011.

Conversely, several studies provide evidence that chromatin alterations impact nuclear organization. Upon ASF1 depletion in HeLa and U2OS cell lines, cells feature abnormal nuclear shapes and mitotic defects (Corpet, De Koning et al. 2011) (Figure 14). This is also seen upon depletion of other chromatin factors, such as subunits of CAF-1 (p60 and p48) (unpublished data). Taken together, these observations imply that disturbing chromatin structure can disorganize the nuclear membrane. Yet, by which mechanisms this is achieved remains unclear.

## **3.3. Cell fate**

### **3.3.1. Asymmetric division**

Redistributing parental histones randomly between daughter strands during replication ensures equal distribution of histone-based information, resulting in two daughter cells identical to the parent cell. Differentiation, however, requires cell fate change. DNA replication provides a window of opportunity to create two epigenetically asymmetric daughter strands, resulting in asymmetric cell division and, in turn, distinct cell types. For example, in the mouse muscle, satellite cells, which are the major producer of myoblasts, divide asymmetrically upon replication (Shinin, Gayraud-Morel et al. 2006, Rocheteau, Gayraud-Morel et al. 2012). In pulse-chase experiments using incorporation of bromodeoxyuridine (BrdU), a subpopulation of cells retain selectively labeled DNA strands, showing that DNA strands are not treated in an identical manner. The self-renewal factor Numb also selectively segregates to one of the daughter cells. This asymmetric process ensures the continuity of a lineage of stem cells, while still producing differentiated cells. These studies monitor asymmetric division of the DNA template. Whether histones are asymmetrically recycled and deposited during this asymmetric division of mouse muscle satellite cells remains to be investigated.

Work in *Drosophila* male germline stem cells also provides evidence of asymmetric division during differentiation and describes the fate of histones in this context (Fuller and Spradling 2007). Monitoring parental versus new histone segregation during germline stem cell division showed that parental histone H3 specifically segregated to the new germline stem cell, while new histones H3 segregated to the gonialblast meant for differentiation (Tran, Lim et al. 2012, Tran, Feng et al. 2013). This mechanism seems mediated by the histone modification H3T3P imposed specifically on parental histones and alteration in this modification leads to differentiation defects (Xie, Wooten et al. 2015).

### **3.3.2. Histone chaperones as a safeguard of cell identity?**

It is clear that chromatin organization regulates many different aspects of the genome, from its expression to its nuclear localization, over several cell generations and, therefore, is a pillar of cell identity. Chromatin organization is modulated during development to determine cell fate; in turn, by manipulating chromatin organization, we may be able to impact cell fate. Interestingly, two recent studies highlighted the role of CAF-1 in this context (Cheloufi, Elling et al. 2015, Ishiuchi, Enriquez-Gasca et al. 2015). Ishiuchi et al. showed that downregulation of CAF-1 enabled the reprogramming of mouse embryonic stem cells into cells resembling 2-cell-stage embryos (2C-like cells), providing the first evidence of reprogramming into totipotency. In mouse fibroblasts, Cheloufi et al. performed a screen and identified CAF-1 as a chromatin factor facilitating cell reprogramming into induced pluripotent stem cells (iPSCs). CAF-1 depletion decreased heterochromatin domains, enabling transcription factor-induced activation of pluripotency genes. Interestingly, the H3K9 methyltransferase SETDB1 was also identified in this screen, highlighting the importance of heterochromatin integrity for cell identity maintenance. Furthermore, a recent study investigated the role of the histone methyltransferase Suv39h1, responsible for H3K9me3, into lineage commitment during T lymphocytes differentiation (Pace, Goudot et al. 2018). The authors showed that Suv31h1-defective T lymphocytes feature defects in silencing of genes related to stemness and memory, increasing their reprogramming capacity. Conversely, ASF1a has been reported to be necessary for maintenance of pluripotency and cellular reprogramming (Gonzalez-Munoz, Arboleda-Estudillo et al. 2014). Considering that ASF1a and ASF1b are involved in multiple pathways, the role of ASF1 in differentiation could be different from CAF-1. Yet, whether depletion of both isoforms ASF1a and ASF1b facilitates cellular reprogramming remains unknown. Taken together, these studies show the importance of chromatin for lineage commitment, and provide evidence that chromatin can be targeted to modulate cell plasticity.



# Question

---



DNA replication provides an opportunity to maintain or change the chromatin landscape. Parental histone recycling is an essential aspect to explore when considering how to ensure transmission of histone-based information, yet how parental histones are handled at the replication fork remains an elusive mechanism. During the course of my PhD, I have tried to address this fundamental question:

### **How are parental histones H3.1 and H3.3 recycled during replication?**

To this end, I focused on two aspects:

1. How do the histone variants H3.1 and H3.3 distribute throughout replication?

In order to investigate how parental H3.1 and H3.3 behaved during replication, I first needed to gain a better view of their distribution throughout the cell cycle, with a particular focus on S phase. I studied H3.1 and H3.3 distribution in the nuclear space.

2. What is the role of ASF1 in the recycling of parental H3.1 and H3.3?

ASF1 was a prime candidate to participate in H3.1 and H3.3 recycling. I directly tested its involvement by monitoring the impact of its depletion on parental histone recycling at replication sites.



# Results

---



During my PhD, I have tried to gain a better understanding of parental histone recycling during DNA replication. I have obtained a series of results, which I summarized in a manuscript, currently under revision for Nature Communications, entitled “High resolution visualization of H3 variants during replication reveals their controlled recycling”.

## 1. Strategy and methodology

Here is a brief overview of the technological approach (summarized in Figure 15), followed by the manuscript.

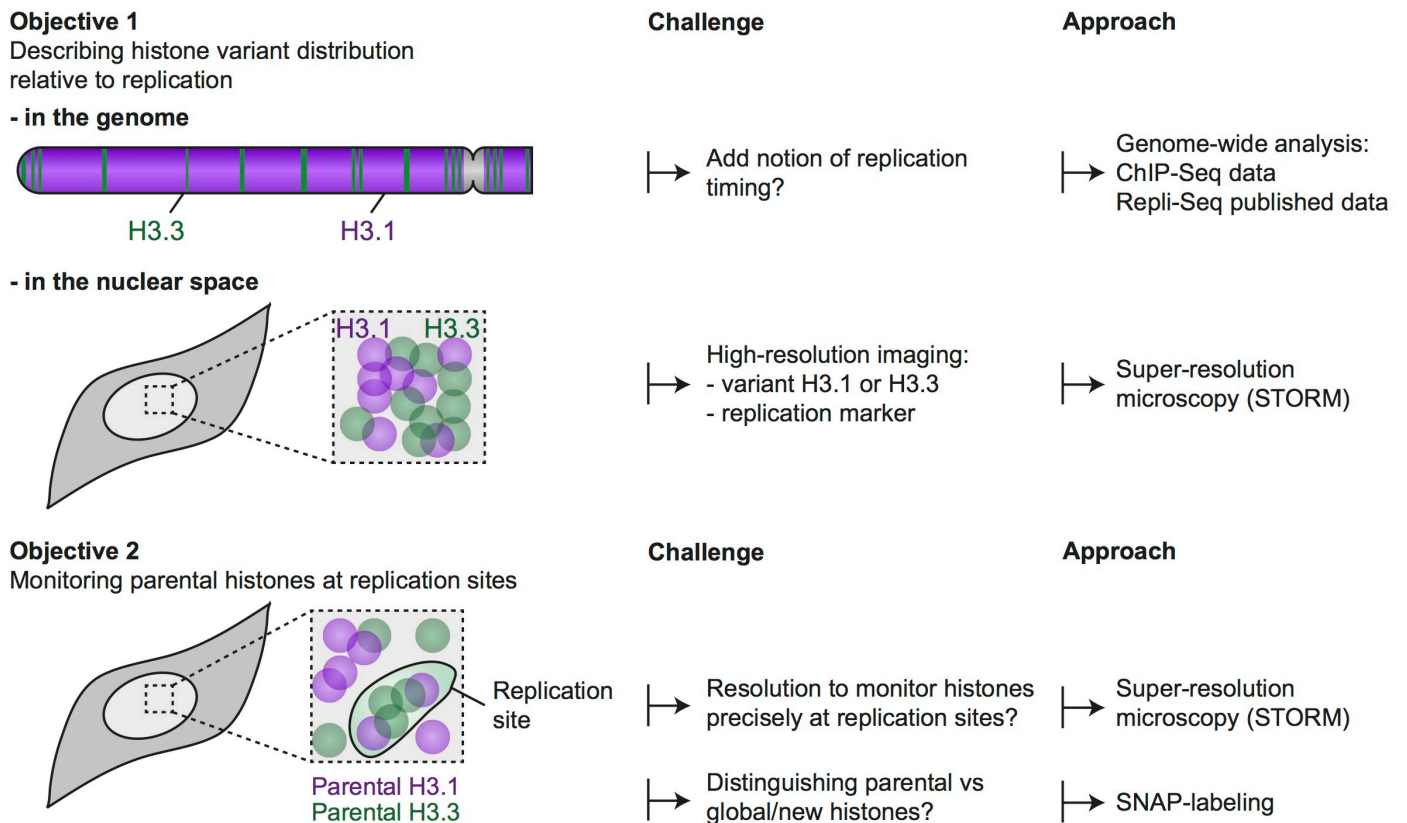


**Figure 15: Experimental approach.**

## **1. How do the histone variants H3.1 and H3.3 distribute throughout replication?**

In order to describe the distribution of H3.1 and H3.3 relative to replication timing, we tried to gain a genomic and spatial view by using (i) a genome-wide analysis and (ii) an imaging approach.

### **Genome-wide distribution of H3.1 and H3.3**

First, Alberto Gatto, bioinformatician in our lab, performed a genome-wide analysis of H3.1 and H3.3 distribution using ChIP-Seq data obtained by Audrey Forest and Jean-Pierre Quivy. Alberto used published Repli-Seq and Nascent RNA-Seq data to analyze H3.1 and H3.3 distribution relative to replication timing and transcriptional activity.

### **Spatial distribution of H3.1 and H3.3**

Second, in order to assess the 3D configuration of H3.1 and H3.3 in the nucleus, I used a microscopy approach. I aimed to visualize simultaneously H3.1/3 and newly synthesized DNA. For the visualization of nascent DNA, I used the modified thymine 5-ethynyl-2'-deoxyuridine (EdU), which is incorporated into newly synthesized DNA when added to the culture medium. This allowed both the identification of replicating cells and the visualization of replication sites. For histone visualization, and considering the next steps of my project, I used a cell line expressing SNAP-tagged H3.1 or H3.3 (see 2.). Concerning the choice of the microscopy approach, I chose a super-resolution microscopy technique in order to visualize histones at replication sites with high resolution. This was important to characterize the 3D configuration of H3.1 and H3.3 beyond what we had previously described with standard microscopy techniques, but also was required for the next step of my project, which consisted in quantifying parental histones at replication sites (see 2.).

## 2. What is the role of ASF1 in the recycling of parental H3.1 and H3.3?

To address the question of the recycling of parental H3.1 and H3.3 during DNA replication, I was faced with a dual technological challenge: (i) to distinguish parental histones from global or new histones and (ii) to gain access to a sufficient resolution to visualize histones precisely at replication sites.

### Specific labeling of parental H3.1 or H3.3

First, in order to distinguish parental histones from global or new histones, I used SNAP-tag labeling, a well-characterized system in our lab (Figure 16) (Keppler et al. 2004, Jansen et al. 2007, Ray-Gallet et al. 2011). In brief, the SNAP-tag can bind covalently to a benzylguanine coupled to a fluorescent or nonfluorescent dye. In a cell line expressing the protein of interest fused to a SNAP-tag - for example H3-SNAP -, a quench step blocks available H3-SNAP with a nonfluorescent dye; a chase step allows synthesis of new available H3-SNAP; and a pulse step labels available H3-SNAP with a fluorescent dye (such as TMR).

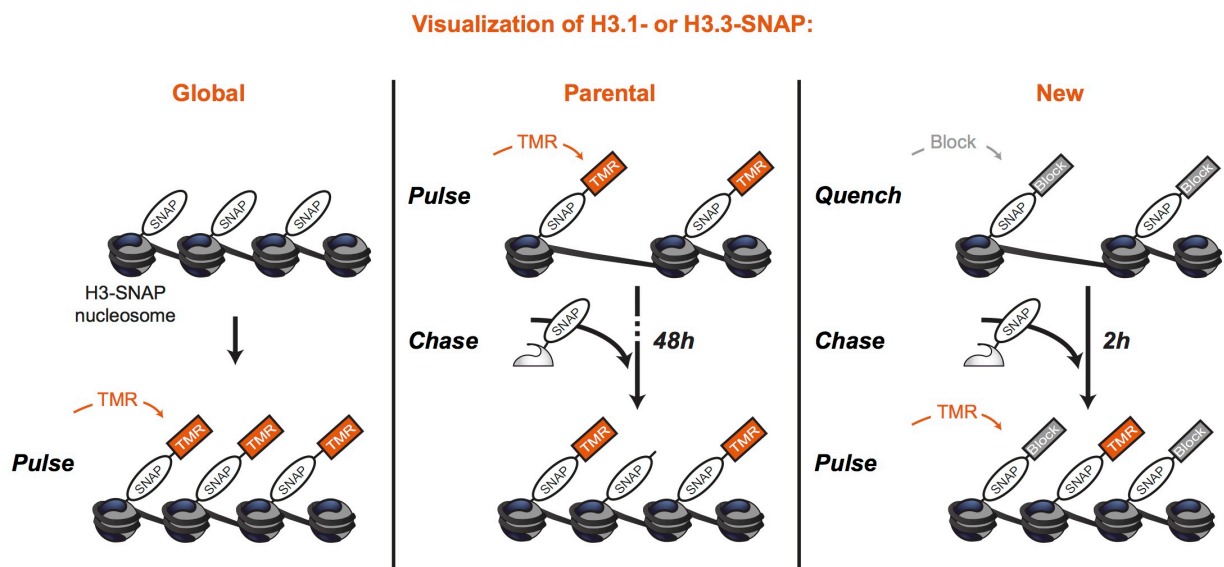


**Figure 16: SNAP-based labeling principle and de novo histone H3 deposition assay.**

Histone H3 is fused to the SNAP-tag, a 20-kDa mutant of the DNA repair protein O6-alkylguanine-DNA alkyltransferase that reacts specifically and rapidly with benzylguanine derivatives, leading to irreversible covalent labeling of the SNAP-tag with a synthetic probe. Specific labeling of global, parental, or new histones in stably expressing H3.1- or H3.3-SNAP cells is based on a pulse, pulse-chase, or quench-chase-pulse experiments, respectively. The quench step labels

parental (preexisting) H3-SNAP with a nonfluorescent SNAP-tag substrate, the chase step allows the synthesis and deposition of new H3-SNAP, and the pulse step labels only the new H3-SNAP with a red fluorescent SNAP-tag substrate (TMR). A triton extraction before fixation of the cells eliminates soluble histones in order to enrich for the nonsoluble, labeled H3-SNAP that contain histones stably bound to chromatin.

Combinations of these three steps allow the specific labeling of (i) global histones (pulse), (ii) parental histones (pulse-chase) or (iii) new histones (quench-chase-pulse). These protocols are more detailed in a method chapter I had the opportunity to write in collaboration with other members of the team entitled: “Functional Characterization of Histone Chaperones Using SNAP-Tag-Based Imaging to Assess De Novo Histone Deposition” (see Annexe).

### High-resolution visualization of H3.1 and H3.3 at replication sites

Next, I needed a sufficient resolution to visualize histones precisely at replication sites. In epifluorescence microscopy images, histone signal locates in the entire nucleus. It is possible and informative to quantify the overall fluorescence intensity in the nucleus; however, in order to selectively visualize and quantify histones located precisely at replication sites, an increased resolution and adapted imaging analysis methodology are necessary. I used Stochastic Optical Reconstruction Microscopy (STORM) (Figure 17).

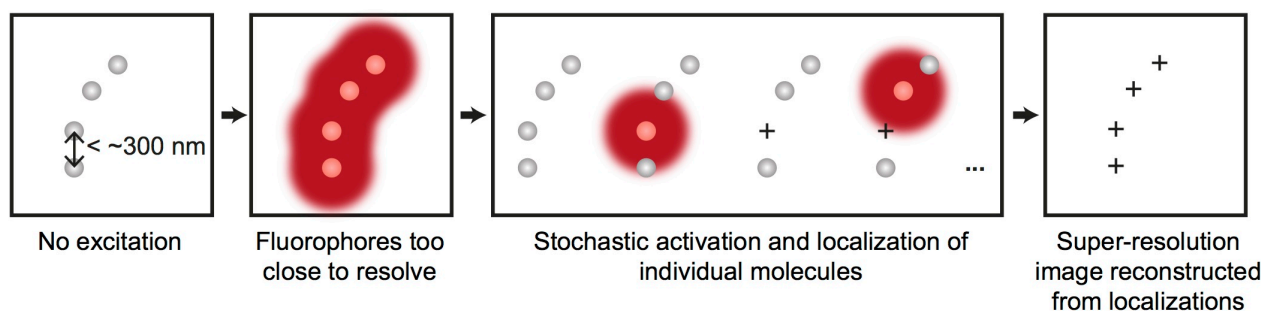


**Figure 17: Principle of Stochastic Optical Reconstruction Microscopy (STORM).**

Adapted from an image on the Huang Lab (UCSF, United States) website.

STORM relies on the property of some fluorophores to stochastically switch between a dark and a fluorescent state. In classical diffraction-limited microscopy, two neighboring fluorophores are fluorescent at the same time. If

they are too close to each other (under 250-300 nm), their fluorescent signals overlap creating a blurred image that cannot be resolved. In STORM microscopy, two neighboring fluorophores are fluorescent at different times. At a given time, only one fluorescent signal is detected, and the localization of the original molecule can be inferred, with a localization precision that can be as low as 10 nm. If we image a sample for a sufficient amount of time, we can accumulate enough localizations to reconstitute an image with a tenfold increase in resolution. In the context of my project, I developed a STORM protocol to visualize histones precisely at replication sites. This technique had never been used in our lab before, so I relied on published method papers as well as a fruitful collaboration with Guillermo Orsi in the team, and the collaborative Pic3i consortium at the Institut Curie. I was able to identify the right imaging conditions - buffer composition and acquisition settings -, use data processing algorithms developed by our collaborators, and write custom programs to analyze the data to answer my biological questions.

In summary, most of my PhD work consisted in approaching the biology of histone chaperones and variants by developing and exploiting the STORM methodology, and I had the opportunity to collaborate with other members of the team to integrate genomic information as well. The full results of this work are presented in the following manuscript.

## **2. Publication**

### **High-resolution Visualization of H3 Variants Reveals their Controlled Recycling**

Clément, C., G. A. Orsi, A. Gatto, A. Forest, B. Hajj, J. Miné-Hattab, M. Garnier, Z. A. Gurard-Levin, J. P. Quivy and G. Almouzni

In revision, Nature Communications

## Title

High-resolution visualization of H3 variants during replication reveals their controlled recycling

## Authors

Camille Clément<sup>1,2</sup>, Guillermo A. Orsi<sup>1,2</sup>, Alberto Gatto<sup>1,2</sup>, Ekaterina Boyarchuk<sup>1,2</sup>, Audrey Forest<sup>1,2</sup>, Bassam Hajj<sup>3</sup>, Judith Miné-Hattab<sup>2,4</sup>, Mickaël Garnier<sup>2,4</sup>, Zachary A. Gurard-Levin<sup>1,2,5</sup>, Jean-Pierre Quivy<sup>1,2</sup>, Geneviève Almouzni<sup>1,2</sup>

1. Institut Curie, PSL Research University, CNRS, UMR3664, Equipe Labellisée Ligue contre le Cancer, F-75005 Paris, France

2. Sorbonne Universités, UPMC Univ Paris 06, CNRS, UMR3664, F-75005 Paris, France

3. Institut Curie, PSL Research University, CNRS, UMR168, Laboratoire Physico-Chimie, F-75005 Paris, France

4. Institut Curie, PSL Research University, CNRS, UMR3664, F-75005 Paris, France

5. Current address: SAMDI Tech, Inc. Chicago, IL 60657, United States

Email corresponding author: [genevieve.almouzni@curie.fr](mailto:genevieve.almouzni@curie.fr)

## Abstract

DNA replication is a challenge for the faithful transmission of parental information to daughter cells, as both DNA and chromatin organization must be duplicated. Replication stress further complicates the safeguard of epigenome integrity. Here, we focus on the transmission of the histone variants H3.3 and H3.1 during replication. We follow their distribution relative to replication timing, first in the genome and, second, in 3D using super-resolution microscopy. We find that H3.3 and H3.1 mark early- and late-replicating chromatin, respectively. In the nucleus, H3.3 forms domains, which decrease in density throughout replication, while H3.1 domains increase in density. Hydroxyurea impairs local recycling of parental histones at replication sites. Similarly, depleting the histone chaperone ASF1 affects recycling, leading to an impaired histone variant landscape. We discuss how faithful transmission of histone variants involves ASF1 and can be impacted by replication stress, with ensuing consequences for cell fate and tumorigenesis.

## Introduction

The genome is partitioned into chromatin domains marked by distinct histone variants and their post-translational modifications<sup>1-3</sup>. A cellular identity profile has emerged on this basis. How this identity is maintained or changed throughout cell division is central to propagate a cell lineage or change cell fate<sup>4</sup>. Chromatin organization undergoes a major challenge during DNA replication. While nucleosomes ahead of the replication fork are disrupted, the corresponding parental histones along with their modifications are recycled on newly synthesized DNA. This process ensures the transmission of parental histone variants with their post-translational modifications<sup>5</sup>. In parallel, de novo deposition of new histones provides a complement to maintain nucleosomal density. While histone deposition occurs rapidly after passage of the fork, restoration of nucleosome positioning and histone post-translational modification profiles takes more time<sup>6,7</sup>. Therefore, it is key to explore how the timing and spatial orchestration of these events participate in maintaining or changing the epigenetic landscape. Notably, replication itself is constantly challenged, and replication stress - caused by secondary DNA structures, DNA damage, nucleotide pool imbalance or mutations in replication proteins - can have short or long term consequences for epigenomic stability<sup>8</sup>. In certain

cases, this can perturb repressive as well as active histone marks, leading to changes in gene expression patterns. Highlighting the potential impact of this phenomenon, replication stress has often been observed in cancer cells, at early stages of their transformation<sup>8,9</sup>.

To date, we have learnt a lot concerning de novo deposition of new histone variants via pathways involving dedicated histone chaperones<sup>10</sup>. Yet, how parental histone variants are handled to be recycled locally in either normal or stressed conditions remains unclear. To gain understanding into these questions, one must consider (i) their distribution in the genome relative to replication timing, (ii) their 3D spatial configuration in the nucleus relative to replication timing, and (iii) the factors involved in their recycling at replication sites in normal and stressed conditions.

The main supply of new histones during replication is provided by increased expression of the replicative histones H3, H4, H2A and H2B<sup>1</sup>. For histone H3, the replicative variants are H3.1 and H3.2<sup>1,2</sup>. In contrast, the H3.3 variant, constitutively expressed, is available throughout all phases of the cell cycle<sup>1,2</sup> and can replace H3.1 at genomic sites undergoing active nucleosome turnover. Consequently, H3.3 is enriched at gene bodies and DNA regulatory elements, suggesting a close association with transcriptional activity, while heterochromatin territories including pericentromeres, transposons and telomeres can also contain this variant<sup>11,12</sup>. Key histone chaperones are involved in de novo deposition of specific histone variants and guide their specific enrichment profiles in the genome<sup>13,14</sup>. The histone chaperone Chromatin Assembly Factor 1 (CAF-1) is specifically associated with H3.1<sup>13</sup> and is key for its deposition coupled to DNA synthesis<sup>15-18</sup>, favored through its interaction with Proliferating Cell Nuclear Antigen (PCNA)<sup>19,20</sup>. Throughout the cell cycle, the replacement H3 variant H3.3 is deposited in a DNA synthesis-independent manner by a complex comprising the histone chaperone Histone Regulator A (HIRA)<sup>12,13,21</sup>, or by the histone chaperone Death-Associated protein (DAXX)<sup>14</sup>. Finally, the H3-H4 chaperone Anti-Silencing Function 1 (ASF1)<sup>22</sup> associates with both H3.1 and H3.3 and has been implicated in their storage as well as histone hand-over for de novo deposition, working in concert with CAF-1 or HIRA respectively<sup>23-27</sup>.

In mammals, ASF1 exists as two paralogs, ASF1a and ASF1b<sup>28</sup>. In mice, loss of ASF1a is embryonic lethal, while ASF1b deficiency leads to viability but impaired fertility<sup>29</sup>, indicating that the two paralogs are not redundant during development<sup>28</sup>. In human cells, co-depletion of both ASF1a and ASF1b impairs replication fork progression<sup>30,31</sup>. Increasing evidence supports the view that ASF1 could be critical in parental histone recycling. ASF1 forms a complex with the MCM2 subunit of the MCM replicative helicase

via a histone H3-H4 bridge<sup>31-33</sup>. Proximity ligation assays enabled the visualization of a fraction of ASF1 at active replisomes<sup>33</sup>. Considering that a recent mass spectrometry study could not reveal the association of ASF1 with the active replicative helicase<sup>34</sup>, ASF1 would likely bind transiently to unload the MCM from parental histones and deliver them to the other side of the replication fork. While structural studies show that ASF1 interacts with an H3-H4 dimer<sup>35</sup>, parental H3-H4 dimers rarely mix with newly synthesized dimers<sup>36</sup>. In the current view, two ASF1 molecules are required to interact with both H3-H4 dimers while an additional step ensures the reassembly of the original tetramer. Importantly, upon hydroxyurea treatment, replication arrest is concomitant with an accumulation of ASF1 loaded with histones carrying post-translational modifications characteristic of parental histones<sup>31,37</sup>. These might be redeposited at unscheduled sites upon replication restart<sup>37</sup>. Although it remains unclear how replication stress affects the spatial distribution of parental histones, the importance of a tight control of histone recycling emerges as a central mechanism for the integrity of the epigenome<sup>8</sup>. The current model places ASF1 in a key position to recycle parental H3.3 and H3.1, yet its exact role and its contribution to maintaining a histone variant landscape needs to be elucidated.

Genome-wide analyses provide a view of how histone variants distribute in the genome. However, their genomic distribution relative to replication timing has never been investigated, contrasting with the extensive characterization of genomic replication patterns directly at the level of DNA<sup>38,39</sup>. Furthermore, advances in super-resolution microscopy have enabled considerable progress in the 3D visualization of either replication sites<sup>40-42</sup> - allowing the quantification of the number and size of single replicons in human and mouse cells<sup>40</sup> -, or histones. Indeed, recent studies visualized histones H2B in different cell types<sup>43,44</sup> and showed that their heterogeneous distribution and density correlate with the pluripotency state<sup>44</sup>. Furthermore, high-resolution visualization of histone post-translational modifications enabled the classification of stem cell states<sup>45</sup>, while imaging of the underlying DNA led to a quantitative description of the compaction levels of different chromatin domains<sup>46</sup>. Although the use of histone marks has traditionally enabled the classification of distinct chromatin states<sup>47,48</sup>, histone variants are lacking in this picture.

In this work, we exploited a dual approach to study histone variants relative to replication timing with a genome-wide analysis and in 3D using super-resolution microscopy. We combined two-color Stochastic Optical Reconstruction Microscopy (STORM)<sup>49,50</sup> - to visualize the histone variants H3.3 and H3.1 relative to replicated DNA - with the SNAP system<sup>12,51,52</sup> - to label specifically global or parental histones. With this

assay, we first visualized H3.3 and H3.1 globally at an unprecedented resolution. While both H3.3 and H3.1 clustered in space, we found a distinct spatial configuration for these variants. H3.3 formed spatial domains whose size was not affected by the cell cycle, but whose density decreased throughout S phase. Unlike H3.3, H3.1 formed domains whose size and density were cell cycle-dependent. We then specifically probed the recycling of parental histone variants. We aimed to perturb histone recycling by targeting (i) DNA itself at the replication fork by inducing replication stress and (ii) histone localization by depleting ASF1. First, we found that replication stress, induced by hydroxyurea, prevented the recycling of parental H3.1 within replicated DNA and impaired its spatial distribution around replicated DNA. Importantly, ASF1 depletion also affected the recycling of parental H3.1 and H3.3 at replication sites both in terms of quantity and spatial distribution. Most remarkably, upon ASF1 depletion, we observed a change in the spatial distribution of both H3.1 and H3.3 in late S phase, but only of H3.1 in early S phase. Considering the longstanding importance of replication timing for distinct functional events, we discuss the implications of our findings for the maintenance of epigenetic states.

## Results

### Genome-wide analysis of the H3 variant landscape

We first aimed to assess the genome-wide distribution of the H3 variants H3.3 and H3.1 relative to replication timing. For this, we performed ChIP-Seq to retrieve H3.3 and H3.1 nucleosomes in asynchronous HeLa cells stably expressing tagged H3.3 or H3.1. For each variant, we analyzed the input-normalized coverage at consecutive windows of 10 kb, using the  $\log_2$  ratio as a proxy for enrichment or depletion in a given region. Consistent with their dynamics, global H3.3 and H3.1 showed inverse genome-wide enrichment profiles (Figure 1A). H3.1 tended to accumulate in broad, megabase-sized chromosomal domains that displayed a proportional H3.3 depletion. Conversely, H3.3-rich regions were narrower and exhibited low H3.1 abundance relative to input.

To investigate the occupancy of both variants in relation to replication timing, we included in our analysis Repli-Seq data from Dellino et al<sup>38</sup>, in which replication sites were mapped in 6 different cell populations (sorted based on DAPI content) corresponding to consecutive S phase fractions ( $S_1$  to  $S_6$ , ranging from early to late replicating). We assigned each of the 10 kb windows to an S phase fraction (chosen as the fraction with the highest mean coverage of BrdU for that window). We evaluated the distribution of H3.3 and H3.1 in each S phase fraction (Figure 1B, C). We found that (i)

H3.3 is mainly enriched at early-replicating regions and depleted at late-replicating ones and (ii) its occupancy anti-correlates with the timing of replication. Conversely, H3.1 is more uniformly distributed and changes less markedly with replication timing. Late-replicating regions are nonetheless more enriched in H3.1 compared to early-replicating regions (with the exception of the S<sub>1</sub> fraction). Genomic regions associated with the S<sub>6</sub> fraction show the largest difference between the two variants.

Early-replicating regions tend to coincide with transcriptionally active, gene-rich domains, which are expected to be enriched in H3.3. To examine whether transcription alone could account for the association between histone variants and replication timing, we then integrated nascent RNA-Seq data from Liang et al<sup>53</sup> in our ChIP-Seq and Repli-Seq analysis. We classified the genomic windows into 4 categories based on the transcriptional activity (low, mid, high) or the absence of measurable activity (none). We then compared, for each expression category, H3.3 or H3.1 occupancy to replication timing, as measured by BrdU incorporation in the S<sub>1</sub> fraction compared to the average incorporation in all S phase fractions. As expected, H3.1 did not correlate with transcriptional activity (Supplementary Figure 1B) and the relation between H3.1 and replication timing was independent of transcription (Figure 1D, E). In agreement with previous studies, transcriptional activity associated with early replication and with higher H3.3 occupancy (Supplementary Figure 1A). Interestingly, however, the association between H3.3 and replication timing proved to be independent of transcriptional activity (Figure 1D, E). Therefore, transcriptional activity alone cannot explain the relationship between H3.3 occupancy and replication timing.

Overall, our approach combining ChIP-Seq, Repli-Seq and nascent RNA-Seq data (i) provides a distribution of H3.3 and H3.1 in the genome, (ii) shows that H3.3 is enriched in early-replicating chromatin, while H3.1 is enriched in late-replicating chromatin, and (iii) differences in transcription do not fully account for the opposite patterns of H3 variants. How do these findings translate into 3D spatial distribution and nuclear geography? Are they valid at the level of single cells? What are the dynamics of H3.3 and H3.1 that establish and maintain this histone variant landscape, in particular in S phase? To address these questions, we developed an assay to visualize histone variants and regions of replicated DNA using super-resolution microscopy.

### **STORM assay to visualize H3 variants and replication sites**

We combined histone monitoring with DNA synthesis labeling. For histones, we exploited two cell lines previously characterized in our laboratory, that stably express

SNAP-tagged H3.3 or H3.1<sup>12</sup>. The versatility of the SNAP-tag labeling system enables to monitor *in vivo* global, parental or new histones<sup>12,51,52</sup> (Figure 2A and Supplementary Figure 7A). For DNA synthesis, we used EdU labeling (later coupled with the fluorophore Alexa 647) and distinguished cells outside S phase, in early S phase and in mid/late S phase based on their typical patterns (Figure 2B, left). Of note, EdU only labels regions that are undergoing replication during the time of the EdU pulse. Therefore, EdU-negative regions comprise both previously replicated and unreplicated regions. Here, to achieve high spatial resolution and perform a quantitative analysis, we used 3D Stochastic Optical Reconstruction Microscopy (STORM), which allows the detection of single molecules<sup>49,50</sup>. We first performed a pulse experiment with EdU labeling and successfully reconstituted STORM images for global H3.3 and H3.1 in cells outside of S phase, in early S phase, and in mid/late S phase (Figure 2B, right, see also Figures 3B and 4B).

We first analyzed the histone signal. Consistent with confocal images, the STORM images showed a broad distribution of H3.1 and H3.3 throughout the nucleus, in cells outside of S phase, in early S phase, and in mid/late S phase (Figure 2B, Figure 3B), while reaching a resolution in the range of 40 nm. At this resolution, we observed that H3.3 and H3.1 distributed heterogeneously in the nucleus, forming groups of detections – reminiscent of those found for histone H2B<sup>44</sup>. To further analyze this signal in the distinct phases, we used a density-based clustering algorithm (DBSCAN) (Supplementary Figure 2A). This clustering method is based on the identification of regions with higher density for H3.3 and H3.1, which we designated as conglomerates (Supplementary Figure 3A and 4A). For each identified histone conglomerate, we measured two parameters: volume and density – which we calculated as the proportion of detections in the nucleus per volume and per conglomerate. We represented the distribution of these parameters for all conglomerates, in cells outside S phase, in early S and in mid/late S (see below).

We next examined the EdU signal. For cells outside of S phase, as expected, the EdU signal was low compared to cells in S phase reflecting background noise and possibly some EdU incorporation due to limited DNA damage (Figure 2B, right). For cells in S phase, we again applied the DBSCAN algorithm to define EdU clusters representative of regions of newly replicated DNA. Here, based on a recent super-resolution microscopy study of replication sites<sup>40</sup>, we chose experimental conditions yielding EdU clusters corresponding to several replicons, ensuring that we had enough histone detections within these clusters for quantitative analysis. In our 600 nm sections, we defined an average of respectively 94 and 82 regions of replicated DNA in early and mid/late S phase cells in the H3.3 cell line, and 122 and 69 in H3.1 (Supplementary Figure 2B), with

volumes in the range of  $1.5 \cdot 10^7 \text{ nm}^3$ , corresponding to a 300 nm diameter sphere (Supplementary Figure 2C). For an entire nucleus, this would approximately translate into 1000 and 900 replicated regions in early and mid/late S phase respectively for H3.3, and 1400 and 800 regions for H3.1, corresponding to about 5 replicons each<sup>40</sup>.

### **H3.3 conglomerates display cell cycle-dependent density**

Using our STORM-SNAP assay, we first aimed to monitor how the global distribution of H3.3 evolved throughout S phase (Figure 3A, B). As a first step, we analyzed all H3.3 conglomerates. H3.3 conglomerates had volumes in the range of  $4 \times 10^5 \text{ nm}^3$  (90 nm diameter). This compares to H2B regions as described by Ricci et al<sup>44</sup> (in the range of 80 nm). The distribution of these volumes was stable throughout S phase and outside S phase (i.e. distributions displayed variability but peaked at identical values and were unrelated to cell cycle stage) (Figure 3C, top, see also Supplementary Figure 4C). In contrast, the density of H3.3 conglomerates evolved throughout S phase, decreasing when progressing from early to mid/late S phase (Figure 3C, bottom, see the peak shift -33%, where "+" and "-" refer to increase and decrease, respectively). Cells outside of S phase displayed an intermediate density distribution. Of note, our assay includes a pre-extraction step to eliminate soluble histones. Although we cannot exclude that this treatment could potentially affect our observations, this is necessary to monitor nucleosomal/chromatin-bound histones. Furthermore, to verify that the changes observed in our analysis did not arise from a bias due to the clustering approach, we applied an independent partitioning method (Voronoi tessellation) to our data as described for the nucleoporin protein TPR<sup>54</sup>. We partitioned the signal into polygons such that each polygon contains a single detection, while their size is inversely proportional to local density (Supplementary Figure 3B). The distribution of polygon sizes confirmed that early S phase cells had more high-density regions than mid/late S phase cells (Supplementary Figure 3C).

As a second step, we conducted the analysis for H3.3 conglomerates near EdU clusters (under 200 nm from cluster center of gravity), thereby comparing conglomerates in early- and late-replicating chromatin at sites of DNA synthesis (Figure 3D, scheme). As in the previous analysis, the volumes of H3.3 conglomerates remained similar (Figure 3D, top), and their density decreased when progressing from early- to late-replicating regions (Figure 3D, bottom, see the peak shift -21%, and summary in Figure 3E).

### **H3.1 conglomerates change in volume and density in S phase**

Similarly, we exploited our assay and analytical method to monitor global H3.1 throughout S phase (Figure 4A, B). H3.1 conglomerates had volumes in the range of 3.5

to  $4.5 \times 10^5 \text{ nm}^3$ . When analyzing H3.1 conglomerate volumes in the whole nucleus, these were slightly larger in early S compared to outside S (+15% peak shift) (Figure 4C, top), in the same size range as the H3.3 conglomerates described above. Indeed, when we directly compared the volumes of H3.1 and H3.3 conglomerates, H3.1 volumes were slightly larger than H3.3 in early S phase (+16% peak shift), while it was the opposite for outside S and mid/late S (-11% and -18% peak shifts) (Supplementary Figure 4B). As these distribution shifts were modest, we looked more specifically at individual cells and refined our observation: H3.1 conglomerates seemed larger in early S than outside S, with intermediary volumes for mid/late (Supplementary Figure 4C). The volume of H3.1 conglomerates within EdU sites followed the same trend between early- and late-replicating chromatin (-13% peak shift) (Figure 4D, top), indicating that H3.1 conglomerates adopt larger volumes when coinciding with early-replicating chromatin. We then measured the density of H3.1 conglomerates and found an increase in mid/late compared to early S phase (+26% peak shift) (Figure 4C, bottom). Of note, the normalization by the total number of detections in the nucleus (Supplementary Figure 4A, right) may in part contribute to this finding. When comparing small surfaces in Voronoi tessellation analysis, we found that mid/late S phase cells had smaller surfaces than early S phase cells (Supplementary Figure 4D), confirming our clustering results. The density of H3.1 conglomerates near EdU sites was also increased in late- compared to early-replicating chromatin (+44% peak shift in mid/late compared to early) (Figure 4D, bottom, and summary in Figure 4E).

We next investigated how histone variants are maintained at sites of DNA synthesis.

### **Monitoring parental histone recycling using the SNAP system**

Our knowledge concerning how histone variants are recycled or discarded at sites of DNA replication remains very limited. To address this question, we labeled specifically parental histone variants using the SNAP system (Figure 5A, B). We used different chase times (0, 24 and 48 hours, corresponding to 0, 1 or 2 cell cycles) and measured the fluorescence intensity in whole nuclei using epifluorescence microscopy in order to monitor the decrease in the histone signal over several cell divisions (Figure 5C and Supplementary Figure 5). If parental histones were lost exclusively by S phase dilution, we would expect an exponential decay, i.e. 50% loss every cell cycle. Instead, we found that both H3.1 and H3.3 are lost at higher rates, consistent with additional replication-independent histone turnover. The increased loss of parental H3.3 compared to H3.1 from 0 to 24 hours is in line with our previous result that H3.3 marks early-replicating regions with higher turnover. We focused on a 48h-chase for the following experiments

for two reasons: (i) in our experimental conditions, it proved the minimum amount of time required for efficient siRNA depletion (see below), and (ii) a 48-hour chase ensured that we specifically examined parental histones without bias linked to cell-cycle variation, for both variants H3.1 and H3.3.

### **Hydroxyurea impairs local recycling of parental histones**

We next used our STORM assay to first monitor parental histones in a context where we expected local parental histone recycling to be affected. For this, we treated HeLa SNAP H3.1 cells with hydroxyurea (HU) for 30 minutes before fixation to uncouple helicase progression from DNA synthesis (Figure 6A). As expected, HU treatment caused reduced EdU signal (consistent with impaired replication) and the appearance of the single-stranded DNA-binding protein RPA at replication sites<sup>31</sup> (Supplementary Figure 6A). At the level of total nuclear fluorescence, we detected a slightly higher retention of parental H3.1 in the HU condition compared to the control, consistent with general replication arrest (Supplementary Figure 6B).

Because of the physical uncoupling between parental DNA unwinding and new DNA synthesis, parental histones disrupted ahead of the fork may not be recycled immediately after. To visualize this, we monitored parental H3.1 at EdU sites in HU-treated cells by STORM (Figure 6B). With low and more dispersed signal for parental histones in STORM images compared to global histones, our clustering approach was inappropriate. Instead we adopted a different strategy: we directly counted the number of parental H3.1 detections in replicated regions (Figure 6C). We normalized to the EdU signal to account for the fact that HU treatment blocks replication, as well as to the total number of H3.1 detections in the nucleus. As predicted, both in early and mid/late S phase, the amount of parental H3.1 decreased significantly in the HU condition compared to the control (-31% and -21% peak shift) (Figure 6D). This suggests that local perturbation of DNA at the replication fork inflicted by HU treatment impairs the local recycling of parental histones, leading to a loss of parental histones in regions of replicated DNA.

### **Hydroxyurea affects parental histone spatial distribution**

We next asked whether local loss of parental histones had further consequences for their spatial distributions around replication sites. To this end, we developed a method to describe the spatial distribution of histone detections (signal A) around replicated DNA (signal B) (histones vs EdU). We measured the number of histone or EdU detections in concentric regions centered at the gravity center of EdU clusters (Figure 6E). To validate this approach, we measured the spatial distribution of newly

synthesized H3.1 (quench-chase-pulse labeling) vs EdU, using data obtained after performing a quench-chase-pulse experiment (Supplementary Figure 7A, B). Unlike parental H3.3 and H3.1 signal located in the entire nucleus, newly synthesized H3.1 exhibits clear enrichment at EdU labeled-sites, as we previously described<sup>15</sup>, providing an ideal context to measure the distance between these two signals. We found that the distance of maximum enrichment between new H3.1 and replication sites centers was 200, 150, and 250 nm in early S phase, mid/late S phase in the interior, and mid/late S phase at the periphery (Supplementary Figure 7C, D). To validate these estimates with an independent approach, we adapted a function (termed m function) from a spatial economics study<sup>55</sup>. This function measures the enrichment between two signals, based on the distances between detections of signal A vs detections of signal B. We tested this on simulated data (Supplementary Figure 7E(i)), then applied it to the new H3.1 data (Supplementary Figure 7E(ii)). This analysis provided a similar estimate of the distance between new H3.1 and EdU as our approach, supporting its validity.

Next, we compared DNA that had been replicated at different times, aiming to detect expected changes in spatial distribution. We performed either a single EdU pulse, or an EdU pulse followed by a 30-minute chase (Supplementary Figure 8A). Using the DBSCAN clustering analysis, we detected larger replicated regions in the EdU pulse-chase than in the EdU pulse (Supplementary Figure 8C). This increase suggested that during the chase period, the organization of the replicated region evolved as a sign of chromatin maturation. We studied the spatial distribution of EdU vs EdU in each experiment, and detected a change towards higher distances in the EdU pulse-chase compared to the EdU pulse (Supplementary Figure 8B), consistent with the clustering result. We concluded that the changes detected in the spatial distribution indeed reflected biological changes, and that earlier-replicated DNA spatially spread further from the center of EdU clusters compared to more recently replicated DNA.

We then applied our method to study the effect of HU treatment on the spatial distribution of parental H3.1 (revealed by pulse-chase labeling) relative to EdU clusters. Upon HU treatment, we observed a clear change in the spatial distribution of parental H3.1 both in early and mid/late S phase (both at the nuclear periphery and interior) (Figure 6F). In all cases, we found that parental H3.1 redistributed at increased distances from replicated DNA following HU treatment, with H3.1 remoteness increased at a scale of hundreds of nanometers.

Overall, our results show that replication stress upon HU treatment not only leads to local loss of histone recycling, but also their unscheduled redistribution at distant nuclear loci, with a potential impact on the epigenomic landscape.

## **ASF1 depletion affects recycling of parental H3.3 and H3.1**

We next investigated which factors recycled histones during DNA replication. As ASF1 was a prime candidate, we performed pulse-chase experiments and downregulated ASF1 (both ASF1a and ASF1b) using small interfering RNA (siRNA) (Supplementary Figure 9A). As previously reported, ASF1 depletion led to slower cell cycle and abnormally shaped nuclei<sup>56</sup>. To check the general effect at a larger scale, we first performed this experiment in cells synchronized with a double thymidine block to verify cell cycle progression, and monitored the dilution of the parental H3.1 signal over two divisions using epifluorescence microscopy (Supplementary Figure 9B). We observed a decrease of the final (48h) to initial (0h) signal ratio in the siASF1 condition, suggesting that, over two divisions, ASF1-depleted cells retained parental H3.1 less efficiently than control cells, while we observed no change in the overall nucleosome density (Supplementary Figure 10).

Additionally, we performed immunofluorescence 48 and 72 hours after ASF1 depletion to assess the status of several H3 post-translational modifications typical for nucleosomal H3 in chromatin<sup>57</sup>. We performed this experiment in an asynchronous population and used confocal microscopy to monitor: euchromatic H3K4me3 and H3K36me3; and heterochromatic H3K27me3 and H3K9me3 (Supplementary Figure 9C). At this resolution, we did not observe changes in the distribution of the euchromatic marks upon siASF1, although the lack of a clearly defined pattern for these marks might mask subtle changes in distribution. In contrast, we observed a change in the pattern of H3K9me3 and H3K27me3 in ASF1 depletion conditions, with a more diffuse signal compared to the distribution of these marks at the nuclear and nucleolar periphery in control cells. We then refined our analysis with an increased resolution focusing on H3K36me3 and H3K9me3 using STORM analysis (Supplementary Figure 11A). We found that H3K9me3 formed domains, which decreased in density in the ASF1-depleted condition compared to the control (-46%), with no clear changes in volume (Supplementary Figure 11B). H3K36me3 domains, on the contrary, were unchanged in density, but decreased in volume (-40%) and were more numerous in the ASF1 knockdown (Supplementary Figure 11C, D). Of note, these marks are reestablished on new histones within one cell cycle<sup>7</sup>, and they feature different dynamics, and therefore cannot be used as a direct proxy for parental histones over long time periods. Overall, these data suggest that ASF1 depletion affects parental histone recycling at the scale of the entire nucleus, while leading to disorganization of histone post-translational modifications.

To evaluate how ASF1 depletion impacts global H3.1 and H3.3, we performed a pulse labeling experiment following siASF1 knockdown and detected H3.1 and H3.3 conglomerates (Supplementary Figure 12A). For both H3.1 and H3.3 conglomerates, S phase changes in volumes and densities followed similar trends in siASF1 cells and control cells, although siASF1 cells displayed more variability and less pronounced changes (Supplementary Figure 12B, C and 13). In particular, when focusing on sites of replicated DNA, the density of H3.3 conglomerates in early- vs late-replicating chromatin was less decreased in the ASF1-depleted condition (-13%) than in the control (-21%), while the density of H3.1 conglomerates increased (+35%) less than the control (+44%). We next aimed to test the effect of ASF1 depletion at sites of replicated DNA, in order to directly assess its involvement on parental histone variant recycling.

We focused on parental histones by performing a pulse-chase experiment after depleting ASF1 (Figure 7A, B), and used STORM imaging to measure the number of parental H3.3 or H3.1 detections at replicated regions (Figure 7C and Supplementary Figure 14D). As for the HU treatment, we normalized to the EdU signal to account for the fact that ASF1 depletion slows down replication. Strikingly, we found that, in early S phase, the amount of parental H3.3 and H3.1 decreased significantly in the ASF1-depleted condition compared to the control (-60% and -18% peak shift) (Figure 7D). H3.3 was more affected than H3.1, although we cannot rule out that this reflects a sampling effect rather than a biological difference. In mid/late S phase, we did not observe changes of this magnitude (Supplementary Figure 14A, B, C). However, it is important to note that our data analysis may be underestimating late S phase defects as we normalized to the total number of detections in the nucleus, which may be affected by early S phase ASF1-dependent defects.

These results show that ASF1 depletion leads to impaired retention of parental H3.3 and H3.1 at replicated regions most notably in early S phase (Supplementary Figure 17A). The similarity with our result in HU-treated cells suggests that ASF1 depletion affects local histone recycling at the replication fork, likely by uncoupling parental histone transfer from replication fork progression. Of note, ASF1 knockdown does not lead to accumulation of  $\gamma$ H2AX<sup>31</sup> (Supplementary Figure 15), suggesting that these effects are not merely a consequence of a DNA damage response.

### **ASF1 depletion impairs H3.3 and H3.1 spatial distribution**

The observed decrease in parental H3.3 and H3.1 at replicated regions in early S phase upon ASF1 depletion raised the question of the fate of these lost parental histones. We hypothesized that they could either be degraded, or, if recycled, positioned at sites

distant from patches of DNA synthesis, which may give rise to changes in their spatial distribution. Therefore, we applied our analytical method to study the impact of ASF1 depletion on the spatial distribution of parental histones around replicated DNA (Figure 8A). As an important control, we observed no difference between the siASF1 and the control conditions in the spatial distribution of EdU (“EdU vs EdU” for early S; mid/late S showed no change either) (Figure 8B and Supplementary Figure 16A, B). This shows that no changes in chromatin compaction or DNA replication speed can account for changes in histone distribution in our analysis. We then investigated whether we could detect differences in histone localization around these sites. We found no difference in the spatial distribution of parental H3.3 vs EdU in early S phase (Figure 8C, left), despite the overall decrease in amounts of parental H3.3 in replicated regions (see Figure 7D, left). This indicates that impaired recycling of histones in replicated regions due to ASF1 depletion does not lead to a shift in their spatial distribution. In contrast, when looking at mid/late S phase cells, both in the nuclear interior and at the nuclear periphery, we noticed a clear change in the spatial distribution of H3.3 towards farther distances (Figure 8C, middle and right). Unlike H3.3, parental H3.1 showed a spatial distribution away from replication sites in both early and mid/late S phase (Figure 8D). Based on these findings, we conclude that, upon ASF1 depletion-mediated impairment of parental histone recycling, a fraction of parental H3.3 and H3.1 is recycled at distant sites from replication sites, at a scale of hundreds of nanometers away (Supplementary Figure 17B). Intriguingly, parental H3.3 in early S phase, while not properly recycled locally, was not detected to be recycled at distant sites.

## Discussion

Histone variants are a key feature of the epigenetic landscape. In this work, we investigated how their distribution was maintained throughout the cell cycle, and whether replication stress reshuffled their organization. First, we established a genome-wide mapping of H3 variants relative to replication timing. Second, using STORM microscopy and SNAP labeling we further gained a spatial and quantitative view of the relationship between histones and regions of replicated DNA, not only globally, but also with a specific focus on parental histones (Supplementary Figure 18). At a global level, we identified distinct 3D units for H3.3 and H3.1. H3.3 forms units corresponding to early-replicating chromatin with a stable volume throughout the cell cycle. Unlike H3.3, H3.1 forms units that vary both in volume and density during the cell cycle. We can

distinguish two categories: (i) in early S, large low-density units likely correspond to deposition of new H3.1 in H3.3-associated chromatin, and (ii) at any time during the cell cycle, small high-density units would mark late-replicating chromatin. We then extended our analysis to the fate of parental H3.3 and H3.1 to follow their recycling at an unprecedented level. Using this approach, we could first evaluate how replication stress impairs the recycling of parental H3.1 both in terms of quantity and spatial distribution. Second, we found that ASF1 depletion affected the local recycling of both parental H3.3 and H3.1 at replication sites, but with a distinctive impact on their spatial distribution around replication sites. Therefore, we demonstrate that mislocalization of parental histones ensues in the context of replication stress or histone mismanagement, thereby leading to profound effects on the epigenome.

Genome-wide analysis of H3 variant distribution relative to replication timing revealed an enrichment of H3.3 in early-replicating chromatin, and H3.1 in late-replicating chromatin. Our combined analysis of nascent RNA-Seq with Repli-Seq and our CHIP-Seq data confirmed that H3.3 occupancy correlated with transcriptional activity and early replication timing. Interestingly however, this analysis revealed that transcription alone is not sufficient to explain the correlation between H3.3 occupancy and replication timing. Thus, other mechanisms are likely in place. One possibility is that physical properties of late-replicating chromatin may specifically exclude H3.3. This could either occur by lack of histone turnover, or impaired access of the H3.3 deposition machinery. Indeed, late-replicating chromatin coincides with heterochromatic regions that display particular isolating properties, such as phase separation -reported in two recent studies<sup>58,59</sup>-, high compaction, as well as the presence of RNAs and chromatin-bound proteins<sup>60</sup>. This could impact H3.3 deposition beyond transcriptional activity alone. While other possibilities cannot be excluded, it will be exciting to explore this avenue in the future using advanced technologies in both physics and genomic studies.

While genomic data allows a precise description of the histone variant landscape, it lacks the spatial view of how variants distribute in the nucleus. Our STORM analysis enables the visualization of H3.3 and H3.1 in 3D and reveals that they adopt distinct configurations. H3.3 forms units whose volume is unaffected by the cell cycle. Intriguingly, the volume of H3.3 unit is also independent of their coincidence with early- or late-replicating chromatin, suggesting that this property is independent of whether H3.3 marks euchromatic or heterochromatic sites. How this spatial feature relates to intrinsic properties that H3.3 itself is an exciting possibility to further examine. In addition, H3.3 conglomerate density decreases from early to late S phase. This suggests

a dilution of H3.3 in S phase, in line with the fact that the replicative H3.1, but not H3.3, is deposited genome-wide in a DNA synthesis-dependent manner<sup>2</sup>. Outside S phase, the density of H3.3 increases compared to late S, likely reflecting a replacement process, with new H3.3 deposition in a DNA synthesis-independent manner at sites where H3.1 had previously been incorporated.

Unlike H3.3, H3.1 forms units with cell cycle-dependent variations in volume and density that we can classify into two categories: (i) large and low density units present mostly in early S phase that would correspond to H3.3-enriched early-replicating chromatin, and (ii) small and dense units present throughout the whole cell cycle that would mark late-replicating chromatin. The first category diminishes progressively throughout and after S phase. We propose that H3.1 occupies early-replicating chromatin only temporarily, as a means to form new nucleosomes as placeholders coupled to DNA synthesis. Later in S phase and outside S phase, H3.1 would progressively be replaced by H3.3 in early-replicating regions, and the first category of small and dense H3.1 conglomerates - typical of late-replicating chromatin - would become predominant. The changes in density between early- and late-replicating chromatin are also consistent with our genome-wide analysis showing H3.1 enrichment in late-replicating regions.

We conclude that variants enable the definition of distinct units with properties impacted by genomic location and S phase progression, providing novel rules to partition the genome in the nucleus in 3D.

Several studies have shed light on the dynamics of parental histone recycling during replication. Radioactive pulse-chase experiments and electron microscopy studies first showed that parental histones segregated on the two daughter strands of DNA<sup>4</sup>. More recently, using Nascent Chromatin Capture (NCC) in human cells, Alabert et al. detected parental histones with their post-translational marks on newly synthesized DNA and followed the dynamics of reestablishment of these marks on new histones<sup>7</sup>. However, the exact mechanism of recycling has remained unclear, and how perturbing this recycling could impact the spatial distribution of parental histones has never been directly addressed.

To test these mechanisms, we first induced replication stress with hydroxyurea treatment<sup>8</sup>. This causes local effects on DNA - with consequences including fork stalling, checkpoint activation and DNA damage -, but its consequences on epigenome maintenance have not been determined. Yet, HU treatment leads to the appearance of single stranded DNA, which may prevent chromatin assembly at the replication fork,

and, supposedly, local recycling of parental histones<sup>37</sup>. We directly tested this latter hypothesis with our STORM assay. Our findings showed unambiguously that HU treatment impaired the recycling of parental H3.1 on replicated DNA. In addition to a loss at replication sites, HU treatment severely impaired the spatial distribution of parental H3.1 in the surrounding region. It would be interesting to monitor the fate of parental histones upon recovery from HU and assess the consequences on the epigenome. Our findings suggest that replication stress may, in some contexts, challenge the integrity of the epigenome and potentially lead to reconfiguration of chromatin territories and unscheduled changes in gene expression. Indeed, in the context of G-quadruplex-induced stress, impediments on replication were associated with changes in histone mark profiles and gene expression in daughter cells<sup>8</sup>. Interestingly, DNA damage has been found to coordinate the establishment of a protective chromatin environment in regions prone to replication stress, through FACT-dependent deposition of macroH2A1.2<sup>61</sup>, highlighting the importance of dedicated chromatin-mediated mechanisms to face replicative stress. It will be interesting to explore how this relates to H3 variants dynamics. We propose that reshuffling of histone variants upon stress may contribute to epigenomic instability. This may be particularly relevant in the context of cancer, considering the possibility that some oncogenes may induce different forms of replication stress<sup>9,62</sup>.

We then investigated the role of factors involved in histone management that could contribute to parental histone recycling. Given that the histone chaperone ASF1 was a prime candidate, we used STORM imaging coupled to the SNAP assay to directly investigate its implication in the recycling and localization dynamics of the parental histone subpopulation. Our results indicated that ASF1 depletion led to (i) a decrease in both parental H3.3 and H3.1 at replicated regions and, importantly, (ii) a change in the spatial redistribution of parental H3.3 and H3.1 relative to replicated regions. When monitoring the effect of ASF1 depletion on conglomerate properties of global H3.3 and H3.1, we detected similar trends as in the control, although less pronounced. In particular, the differences between early- and late-replicating chromatin were decreased. We propose that ASF1 depletion affects variant genomic distribution, while not affecting global S phase dynamics - such as H3.1 deposition and concomitant H3.3 dilution.

Importantly, the similarity between our results on parental histones following HU treatment and the ASF1 phenotype supports a model in which ASF1 functions directly at the fork to recycle parental histones locally, in line with its capacity to form a complex

with the MCM helicase<sup>31-33</sup>, potentially in partnership with additional factors to reform nucleosomes. In this model, absence of ASF1 would uncouple the progression of the fork from the transmission of parental histones. As ASF1 depletion, unlike HU treatment, does not trigger replication stress checkpoints - allowing either time for repair or replication arrest as a means to prevent propagation of an abnormal state -, this situation is particularly dangerous for the cell, with potential long-term implications for genome and epigenome integrity. Importantly, codepletion of ASF1a and ASF1b can induce the Alternative Lengthening of Telomeres (ALT) pathway<sup>63</sup>. Telomeres are particularly challenging for replication, as they are prone to fork stalling, formation of secondary DNA structures and DNA damage<sup>64</sup>. In this context, the added stress caused by ASF1 depletion, which prevents parental histone transfer for chromatin reassembly at the fork, might render telomeric regions particularly vulnerable and exposed, triggering in some cases the ALT response. Inversely, it would be interesting to know how ASF1 overexpression may impact the recycling of parental histone variants. In particular, the isoform ASF1b is overexpressed in cancer<sup>56</sup>, yet it is unclear whether the two isoforms ASF1a and ASF1b have different roles in recycling H3.3 and H3.1 during proliferation. Taken together, these data further emphasize the importance of histone management in the maintenance of the epigenome.

In absence of ASF1, we detect changes in the spatial distribution of parental histones. Such changes may reflect that parental histones are recycled at sites distant from their original location. More specifically, this is the case for H3.3 in mid/late S phase and for H3.1 during all S phase, but not for H3.3 in early S phase. ASF1 depletion did not seem to give rise to a spatial redistribution of the replicated DNA itself, as probed with EdU, suggesting a specific impact on histone localization. How histone variants are handled in this context remains to be elucidated. The most simple hypothesis is that parental histones, if not secured in the vicinity of the replication fork, are treated as new histones and reincorporated further away from their original location by de novo deposition pathways, such as CAF-1-mediated for H3.1, and HIRA- or DAXX-mediated for H3.3. The distinct fate of parental H3.3 in early S phase may reveal a safeguard mechanism where a fraction of H3.3 would be retargeted locally - while the rest would be degraded -, maintaining the spatial distribution of H3.3 in these regions. This could involve, for example, the presence of HIRA and RPA<sup>65</sup>. In this context, it would be interesting to investigate the implication of factors associated with the replication machinery in the recycling of parental histones. Furthermore, we observe changes in the distribution of some histone modifications (H3K9me3 and H3K27me3, H3K36me3). We hypothesize

that this may arise from relocation of parental modification-bearing histone variants away from their cognate sites during S phase.

More generally, the presence of DNA damage, transcription machineries<sup>66</sup>, or non-nucleosome material<sup>60</sup>, and the asymmetry between leading and lagging strand might interfere with histone recycling and influence the fate of each variant, both in presence and absence of ASF1. Importantly, ASF1 has been implicated in buffering H3-H4 dimers with Nuclear Autoantigenic Sperm Protein (NASP)<sup>23</sup> and in handing them off to CAF-1 and HIRA for de novo deposition<sup>24-27</sup>. It is unclear whether, in absence of ASF1, parental H3-H4 are released as tetramers or as dimers<sup>67</sup>, how the histone soluble pool is affected, and how other chaperones can bypass ASF1 function and directly handle tetramers or dimers for their deposition. Notably, parental histones carry post-translational modifications – some of which are more prevalent on specific variants<sup>57</sup> - that may impact their affinity for other factors and, in turn, their fate<sup>2</sup>.

Taken together, our observations suggest that ASF1 depletion reshapes the histone variant balance in chromatin during S phase, which may affect transcriptional status. Future work should address the details of the precise mechanism, its regulation, and the potential role for other factors in parental histone recycling. Maintaining histone variants at the exact same position during replication encourages a cell to commit to its lineage. Inversely, their loss provides an opportunity to reshape the chromatin landscape. In line with this view, recent studies showed that depletion of CAF-1 facilitated cell reprogramming by pluripotency factors<sup>68,69</sup>. Based on our findings, it is tempting to envisage a similar role for ASF1 in this context. However, considering that ASF1a has been reported to be necessary for maintenance of pluripotency and cellular reprogramming<sup>70</sup> and that ASF1a and ASF1b are involved in multiple pathways<sup>28</sup>, the role of ASF1 in differentiation is likely distinct from CAF-1 and awaits further investigation. In particular, in contexts such as the establishment of monoallelic expression - where early replication of the expressed allele coincides with chromatin accessibility<sup>71</sup> -, it would be interesting to know whether ASF1 and the distribution of histone variants affect replication timing and, in turn, the differentiation program.

## Methods

### H3.3- and H3.1-SNAP labeling in vivo

We used cell lines stably expressing H3.3-SNAP-3xHA or H3.1-SNAP- 3xHA in HeLa cells previously used and characterized<sup>12</sup>. These cell lines have been tested negative for mycoplasma contamination. For the pulse experiments, we incubated cells in complete

medium containing 2  $\mu\text{M}$  of SNAP-Cell TMR-Star (New England Biolabs) and 10  $\mu\text{M}$  of EdU (5-ethynyl-20-deoxyuridine) during 20 min for labeling. We did two quick washes with PBS then reincubated the cells in complete medium for 30 min to allow excess SNAP-Cell TMR-Star to diffuse out. We then moved on to extraction and fixation protocol. For the pulse-chase experiments, we incubated cells with medium containing 2  $\mu\text{M}$  of SNAP-Cell TMR-Star during 20 min for labeling, did two PBS washes, and reincubated the cells in complete medium for 30 min, then washed twice with PBS again. We incubated the cells in complete medium for a chase period of 48 hours. We then washed twice with PBS and reincubated in complete medium containing 10  $\mu\text{M}$  of EdU for 30 min, before moving on to extraction and fixation protocol. For the quench-chase-pulse experiments, we incubated cells in complete medium containing 10  $\mu\text{M}$  of SNAP-Cell Block (New England Biolabs) to quench SNAP-tag activity, and then performed two PBS washes and 30 min incubation in complete medium to allow the SNAP-Cell Block to diffuse out. We incubated in complete medium for a 2h chase period, then performed a pulse step as described above. At least three independent experiments were performed for each condition.

### **Extraction and fixation followed by EdU detection**

We performed a pre-extraction of cells prior to fixation for 5 min with 0.5% Triton in CSK buffer (10 mM PIPES [pH 7], 100 mM NaCl, 300 mM sucrose, 3 mM  $\text{MgCl}_2$ , protease inhibitors), then washed quickly with CSK and performed a 5 min CSK wash. We then fixed cells in 2% paraformaldehyde for 20 min. We blocked cells with BSA (3% in PBS) before performing Click reaction to reveal the EdU (Click-iT EdU Alexa Fluor 647 imaging kit, Invitrogen). We mounted the coverslips in PBS containing 5 mM of MEA (Mercaptoethylamine, 30070, Sigma) on cavity slides (BR475505, Sigma) and sealed with Twinsil sealing medium (Rotec) before STORM imaging. We changed the mounting buffer between every acquisition.

### **siRNA transfection and drug treatment**

In the pulse-chase experiments, we performed a siRNA transfection prior to the pulse-chase using Lipofectamine RNAimax (Invitrogen). We used siRNA previously characterized<sup>30,31</sup> against ASF1a (GUGAAGAAUACGAUCAAGUUU) and ASF1b (CAACGAGUACCUCAACCCUUU) at 100 nM concentration (siRNA purchased from Dharmacon). In hydroxyurea experiments, cells were treated with 3mM HU for 30 minutes prior to extraction and fixation protocol.

## **Micrococcal Nuclease sensitivity assay**

One million cells of each indicated condition were collected, washed twice in PBS and nuclei were extracted in 150mM NaCl, 50mM Tris-HCl pH 7.5, 2mM MgCl<sub>2</sub>, 0.1% Triton, 0.5% NP-40. Pelleted nuclei were resuspended in 150mM NaCl, 50mM Tris-HCl pH 7.5, 2mM MgCl<sub>2</sub>, 0.1% Triton, 5mM CaCl<sub>2</sub> buffer, containing 2 units of S7 Micrococcal Nuclease (ThermoFisher Scientific EN0181) and incubated at 37°C. At each time point, 20% of the sample was collected and mixed with an equal volume of 150mM NaCl, 50mM Tris-HCl pH 7.5, 2mM MgCl<sub>2</sub>, 0.1% Triton, 10mM EGTA to stop the digestion reaction. DNA was extracted, analyzed by electrophoresis in a 1% agarose gel with Sybr Safe dye (Invitrogen) and photographed under UV light using a ChemiDoc Gel Imaging System (Bio Rad). Images were analyzed with Fiji software to extract density profiles.

## **STORM imaging**

We acquired 3D STORM images on a custom setup based on a Nikon iSPT-PALM inverted microscope. We excited Alexa 647 - used to label EdU - with a 640-nm laser with a power of 10.8 mW at the sample. We excited TMR - used to label histones - with a 560-nm laser with a power of 41.3 mW at the sample. In addition, both for Alexa 647 and TMR, we used a 405-nm Coherent laser with a power of 18.5  $\mu$ W at the sample. We imaged the fluorescence from the activated Alexa 647 and TMR molecules with an EM-CCD camera (Ixon Ultra 897 Andor) using a 100x/1.45NA (Nikon) objective. Using this objective, the image pixel size was 160 nm. We used a cylindrical lens (Melles Griot) for 3D<sup>72</sup>. We controlled the microscope with NIS software (Nikon). The number of acquisitions for each experiment is indicated in Figure Legends.

We detected the localizations in STORM movies with a custom algorithm as in Sergé et al<sup>73</sup>. For data visualization, detections were rendered using the ViSP software as an isotropic Gaussian whose full-width half-maximum was 40 nm<sup>74</sup>. We performed z stacks on fluorescent beads (TetraSpeck Microspheres, ThermoFisher) for z calibration. We also used fluorescent beads monitored during STORM image acquisition to correct for sample drift<sup>75</sup> and to align the two signals. When two localizations were detected in consecutive frames within a 50-nm radius, we considered them as one.

## **STORM data analysis**

We identified conglomerates of H3.3 and H3.1 or replication foci using the density-based clustering algorithm DBSCAN<sup>76</sup>. DBSCAN uses two input parameters – Eps and MinPts – and determines that a point is in a cluster if at least MinPts points are within a distance

of Eps. We used an Eps value of 75 nm and a Minpts of 10 for DBSCAN analysis. For replication foci, we only used clusters with a detection number above a threshold value (100) for further analysis.

To measure the volume of the conglomerates, we used the convex hull function in Matlab. For the density, we calculated the number of detections - normalized by the total number of detections in the nucleus - divided by the volume. We visualized the volume and density as distribution plots using the ksdensity function in Matlab. When looking at H3.3 or H3.1 conglomerates at replication sites, we selected the ones located under 200 nm from the center of gravity of an EdU cluster; we also tested selecting conglomerates directly situated in an EdU cluster using the convex hull function, which yielded the same results. To study parental H3.3 or H3.1 at replication sites, we calculated the number of H3.3 or H3.1 detections located in the replication foci - normalized by the total number of H3.3 or H3.1 detections in the nucleus - and normalized to the EdU signal, accounting for differences in replicative behavior, including between the two cell lines. This was also visualized as a distribution plot using ksdensity. When comparing populations, we used a Mann-Whitney-Wilcoxon test. For comparison between scatter plots, error bars represent standard deviation and we used a t test. p-values:  $p > 0,05$  was annotated "ns" (non significant);  $0,01 < p < 0,05$  was noted \*;  $0,001 < p < 0,01$  was noted \*\*;  $p < 0,001$  was noted \*\*\*. For the study of spatial distribution, for each replication site, we assigned each surrounding detection of histones (for "histones vs EdU")/EdU (for "EdU vs EdU") to a 50 nm wide concentric region around the center of gravity of the replication site based on its distance to the center of gravity. The number of detections counted in each region was normalized by the volume of the corresponding region and plotted in a bar plot. For the alternative method, we modified the m function from Lang et al<sup>55</sup>. We considered the distances between all the histone detections vs all the EdU detections and normalized to the distances between detections from two randomly distributed signals. In the plotted graph, when the function is above 1, it indicates attraction, while below 1 indicates repulsion.

## **Immunofluorescence and epifluorescence microscopy**

For standard epifluorescence imaging of histone post-translational modifications, after blocking with BSA and Click reaction for EdU labeling, coverslips were incubated with primary and secondary antibodies and stained with DAPI. Coverslips were mounted in Vectashield medium. We used an AxioImager Zeiss Z1 microscope with a 63x objective. For confocal images, we used a Confocal Zeiss LSM780, and images were acquired using

63x/1.4NA under Zen blue software (Zeiss – Germany). Antibodies were used at the following dilutions: H3K9me3 1:1000 (39765, ActiveMotif), H3K27me3 1:500 (07-449, Millipore), H3K4me3 1:500 (07-473, Millipore), H3K36me3 1:500 (ab9050, Abcam),  $\gamma$ H2AX (05-636, Euromedex).

### **H3.3 and H3.1 ChIP and ChIP-seq data analysis**

We performed HA-tag ChIP-seq from the HeLa H3.3-SNAP-3xHA and HeLa H3.1-SNAP-3xHA cell lines as described in Rotem et al<sup>77</sup>. We used 4 million cells digested in 100  $\mu$ L with MNase for 8 min at 37°C (3 units/million cell). We performed HA-ChIP by incubating chromatin (100  $\mu$ L) supplemented with 500  $\mu$ L incubation buffer (Tris HCl 50mM pH7.5, NaCl 100mM, BSA 0.5%, protease inhibitors tablet cocktail, Roche) with anti-HA beads (10  $\mu$ L) (Roche diagnostics). After overnight incubation on a rotating wheel at 4°C and following washes, we collected beads in 20  $\mu$ L TE. We eliminated RNA contaminant by adding 2  $\mu$ L RNase A (10  $\mu$ g/ $\mu$ L) and incubating 30 minutes at 37°C. We eluted DNA by adding 2  $\mu$ L Proteinase K (20  $\mu$ g/ $\mu$ L), 2.5  $\mu$ L SDS 2% and incubating 2 hours at 37°C. DNA was then purified with Agencourt AMPure XP Beads (Beckman Coulter) according to manufacturer recommendations in 20  $\mu$ L water. Sequencing libraries (TruSeq ChIPseq) were prepared with 15 ng of DNA and pair-end sequenced on HiSeq2500 at the Institut Curie NGS sequencing platform.

Reads were aligned to the human genome version hg19/GRCh37 with Bowtie2<sup>78</sup> (version 2.2.9), run in paired-end mode using the --very-sensitive parameter. Genome-wide coverage in bedGraph format was obtained for each alignment using bedtools<sup>79</sup> (version 2.17.0) after sorting and indexing the corresponding BAM file with samtools<sup>80</sup> (version 1.1). Custom Python scripts were used to compute the mean per-base coverage at consecutive 10 kb bins along each chromosome, after normalizing the read counts to the total sequencing depth for each sample. The  $\log_2$  ratio to input at non-zero bins was used as a proxy for H3 enrichment.

### **Data and Code availability**

All relevant data and analysis code for genome-wide and imaging experiments are available from the authors upon request. Raw sequencing data is available on NCBI SRA (pending accession number).

## **Acknowledgments**

We thank Antoine Coulon and the members of the PIC3i "UNDERSTAND DYNAMIC ARC" for helpful discussions, Shauna Katz and Dominique Ray-Gallet for critical reading of the manuscript, Chloé Guedj, Patricia Le Baccon and the PICT-IBiSA platform for help with the iSPT-PALM microscope. This work was supported by la Ligue Nationale contre le Cancer (Equipe labellisée Ligue), ANR-11-LABX-0044\_DEEP and ANR-10-IDEX-0001-02 PSL, ANR-12-BSV5-0022-02 "CHAPINHIB", ANR-14-CE16-0009 "Epicure", ANR-14-CE10-0013 "CELLECTCHIP", EU project 678563 "EPOCH28", ERC-2015-ADG- 694694 "ChromADICT", ANR-16-CE15-0018 "CHRODYT", ANR-16-CE12-0024 "CHIFT", ANR-16-CE11-0028 « REPLICAF », and "Parisian Alliance of Cancer Research Institutes ". High-throughput sequencing and Library preparation has been performed by the ICGex NGS platform of the Institut Curie supported by the grants ANR-10-EQPX-03 (Equipex) and ANR-10-INBS-09-08 (France Génomique Consortium) from the Agence Nationale de la Recherche ("Investissements d'Avenir" program), by the Canceropole Ile-de-France and by the SiRIC-Curie program - SiRIC Grant "INCa-DGOS- 4654".

## **Conflict of interest**

The authors declare no conflict of interest.

## **Author contributions**

G.A. supervised the work. G.A. and C.C. conceived the overall strategy and wrote the paper. C.C. performed epifluorescence and STORM experiments and analyzed STORM data. G.A.O. performed epifluorescence, confocal and STORM experiments, analyzed STORM data, and wrote corresponding parts in the paper. A.G. analyzed the epigenomics data and wrote corresponding parts of the paper. E.B. performed STORM microscopy experiments. A.F. performed the chromatin immunoprecipitation experiments. B.H. and J.M-H. built the custom PALM/STORM microscope. M.G. developed tools for image analysis. Z.A.G-L. conceived and analyzed cell biology experiments. J.P.Q. designed the chromatin immunoprecipitation experiments and wrote corresponding parts of the paper. Critical reading and discussion of all data involved all authors.

## References

- 1 Talbert, P. B. & Henikoff, S. Histone variants--ancient wrap artists of the epigenome. *Nat Rev Mol Cell Biol* **11**, 264-275, doi:10.1038/nrm2861 (2010).
- 2 Gurard-Levin, Z. A. & Almouzni, G. Histone modifications and a choice of variant: a language that helps the genome express itself. *F1000Prime Rep* **6**, 76, doi:10.12703/P6-76 (2014).
- 3 Romanoski, C. E., Glass, C. K., Stunnenberg, H. G., Wilson, L. & Almouzni, G. Epigenomics: Roadmap for regulation. *Nature* **518**, 314-316, doi:10.1038/518314a (2015).
- 4 Groth, A., Rocha, W., Verreault, A. & Almouzni, G. Chromatin challenges during DNA replication and repair. *Cell* **128**, 721-733, doi:10.1016/j.cell.2007.01.030 (2007).
- 5 Probst, A. V., Dunleavy, E. & Almouzni, G. Epigenetic inheritance during the cell cycle. *Nat Rev Mol Cell Biol* **10**, 192-206, doi:10.1038/nrm2640 (2009).
- 6 Ramachandran, S. & Henikoff, S. Transcriptional Regulators Compete with Nucleosomes Post-replication. *Cell* **165**, 580-592, doi:10.1016/j.cell.2016.02.062 (2016).
- 7 Alabert, C. *et al.* Two distinct modes for propagation of histone PTMs across the cell cycle. *Genes Dev* **29**, 585-590, doi:10.1101/gad.256354.114 (2015).
- 8 Svikovic, S. & Sale, J. E. The Effects of Replication Stress on S Phase Histone Management and Epigenetic Memory. *J Mol Biol* **429**, 2011-2029, doi:10.1016/j.jmb.2016.11.011 (2017).
- 9 Macheret, M. & Halazonetis, T. D. DNA replication stress as a hallmark of cancer. *Annu Rev Pathol* **10**, 425-448, doi:10.1146/annurev-pathol-012414-040424 (2015).
- 10 Gurard-Levin, Z. A., Quivy, J. P. & Almouzni, G. Histone chaperones: assisting histone traffic and nucleosome dynamics. *Annu Rev Biochem* **83**, 487-517, doi:10.1146/annurev-biochem-060713-035536 (2014).
- 11 Goldberg, A. D. *et al.* Distinct factors control histone variant H3.3 localization at specific genomic regions. *Cell* **140**, 678-691, doi:10.1016/j.cell.2010.01.003 (2010).
- 12 Ray-Gallet, D. *et al.* Dynamics of histone H3 deposition in vivo reveal a nucleosome gap-filling mechanism for H3.3 to maintain chromatin integrity. *Mol Cell* **44**, 928-941, doi:10.1016/j.molcel.2011.12.006 (2011).

- 13 Tagami, H., Ray-Gallet, D., Almouzni, G. & Nakatani, Y. Histone H3.1 and H3.3 complexes mediate nucleosome assembly pathways dependent or independent of DNA synthesis. *Cell* **116**, 51-61 (2004).
- 14 Drane, P., Ouararhni, K., Depaux, A., Shuaib, M. & Hamiche, A. The death-associated protein DAXX is a novel histone chaperone involved in the replication-independent deposition of H3.3. *Genes Dev* **24**, 1253-1265, doi:10.1101/gad.566910 (2010).
- 15 Smith, S. & Stillman, B. Purification and characterization of CAF-I, a human cell factor required for chromatin assembly during DNA replication in vitro. *Cell* **58**, 15-25 (1989).
- 16 Gaillard, P. H. *et al.* Chromatin assembly coupled to DNA repair: a new role for chromatin assembly factor I. *Cell* **86**, 887-896 (1996).
- 17 Quivy, J. P., Grandi, P. & Almouzni, G. Dimerization of the largest subunit of chromatin assembly factor 1: importance in vitro and during *Xenopus* early development. *Embo J* **20**, 2015-2027, doi:10.1093/emboj/20.8.2015 (2001).
- 18 Mattioli, F. *et al.* DNA-mediated association of two histone-bound CAF-1 complexes drives tetrasome assembly in the wake of DNA replication. *Elife* **6**, doi:10.7554/eLife.22799 (2017).
- 19 Shibahara, K. & Stillman, B. Replication-dependent marking of DNA by PCNA facilitates CAF-1-coupled inheritance of chromatin. *Cell* **96**, 575-585 (1999).
- 20 Moggs, J. G. *et al.* A CAF-1-PCNA-mediated chromatin assembly pathway triggered by sensing DNA damage. *Mol Cell Biol* **20**, 1206-1218 (2000).
- 21 Lamour, V. *et al.* A human homolog of the *S. cerevisiae* HIR1 and HIR2 transcriptional repressors cloned from the DiGeorge syndrome critical region. *Hum Mol Genet* **4**, 791-799 (1995).
- 22 Le, S., Davis, C., Konopka, J. B. & Sternglanz, R. Two new S-phase-specific genes from *Saccharomyces cerevisiae*. *Yeast* **13**, 1029-1042, doi:10.1002/(SICI)1097-0061(19970915)13:11<1029::AID-YEA160>3.0.CO;2-1 (1997).
- 23 Cook, A. J., Gurard-Levin, Z. A., Vassias, I. & Almouzni, G. A specific function for the histone chaperone NASP to fine-tune a reservoir of soluble H3-H4 in the histone supply chain. *Mol Cell* **44**, 918-927, doi:10.1016/j.molcel.2011.11.021 (2011).
- 24 Tyler, J. K. *et al.* The RCAF complex mediates chromatin assembly during DNA replication and repair. *Nature* **402**, 555-560, doi:10.1038/990147 (1999).

- 25 Mello, J. A. *et al.* Human Asf1 and CAF-1 interact and synergize in a repair-coupled nucleosome assembly pathway. *EMBO Rep* **3**, 329-334, doi:10.1093/embo-reports/kvf068 (2002).
- 26 Daganzo, S. M. *et al.* Structure and function of the conserved core of histone deposition protein Asf1. *Curr Biol* **13**, 2148-2158 (2003).
- 27 Tang, Y. *et al.* Structure of a human ASF1a-HIRA complex and insights into specificity of histone chaperone complex assembly. *Nat Struct Mol Biol* **13**, 921-929, doi:10.1038/nsmb1147 (2006).
- 28 Abascal, F. *et al.* Subfunctionalization via adaptive evolution influenced by genomic context: the case of histone chaperones ASF1a and ASF1b. *Mol Biol Evol* **30**, 1853-1866, doi:10.1093/molbev/mst086 (2013).
- 29 Messiaen, S. *et al.* Loss of the histone chaperone ASF1B reduces female reproductive capacity in mice. *Reproduction* **151**, 477-489, doi:10.1530/REP-15-0327 (2016).
- 30 Groth, A. *et al.* Human Asf1 regulates the flow of S phase histones during replicational stress. *Mol Cell* **17**, 301-311, doi:10.1016/j.molcel.2004.12.018 (2005).
- 31 Groth, A. *et al.* Regulation of replication fork progression through histone supply and demand. *Science* **318**, 1928-1931, doi:10.1126/science.1148992 (2007).
- 32 Richet, N. *et al.* Structural insight into how the human helicase subunit MCM2 may act as a histone chaperone together with ASF1 at the replication fork. *Nucleic Acids Res*, doi:10.1093/nar/gkv021 (2015).
- 33 Huang, H. *et al.* A unique binding mode enables MCM2 to chaperone histones H3-H4 at replication forks. *Nat Struct Mol Biol* (2015).
- 34 Campos, E. I. *et al.* Analysis of the Histone H3.1 Interactome: A Suitable Chaperone for the Right Event. *Mol Cell*, doi:10.1016/j.molcel.2015.08.005 (2015).
- 35 Mousson, F. *et al.* Structural basis for the interaction of Asf1 with histone H3 and its functional implications. *Proc Natl Acad Sci U S A* **102**, 5975-5980, doi:10.1073/pnas.0500149102 (2005).
- 36 Xu, M. *et al.* Partitioning of histone H3-H4 tetramers during DNA replication-dependent chromatin assembly. *Science* **328**, 94-98, doi:10.1126/science.1178994 (2010).
- 37 Jasencakova, Z. *et al.* Replication stress interferes with histone recycling and predeposition marking of new histones. *Mol Cell* **37**, 736-743, doi:10.1016/j.molcel.2010.01.033 (2010).

- 38 Dellino, G. I. *et al.* Genome-wide mapping of human DNA-replication origins: levels of transcription at ORC1 sites regulate origin selection and replication timing. *Genome Res* **23**, 1-11, doi:10.1101/gr.142331.112 (2013).
- 39 Petryk, N. *et al.* Replication landscape of the human genome. *Nat Commun* **7**, 10208, doi:10.1038/ncomms10208 (2016).
- 40 Chagin, V. O. *et al.* 4D Visualization of replication foci in mammalian cells corresponding to individual replicons. *Nat Commun* **7**, 11231, doi:10.1038/ncomms11231 (2016).
- 41 Baddeley, D. *et al.* Measurement of replication structures at the nanometer scale using super-resolution light microscopy. *Nucleic Acids Res* **38**, e8, doi:10.1093/nar/gkp901 (2010).
- 42 Zessin, P. J., Finan, K. & Heilemann, M. Super-resolution fluorescence imaging of chromosomal DNA. *J Struct Biol* **177**, 344-348, doi:10.1016/j.jsb.2011.12.015 (2012).
- 43 Bohn, M. *et al.* Localization microscopy reveals expression-dependent parameters of chromatin nanostructure. *Biophys J* **99**, 1358-1367, doi:10.1016/j.bpj.2010.05.043 (2010).
- 44 Ricci, M. A., Manzo, C., Garcia-Parajo, M. F., Lakadamyali, M. & Cosma, M. P. Chromatin fibers are formed by heterogeneous groups of nucleosomes in vivo. *Cell* **160**, 1145-1158, doi:10.1016/j.cell.2015.01.054 (2015).
- 45 Kim, J. J. *et al.* Optical High Content Nanoscopy of Epigenetic Marks Decodes Phenotypic Divergence in Stem Cells. *Sci Rep* **7**, 39406, doi:10.1038/srep39406 (2017).
- 46 Boettiger, A. N. *et al.* Super-resolution imaging reveals distinct chromatin folding for different epigenetic states. *Nature* **529**, 418-422, doi:10.1038/nature16496 (2016).
- 47 Rivera, C. M. & Ren, B. Mapping human epigenomes. *Cell* **155**, 39-55, doi:10.1016/j.cell.2013.09.011 (2013).
- 48 Fillion, G. J. *et al.* Systematic protein location mapping reveals five principal chromatin types in *Drosophila* cells. *Cell* **143**, 212-224, doi:10.1016/j.cell.2010.09.009 (2010).
- 49 Rust, M. J., Bates, M. & Zhuang, X. Sub-diffraction-limit imaging by stochastic optical reconstruction microscopy (STORM). *Nat Methods* **3**, 793-795, doi:10.1038/nmeth929 (2006).
- 50 Betzig, E. *et al.* Imaging intracellular fluorescent proteins at nanometer resolution. *Science* **313**, 1642-1645, doi:10.1126/science.1127344 (2006).

- 51 Keppler, A. *et al.* A general method for the covalent labeling of fusion proteins with small molecules in vivo. *Nat Biotechnol* **21**, 86-89, doi:10.1038/nbt765 (2003).
- 52 Jansen, L. E., Black, B. E., Foltz, D. R. & Cleveland, D. W. Propagation of centromeric chromatin requires exit from mitosis. *J Cell Biol* **176**, 795-805, doi:10.1083/jcb.200701066 (2007).
- 53 Liang, K. *et al.* Mitotic Transcriptional Activation: Clearance of Actively Engaged Pol II via Transcriptional Elongation Control in Mitosis. *Mol Cell* **60**, 435-445, doi:10.1016/j.molcel.2015.09.021 (2015).
- 54 Andronov, L., Orlov, I., Lutz, Y., Vonesch, J. L. & Klaholz, B. P. ClusterViSu, a method for clustering of protein complexes by Voronoi tessellation in super-resolution microscopy. *Sci Rep* **6**, 24084, doi:10.1038/srep24084 (2016).
- 55 Lang, G., Marcon, E. & Puech, F. Distance-Based Measures of Spatial Concentration: Introducing a Relative Density Function. (2015).
- 56 Corpet, A. *et al.* Asf1b, the necessary Asf1 isoform for proliferation, is predictive of outcome in breast cancer. *Embo J* **30**, 480-493, doi:10.1038/emboj.2010.335 (2011).
- 57 Loyola, A., Bonaldi, T., Roche, D., Imhof, A. & Almouzni, G. PTMs on H3 variants before chromatin assembly potentiate their final epigenetic state. *Mol Cell* **24**, 309-316, doi:10.1016/j.molcel.2006.08.019 (2006).
- 58 Strom, A. R. *et al.* Phase separation drives heterochromatin domain formation. *Nature* **547**, 241-245, doi:10.1038/nature22989 (2017).
- 59 Larson, A. G. *et al.* Liquid droplet formation by HP1alpha suggests a role for phase separation in heterochromatin. *Nature* **547**, 236-240, doi:10.1038/nature22822 (2017).
- 60 Imai, R. *et al.* Density imaging of heterochromatin in live cells using orientation-independent-DIC microscopy. *Mol Biol Cell*, doi:10.1091/mbc.E17-06-0359 (2017).
- 61 Kim, J. *et al.* Replication Stress Shapes a Protective Chromatin Environment across Fragile Genomic Regions. *Mol Cell* **69**, 36-47 e37, doi:10.1016/j.molcel.2017.11.021 (2018).
- 62 Macheret, M. & Halazonetis, T. D. Intragenic origins due to short G1 phases underlie oncogene-induced DNA replication stress. *Nature* **555**, 112-116, doi:10.1038/nature25507 (2018).

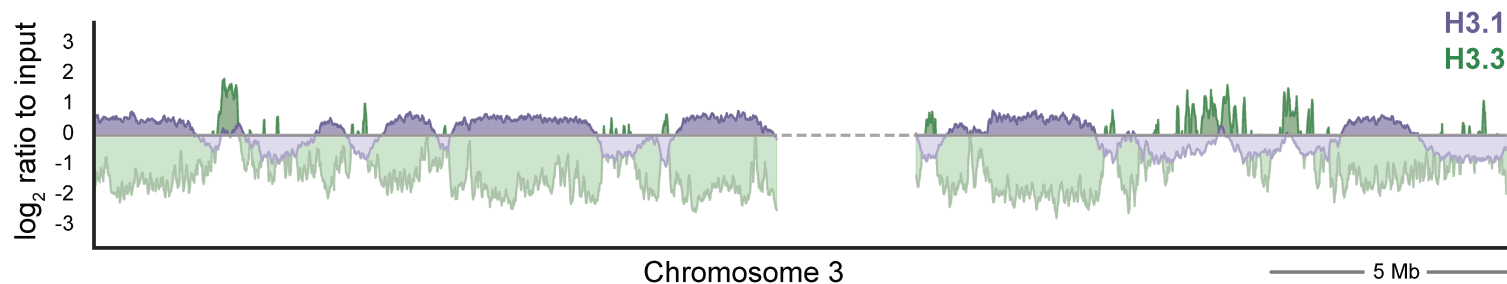
- 63 O'Sullivan, R. J. *et al.* Rapid induction of alternative lengthening of telomeres by depletion of the histone chaperone ASF1. *Nat Struct Mol Biol* **21**, 167-174, doi:10.1038/nsmb.2754 (2014).
- 64 Gilson, E. & Geli, V. How telomeres are replicated. *Nat Rev Mol Cell Biol* **8**, 825-838, doi:10.1038/nrm2259 (2007).
- 65 Zhang, H. *et al.* RPA Interacts with HIRA and Regulates H3.3 Deposition at Gene Regulatory Elements in Mammalian Cells. *Mol Cell* **65**, 272-284, doi:10.1016/j.molcel.2016.11.030 (2017).
- 66 Hamperl, S., Bocek, M. J., Saldivar, J. C., Swigut, T. & Cimprich, K. A. Transcription-Replication Conflict Orientation Modulates R-Loop Levels and Activates Distinct DNA Damage Responses. *Cell* **170**, 774-786 e719, doi:10.1016/j.cell.2017.07.043 (2017).
- 67 Ray-Gallet, D. & Almouzni, G. Molecular biology. Mixing or not mixing. *Science* **328**, 56-57, doi:10.1126/science.1188653 (2010).
- 68 Cheloufi, S. *et al.* The histone chaperone CAF-1 safeguards somatic cell identity. *Nature* (2015).
- 69 Ishiuchi, T. *et al.* Early embryonic-like cells are induced by downregulating replication-dependent chromatin assembly. *Nat Struct Mol Biol*, doi:10.1038/nsmb.3066 (2015).
- 70 Gonzalez-Munoz, E., Arboleda-Estudillo, Y., Otu, H. H. & Cibelli, J. B. Cell reprogramming. Histone chaperone ASF1A is required for maintenance of pluripotency and cellular reprogramming. *Science* **345**, 822-825, doi:10.1126/science.1254745 (2014).
- 71 Levin-Klein, R. *et al.* Clonally stable V $\kappa$  allelic choice instructs I $\kappa$  repertoire. *Nat Commun* **8**, 15575, doi:10.1038/ncomms15575 (2017).
- 72 Jones, S. A., Shim, S. H., He, J. & Zhuang, X. Fast, three-dimensional super-resolution imaging of live cells. *Nat Methods* **8**, 499-508, doi:10.1038/nmeth.1605 (2011).
- 73 Serge, A., Bertaux, N., Rigneault, H. & Marguet, D. Dynamic multiple-target tracing to probe spatiotemporal cartography of cell membranes. *Nat Methods* **5**, 687-694, doi:10.1038/nmeth.1233 (2008).
- 74 El Beheiry, M. & Dahan, M. ViSP: representing single-particle localizations in three dimensions. *Nat Methods* **10**, 689-690, doi:10.1038/nmeth.2566 (2013).
- 75 Huang, B., Wang, W., Bates, M. & Zhuang, X. Three-dimensional super-resolution imaging by stochastic optical reconstruction microscopy. *Science* **319**, 810-813, doi:10.1126/science.1153529 (2008).

- 76 Ester, M., Kriegel, H. P., Sander, J. & Xu, X. A Density-Based Algorithm for Discovering Clusters in Large Spatial Databases with Noise. *KDD'96 Proceedings of the Second International Conference on Knowledge Discovery and Data Mining*, 226–231 (1996).
- 77 Rotem, A. *et al.* Single-cell ChIP-seq reveals cell subpopulations defined by chromatin state. *Nat Biotechnol* **33**, 1165-1172, doi:10.1038/nbt.3383 (2015).
- 78 Langmead, B. & Salzberg, S. L. Fast gapped-read alignment with Bowtie 2. *Nat Methods* **9**, 357-359, doi:10.1038/nmeth.1923 (2012).
- 79 Quinlan, A. R. & Hall, I. M. BEDTools: a flexible suite of utilities for comparing genomic features. *Bioinformatics* **26**, 841-842, doi:10.1093/bioinformatics/btq033 (2010).
- 80 Li, H. *et al.* The Sequence Alignment/Map format and SAMtools. *Bioinformatics* **25**, 2078-2079, doi:10.1093/bioinformatics/btp352 (2009).

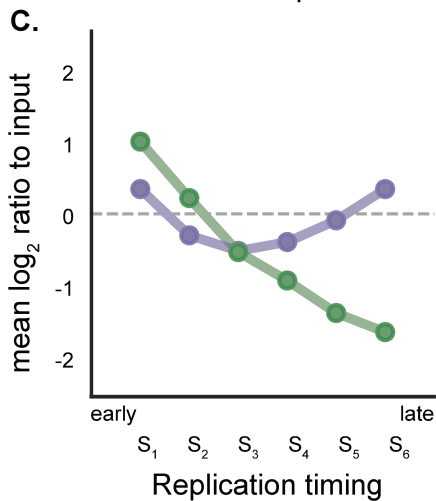
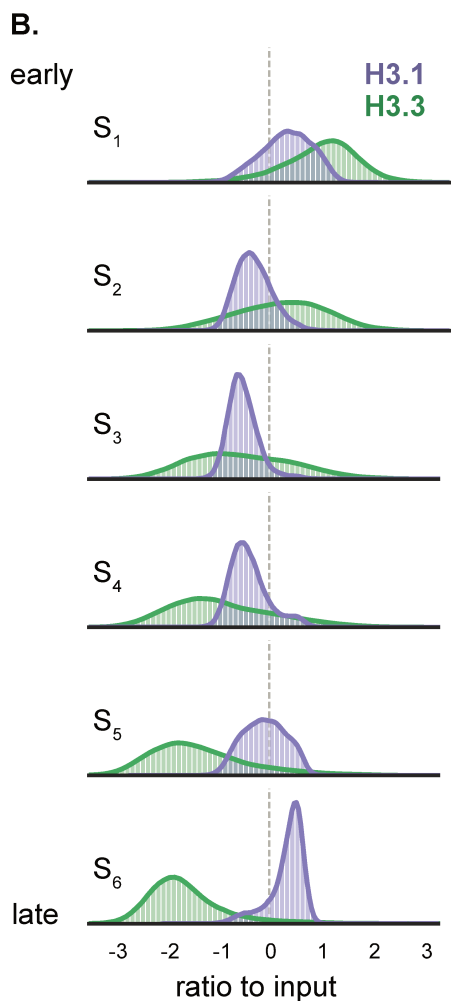


Figure 1

A. ChIP-Seq:



B. ChIP-Seq vs Repli-Seq:



D. ChIP-Seq vs Repli-Seq vs nascent RNA-Seq:

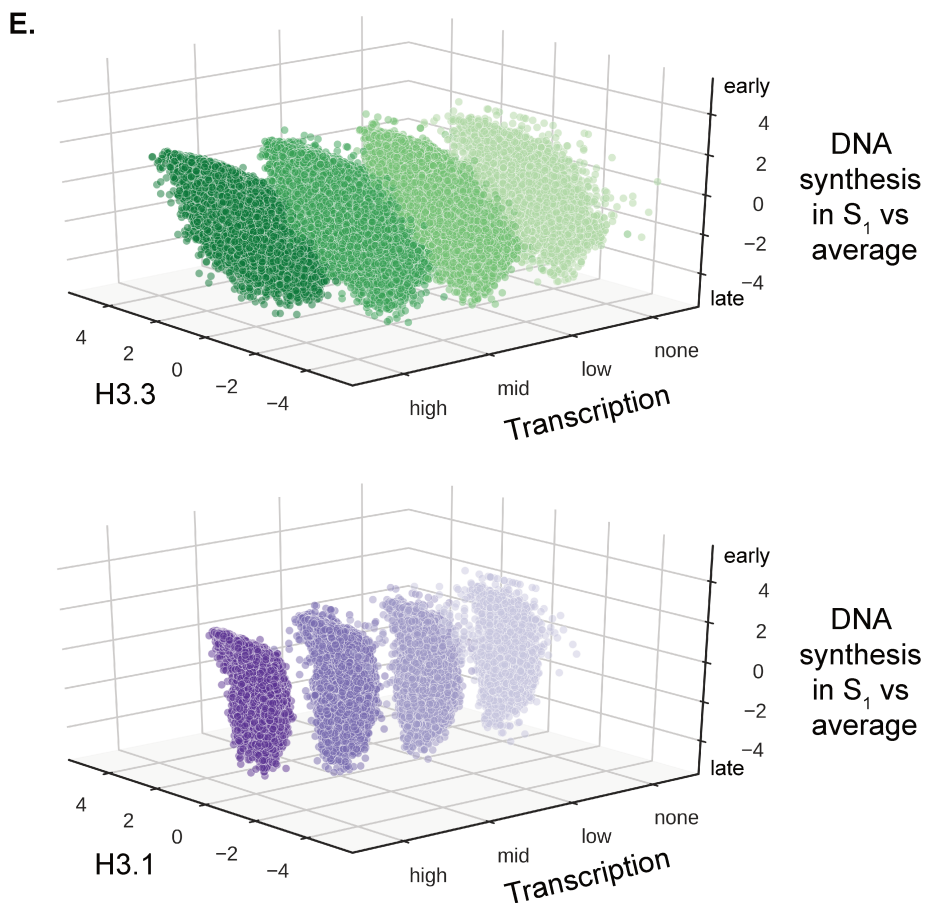
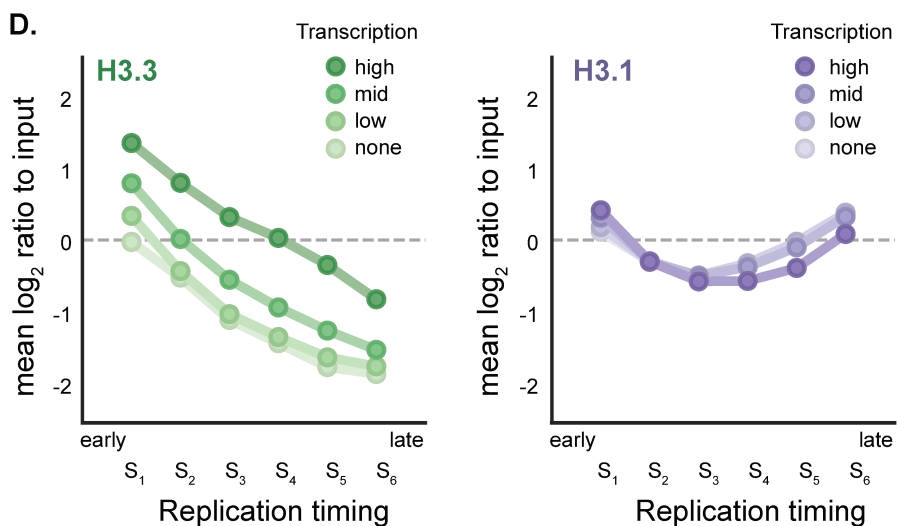


Figure 1 – Global H3.3 and H3.1 genome-wide occupancy relative to replication timing and transcriptional activity

A. H3.3 and H3.1 genomic coverage normalized to input (chromosome 3 centromeric band  $\pm$  15 Mb, x-axis). The y-axis shows the  $\log_2$  ratio between the mean per-base number of reads from H3.3 (green) and H3.1 (purple) and their respective input, at consecutive 10 kb bins (smoothed over 5 non-zero bins). Enriched regions (i.e.  $\log_2$  ratio  $\geq 0$ ) are highlighted in darker colors.

B. H3.3 and H3.1 occupancy by replication timing: the panels show the histogram and Gaussian kernel density corresponding to the  $\log_2$  ratio to input for H3.3 (green) and H3.1 (purple) at 10 kb regions ranked by replication timing from early to late (S phase fraction with the highest mean coverage in Repli-Seq data from Dellino et al. 2013).

C. Mean values corresponding to B.

D. H3.3 and H3.1 occupancy by replication timing at increasing levels of nascent transcription: the mean  $\log_2$  ratio to input for H3.3 (green, left) and H3.1 (purple, right) at 10 kb regions ranked by replication timing (as in B) and transcription percentile (based on nascent RNA-Seq data from Liang et al. 2015). The color gradient represents increasing levels of nascent transcription computed from the  $\log_2$ -transformed mean coverage: absence of measurable transcription (none), lower 10th percentile (low), 10th to 90th percentile (mid) or upper 10th percentile (high).

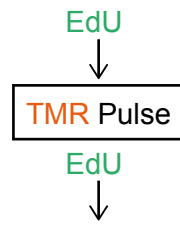
E. H3.3 and H3.1 correlation with early DNA synthesis at increasing transcription levels. H3.3 (top) and H3.1 (bottom)  $\log_2$  ratio to input (x-axis) against S1 coverage normalized to the average over all fractions ( $\log_2$  ratio, z-axis) at 10 kb regions ranked by transcriptional status (y-axis). The rank reflects the level of nascent transcription as described above.

Figure 2

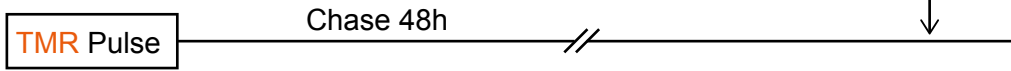
A. Labeling scheme:

Histones  
H3.1 or H3.3 / Replicated  
DNA

Global



Parental



B.

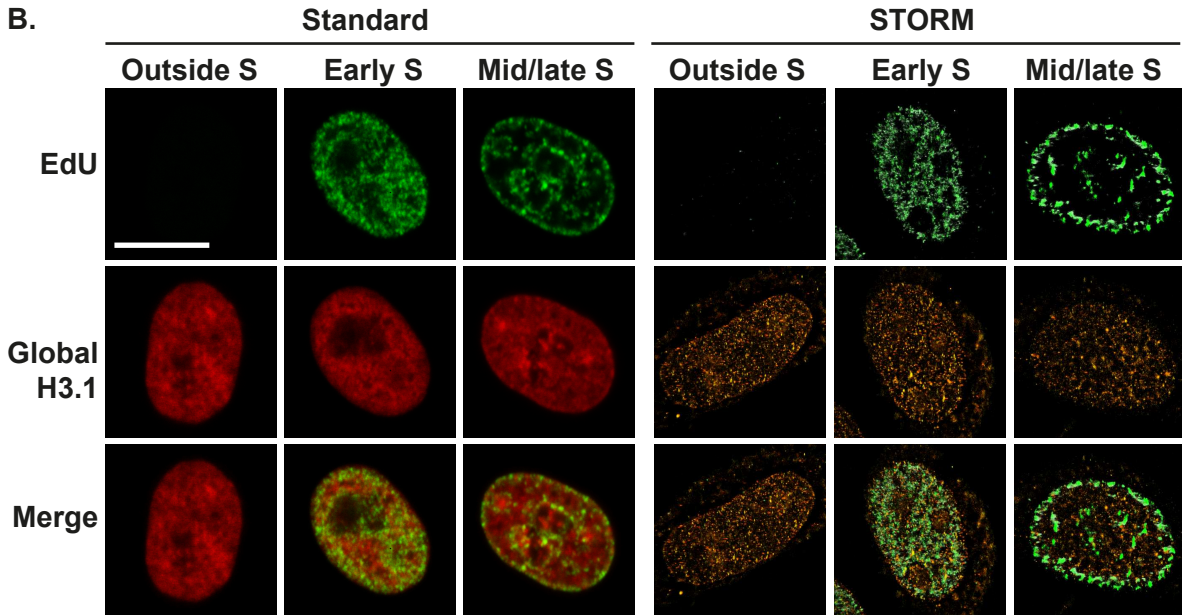


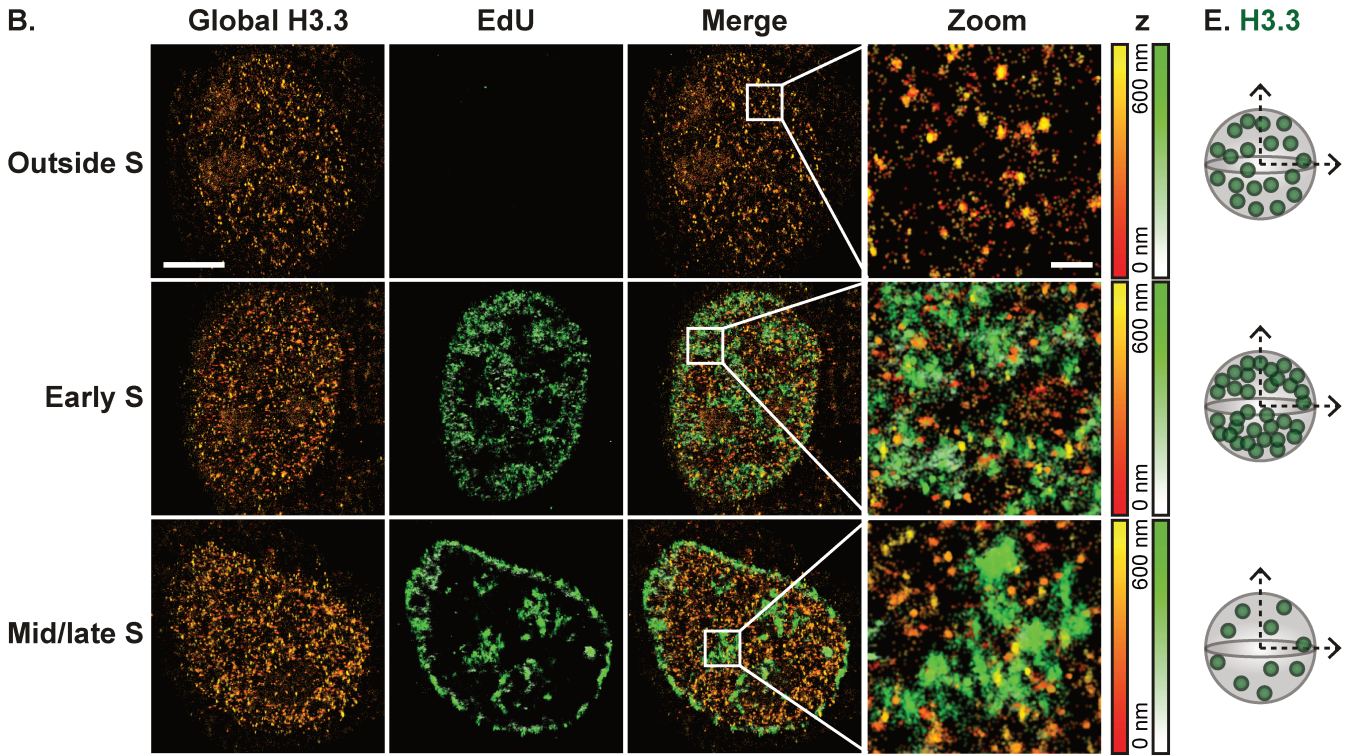
Figure 2 – Tracking histone H3 variants with STORM microscopy

A. Labeling scheme using H3.3- or H3.1-SNAP to follow global (top) or parental (bottom) histones. A pulse using the fluorophore TMR (orange) labels SNAP-tagged H3.3 or H3.1. EdU incorporation at the end of the assay allows the detection of replicated DNA (green). This EdU labeling is carried out either during the TMR pulse to compare global H3 distribution with patches of DNA synthesis, or after a chase period that allows synthesis and deposition of new unlabeled H3.3- or H3.1-SNAP. The latter enables the localization of 48h-old parental histones with new patches of DNA synthesis. In all cases, we eliminate soluble histones by triton extraction prior to fixation in order to analyze chromatin bound H3.3 or H3.1 fractions.

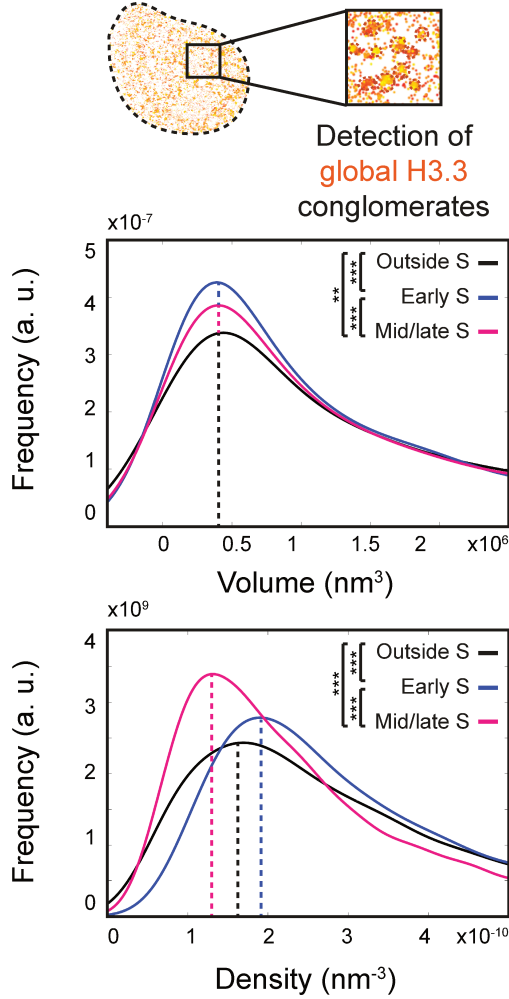
B. Left panels: confocal images of global H3.1 (TMR, red) and replicated DNA (EdU, green) at different S phase stages and outside S. Cells outside S phase are EdU negative, early S phase shows patterns broadly labeling the nucleus with the exception of the nucleoli, and mid/late S phase shows patterns with clear enrichment at the nuclear periphery and around nucleoli. Right panels: STORM images of global H3.1 (TMR, orange) and replicated DNA (EdU, green) in cells outside S phase, early S phase and mid/late S phase. We used the ViSP software to render STORM images. Scale bars represent 10  $\mu\text{m}$ .

Figure 3

A. Labeling scheme: **Global histone H3.3** / **Replicated DNA** TMR + EdU Pulse



**C. Whole nucleus**



**D. Replicated DNA**

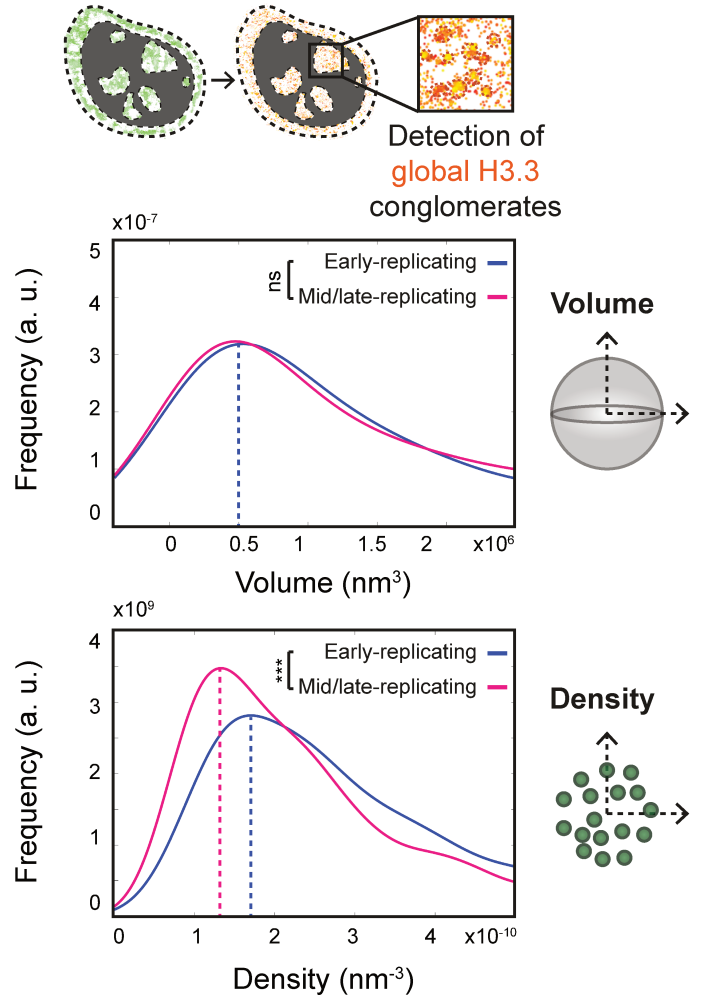


Figure 3 – Global distribution of H3.3 throughout S phase using STORM assay

A. Labeling scheme using H3.3-SNAP to follow global H3.3 as described in Figure 2.

B. Representative STORM images of global H3.3 (TMR, orange) and replicated DNA (EdU, green) in HeLa H3.3-SNAP. EdU labeling, as described in Figure 2, allows the selection of cells outside S phase, in early S phase and mid/late S phase. The color gradient corresponds to the z range. Scale bars represent 5  $\mu\text{m}$ . Insets represent enlarged images of selected area where scale bars correspond to 600 nm.

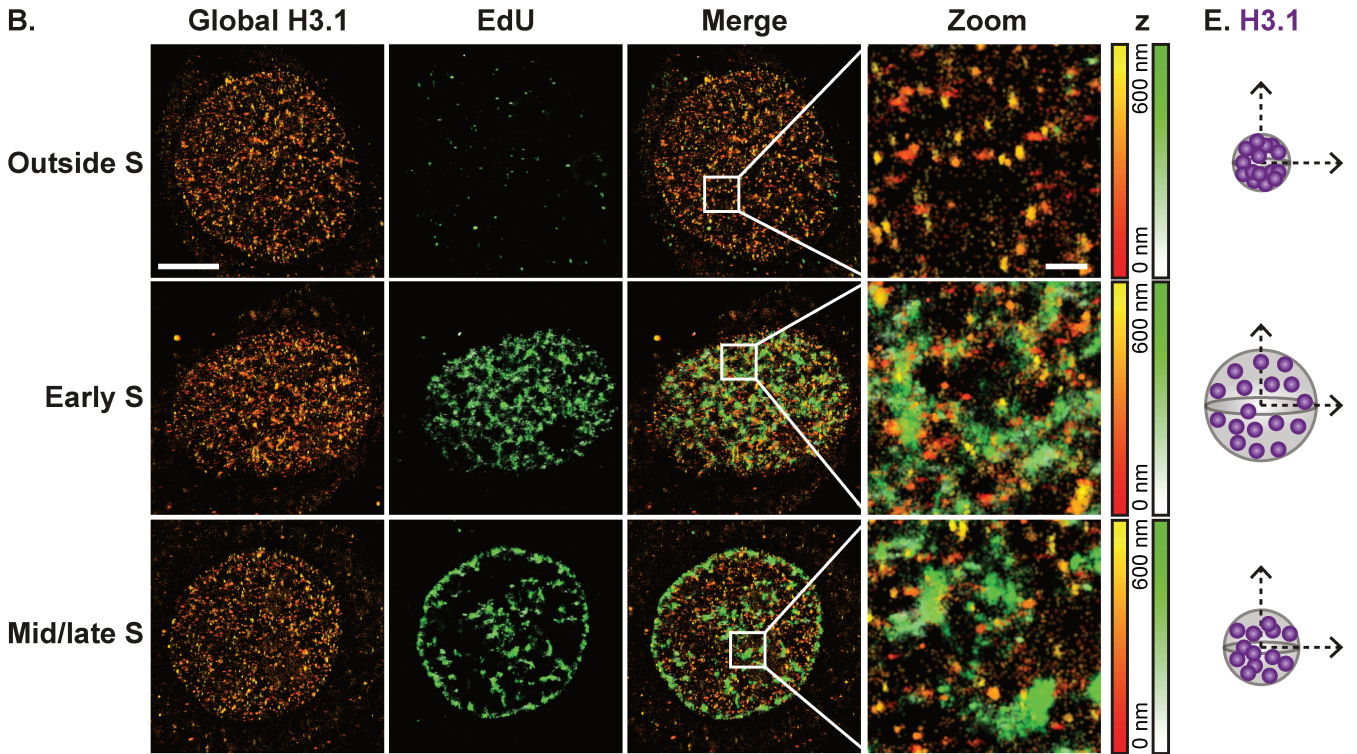
C. For the H3.3-enriched areas - defined as conglomerates - in the whole nucleus: the plots show the distribution of volume (top) or density (bottom) of H3.3 conglomerates in cells outside S phase (black), in early S phase (blue), and in mid/late S phase (magenta). For C and D, N=11, 8, and 10 cells for outside S phase, early S phase and mid/late S phase respectively. p-values (using a Mann-Whitney-Wilcoxon test): (\*\*\*)  $p \leq 0.001$ ; (\*\*)  $p \leq 0.01$ ; (\*)  $p \leq 0.05$ ; (ns) not significant.

D. For H3.3 conglomerates in regions of replicated DNA, the plots show the distribution of volume (top) or density (bottom) of H3.3 conglomerates in cells in early S phase (blue), and in mid/late S phase (magenta).

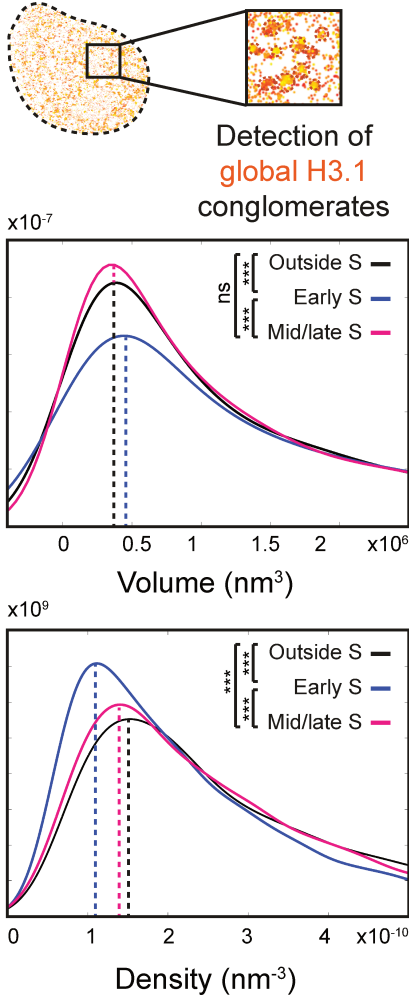
E. Scheme summarizing the changes in volume and density of H3.3 conglomerates outside S phase, in early S phase, and in mid/late S phase.

Figure 4

A. Labeling scheme: **Global histone H3.1** / **Replicated DNA** TMR + EdU Pulse



**C. Whole nucleus**



**D. Replicated DNA**

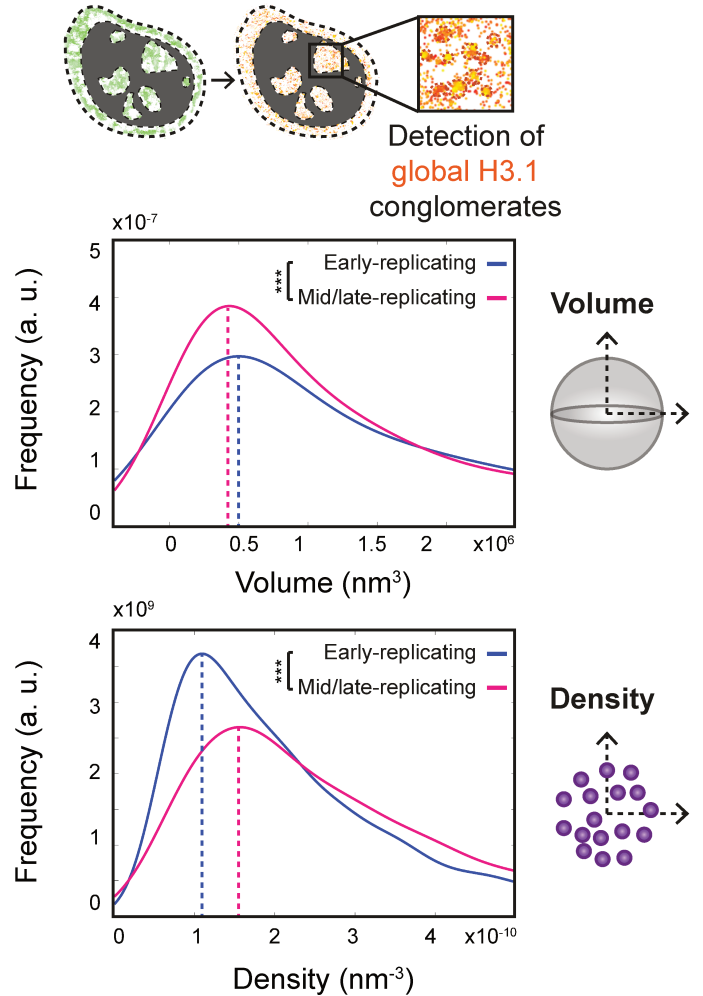


Figure 4 – Global distribution of H3.1 throughout S phase using STORM assay

A. Labeling scheme using H3.1-SNAP to follow global H3.1 as described in Figure 2.

B. Representative STORM images of global H3.1 (TMR, orange) and replicated DNA (EdU, green) in HeLa H3.1-SNAP. EdU labeling, as described in Figure 2, allows the selection of cells outside S phase, in early S phase and mid/late S phase. The color gradient corresponds to the z range. Scale bars represent 5  $\mu\text{m}$ . Insets represent enlarged images of selected area where scale bars correspond to 600 nm.

C. For the H3.1-enriched areas - defined as conglomerates - in the whole nucleus: the plots show the distribution of volume (top) or density (bottom) of H3.1 conglomerates in cells outside S phase (black), in early S phase (blue), and in mid/late S phase (magenta). For C and D, N=9, 10, and 13 cells for outside S phase, early S phase and mid/late S phase respectively. p-values (using a Mann-Whitney-Wilcoxon test): (\*\*\*)  $p \leq 0.001$ ; (\*\*)  $p \leq 0.01$ ; (\*)  $p \leq 0.05$ ; (ns) not significant.

D. For H3.1 conglomerates in regions of replicated DNA: the plots show the distribution of volume (top) or density (bottom) of H3.1 conglomerates in cells in early S phase (blue), and in mid/late S phase (magenta).

E. Scheme summarizing the changes in volume and density of H3.1 conglomerates outside S phase, in early S phase, and in mid/late S phase.

Figure 5

A. Labeling scheme:

Parental histone H3.3 or H3.1

0h

TMR Pulse

24h

TMR Pulse

Chase 24h

48h

TMR Pulse

Chase 48h

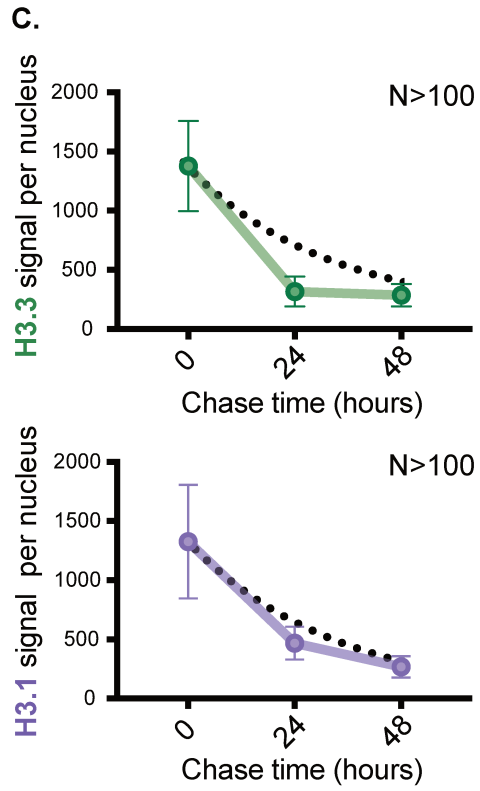
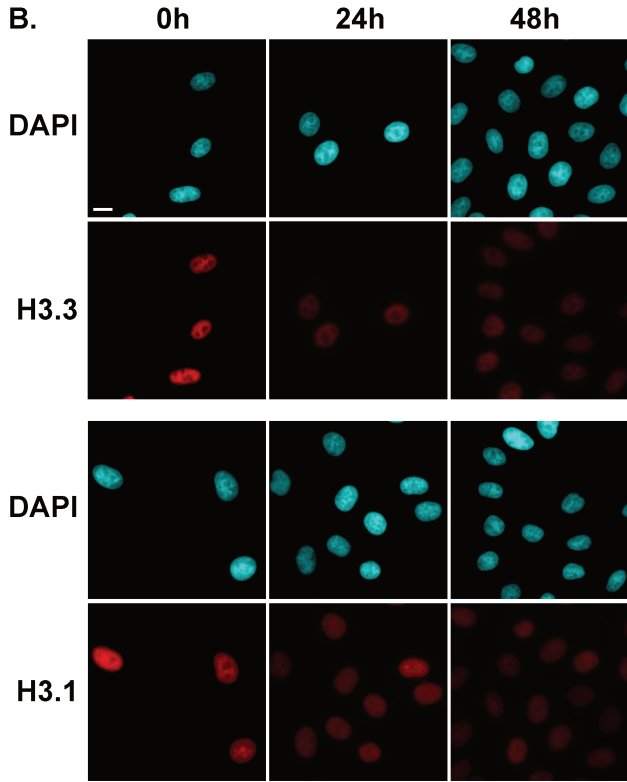


Figure 5 – Tracking parental H3.3 and H3.1

A. Labeling scheme using H3.3- or H3.1-SNAP to follow parental H3.3 or H3.1 as described in Figure 2. We used three different chase times: 0h, 24h and 48h (equivalent to tracking global, 24h-old and 48h-old histones).

B. Standard epifluorescence images of histones H3.3 or H3.1 after a chase of 0h, 24h and 48h. DAPI stains nuclei. Scale bars represent 10  $\mu\text{m}$ .

C. The plots show the quantification of the fluorescence for H3.3 or H3.1 after different chase times. Dashed lines correspond to how the signal would decrease by cell division-dependent dilution only, determined using the growth rate of each cell line HeLa H3.3- and H3.1-SNAP.

Figure 6

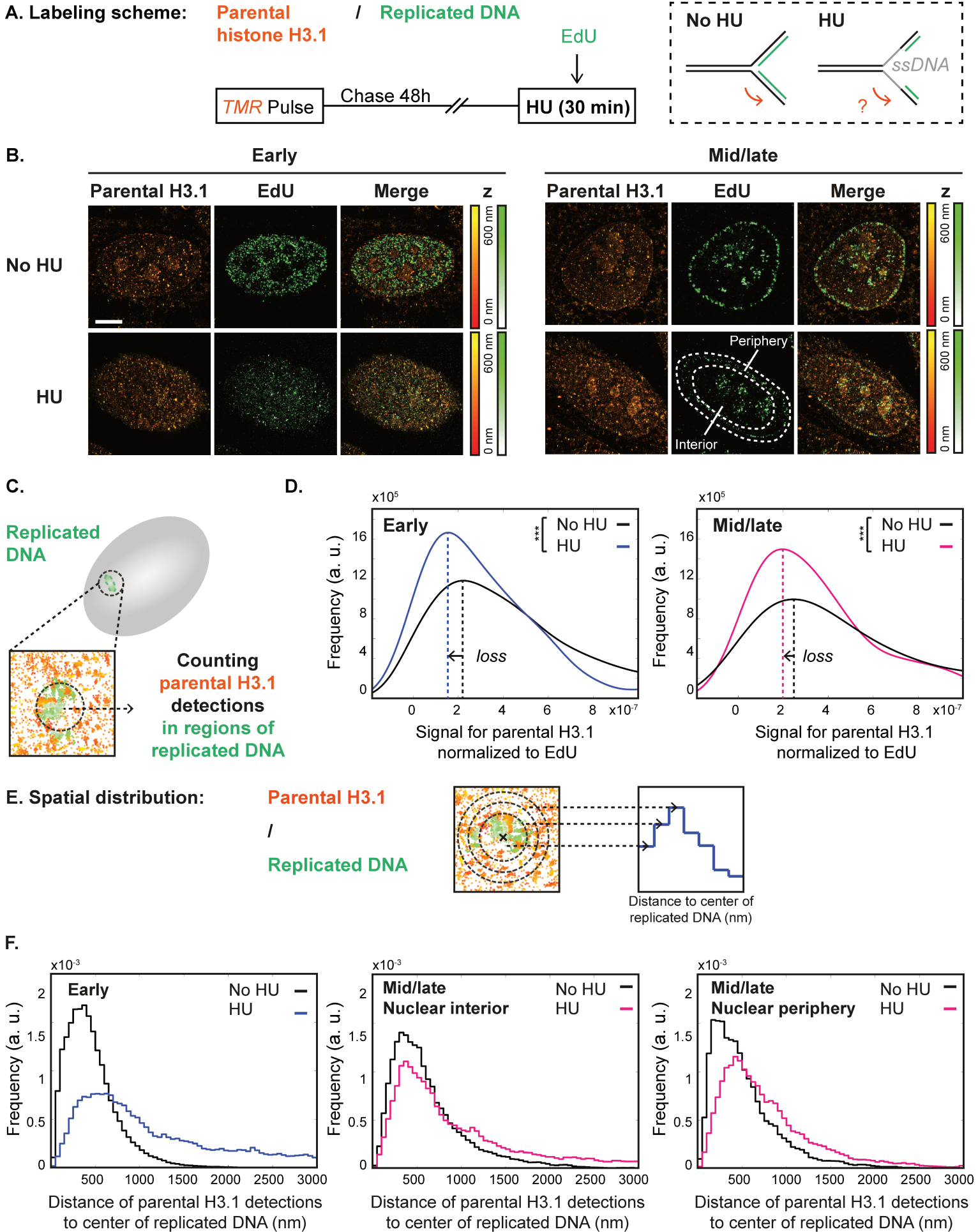


Figure 6 – Effect of hydroxyurea treatment on parental H3.1 recycling at replication sites.

A. Labeling scheme using H3.1-SNAP to follow parental or H3.1 as described in Figure 2. In addition, we perform a 30 min hydroxyurea (HU) treatment prior to fixation. The dashed box depicts DNA at the replication fork with or without HU treatment: parental DNA (black), newly synthesized DNA (green), or single-stranded DNA (grey).

B. Representative STORM images of parental H3.1 (TMR, orange) and replicated DNA (EdU, green) in HeLa H3.1-SNAP in early and mid/late S phase. The color gradient corresponds to the z range. Scale bars represent 5  $\mu\text{m}$ .

C. Calculation method for the signal for parental H3.1 normalized to EdU: in regions of replicated DNA, we counted parental H3.1 detections and normalized to the EdU detections and the total parental H3.1 detections in the nucleus.

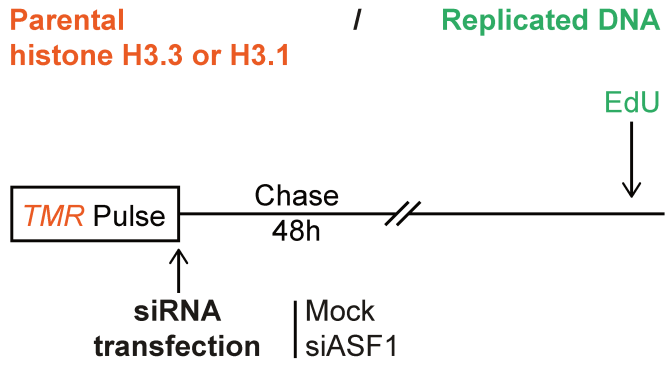
D. Distribution of the signal for parental H3.1 (right) normalized to EdU in early S phase in control (No HU, black) and HU-treated cells (HU, blue or pink) in early (left) or mid/late (right) S phase cells. In the No HU condition, N=10 cells for early S and N=9 cells for mid/late S. In the HU condition, N=8 cells for early S and N=10 cells for mid/late S. p-values (using a Mann-Whitney-Wilcoxon test): (\*\*\*)  $p \leq 0.001$ ; (\*\*)  $p \leq 0.01$ ; (\*)  $p \leq 0.05$ ; (ns) not significant.

E. Analysis method for the spatial distribution of parental H3.1 relative to replicated DNA. For each region of replicated DNA, we defined 50 nm wide concentric zones centered on the center of gravity of the replicated DNA site. We assigned surrounding detections of parental H3.1 to zones based on their distance to the center. The number of detections counted in each region was normalized to the volume of the corresponding region.

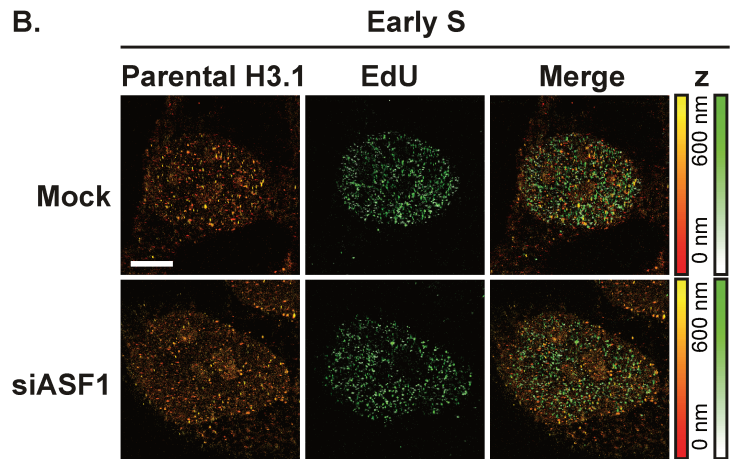
F. Spatial distribution of parental H3.1 relative to replicated DNA. The plots show the distributions of the distances of parental H3.1 to the center of replicated DNA sites for control (black) and HU-treated cells (blue or pink) in early S phase cells (left), interior of mid/late S phase cells (middle), and periphery of mid/late S phase cells (right).

Figure 7

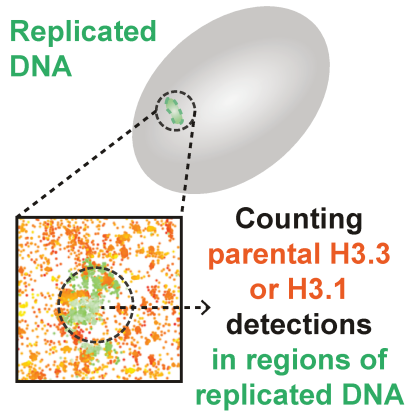
A. Labeling scheme



B.



C.



D. Early S

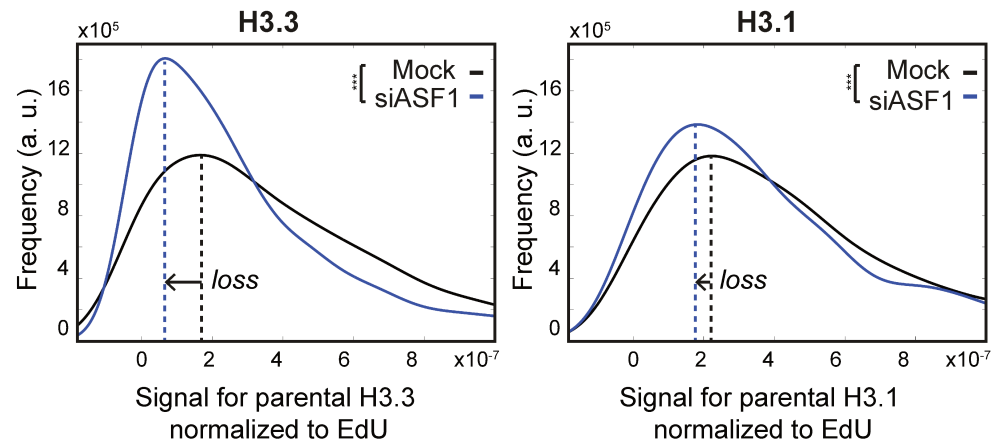


Figure 7 – Effect of ASF1 depletion on the recycling of parental H3.3 and H3.1 at replicated DNA regions

A. Labeling scheme using H3.3- or H3.1-SNAP to follow parental H3.3 or H3.1 as described in Figure 2. In addition, we perform a siRNA transfection (mock or against ASF1) immediately following the TMR pulse labeling histones and prior to the 48h-chase.

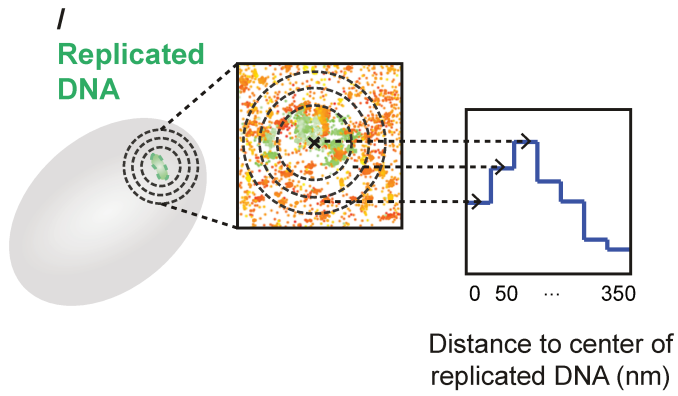
B. Representative STORM images of parental H3.1 (TMR, orange) and replicated DNA (EdU, green) in HeLa H3.1-SNAP in early S phase. The color gradient corresponds to the z range. Scale bars represent 5  $\mu\text{m}$ .

C. Calculation method for the signal for parental H3.3/1 normalized to EdU as described in Figure 6C.

D. The plot shows the distribution of the signal for parental H3.3 (left) or H3.1 (right) normalized to EdU in early S phase in control (mock, black) and ASF1-depleted cells (siASF1, blue). For H3.3, in the mock condition, N=11 cells, and in the siASF1 condition, N=10 cells. For H3.1, in the mock condition, N=10 cells, and in the siASF1 condition, N=10 cells. p-values (using a Mann-Whitney-Wilcoxon test): (\*\*\*)  $p \leq 0.001$ ; (\*\*)  $p \leq 0.01$ ; (\*)  $p \leq 0.05$ ; (ns) not significant.

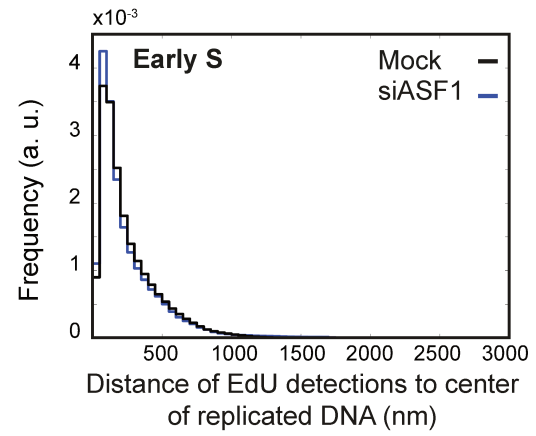
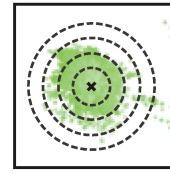
Figure 8

A. Parental H3.3 or H3.1 spatial distribution

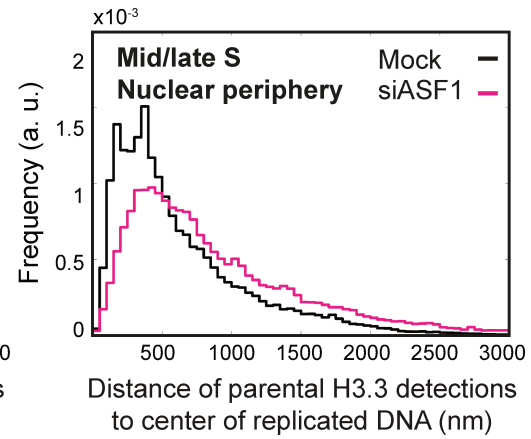
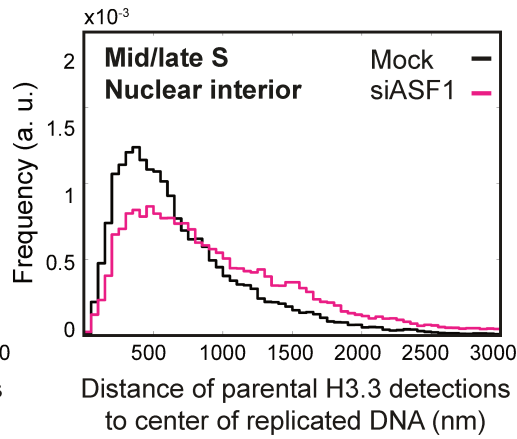
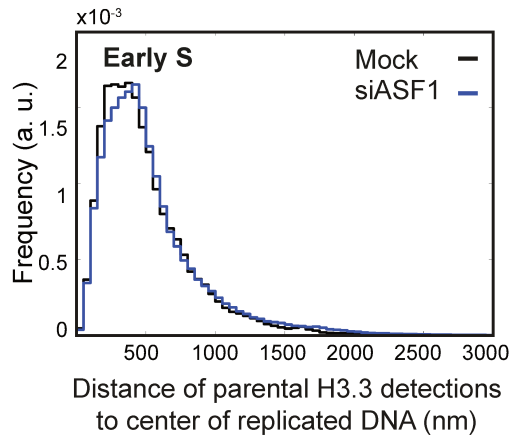


B. Control

EdU vs EdU



C. H3.3



D. H3.1

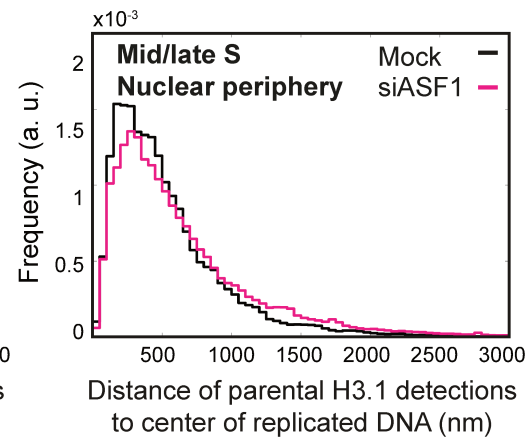
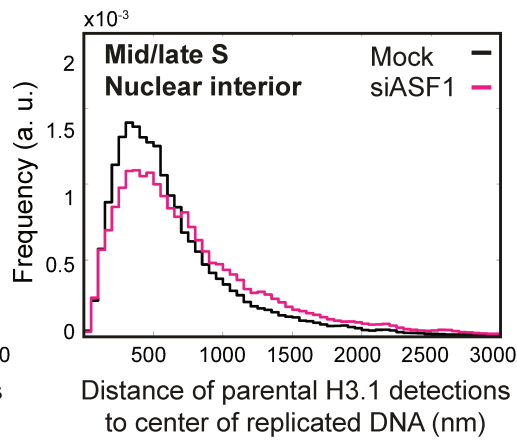
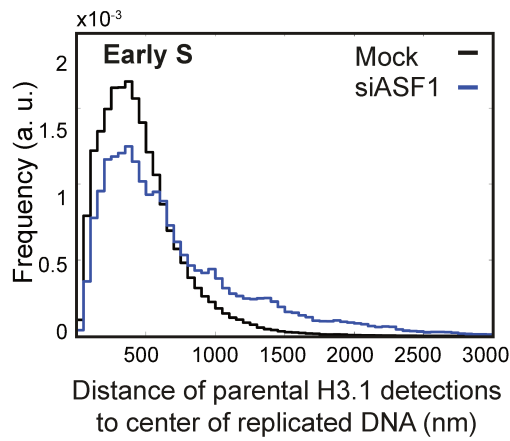


Figure 8 – Effect of ASF1 depletion on the spatial distribution of parental H3.3 and H3.1 throughout S phase

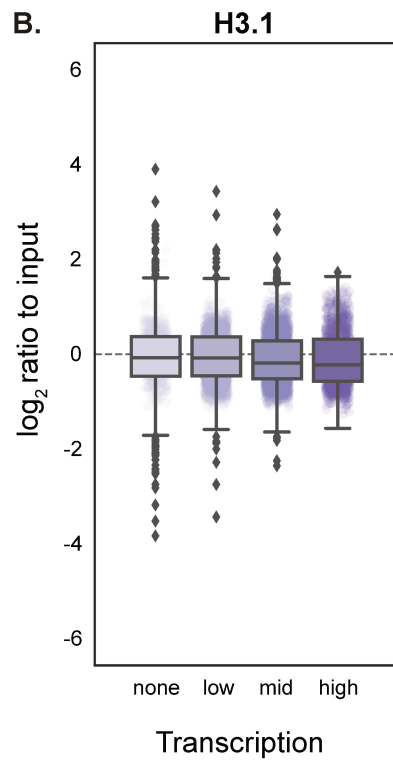
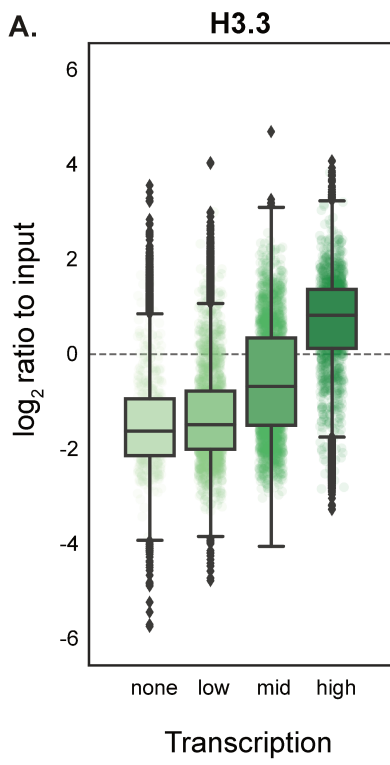
A. Analysis method for the spatial distribution of parental H3.3 and H3.1 relative to replicated DNA as described in Figure 6E.

B. Spatial distribution of EdU relative to replicated DNA. The plot shows the distribution of the distances of EdU detections to the center of replicated DNA sites for control (black) and ASF1-depleted (blue) early S phase cells. For B-D, the same cells were used as in Figure 7.

C. Spatial distribution of parental H3.3 relative to replicated DNA. The plots show the distributions of the distances of parental H3.3 to the center of replicated DNA sites for control (black) and ASF1-depleted cells (blue or pink) in early S phase cells (left), interior of mid/late S phase cells (middle), and the periphery of mid/late S phase cells (right).

D. Spatial distribution of parental H3.1 relative to replicated DNA. The plots show the distributions of the distances of parental H3.1 to the center of replicated DNA sites for control (black) and ASF1-depleted cells (blue or pink) in early S phase cells (left), interior of mid/late S phase cells (middle), and the periphery of mid/late S phase cells (right).

Supplementary Figure 1



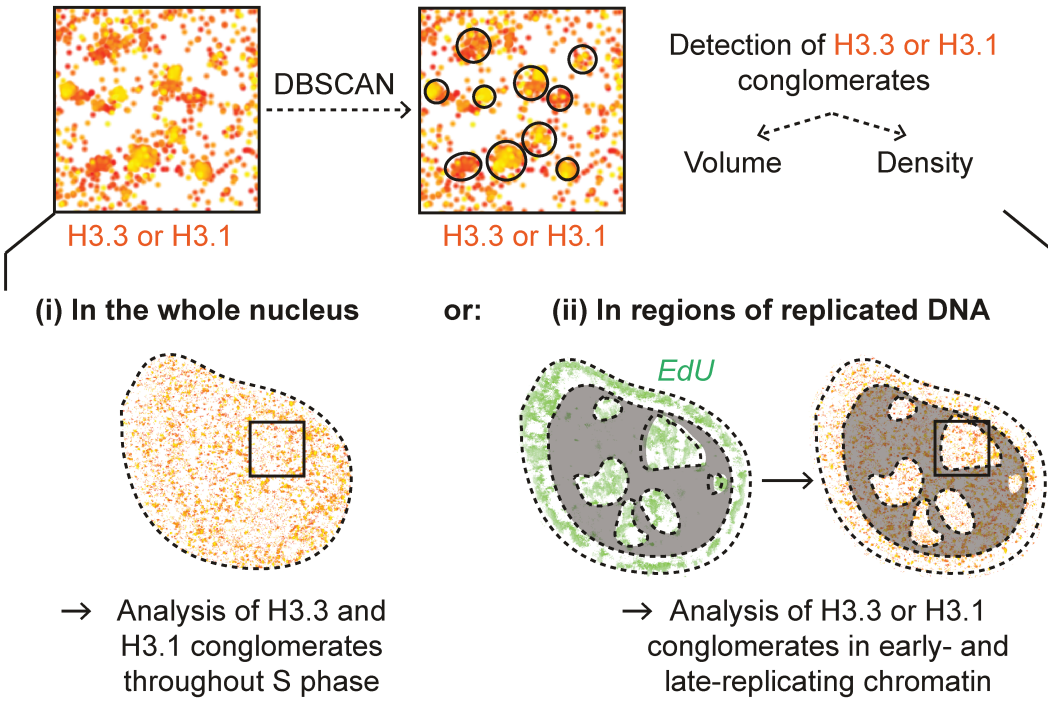
### Supplementary Figure 1

A. H3.3 distribution by transcription levels. For A and B, the box plots show, respectively, the distribution of H3.3 and H3.1 log<sub>2</sub> ratios to input (y-axis) at 10 kb regions ranked by transcriptional status (x-axis). The rank reflects the level of nascent transcription, from none to low (lower 10<sup>th</sup> percentile), mid (10<sup>th</sup> to 90<sup>th</sup> percentile) or high (upper 10<sup>th</sup> percentile) (highlighted with increasingly darker colors).

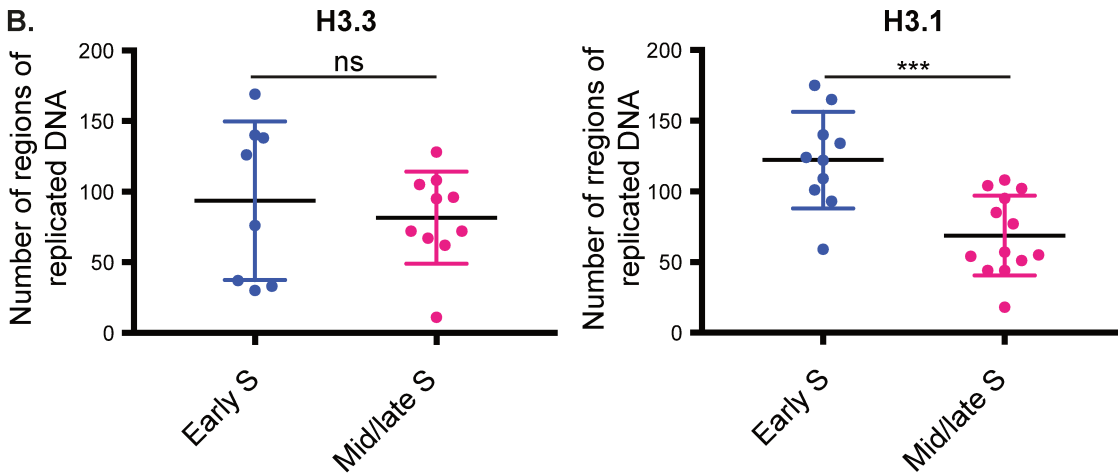
B. H3.1 distribution by transcription levels.

Supplementary Figure 2

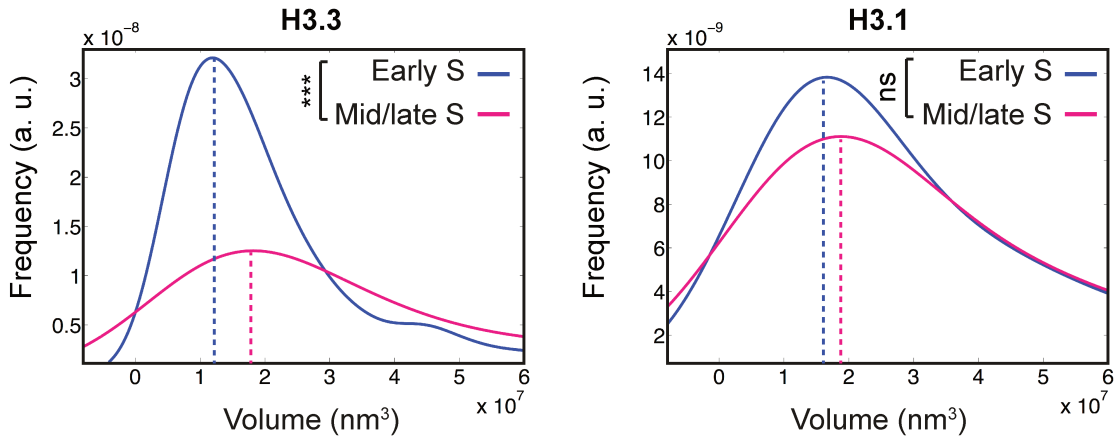
A. Data analysis



B.



C.



## Supplementary Figure 2

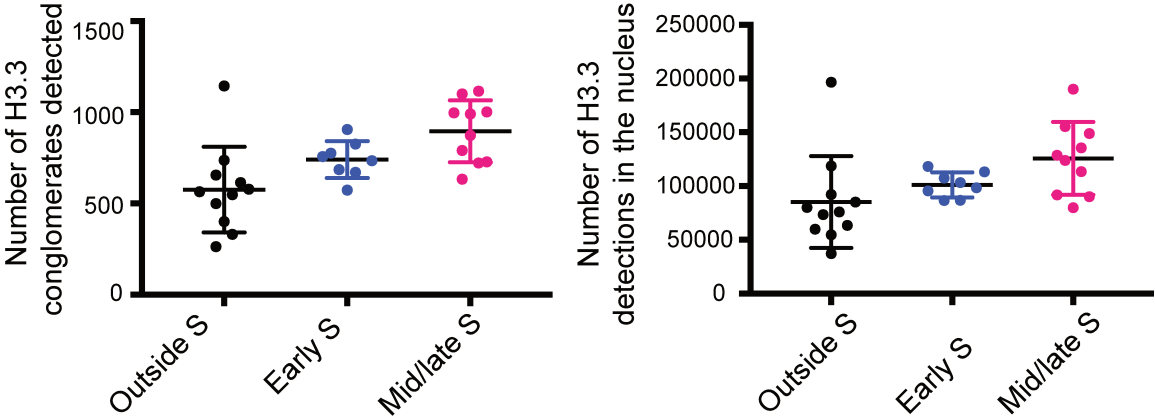
A. Analysis of the H3.3 or H3.1 signal. The DBSCAN clustering algorithm groups together detections with enough neighbors in a given radius. We refer to the isolated clusters as H3.3 or H3.1 conglomerates. We analyze the volume and density of these conglomerates.

B. Number of regions or replicated DNA detected using the DBSCAN approach applied to the EdU signal in our HeLa H3.3- (left) or H3.1-SNAP (right) cell lines. Error bars represent standard deviation. p-values (using a t test): (\*\*\*)  $p \leq 0.001$ ; (\*\*)  $p \leq 0.01$ ; (\*)  $p \leq 0.05$ ; (ns) not significant.

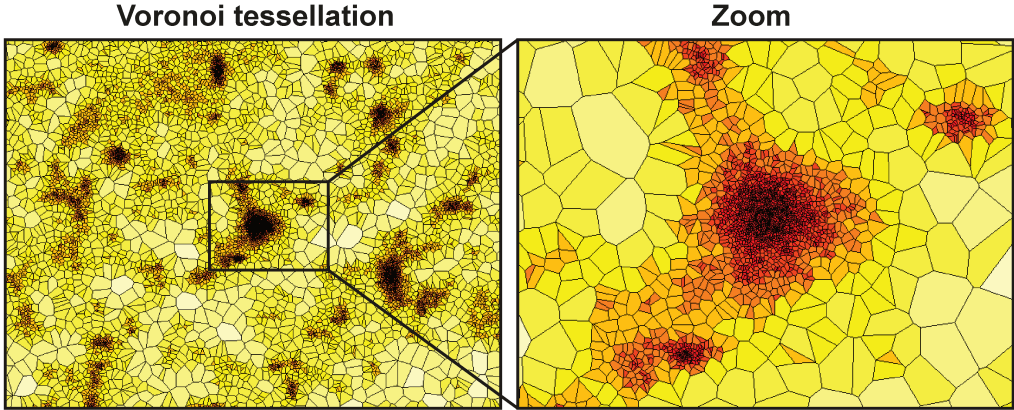
C. The plots show the distribution of volumes of regions of replicated DNA in our HeLa H3.3- (left) or H3.1-SNAP (right) cell lines. Error bars represent standard deviation. p-values (using a Mann-Whitney-Wilcoxon test): (\*\*\*)  $p \leq 0.001$ ; (\*\*)  $p \leq 0.01$ ; (\*)  $p \leq 0.05$ ; (ns) not significant.

Supplementary Figure 3

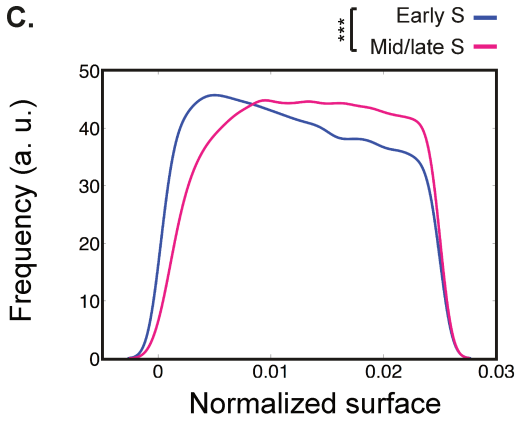
A.



B.



C.



Supplementary Figure 3

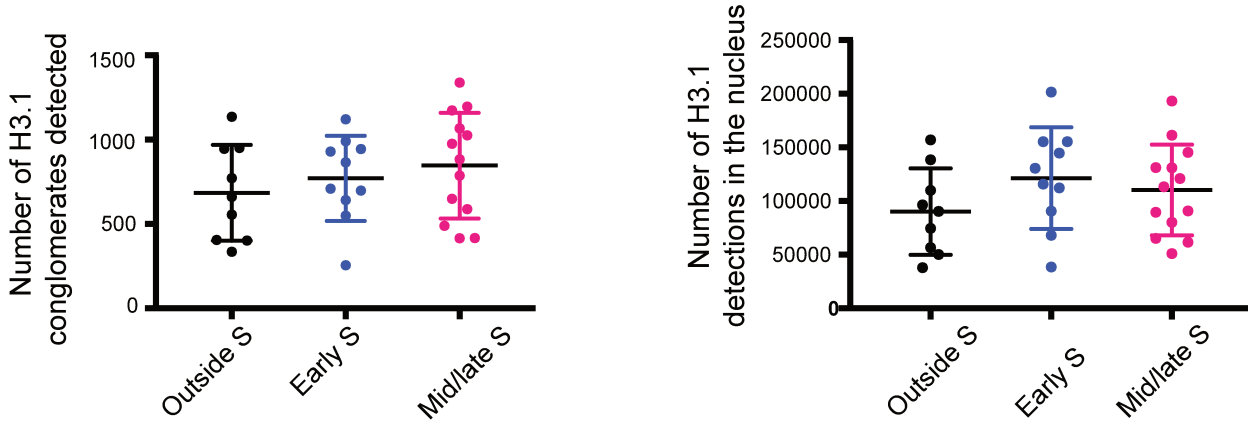
A. (Left) Number of H3.3 conglomerates detected; (right) total number of H3.3 detections in the nucleus. 20 000 frames were used. Error bars represent standard deviation.

B. Voronoi tessellation of STORM data. This partitions the signal into polygons such that each polygon contains a single detection. Large polygons (yellow) correspond to low-density regions and small polygons (dark red) correspond to high-density regions.

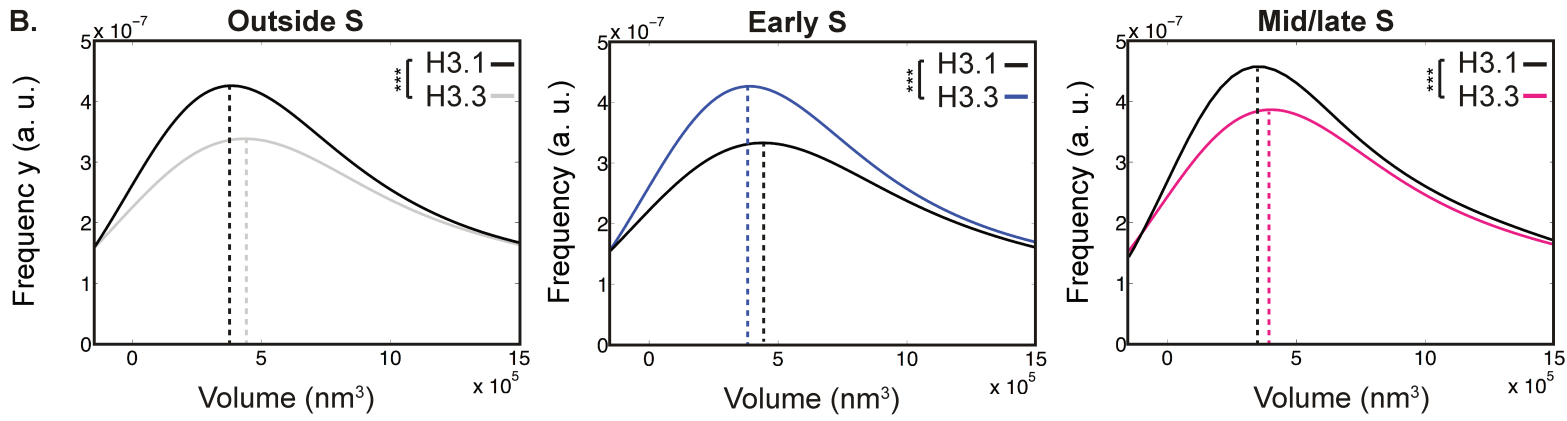
C. Voronoi surface analysis: the plot shows the distribution of small surfaces in cells in early S phase (blue) and in mid/late S phase (magenta). For early S, N=8 cells and, for mid/late S, N=10 cells. p-values (using a Mann-Whitney-Wilcoxon test): (\*\*\*)  $p \leq 0.001$ ; (\*\*)  $p \leq 0.01$ ; (\*)  $p \leq 0.05$ ; (ns) not significant.: (\*\*\*)  $p \leq 0.001$ ; (\*\*)  $p \leq 0.01$ ; (\*)  $p \leq 0.05$ ; (ns) not significant.

Supplementary Figure 4

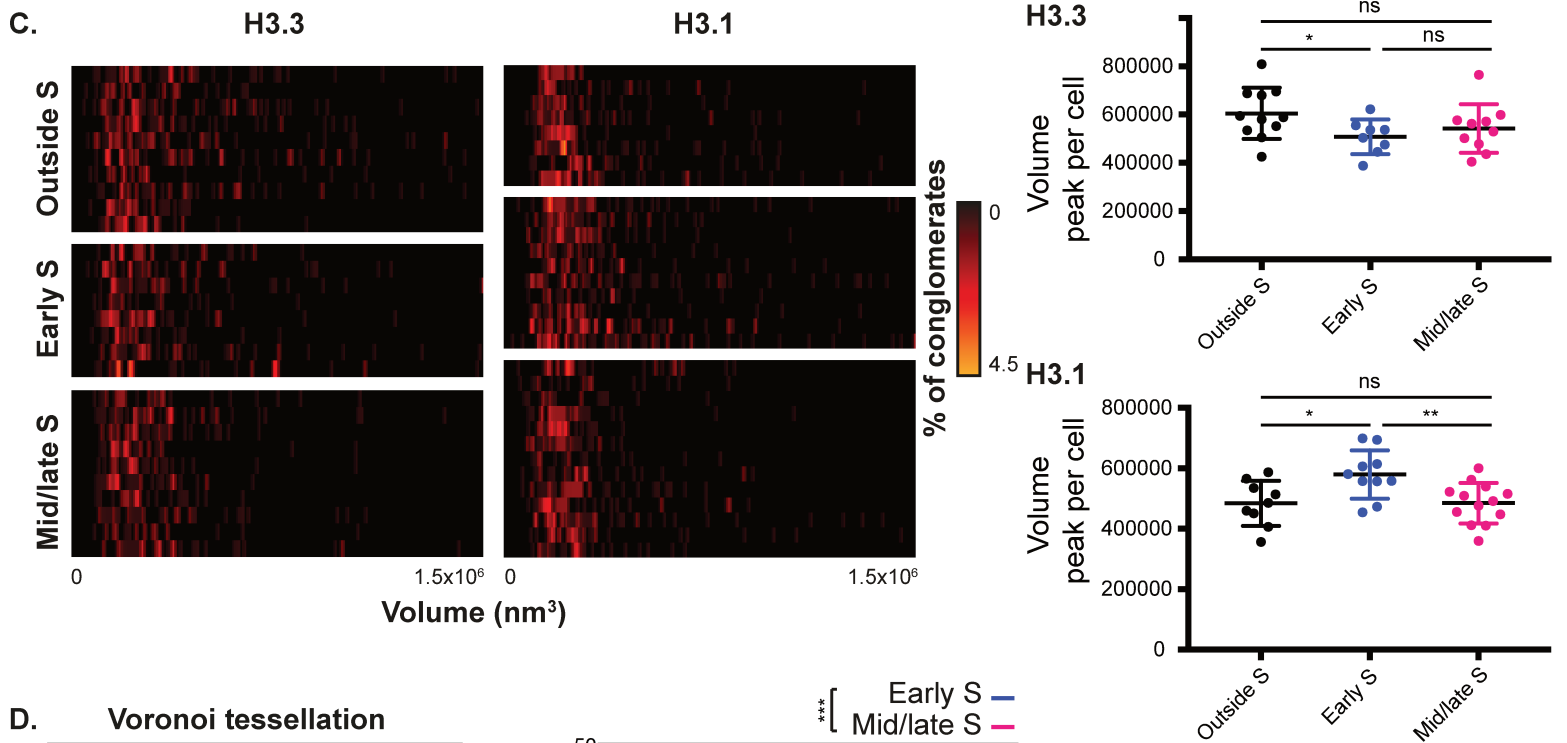
A.



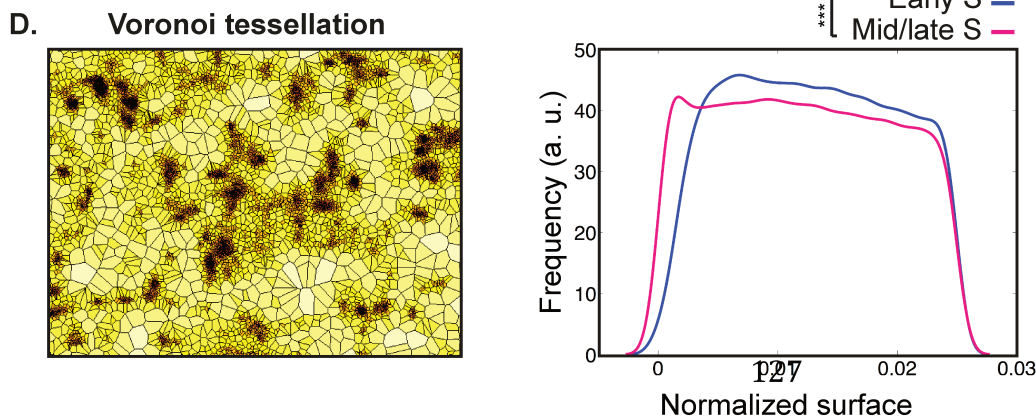
B.



C.



D.



Supplementary Figure 4

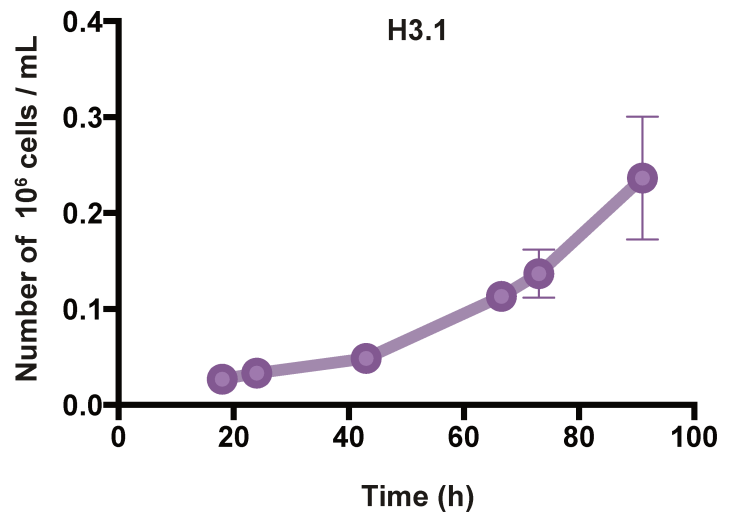
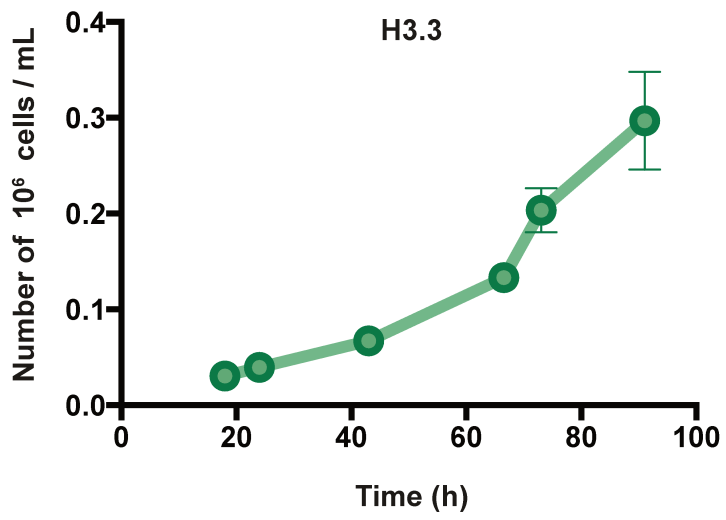
A. (Left) Number of H3.1 conglomerates detected; (right) total number of H3.1 detections in the nucleus. 20 000 frames were used. Error bars represent standard deviation.

B. The plots show the distributions of the volume of H3.3 or H3.1 conglomerates in cells outside S phase (left), in early S phase (middle), and in mid/late S phase (right).

C. Conglomerate volume distributions in individual cells. (Left) Each row represents a single cell where the percentage of conglomerates falling in every 7500 nm<sup>3</sup> bin was calculated and normalized for display. Heatmaps are unsorted within each group. (Right) Scatter plot of the corresponding volume peaks cell by cell. Error bars represent standard deviation. p-values (using a t test): (\*\*\*) p≤0.001; (\*\*) p≤ 0.01; (\*) p≤ 0.05; (ns) not significant. Error bars represent standard deviation.

D. (Left) Voronoi tessellation of STORM data. This partitions the signal into polygons such that each polygon contains a single detection. Large polygons (yellow) correspond to low-density regions and small polygons (dark red) correspond to high-density regions. (Right) Voronoi surface analysis: the plot shows the distribution of small surfaces in cells in early S phase (blue) and in mid/late S phase (magenta). For early S, N=10 cells and for mid/late S, 13 cells. p-values (using a Mann-Whitney-Wilcoxon test): (\*\*\*) p≤0.001; (\*\*) p≤ 0.01; (\*) p≤ 0.05; (ns) not significant. Error bars represent standard deviation.

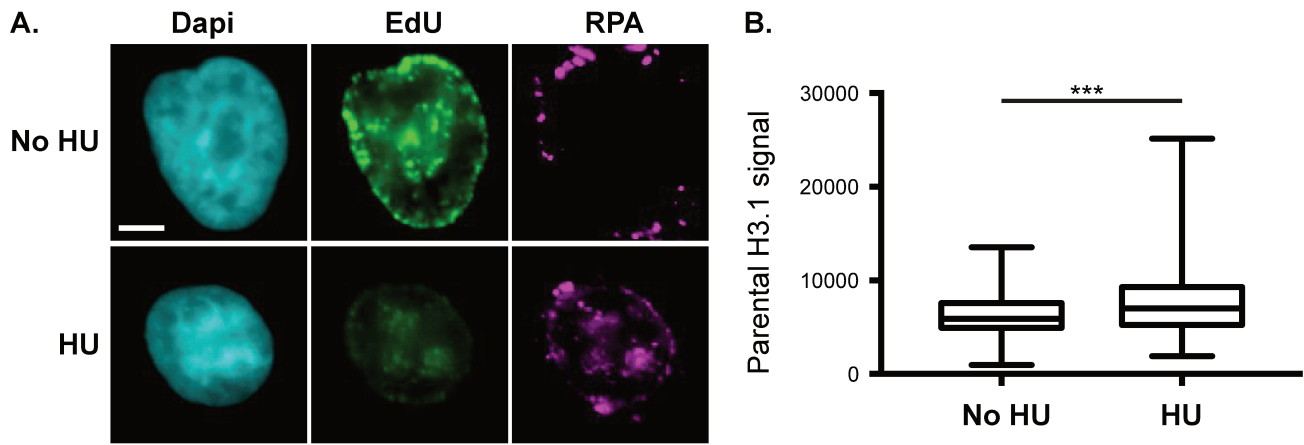
Supplementary Figure 5



Supplementary Figure 5

Growth curves corresponding to the two cell lines HeLa H3.3- and H3.1-SNAP. Error bars represent standard deviation. Three experimental replicates were used.

Supplementary Figure 6



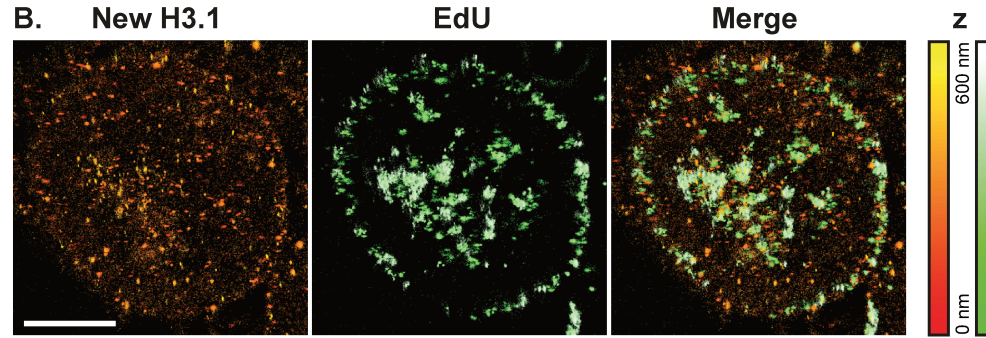
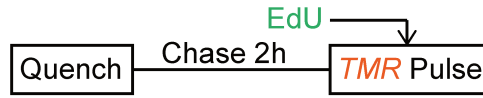
Supplementary Figure 6

A. RPA staining (magenta) and EdU staining (green) in control and HU-treated conditions, revealed by immunofluorescence. DAPI stains nuclei (cyan). The images were acquired using an epifluorescence microscope. Scale bars represent 5  $\mu\text{m}$ .

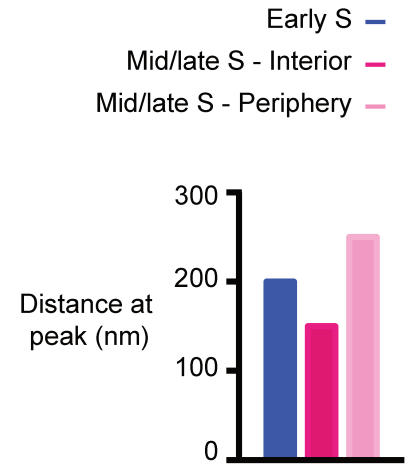
B. Quantification of parental H3.1 signal using epifluorescence microscopy in the control and HU-treated condition. p-values (using a t test): (\*\*\*)  $p \leq 0.001$ ; (\*\*)  $p \leq 0.01$ ; (\*)  $p \leq 0.05$ ; (ns) not significant.

# Supplementary Figure 7

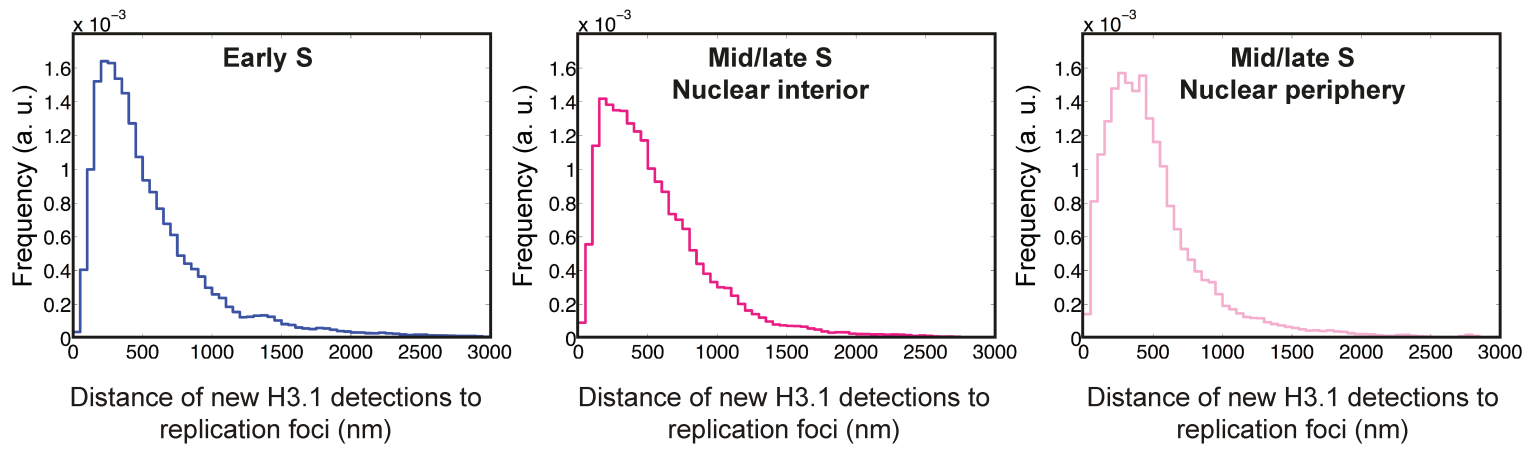
**A. Labeling scheme:** **New histones H3.1** / **Replicated DNA**



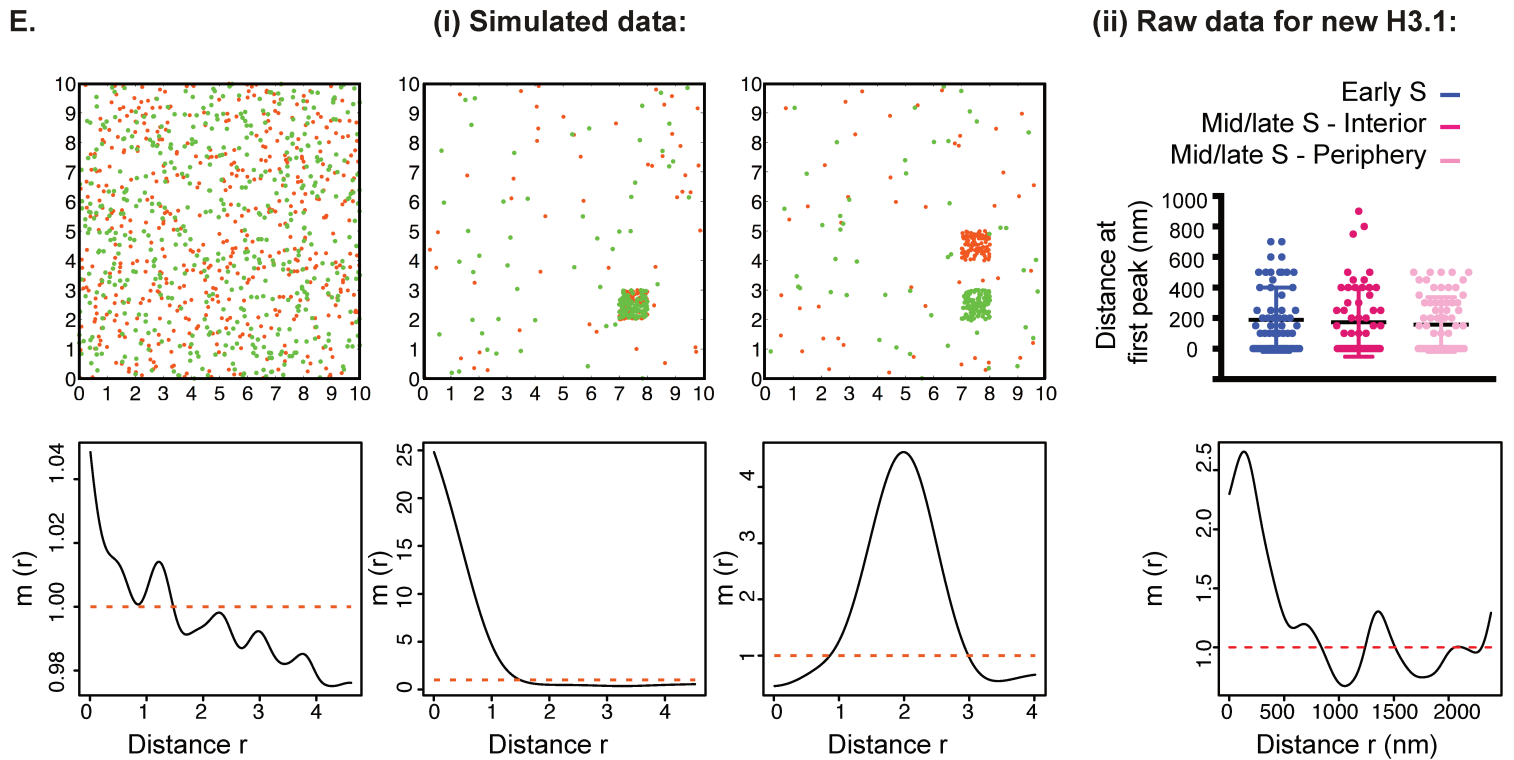
**D.**



**C.**



**E.**



### Supplementary Figure 7

A. Labeling scheme using H3.1-SNAP to follow new histones. A quench step labels all preexisting histones with a non-fluorescent dye. A chase step allows synthesis and deposition of new unlabeled H3.1-SNAP. A pulse using the fluorophore TMR (orange) labels H3.1-SNAP. The EdU labeling and triton extraction are as described in Figure 2.

B. Representative STORM images of new H3.1 (TMR, orange) and replicated DNA (EdU, green) in HeLa H3.1-SNAP. The color gradient corresponds to the z range. Scale bars represent 5  $\mu\text{m}$ .

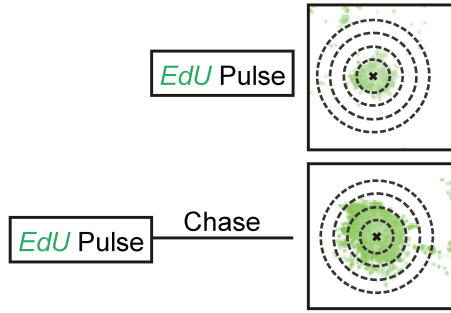
C. The plots show the distributions of the distances of new H3.1 to the center of replicated DNA in early S phase cells (left), mid/late S phase cells in the nuclear interior (middle), and mid/late S phase cells at the nuclear periphery (right).

D. Distance at the peak in the distribution plots in B for cells in early S phase (blue), mid/late S phase cells in the nuclear interior (dark pink), and at the nuclear periphery (light pink).

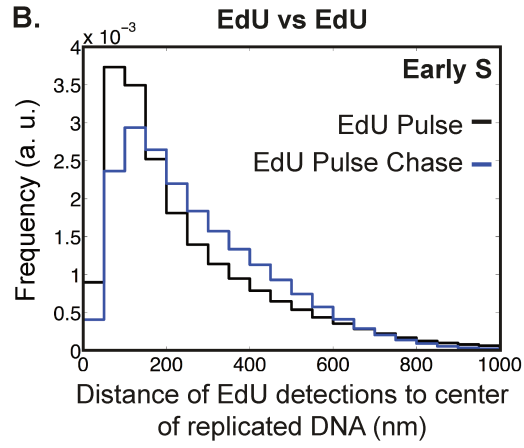
(i) (Top) Simulated data of two signals for (left) randomly distributed populations, (middle) two colocalizing signals, and (right) two signals at a fixed distance from each other. (Bottom) m function plotting the enrichment of the orange signal relating to the green in the three cases. Region of the graph above 1 (dashed orange line) indicates attraction. (ii) m function applied to the signal of new H3.1 and the signal of EdU. In each cell, we applied the function locally to 8 zones at the nuclear periphery and 8 zones in the nuclear interior. (Bottom) Example of m function for one zone. (Top) The scatter plot indicates the distance at the maximum of the first peak for each zone. Due to low signal in some zones, some m functions did not feature a peak of enrichment and were excluded. Error bars represent standard deviation.

# Supplementary Figure 8

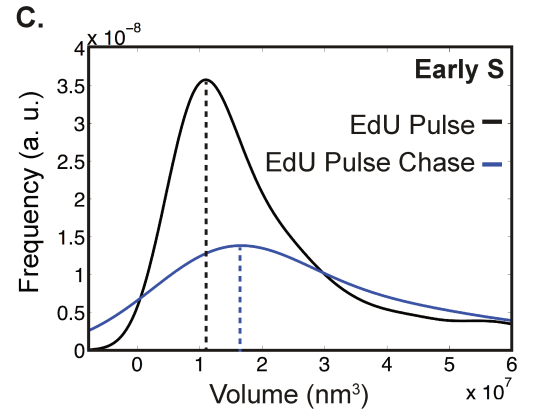
A.



B.



C.



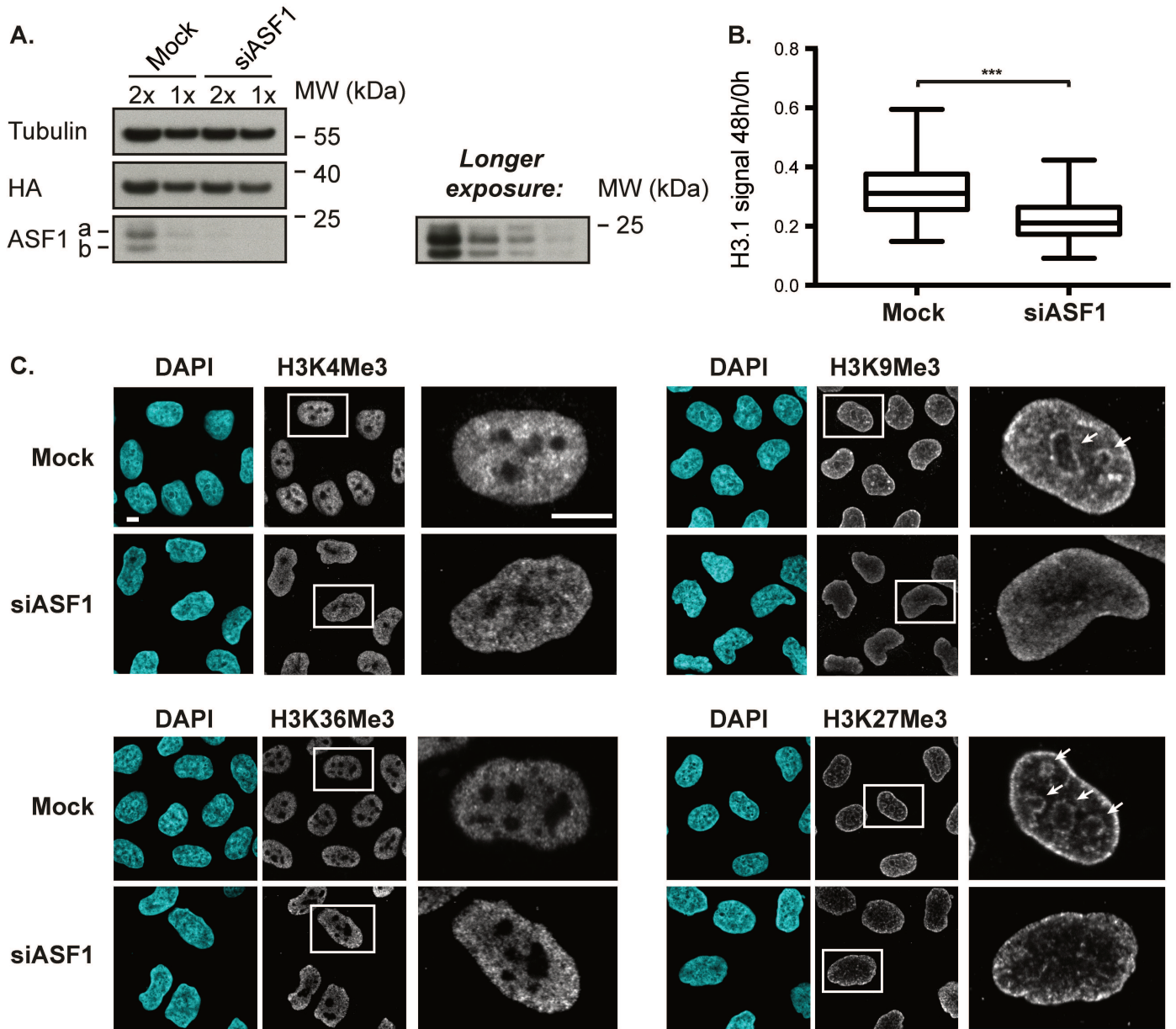
Supplementary Figure 8

A. Scheme of the experiment: we either performed a single EdU pulse (EdU pulse), or an EdU pulse followed by a 30 min-chase (EdU pulse-chase) in HeLa H3.1-SNAP.

B. Distribution plots of the distances of EdU detections to the center of replicated DNA for the EdU pulse (black) and EdU pulse-chase (blue) in early S phase cells.

C. The plot shows the distribution of the volume of regions of replicated DNA in cells for the EdU pulse (black) and EdU pulse-chase (blue) in early S phase cells.

Supplementary Figure 9



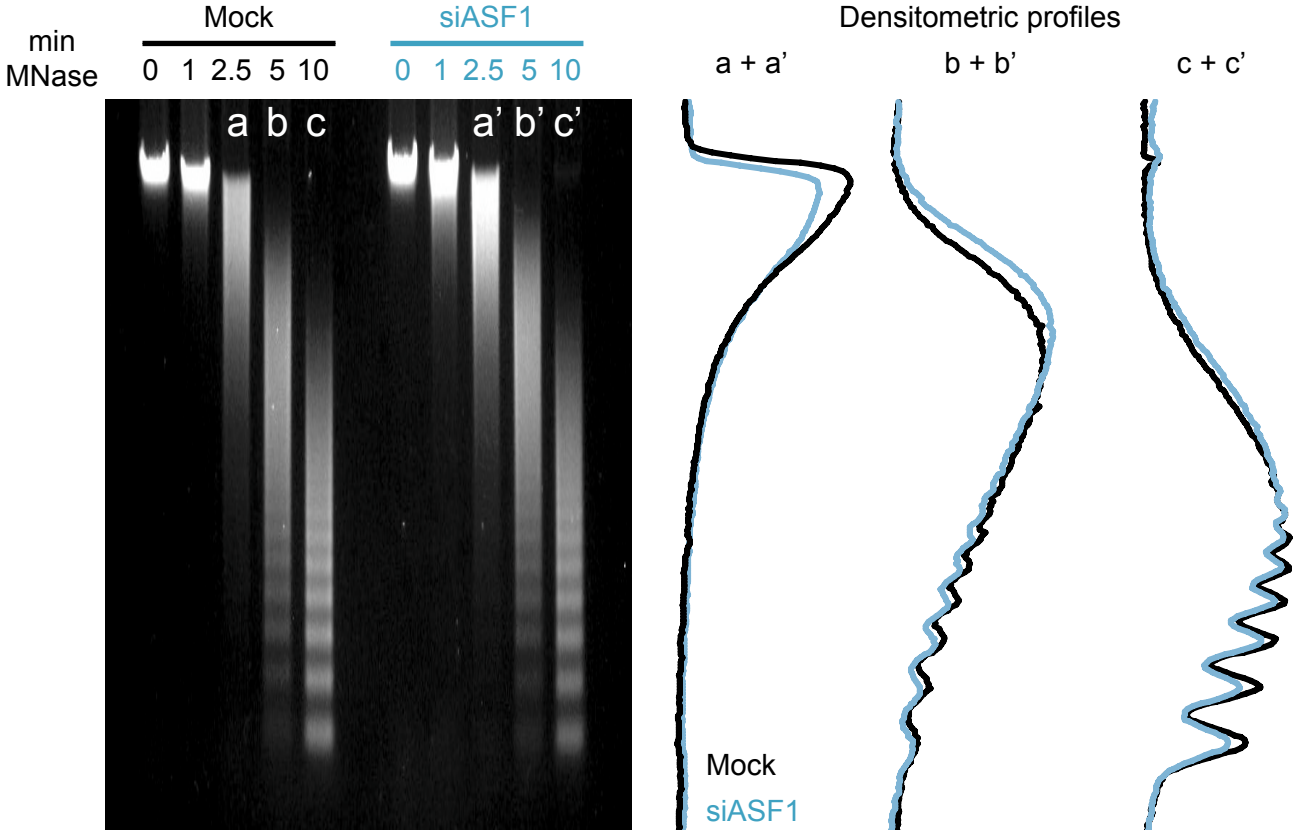
Supplementary Figure 9

A. Western Blot analysis of ASF1a and ASF1b knockdown efficiency using siRNA against ASF1. The SNAP H3.1 also contains a HA-tag, which was probed for in this Western Blot.

B. Ratio between the final (48h-chase after pulse, about two divisions) and the initial (0h after pulse) H3.1 signal in the whole nucleus in mock versus siASF1-transfected cells following a pulse-chase experiment in a synchronized population. An epifluorescence microscope was used. p-values (using a t test): (\*\*\*)  $p \leq 0.001$ ; (\*\*)  $p \leq 0.01$ ; (\*)  $p \leq 0.05$ ; (ns) not significant.

C. H3K4me3, H3K36me3, H3K27me3 and H3K9me3 staining (white) in control and ASF1-depleted conditions, revealed by immunofluorescence in HeLa H3.1-SNAP cells. DAPI stains nuclei (blue). The images were acquired using a confocal microscope. Scale bars represent 10  $\mu\text{m}$ .

Supplementary Figure 10



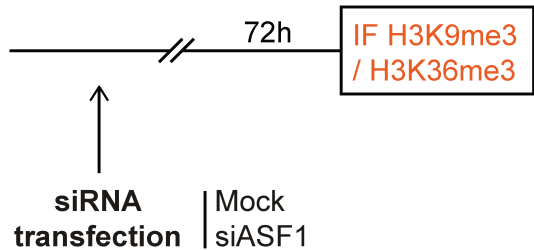
Supplementary Figure 10

MNase sensitivity analysis. Agarose gel electrophoresis of total DNA extracted from Mock or siASF1 cells after the indicated times of MNase treatment (left). Densitometric plots comparing digestion profiles at 2.5, 5 and 10 minutes of digestion show no change between the two conditions (right).

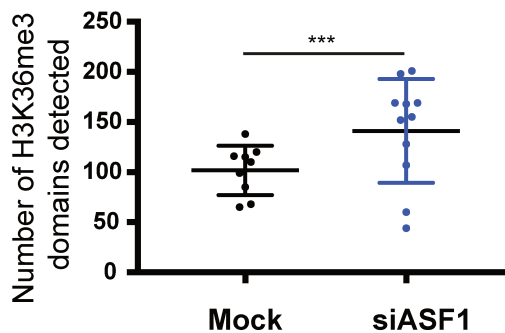
Supplementary Figure 11

A. Labeling scheme:

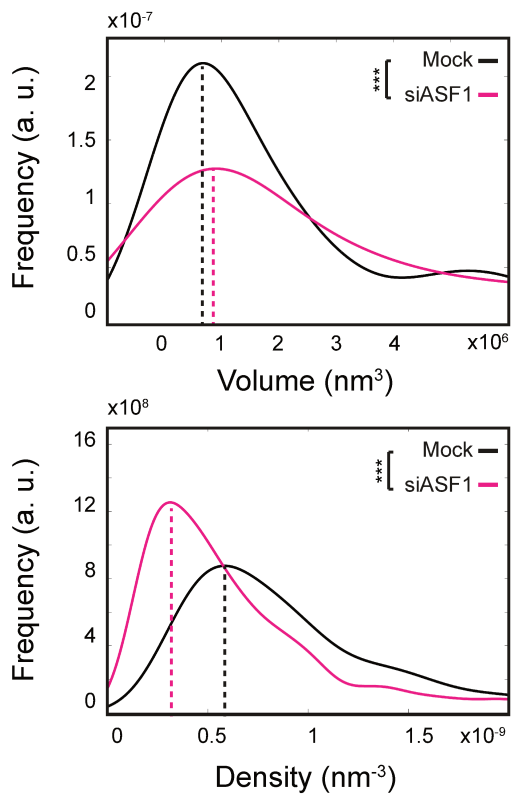
**Histone modification**



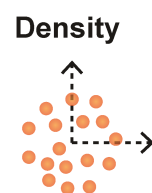
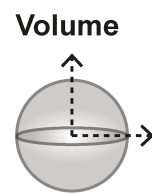
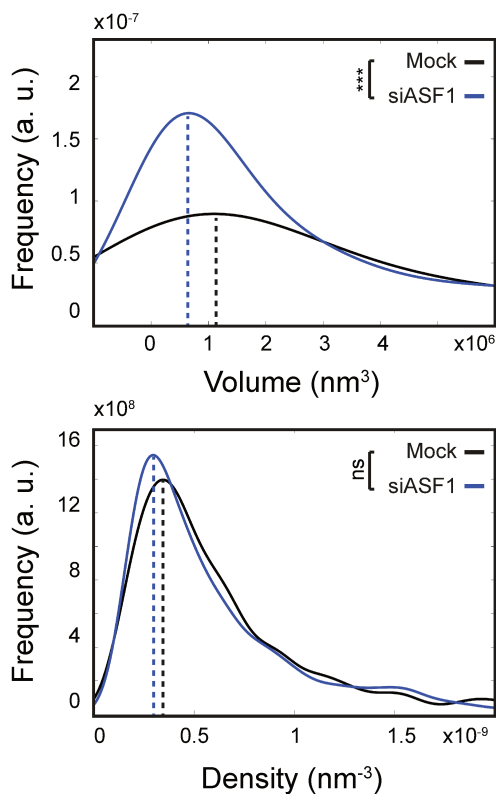
C.



B. H3K9me3



D. H3K36me3



Supplementary Figure 11

A. Labeling scheme for H3K9me3 and H3K36me3 stainings in HeLa H3.1-SNAP in upon siRNA treatment (mock or siASF1).

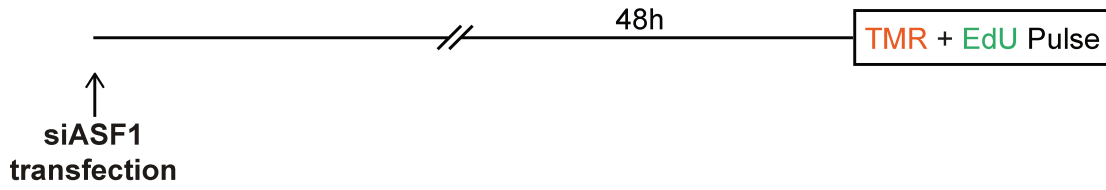
B. The plots show the distribution of volume (top) or density (bottom) of H3K9me3 domains in cells in early S phase in mock (N=4 cells) and ASF1-depleted cells (N=7 cells). For B and D, p-values (using a Mann-Whitney-Wilcoxon test): (\*\*\*)  $p \leq 0.001$ ; (\*\*)  $p \leq 0.01$ ; (\*)  $p \leq 0.05$ ; (ns) not significant. p-values (using a t test): (\*\*\*)  $p \leq 0.001$ ; (\*\*)  $p \leq 0.01$ ; (\*)  $p \leq 0.05$ ; (ns) not significant. Error bars represent standard deviation.

C. Number of H3K36me3 domains detected.

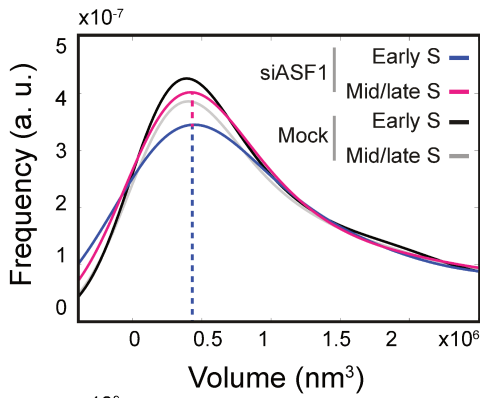
D. The plots show the distribution of volume (top) or density (bottom) of H3K36me3 domains in cells in early S phase in mock (N=9 cells) and ASF1-depleted cells (N=11 cells).

Supplementary Figure 12

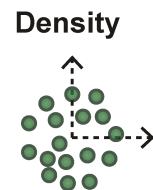
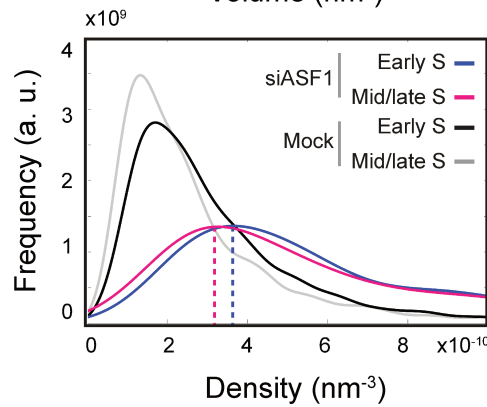
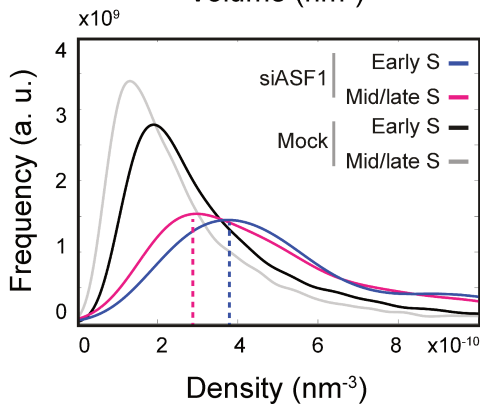
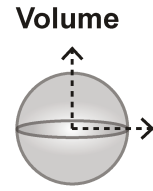
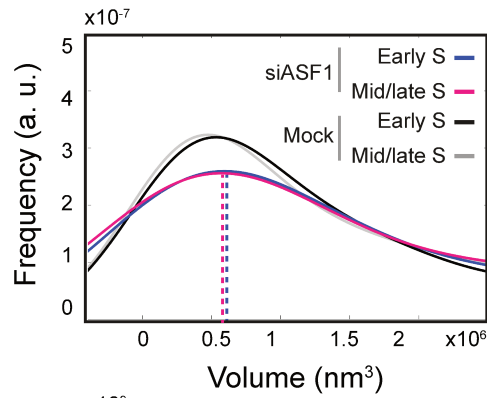
A. Labeling scheme: **Global histone H3.1/3** / **Replicated DNA**



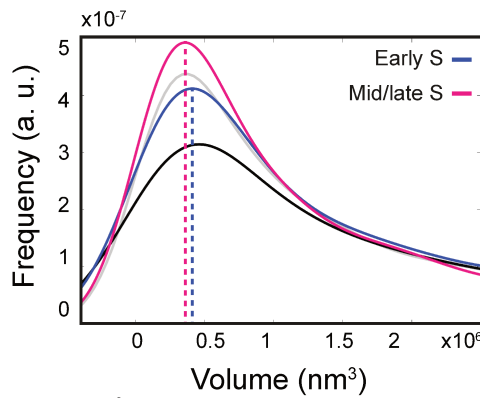
B. H3.3 Whole nucleus



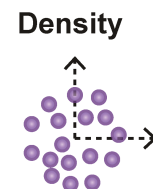
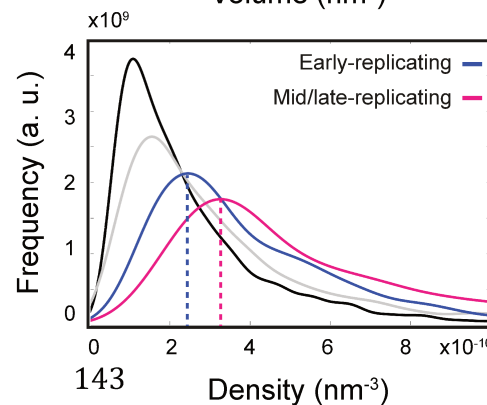
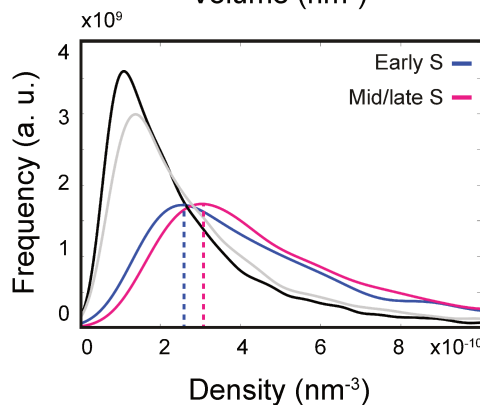
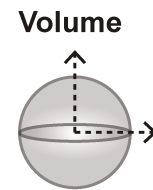
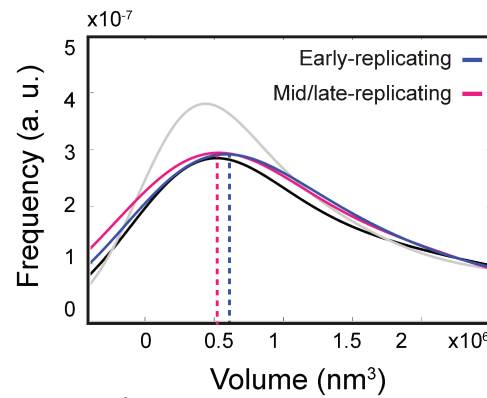
Replicated DNA



C. H3.1 Whole nucleus



Replicated DNA



## Supplementary Figure 12

Global distribution of H3.3/1 upon ASF1 depletion throughout S phase using STORM assay

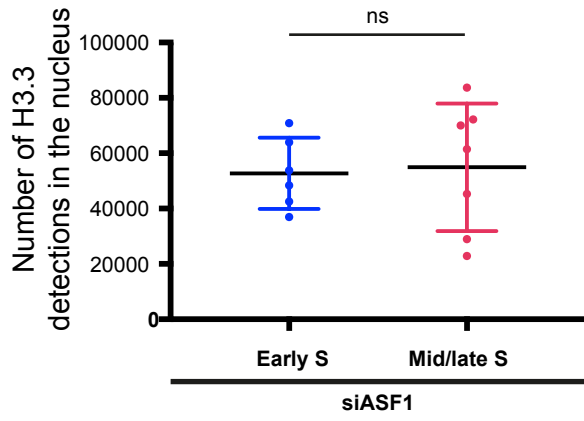
A. Labeling scheme using H3.3/1-SNAP to follow global H3.3/1 as described in Figure 2 upon siASF1 treatment.

B. (Left) For H3.3- conglomerates in the whole nucleus: the plots show the distribution of volume (top) or density (bottom) of H3.3 conglomerates in cells in early S phase (blue), and in mid/late S phase (magenta) upon ASF1 depletion or in the mock condition (black and grey for early and mid/late, respectively) as in Figure 3. (Right) For H3.3 conglomerates in regions of replicated DNA: the plots show the distribution of volume (top) or density (bottom) of H3.3 conglomerates in cells in early S phase (blue), and in mid/late S phase (magenta) upon ASF1 depletion or in the mock condition (black and grey for early and mid/late, respectively) as in Figure 3. N=6 and 7 cells for early S phase and mid/late S phase respectively upon ASF1 depletion.

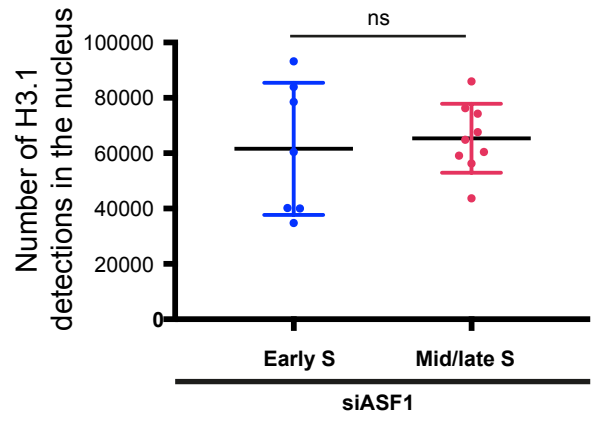
C. (Left) For H3.1- conglomerates in the whole nucleus: the plots show the distribution of volume (top) or density (bottom) of H3.1 conglomerates in cells in early S phase (blue), and in mid/late S phase (magenta) upon ASF1 depletion or in the mock condition (black and grey for early and mid/late, respectively) as in Figure 4. (Right) For H3.1 conglomerates in regions of replicated DNA: the plots show the distribution of volume (top) or density (bottom) of H3.1 conglomerates in cells in early S phase (blue), and in mid/late S phase (magenta) upon ASF1 depletion or in the mock condition (black and grey for early and mid/late, respectively) as in Figure 4. N=7 and 9 cells for early S phase and mid/late S phase respectively upon ASF1 depletion.

# Supplementary Figure 13

**A.**



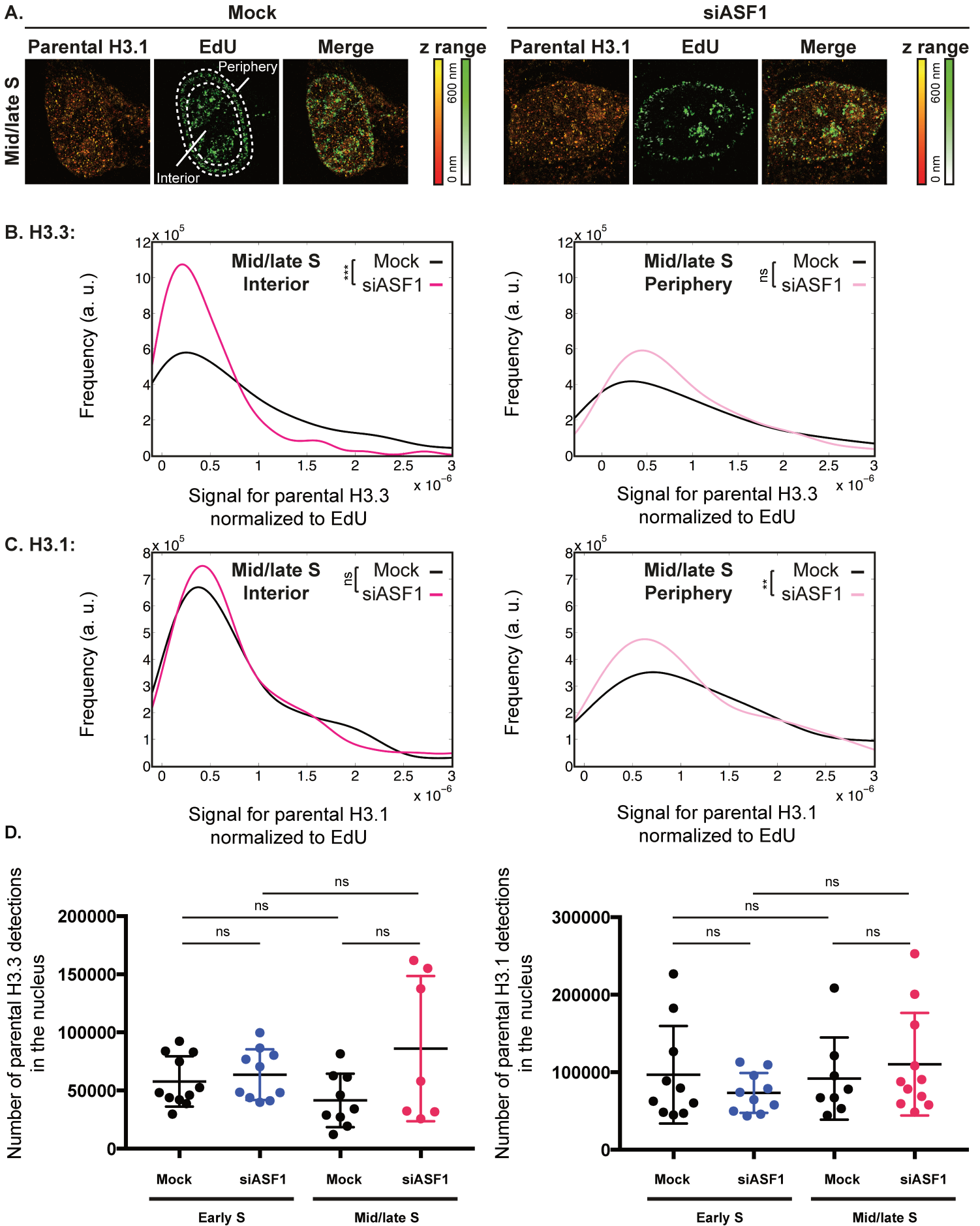
**B.**



### Supplementary Figure 13

Total number of H3.3 (left) or H3.1 (right) detections in the nucleus corresponding to the experiment described in Supplementary Figure 12. 5000 frames were used. p-values (using a t test): (\*\*\*)  $p \leq 0.001$ ; (\*\*)  $p \leq 0.01$ ; (\*)  $p \leq 0.05$ ; (ns) not significant. Error bars represent standard deviation.

Supplementary Figure 14



Supplementary Figure 14

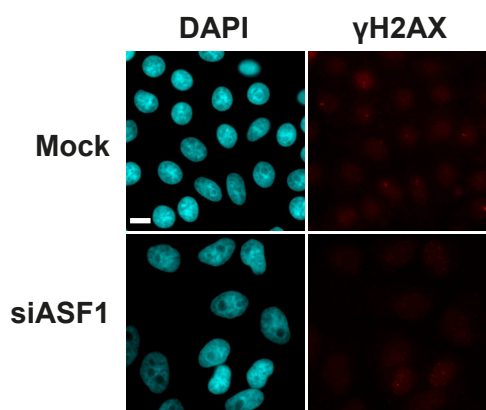
A. Representative STORM images of parental H3.1 (TMR, orange) and replicated DNA (EdU, green) in HeLa H3.1-SNAP in mid/late S phase. The color gradient corresponds to the z range. Scale bars represent 5  $\mu\text{m}$ .

B. The plots show the distributions of the signal for parental H3.3 normalized to EdU in mid/late S phase (left) in the nuclear interior in control (mock, black) and ASF1-depleted cells (siASF1, dark pink). And (right) at the nuclear periphery in control (mock, black) and ASF1-depleted cells (siASF1, light pink). In the mock condition, N=9 cells, and in the siASF1 condition, N=7 cells. For B and C, p-values (using a Mann-Whitney-Wilcoxon test): (\*\*\*)  $p \leq 0.001$ ; (\*\*)  $p \leq 0.01$ ; (\*)  $p \leq 0.05$ ; (ns) not significant.

C. The plots show the distributions of the signal for parental H3.1 normalized to EdU in mid/late S phase (left) in the nuclear interior in control (mock, black) and ASF1-depleted cells (siASF1, dark pink) and (right) at the nuclear periphery in control (mock, black) and ASF1-depleted cells (siASF1). In the mock condition, N=8 cells, and in the siASF1 condition, N=11 cells.

D. Total number of parental H3.3 (left) or H3.1 (right) detections in the nucleus. p-values (using a t test): (\*\*\*)  $p \leq 0.001$ ; (\*\*)  $p \leq 0.01$ ; (\*)  $p \leq 0.05$ ; (ns) not significant. Error bars represent standard deviation.

Supplementary Figure 15

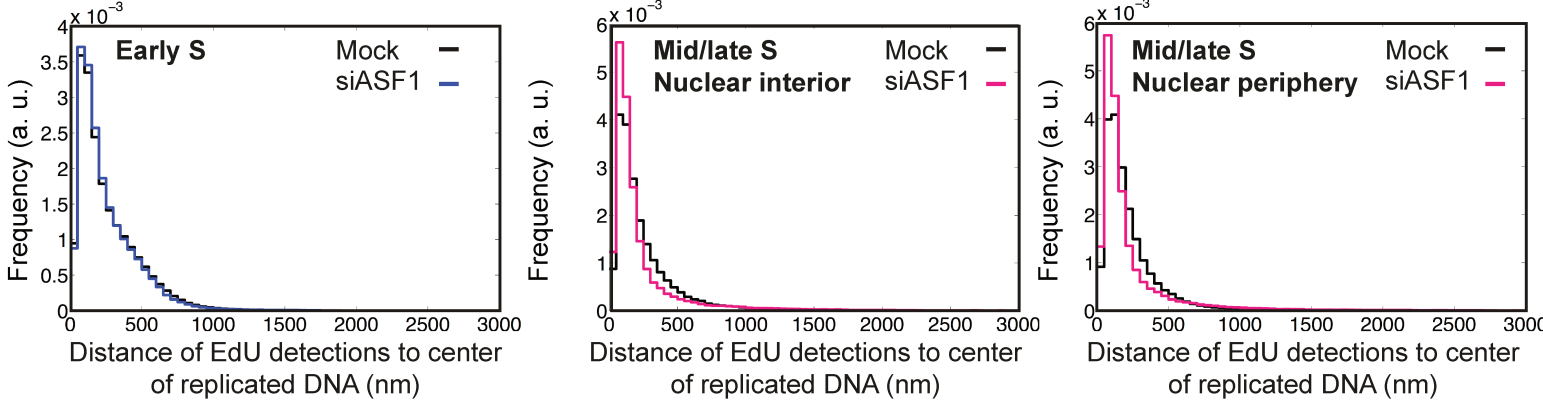


Supplementary Figure 15

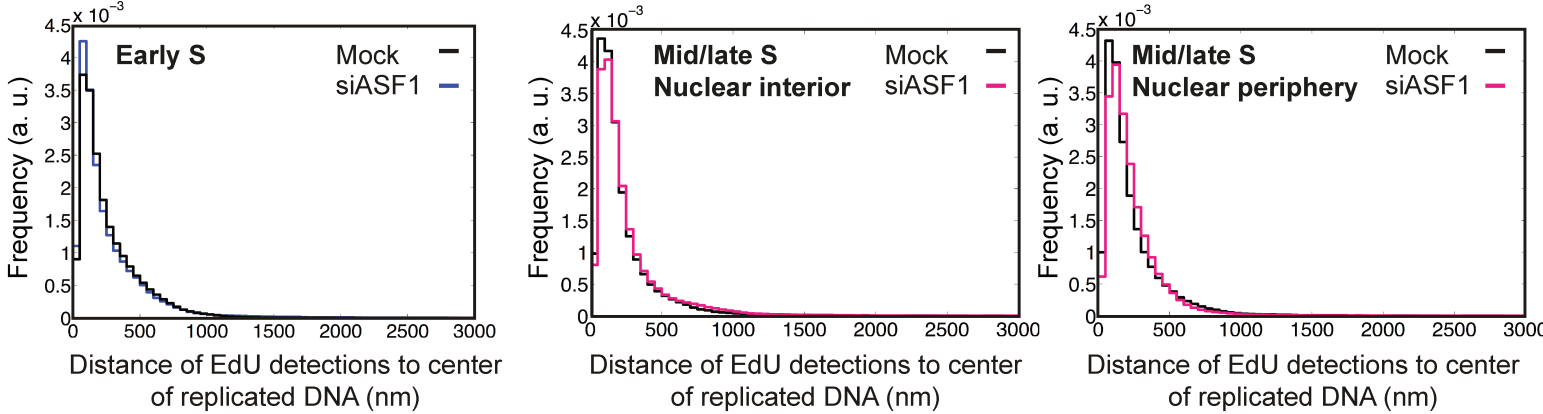
$\gamma$ H2AX staining (red) in control and ASF1-depleted conditions, revealed by immunofluorescence in HeLa H3.1-SNAP cells. DAPI stains nuclei (blue). The images were acquired using an epifluorescence microscope. Scale bars represent 10  $\mu$ m.

Supplementary Figure 16

A. H3.3



B. H3.1



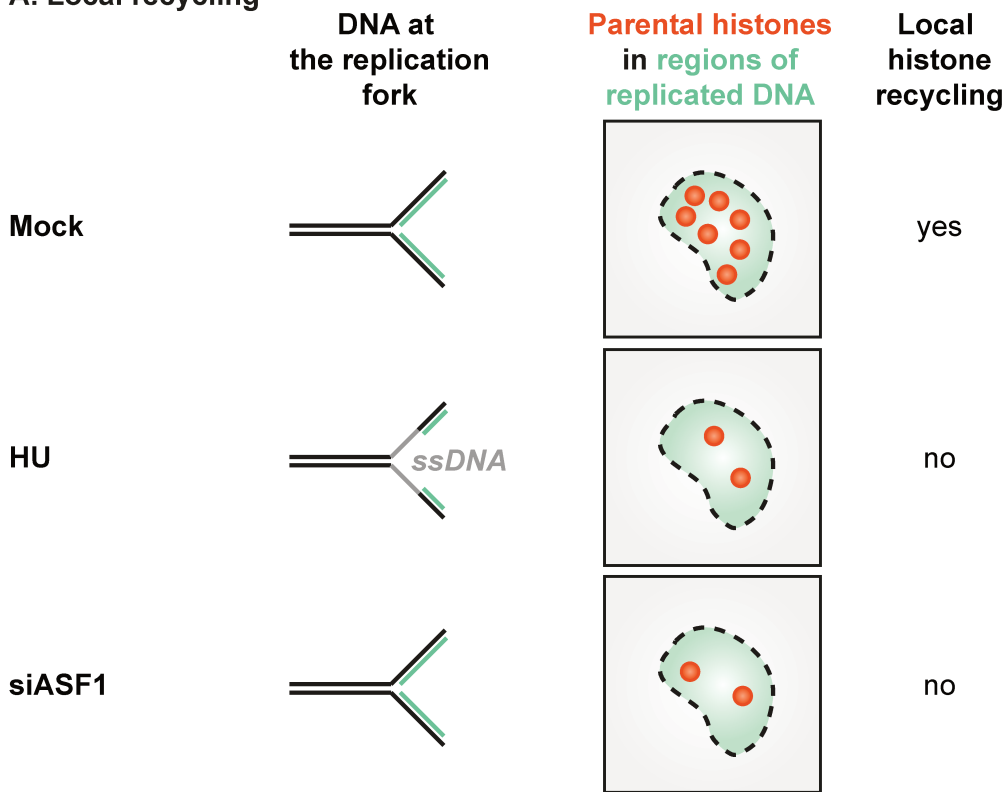
Supplementary Figure 16

A. Spatial distribution of EdU relative to replicated DNA corresponding to experiment described in Figure 8C in HeLa H3.3-SNAP. The plot shows the distribution of the distances of EdU detections to the center of replicated DNA sites for control (black) and ASF1-depleted (blue, pink) cells. The same cells were used as in Figure 8C.

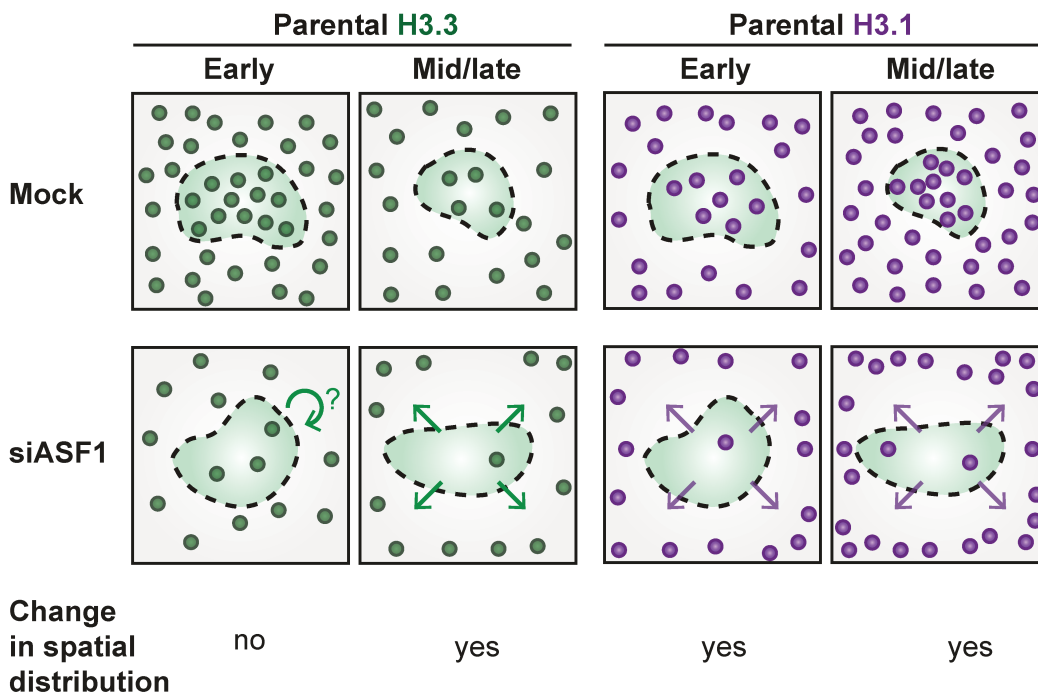
B. Spatial distribution of EdU relative to replicated DNA corresponding to experiment described in Figure 8D in HeLa H3.1-SNAP. The plot shows the distribution of the distances of EdU detections to the center of replicated DNA sites for control (black) and ASF1-depleted (blue, pink) cells. The same cells were used as in Figure 8D.

Supplementary Figure 17

A. Local recycling



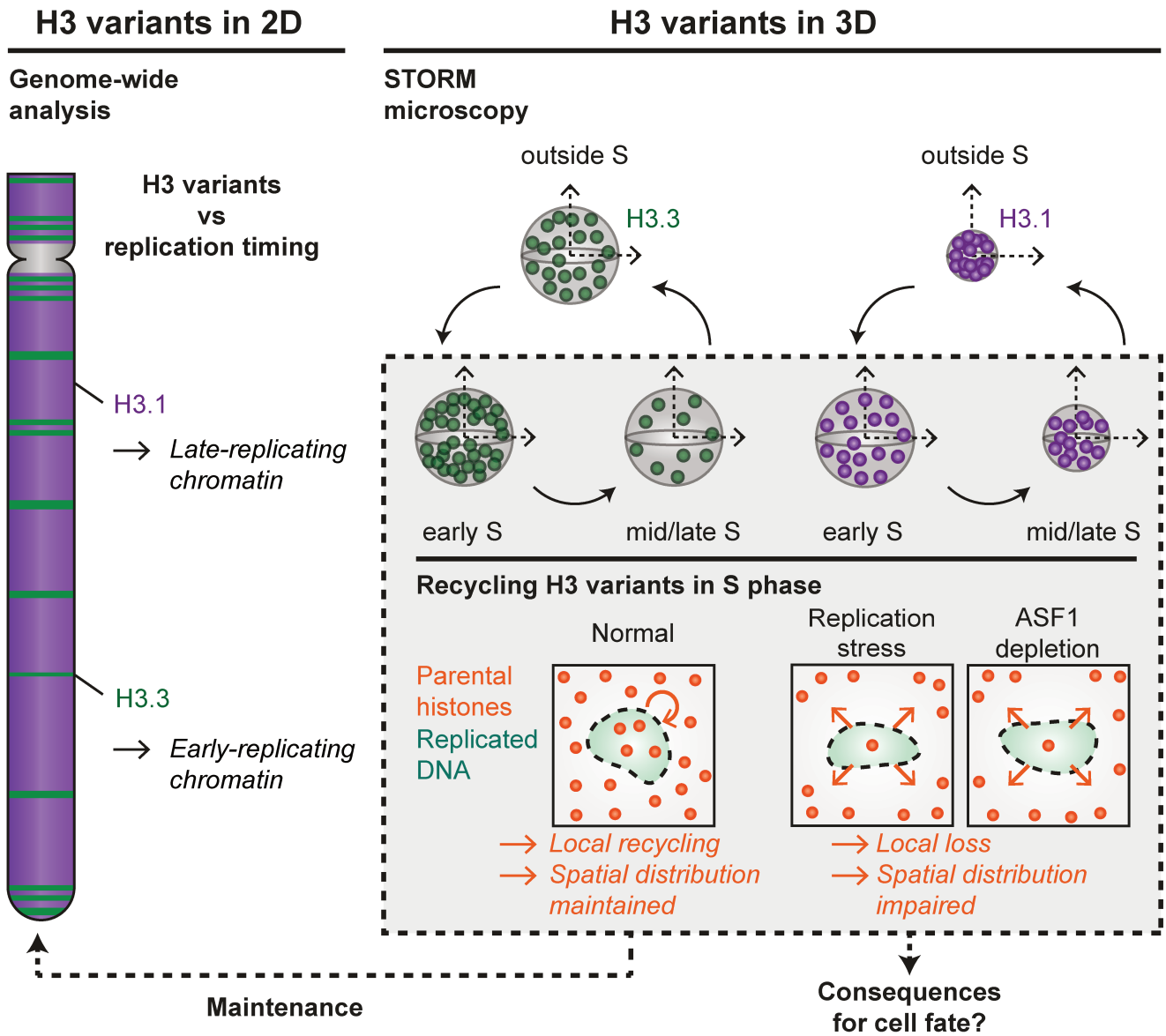
B. Spatial distribution



Supplementary Figure 17

A. Scheme summarizing the effect of HU treatment or ASF1 depletion on local recycling of parental histones.

B. Scheme summarizing the effect of ASF1 depletion on spatial distribution of parental histones relative to replication sites.



Supplementary Figure 18

Graphical abstract

# Discussion

---



At the beginning of my PhD, I had the opportunity to write a News and Views article following the publication of “A unique binding mode enables MCM2 to chaperone histones H3-H4 at replication forks” by Huang et al. in 2015. This article described the structure of the MCM2 subunit of the MCM helicase with either a H3-H4 tetramer, or a H3-H4 dimer and ASF1, providing insight into how MCM2 and ASF1 may co-chaperone parental H3-H4 at the replication fork. In our News and Views, we discussed the implications of this work and raised a number of questions that were at the core of my PhD project.

Publication:

**MCM2 binding to histones H3-H4 and ASF1 supports a tetramer-to-dimer model for histone inheritance at the replication fork**

Clément, C. and G. Almouzni

2015, Nature Structural and Molecular Biology, 22(8): 587-589.

# MCM2 binding to histones H3–H4 and ASF1 supports a tetramer-to-dimer model for histone inheritance at the replication fork

Camille Clément & Geneviève Almouzni

**MCM2, a component of the replicative helicase, can bind histones H3–H4 in both tetrameric and dimeric form, depending on the presence of the histone chaperone ASF1. A structural analysis of the complexes now sheds light on key domains in the MCM2 protein that prove important for cell proliferation.**

During DNA replication, the replication machinery acts on a chromatin template. The resultant challenge is two-fold: ahead of the fork, nucleosomal organization must be disrupted to allow the machinery to progress; behind the fork, the newly synthesized DNA must be repackaged. Histones, the protein fabric of the nucleosome, cycle through disruption of nucleosomes, recycling and *de novo* deposition (Fig. 1). In principle, for each nucleosome disrupted by fork progression, the cell must supply two in order to reproduce an equivalent nucleosomal density on the replicated daughter chromatids. This supply involves both recycling of parental histones and deposition of new histones<sup>1</sup>. How this choreography of histones at the replication fork is orchestrated has been a long-standing puzzle. A key question is whether the recycling of parental histones involves the direct transfer of a tetramer or its splitting into two dimers.

In this issue, Patel, Groth and colleagues explored how MCM2, a key subunit of the replicative helicase, binds to H3–H4 (ref. 2). Their structural analysis shows two binding modes. In the first mode, MCM2 binds an H3–H4 tetramer by replacing both DNA and

histones H2A–H2B in a nucleosome core particle. In the second mode, MCM2 binds a dimer of H3–H4 engaged in an interaction with the ASF1 histone chaperone. The first structure is consistent with the recent report from Richet *et al.*<sup>3</sup>. The second configuration relies on the capacity of the histone chaperone ASF1 to disrupt the histone tetramer<sup>4–6</sup>. Importantly, the authors identified key point mutations in MCM2 that prevent complex formation and impede cell proliferation *in vivo*. Notably, point mutants in the histone-binding surface of MCM2 also disrupt binding to CDC45, a component of the active

helicase complex. This suggests that the interaction of MCM2 with histones involving a tetramer-to-dimer transition is important for the proper function of the replication machinery. The work provides a molecular framework coordinating histone H3–H4 recycling with replication-fork progression. Finally, after finding that MCM2 binds all H3 variants (H3.1, H3.2, H3.3 and CENP-A), the authors proposed that this mechanism to handle histones probably applies throughout the entire genome.

MCM2 binding to histones was discovered almost 20 years ago<sup>7</sup>. The hypothesis that the

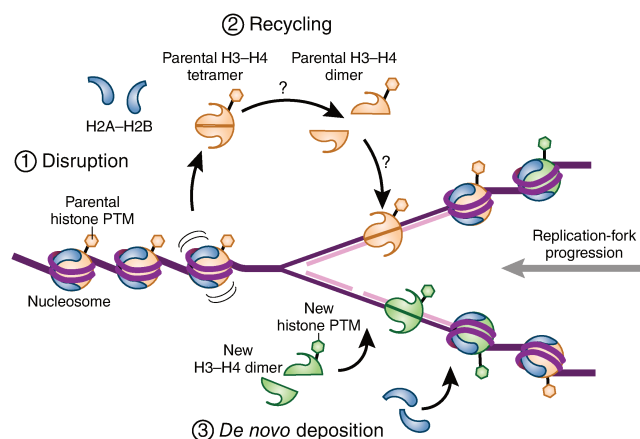


**Figure 1** Dynamics of histones at the replication fork. (1) For each parental nucleosome disrupted by replication-fork passage (indicated by the gray arrow), an H3–H4 tetramer or two H3–H4 dimers are made available. (2) The histones are in turn recycled on newly synthesized DNA either directly as a tetramer or as two dimers. (3) New histones are deposited on nascent DNA to ensure a full complement of nucleosomes on the nascent DNA. Recycling of parental histones and *de novo* deposition are thought to occur randomly on both the leading and the lagging strands. Here, for clarity, *de novo* deposition is depicted on the bottom strand. PTM, post-translational modification. Adapted with permission from ref. 24, Elsevier.

Camille Clément and Geneviève Almouzni are at the Institut Curie, Paris Sciences et Lettres Research University, “Nuclear Dynamics,” UMR3664, CNRS, Université Pierre et Marie Curie, Paris, France. Geneviève Almouzni is Director of the Research Center, Institut Curie, and coordinator of the Network of Excellence EpiGeneSys. e-mail: [genevieve.almouzni@curie.fr](mailto:genevieve.almouzni@curie.fr)

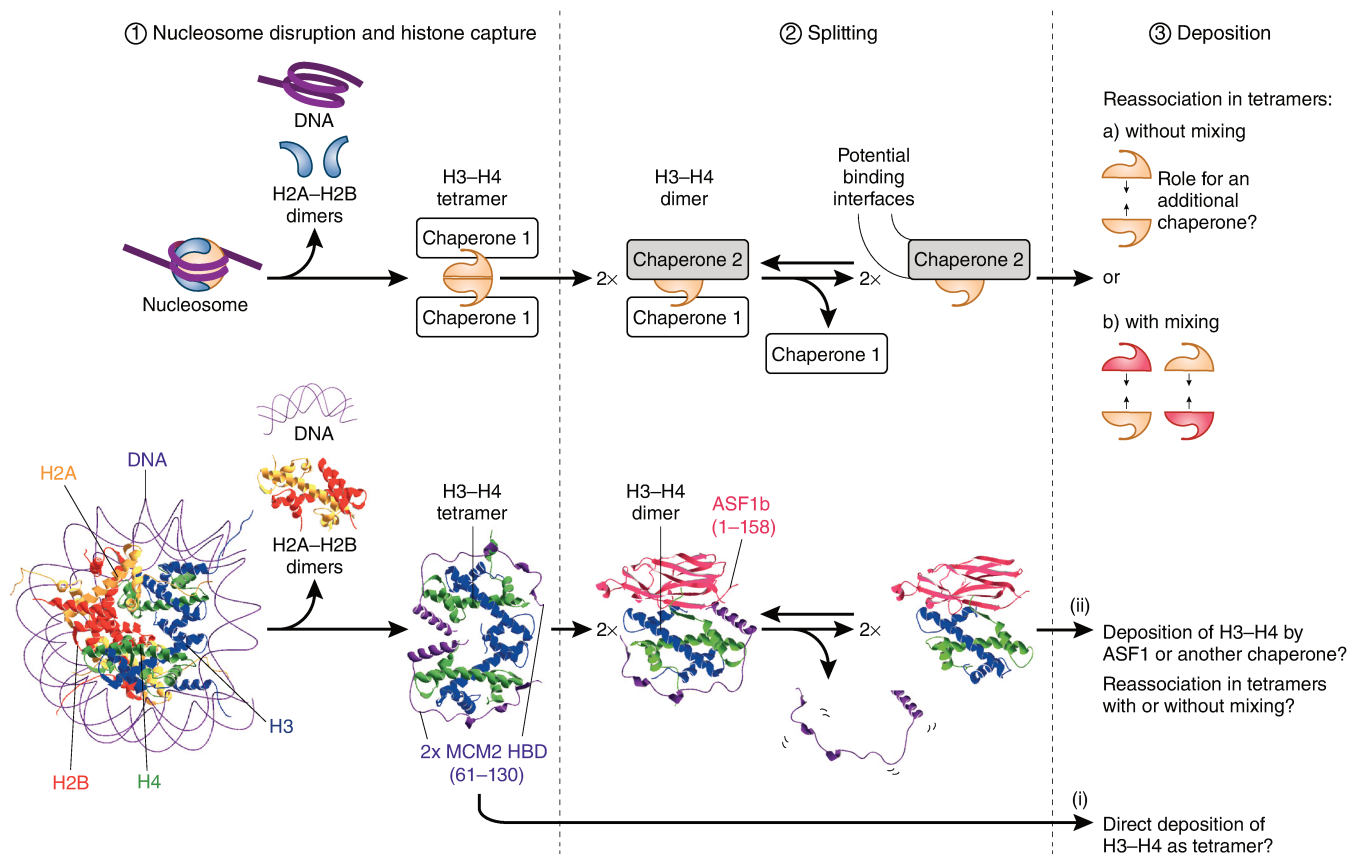


**Figure 2** MCM2 binding to both histones H3-H4 and ASF1 supports a tetramer-to-dimer model in the recycling of parental H3-H4 at the replication fork. (1) Nucleosome disruption and histone capture. Once evicted from DNA, nucleosomal H3-H4 (PDB 1A0I<sup>25</sup>) can be directly transferred to MCM2 as a tetramer, thus forming a 2:2:2 MCM2-H3-H4 complex (in which MCM2 binds H3-H4 by replacing DNA and H2A-H2B) (PDB 5BNV<sup>2</sup>). The 1:2:2 MCM2-H3-H4 configuration is also possible. (2) Splitting. ASF1 can split the MCM2-bound H3-H4 tetramer to form a 1:1:1:1 MCM2-H3-H4-ASF1 complex (PDB 5B00 (ref. 2)). This configuration could coexist with the 1:1:1 ASF1-H3-H4 complex (PDB 2I05 (ref. 6)). (3) Deposition. Parental H3-H4 could be directly deposited as tetramers after transfer to MCM2 (i) or be deposited as dimers after splitting by ASF1 (ii). This latter option could implicate an additional histone chaperone in reforming a tetramer with either no mixing (a) or mixing with additional H3-H4 dimers (depicted in red) (b).

MCM2 histone-chaperone function could be relevant during replication was first proposed during investigation of another H3-H4 histone chaperone, ASF1. Indeed, depletion of ASF1 was found to slow cells in S phase by affecting replication-fork progression, and protein-complex analysis in cells showed that MCM proteins cofractionated with ASF1 (refs. 8,9). Further investigation led to the discovery that H3-H4 forms a bridge between ASF1 and MCM2. Moreover, in cells challenged with hydroxyurea, single-stranded DNA, which usually forms when the MCM helicase functions in a manner that is uncoupled from DNA polymerization, is not detectable upon ASF1 depletion<sup>9</sup>. Furthermore, post-translational modifications that are typical of histones already assembled into chromatin<sup>10</sup>—termed parental histones—were found in the MCM2-H3-H4-ASF1 complex<sup>9,11</sup>. Together, these data led to a model in which the MCM2-ASF1 partnership in histone binding could allow these proteins to function as a multichaperone complex that acts as a platform to keep parental H3-H4

near the replication fork and enables histone recycling and deposition onto newly replicated DNA. Until now, however, the stoichiometry and detailed structure of the complex, both of which are essential for understanding of the complex's function, remained to be elucidated.

Patel, Groth and colleagues<sup>2</sup> now have presented two important structures. The first structure shows that MCM2 binds a tetramer of H3-H4 in a way that would exclude its binding to DNA and to H2A-H2B. This structure is in good agreement with a recent model based on a separate crystal study<sup>3</sup>. This mode of binding implies that, once evicted from DNA by the force of the helicase (possibly acting with remodeling factors), nucleosomal H3-H4 could be directly transferred to MCM2 as a tetramer, and after this step tetrameric H3-H4 could simply be directly loaded onto the newly synthesized DNA. Importantly, although the authors solved the structure featuring two MCM2 proteins with an H3-H4 tetramer, they found that the complex with only one MCM2

bound to an H3-H4 tetramer is also possible, a configuration that would probably be more relevant at active replication forks *in vivo*. The second structure solved by Patel, Groth and colleagues<sup>2</sup> consists of the histone-binding domain of MCM2 (amino acids (aa) 61–130), most of histone H3.3 (aa 57–135) and the N-terminal part of ASF1b (aa 1–158). The use of a clever fusion of the MCM2 histone-binding domain and ASF1b via a peptide linker allowed the authors to solve the first structure of two chaperones cotargeting an H3-H4 dimer at 2.30-Å resolution. Once this 1:1:1:1 complex has formed, ASF1-H3-H4 can in turn either directly lead to H3-H4 deposition or interact with another partner.

This integration of ASF1 into the scheme suggests a disruption of H3-H4 into dimers. However, there is substantial evidence that parental H3-H4 dimers are not mixed with newly synthesized dimers<sup>12</sup>, thus suggesting a mechanism by which the parental H3-H4 tetramer is split but then reunited when it is deposited behind the fork (Fig. 2).

For example, the non-histone-binding side of ASF1 contains a binding pocket that mediates a direct interaction with one subunit of either the H3.1-chaperone CAF-1 or the H3.3-chaperone HIRA complex<sup>13,14</sup>. Although the structure of these overall complexes is still lacking, the structure of UBN1, a subunit of the HIRA complex, with H3.3-H4 and ASF1, has just been solved, thus providing another structure of two chaperones cotargeting an H3-H4 dimer<sup>15</sup>. Importantly, the ability of the largest subunit of CAF-1 to dimerize and bind PCNA<sup>16,17</sup> could allow the formation of a 2:2:2:2 H3-H4-ASF1-CAF-1 complex. The CAF-1 dimer would then promote deposition of the two H3-H4 dimers, thus allowing the reformation of a tetramer. The regulation of CAF-1 dimerization by a Dbf4-dependent kinase could further enable dynamic control of the process<sup>18</sup>. This overall scenario would ensure the maintenance of the tetramer association present in the parental tetramer, through a splitting-and-reassociation mode consistent with the observation that old H3.1-H4 dimers rarely mix with new<sup>12</sup>. Although, in principle, a direct H3-H4 tetramer transfer could occur without invoking an intermediate with ASF1 during normal replication, ASF1 may be necessary in the presence of replication-fork barriers or replication stress. Indeed, by freeing MCM2 of histones through capture by ASF1, the helicase could continue progressing. Under these conditions, the appearance of mixed tetramers should be favored by enabling splitting into dimers that could not immediately reassociate behind the fork. Thus, the situation either at specific chromatin domains (for example at telomeres, known to represent replication-fork barriers) or during replication stress should be examined. The most extreme scenario would lead to a loss of parental marks over substantial regions.

Although these mechanisms can operate in the recycling of parental nucleosomes on newly replicated DNA, new histones are also deposited. The coordination and efficacy of these events determine nucleosomal density behind the fork. The supply of newly synthesized histones, in a soluble pool in which they are chaperoned by several complexes, is also highly regulated. In particular, the multichaperone complex known as the ASF1-H3-H4 dimer-NASP complex, can buffer

new H3-H4 and protect them from degradation via the chaperone-mediated autophagy pathway<sup>19</sup>. Interestingly, in the present study, the authors also identified a soluble pool of the MCM2-H3-H4-ASF1 complex that could act to protect soluble histones from degradation. Whether this also entails protection from chaperone-mediated-autophagy remains to be studied.

The finding that MCM2 can bind all H3 variants (H3.1, H3.2, H3.3 and CENP-A) prompts the attractive hypothesis that the handling of histones by MCM2 represents a common first step in the recycling mechanism genome wide. Although the authors could observe the interaction between MCM2 and CENP-A in cells expressing tagged proteins, whether this can be detected for endogenous proteins remains to be determined. Indeed, as previously reported, certain interactions occur upon imbalance in expression<sup>20</sup>, and it would be informative to learn under which circumstances these interactions can take place. This is particularly interesting given that mixed particles can be detected with the CENP-A-H4-H3.3-H4 complex<sup>20,21</sup>. Nevertheless, the issue of CENP-A recycling during replication remains an open issue, and future work will be needed to better understand how to maintain centromeric chromatin through cell division. Furthermore, how parental tetramers are maintained as tetramers or disrupted into dimers during development, when changes in histone dosage can occur, and whether this is different on the leading strand and the lagging strand, can be particularly relevant for asymmetric division. Disruption of these processes would probably perturb development, as observed in the formation of bilateral asymmetry in the *Caenorhabditis elegans* nervous system<sup>22</sup>.

Patel, Groth and colleagues<sup>2</sup> have provided critical structural data as a solid foundation supporting how histone H3-H4 can be recycled during DNA replication with a control on tetramer transmission. The identification and characterization of the interaction of MCM2 with histones and its exact impact on replication will be a fascinating challenge to tackle. For this, new approaches will be needed, and progress in genome editing to regulate the dosage of molecular components combined with single-molecule imaging will be useful to

more specifically determine how the interrelationships between the different component can be affected. Finally, considering that chromatin dynamics extends to other metabolic processes, such as DNA repair and transcription, whether similar mechanisms are at work in these cases would be very interesting to explore. During transcription, for example, passage of the transcription machinery is also accompanied by histone dynamics. In this context, the structure of the chaperone suppressors of Ty insertions 2 (Spt2) with an H3-H4 tetramer recently characterized by Patel's group could enable recycling as tetramers during transcription<sup>23</sup>. Whether Spt2 could also interact with ASF1 to allow transition to histone dimers would be interesting to explore.

Ultimately, finding out how each of the various histone chaperones bind to dimers, tetramers or both, and to partner chaperones, will be essential to place them in a network that precisely orchestrates histone traffic in all its forms and at all times during the life of a cell.

#### COMPETING FINANCIAL INTERESTS

The authors declare no competing financial interests.

1. Probst, A.V., Dunleavy, E. & Almouzni, G. *Nat. Rev. Mol. Cell Biol.* **10**, 192–206 (2009).
2. Huang, H. *et al. Nat. Struct. Mol. Biol.* **22**, 618–626 (2015).
3. Richet, N. *et al. Nucleic Acids Res.* **43**, 1905–1917 (2015).
4. Mousson, F. *et al. Proc. Natl. Acad. Sci. USA* **102**, 5975–5980 (2005).
5. English, C.M. *et al. Cell* **127**, 495–508 (2006).
6. Natsume, R. *et al. Nature* **446**, 338–341 (2007).
7. Ishimi, Y. *et al. J. Biol. Chem.* **271**, 24115–24122 (1996).
8. Groth, A. *et al. Mol. Cell* **17**, 301–311 (2005).
9. Groth, A. *et al. Science* **318**, 1928–1931 (2007).
10. Loyola, A. *et al. Mol. Cell* **24**, 309–316 (2006).
11. Jasencakova, Z. *et al. Mol. Cell* **37**, 736–743 (2010).
12. Xu, M. *et al. Science* **328**, 94–98 (2010).
13. Tang, Y. *et al. Nat. Struct. Mol. Biol.* **13**, 921–929 (2006).
14. Abascal, F. *et al. Mol. Biol. Evol.* **30**, 1853–1866 (2013).
15. Ricketts, D.M. *et al. Nat. Commun.* **6**, 7711 (2015).
16. Quivy, J.P., Grandi, P. & Almouzni, G. *EMBO J.* **20**, 2015–2027 (2001).
17. Shibahara, K. & Stillman, B. *Cell* **96**, 575–585 (1999).
18. Gérard, A. *et al. EMBO Rep.* **7**, 817–823 (2006).
19. Cook, A.J. *et al. Mol. Cell* **44**, 918–927 (2011).
20. Lacoste, N. *et al. Mol. Cell* **53**, 631–644 (2014).
21. Arimura, Y. *et al. Sci. Rep.* **4**, 7115 (2014).
22. Nakano, S., Stillman, B. & Horvitz, H.R. *Cell* **147**, 1525–1536 (2011).
23. Chen, S. *et al. Genes Dev.* **29**, 1326–1340 (2015).
24. Corpet, A. & Almouzni, G. *Trends Cell Biol.* **19**, 29–41 (2009).
25. Luger, K. *et al. Nature* **389**, 251–260 (1997).

During the course of my PhD, I aimed to gain a better understanding of how the histone variant landscape was transmitted through replication and whether replication stress reshuffled their organization. First, in collaboration with other members of my team, we established a 2D genome-wide mapping of H3 variants relative to replication timing. Second, I developed a STORM microscopy approach to visualize histones in the nucleus and precisely at replication sites. By combining this method with SNAP labeling, I was able to gain a spatial and quantitative view of the relationship between histones and replication sites, not only globally, but also with a specific focus on the parental subpopulation of histones. At a global level, I identified distinct 3D units for H3.3 and H3.1. H3.3 forms units corresponding to early-replicating chromatin with a stable volume throughout the cell cycle. Unlike H3.3, H3.1 forms units that vary both in volume and density during the cell cycle: (i) in early S, large low-density units correspond to deposition of new H3.1 in H3.3-associated chromatin, and (ii) at any time during the cell cycle, small high-density units mark late-replicating chromatin. I then extended the analysis to the fate of parental H3.3 and H3.1 to follow their recycling. Using this approach, I first measured how replication stress impairs the recycling of parental H3.1 both in terms of quantity and spatial distribution. Then I aimed to gain mechanistic insight into how histones were recycled and tested the implication of ASF1. I found that ASF1 depletion affected the local recycling of both parental H3.3 and H3.1 at replication sites, but with a distinctive impact on their spatial distribution around replication sites. The implications of these findings for the epigenome are discussed in the manuscript above; here are additional elements of discussion.

### **Spatial distribution of histone modifications**

When perturbing the recycling of parental histones by targeting ASF1, we showed that the spatial distribution of histone variants was altered. These parental histone variants carry post-translational modifications, which are constantly dynamically erased or written. Is the distribution of these modifications also altered, or are they maintained via other mechanisms? We tried to address this question by performing immunofluorescence staining of a few histone marks upon ASF1 knockdown, namely H3K4me3, H3K36me3 (two

early-replicating euchromatic marks), as well as H3K9me3 and H3K27me3 (two late-replicating heterochromatic marks). Both the heterochromatic marks were affected, as the signal was more diffuse in the nucleus in the ASF1-depleted cells than in the control cells, where there was enrichment of the marks at the nuclear periphery and around the nucleoli. Conversely, neither of the euchromatic marks seemed affected. Since the signal for these marks was homogenous with no clearly detectable pattern, however, it is still possible that ASF1 depletion affects the distribution in a way we cannot detect with standard microscopy. In order to better characterize the effect of ASF1 depletion on histone marks, it would be interesting to use STORM as well as epigenomic approaches. With an increased resolution and with the genomics dimensions, we may be able to better describe the effect on H3K9me3 and H3K27me3, and possibly detect subtle alterations in H3K4me3 and H3K36me3. Overall, my current data suggests that the most affected marks are heterochromatic; this is consistent with the fact that H3K9me3 and H3K27me3 are maintained in a manner that relies on the parental histone marks template.

### **Recycling histones at specific genomic loci**

In my project, I studied the recycling of parental histones in general, and in early-replicating versus late-replicating regions of the genome. It would be very interesting to take it one step further and look at specific genomic loci.

A first locus of interest would be telomeres. Telomeres are fragile regions, prone to DNA secondary structures, replication fork stalling and DNA damage. Handling histones in these regions may require additional steps or factors. For example, ATRX, which is known to resolve G-quadruplex and is recruited to telomeres, is a good candidate to participate in histone recycling in this context. Are telomeres more dependent on ASF1 for histone recycling? Do they rely on other factors? Our collaborators O'Sullivan et al showed that ASF1 depletion could lead to the induction of the Alternative Lengthening of Telomeres pathway (O'Sullivan et al. 2014). One model is that ASF1 depletion affects chromatin assembly at the fork, thereby facilitating formation of DNA secondary structures and DNA damage. The ALT pathway would be triggered as a response.

How histones are recycled at centromeres would also be essential to decipher. Indeed, the centromeric variant CenH3, marker of the centromere and essential for kinetochore assembly, is not deposited de novo in S phase but in late mitosis. Therefore, during S phase, maintenance of centromere epigenetic identity relies solely on recycling parental CenH3. Yet, how this is achieved is unknown. HJURP is the histone chaperone dedicated to CenH3. Using the SNAP system and pulse-chase experiments to label specifically parental CenH3 could shed light on the implication of HJURP in CenH3 recycling during replication. While ASF1 recycles parental H3.1 and H3.3, it has never been found in complex with CenH3 and is an unlikely candidate to chaperone this variant during replication. However, I would still like to check whether ASF1 depletion affects CenH3 distribution and centromere structure, as we cannot rule out that, by affecting surrounding H3.1 and H3.3, ASF1 could indirectly perturb CenH3 recycling.

### **Effect on transcription**

The first potential consequence of reshaping the epigenome – both in terms of variant and histone modification distribution – that comes to mind is the effect on gene expression. Interestingly, a recent study in yeast highlighted the role of ASF1 in expression homeostasis in S phase (Voichek et al. 2016). During DNA replication, the genetic material gradually doubles. Once a gene is duplicated two possible outcomes for mRNA production are possible: (i) doubling of mRNA production and (ii) downregulation of the mRNA production to maintain a balance. In eukaryotes, the second hypothesis occurs and is termed expression homeostasis. In order to gain insight into this mechanism, Voichek et al performed a screen in yeast to identify factors involved in downregulating expression of duplicated genes in S phase. The two best candidates they identified were ASF1 and the acetyltransferase Rtt109, both factors involved in the H3K56ac modification in yeast, essential in the context of de novo histone deposition during replication. Indeed, in absence of ASF1, expression homeostasis was lost and mRNA production doubled when DNA content doubled. By which means ASF1 may regulate gene expression in this context is unclear. One possibility is that, in absence of ASF1, de novo deposition of histones would decrease at replication sites, leading to a decrease in nucleosome

density. Considering that nucleosomes form a barrier to transcription, this could lead to increased mRNA production at these sites. Another hypothesis is related to histone recycling: ASF1 depletion may impair transmission of parental histones with their marks, and, indirectly, transmission of transcription factors. With no memory of the previous transcriptional state, transcription of replicated sites may be altered, leading to the global loss in expression homeostasis. Whether ASF1 impacts expression homeostasis in humans, however, is completely unknown. In this context, a postdoc in our lab, Shweta Mendiratta, is currently investigating ASF1 role during transcription in S phase in human cells, developing a nascent RNA sequencing approach. This project is ongoing in the lab and should provide valuable insight into the role of ASF1 in S phase, this time from the transcription angle. It will be particularly interesting to compare with the yeast work to find out how ASF1 and other histone chaperones such as HIRA may collaborate in regulating transcription and how this relates to events in S phase.

### **Nuclear architecture**

One of the most intriguing aspects of the ASF1 depletion phenotype on cells is the appearance of abnormal nuclear shapes (Corpet et al. 2011). When filming HeLa cells upon ASF1 knockdown, it seems that these shapes appear in late mitosis upon reformation of the nuclear membrane, suggesting that nuclear membrane proteins cannot reorganize properly when chromatin is disorganized. Why does the nuclear envelope need chromatin? The connection between lamins and histones, in particular H3K9me3 and HP1, likely play a role, and disorganization of H3K9me3 due to ASF1 knockdown may prevent proper membrane reformation. The case of ASF1 could thus be a good system to functionally study the impact of chromatin-based information inheritance on nuclear organization. Still, by which mechanisms this is achieved remains unknown and requires further investigation. It would be interesting to test the physical properties of these abnormal membranes, in particular their response to external forces and deformations, especially considering that such structural defects are found in a number of diseases including laminopathies, or even

cancer. From this perspective, it would also be interesting to check if alterations of ASF1 are indeed associated to laminopathies in patient samples.

### **Development and disease**

ASF1b is overexpressed in cancer and its level of expression can serve as a prognostic marker (Corpet et al. 2011, Montes de Oca et al 2015). The most parsimonious explanation is that proliferating cells need increased chromatin assembly, and, therefore, increased chromatin assembly factors such as ASF1 and CAF-1. However, other histone chaperones involved in chromatin assembly, such as the HIRA complex, do not show this association. An alternative view could be that an excess of ASF1 may help cells to overcome replication stress, which is a major cause of genomic instability in tumorigenesis. By protecting replicative chromatin, ASF1 may help propagate precancerous lesions and mutations. Given the importance of the interconnection between genome and epigenome stability in tumor biology, our approach targeting ASF1 may provide an entry point to study how unbalancing the epigenome impacts tumorigenesis. Another crucial context where histone inheritance greatly impacts genome function is development. DNA replication provides a window of opportunity for a cell to copy its identity, or to change its identity. The epigenome is gradually shaped during development and differentiation; targeting the epigenome may provide means to modulate cell fate. Indeed, several recent studies have shown that targeting chromatin factors could affect cell state: depletion of CAF-1 can facilitate cellular reprogramming (Cheloufi et al. Ischiushi et al.), while Suv31h depletion leads to defects in silencing of genes linked to stemness and memory (Pace et al.). How ASF1 fits into this picture is an open question.



# Conclusion

---



My PhD project aimed to gain insight into how histone variants are recycled during replication.

First, my contribution was technological, as I developed a new microscopy approach (STORM) in the lab to visualize histone variants at an unprecedented resolution. This required adjusting the experimental conditions, defining the acquisition settings, and writing algorithms to analyze the data. I combined this approach with the well-characterized SNAP labeling system, enabling to monitor a specific subpopulation – in my case parental - of histones. This allowed the establishment of a pipeline to further study other dynamic events associated with histone variants.

Second, the biological results I obtained using this technology provided a series of important contributions. First, we established how the histone variant landscape (for H3.1 and H3.3) is organized and transmitted during replication. A second contribution is the finding that ASF1 is involved in recycling parental histones during replication. This is the first direct evidence to my knowledge. Interfering with histone handling at the replication fork by depleting ASF1 prevents histone variants to recycle locally. Instead, they likely redistribute randomly, thereby unbalancing the epigenome.

The approach developed during my PhD will surely provide a strong basis to help us gain a better understanding of histone variant dynamics in other contexts. For example, a similar methodology could be used to study histone dynamics and the role of chaperones at specific genomic loci, including the centromere, or in different contexts, such as transcription.

Ultimately, a clear understanding of how histone variant reshuffling impairs genome function, not only in cellular models but also in the context of development, cell fate and in a whole organism, will emerge. This complete characterization will underline the exact epigenetic role of histone variants and their escort partners, histone chaperones.



# Annexes

---



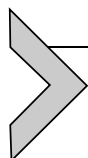
Publication:

**Functional Characterization of Histone Chaperones Using SNAP-Tag-Based Imaging to Assess De Novo Histone Deposition**

Clément, C., I. Vassias, D. Ray-Gallet and G. Almouzni

2016, *Methods in Enzymology*, 573: 97-117.





# Functional Characterization of Histone Chaperones Using SNAP-Tag-Based Imaging to Assess De Novo Histone Deposition

C. Clément<sup>\*,†</sup>, I. Vassias<sup>\*,†</sup>, D. Ray-Gallet<sup>\*,†</sup>, G. Almouzni<sup>\*,†,1</sup>

<sup>\*</sup>Institut Curie, PSL Research University, CNRS, UMR3664, Equipe Labellisée Ligue contre le Cancer, Paris, France

<sup>†</sup>Sorbonne Universités, UPMC Univ Paris 06, CNRS, UMR3664, Paris, France

<sup>1</sup>Corresponding author: e-mail address: genevieve.almouzni@curie.fr

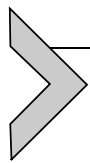
## Contents

|   |     |
|---|-----|
| 1. Introduction   | 98  |
| 2. The SNAP-Tag System to Visualize in vivo New Histone Incorporation into Chromatin: A De Novo Histone Deposition Assay in Cells | 100 |
| 2.1 Establishment of Cell Lines Expressing SNAP-Tagged Histones   | 100 |
| 2.2 Protocol for the “Quench-Chase-Pulse” Assay   | 103 |
| 3. De Novo Histone Deposition Assay Coupled with Histone Chaperone Depletion and Labeling of Replicating Cells                    | 106 |
| 4. De Novo Histone Deposition Assay Coupled with Histone Chaperone Depletion in Response to UV-DNA Damage                         | 108 |
| 5. Imaging and Quantifying SNAP Labeling  | 111 |
| 6. Interpreting the De Novo Histone Deposition Assay Coupled with Histone Chaperone Depletion                                     | 113 |
| 7. Conclusion and Perspectives  | 113 |
| Acknowledgments   | 115 |
| References  | 115 |

## Abstract

Histone chaperones—key actors in the dynamic organization of chromatin—interact with the various histone variants to ensure their transfer in and out of chromatin. In vitro chromatin assembly assays and isolation of protein complexes using tagged histone variants provided first clues concerning their binding specificities and mode of action. Here, we describe an in vivo method using SNAP-tag-based imaging to assess the de novo deposition of histones and the role of histone chaperones. This method exploits cells expressing SNAP-tagged histones combined with individual cell imaging

to visualize directly de novo histone deposition in vivo. We show how, by combining this method with siRNA-based depletion, we could assess the function of two distinct histone chaperones. For this, we provide the details of the method as applied in two examples to characterize the function of the histone chaperones CAF-1 and HIRA. In both cases, we document the impact of their depletion on the de novo deposition of the histone variants H3.1 and H3.3, first in a normal context and second in response to DNA damage. We discuss how this cellular assay offers means to define in a systematic manner the function of any chosen chaperone with respect to the deposition of a given histone variant.



## 1. INTRODUCTION

Distinct regions of the genome are marked at the level of chromatin by specific histone variants and their modifications. Variants of histone H3, for example, include the replicative form H3.1, the replacement form H3.3, and the centromeric variant CenH3 (CENP-A) (Szenker, Ray-Gallet, & Almouzni, 2011). Despite their high sequence conservation—H3.1 and H3.3 differ by only five amino acids—these variants participate in marking specific regions of the genome, such as zones of active transcription, DNA repair, or the centromere (Talbert & Henikoff, 2010). Histone chaperones are key actors of histone variant management (De Koning, Corpet, Haber, & Almouzni, 2007; Gurard-Levin, Quivy, & Almouzni, 2014). They can direct histone incorporation into chromatin at the appropriate time in the cell cycle, for example, during DNA replication when a supply of new histones is required at the time of genome duplication, or during DNA damage. Providing the proper histone variant at the right place and the right time is of major importance for cellular fate and development (Santoro & Dulac, 2015; Szenker, Lacoste, & Almouzni, 2012). Indeed, improper histone variant distribution and unbalanced situations directly impact genome function and have been associated with several pathological situations (Filipescu, Muller, & Almouzni, 2014). Thus, characterizing the precise role of histone chaperones in the incorporation of histone variants into chromatin is of critical importance. To this goal, we have developed sensitive and specific assays to monitor histone variant deposition in vivo.

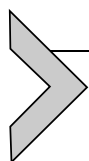
Following the discovery of the first histone chaperones (Laskey, Honda, Mills, & Finch, 1978; Smith & Stillman, 1989), in vitro chromatin assembly assays using crude cell extracts (Gaillard, Roche, & Almouzni, 1999; Ray-Gallet & Almouzni, 2004) revealed two distinct major pathways for histone deposition (Kaufman & Almouzni, 2006). These two pathways allow

histone deposition either (i) coupled to DNA synthesis or (ii) independent of DNA synthesis. Cellular fractionation and complementation assays enabled to assign a key role to chromatin assembly factor 1 (CAF-1) in the DNA synthesis-coupled deposition (Stillman, 1986). Biochemical characterization of the complex identified three subunits, namely p48, p60, and p150 (Smith & Stillman, 1989). This complex is important not only during DNA replication but also during nucleotide excision repair (NER), a DNA repair pathway that requires DNA synthesis (Gaillard et al., 1996). The use of cell lines stably expressing epitope-tagged H3 variants combined with biochemical purification of these variants established that CAF-1 was selective for H3.1 (Tagami, Ray-Gallet, Almouzni, & Nakatani, 2004). To date, no other H3.1-dedicated chaperone has been described. Details concerning its function are provided in De Koning et al. (2007) and Gurard-Levin et al. (2014). Concerning DNA synthesis-independent histone deposition, the importance of the chaperone histone regulator A (HIRA) was first established using in vitro assays (Ray-Gallet et al., 2002). Given that chromatin disruption and dynamics are also important during transactions that do not involve DNA synthesis, for example during transcription, this pathway also engaged active research. Specifically, experiments in *Xenopus* egg extracts depleted for HIRA demonstrated that HIRA is critical for chromatin assembly in the absence of DNA synthesis. The HIRA complex—which contains HIRA, Ubinuclein 1 (UBN1), and calcineurin-binding protein 1 (CABIN1)—is one of the H3.3-selective histone chaperones (Tagami et al., 2004). Further details can be found in Gurard-Levin et al. (2014).

While these in vitro assays proved critical to define distinct nucleosome assembly pathways and highlight key histone chaperones (Ray-Gallet & Almouzni, 2004), further progress was hampered by the lack of method to assess the function of histone chaperones in vivo at a cellular level. The advent of the SNAP-tag system (Keppler et al., 2003) offered a unique tool to specifically visualize new histone variants and to monitor their de novo deposition at a cellular level (Jansen, Black, Foltz, & Cleveland, 2007; Ray-Gallet et al., 2011). By tagging individual histone variants, and following their fate within cells at specific times during the cell cycle or during particular genomic events, it provides a powerful method to characterize the function of histone chaperones in vivo. Importantly, with this technique, it is possible, with single-cell resolution, to detect variations within a heterogeneous cell population, variations that are otherwise averaged with more global approaches. Furthermore, at the subcellular level, it is possible to distinguish particular patterns for histone deposition within individual nuclei. In addition, when coupled with quantitative microscopy approaches

to measure histone deposition in a population of cells, one can accurately scale various types of impact on histone deposition.

Here, we describe the use of the SNAP-tag system combined with siRNA depletion of individual histone chaperones to evaluate their role in the deposition of the histone variants H3.1 and H3.3. We document how this system was critical to unravel the *in vivo* role of histone chaperones in (i) the global deposition of histones (Ray-Gallet et al., 2011), (ii) cell cycle-dependent histone deposition (Ray-Gallet et al., 2011), and (iii) histone deposition in response to DNA damage (Adam, Polo, & Almouzni, 2013).



## 2. THE SNAP-TAG SYSTEM TO VISUALIZE *IN VIVO* NEW HISTONE INCORPORATION INTO CHROMATIN: A DE NOVO HISTONE DEPOSITION ASSAY IN CELLS

The SNAP-tag is a mutant of the human DNA repair protein O<sup>6</sup>-alkylguanine-DNA alkyltransferase that specifically and covalently binds to benzylguanine, in an irreversible manner (Keppler et al., 2003). It can be fused to a protein of interest and this epitope-tagged protein can be expressed in cells. Importantly, cell-permeable fluorescent or nonfluorescent substrates (derivatives of benzylguanine) that react with the SNAP-tag are available (Fig. 1A and Table 1). This enables, *in vivo*, the specific visualization of newly synthesized proteins and the use in “quench-chase-pulse” assays (Fig. 1B) (Bodor, Rodriguez, Moreno, & Jansen, 2012): the “quench” step irreversibly labels all preexisting SNAP-tagged proteins with a nonfluorescent dye; the “chase” period allows for new SNAP-tagged proteins—which are not quenched—to be synthesized; and finally, the “pulse” step labels these new proteins with a fluorescent dye. To visualize newly synthesized molecules specifically, we performed this “quench-chase-pulse” assay using cell lines expressing SNAP-tagged H3.1 or H3.3. To concentrate on new histones that are chromatin-incorporated, a further step has to be performed via a triton extraction enabling the elimination of soluble histones.

### 2.1 Establishment of Cell Lines Expressing SNAP-Tagged Histones

The first SNAP-tagged cell line was devised to visualize the deposition of the centromeric histone variant, CENP-A (Jansen et al., 2007). To establish HeLa cell lines stably expressing either H3.1 or H3.3 tagged with one

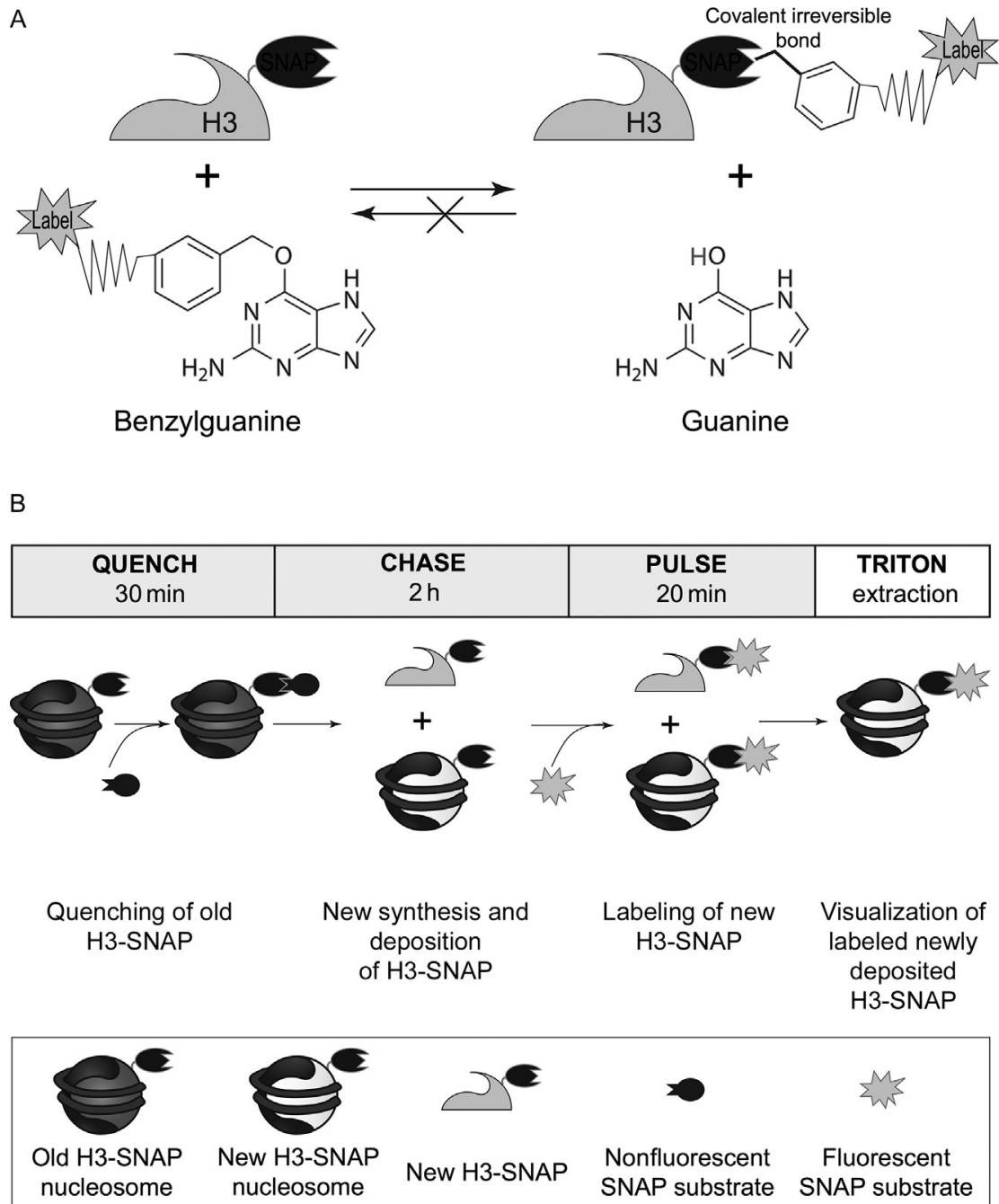


**Fig. 1** SNAP-based labeling principle and de novo histone H3 deposition assay. (A) Histone H3 is fused to the SNAP-tag, a 20-kDa mutant of the DNA repair protein O<sup>6</sup>-alkylguanine-DNA alkyltransferase that reacts specifically and rapidly with benzylguanine derivatives, leading to irreversible covalent labeling of the SNAP-tag with a synthetic probe. Many SNAP-tag substrates are cell permeable, permitting labeling of histone H3 in live cells (see Table 1). (B) Our de novo histone H3 deposition assay in stably expressing H3.1- or H3.3-SNAP cells is based on a “quench-chase-pulse” experiment. The “quench” step labels old (preexisting) H3-SNAP with a nonfluorescent SNAP-tag substrate, the “chase” step allows the synthesis and deposition of new H3-SNAP, and the “pulse” step labels only the new H3-SNAP with a red fluorescent SNAP-tag substrate (TMR). A triton extraction before fixation of the cells eliminates soluble histones in order to enrich for the nonsoluble labeled H3-SNAP that contain newly deposited histones stably bound to chromatin.

**Table 1** List of Commercially Available Cell-Permeable Fluorescent Substrates Used to Label SNAP-Tag Fusion Proteins Inside Living Cells (Purchased from New England Biolabs)

|  | Excitation (nm) | Emission (nm) |
|--|-----------------|---------------|
| SNAP-Cell <sup>®</sup> 360                       | 357             | 437           |
| SNAP-Cell <sup>®</sup> 505-Star                  | 504             | 532           |
| SNAP-Cell <sup>®</sup> Fluorescein               | 500             | 532           |
| SNAP-Cell <sup>®</sup> Oregon Green <sup>®</sup> | 490             | 514           |
| SNAP-Cell <sup>®</sup> TMR-Star                  | 554             | 580           |
| SNAP-Cell <sup>®</sup> 430                       | 421             | 444–485       |
| SNAP-Cell <sup>®</sup> 647-SiR                   | 645             | 661           |

SNAP-tag and three Human influenza hemagglutinin (HA) epitopes, derivatives of this approach have been used (Jansen et al., 2007; Ray-Gallet et al., 2011). Indeed, the H3.1 or H3.3 open-reading frames (ORFs) amplified from complementary DNA by PCR were cloned between the KpnI/XhoI sites of pCENP-A-SNAP-3XHA (Jansen et al., 2007), replacing the CENP-A gene. The resulting H3.1-SNAP-3xHA or H3.3-SNAP-3xHA ORFs were subcloned into pBABE and used for retroviral production and delivery into HeLa cells as described previously (Shah et al., 2004). After selection with Blasticidin S (5 mg/mL, Calbiochem), monoclonal lines were isolated by flow cytometry. Most importantly for our assays, we verified that the selected clones showed low expression levels of tagged H3.1 and H3.3 as compared to the endogenous counterparts to be able to use them as tracers (Ray-Gallet et al., 2011). Considering that the presence of the tag could potentially interfere with the functionality of the protein and impact cell properties, we also verified that they did not significantly alter cell cycle progression and general cellular properties. In addition, we also generated independently two other stable U2OS cell lines expressing H3.1-SNAP or H3.3-SNAP by cloning the genes into a pSNAPm vector (N9172S, NEB), transfection and G418 selection (400 µg/mL) of single-cell clones (Dunleavy, Almouzni, & Karpen, 2011). Considering recent advances in genome editing, the use of technologies such as the CRISPR/Cas9 system is now an attractive option that we would recommend to tag the endogenous proteins of interest directly at their natural site. The use of distinct cell lines and independent methods can be most useful to verify the generality of the properties observed in a particular context.

## 2.2 Protocol for the “Quench-Chase-Pulse” Assay

### 2.2.1 Cell Culture Conditions

Grow cells expressing the SNAP-tagged histone on glass coverslips (12 mm diameter, 0.17 mm thickness) in Dulbecco’s modified Eagle’s medium, 10% newborn calf serum, penicillin, and streptomycin (complete medium). Incubate cells in a humidified 37°C incubator with 5% CO<sub>2</sub> until they reach the desired confluence (70–80%). Labeling and washing volumes are given for one coverslip in a 24-well plate.

### 2.2.2 Quench

- Replace the medium with 200 µL of complete medium with 10 µM SNAP-Cell Block (S9106S, New England Biolabs)
- Incubate at 37°C, 5% CO<sub>2</sub> for 30 min
- Wash cells twice with 1 mL of PBS
- Replace PBS with 1 mL of complete medium and incubate at 37°C, 5% CO<sub>2</sub> for 30 min to allow the excess SNAP-Cell Block to diffuse out
- Wash cells twice with 1 mL of PBS

### 2.2.3 Chase

- Replace PBS with 1 mL of complete medium
- Incubate at 37°C, 5% CO<sub>2</sub> for an appropriate time of “chase,” to allow new SNAP-tagged histones to be synthesized and incorporated into chromatin. We typically use a “chase” period of 2 h

### 2.2.4 Pulse

- Replace medium with 200 µL of complete medium with 2 µM fluorescent SNAP-Cell TMR-Star (tetramethylrhodamine, “TMR” in Figs. 2–4) (S9105S, New England Biolabs). Note that other SNAP-tag fluorescent substrates are available (see Table 1)
- Incubate at 37°C, 5% CO<sub>2</sub> for 20 min
- Wash cells twice with 1 mL of PBS
- Replace PBS with 1 mL of complete medium
- Incubate at 37°C, 5% CO<sub>2</sub> for 30 min, to allow the excess SNAP-Cell TMR-Star to diffuse out
- Wash cells twice with 1 mL of PBS

### 2.2.5 Triton Extraction

In this step, the goal is to try and eliminate soluble proteins and enrich for chromatin-incorporated histones

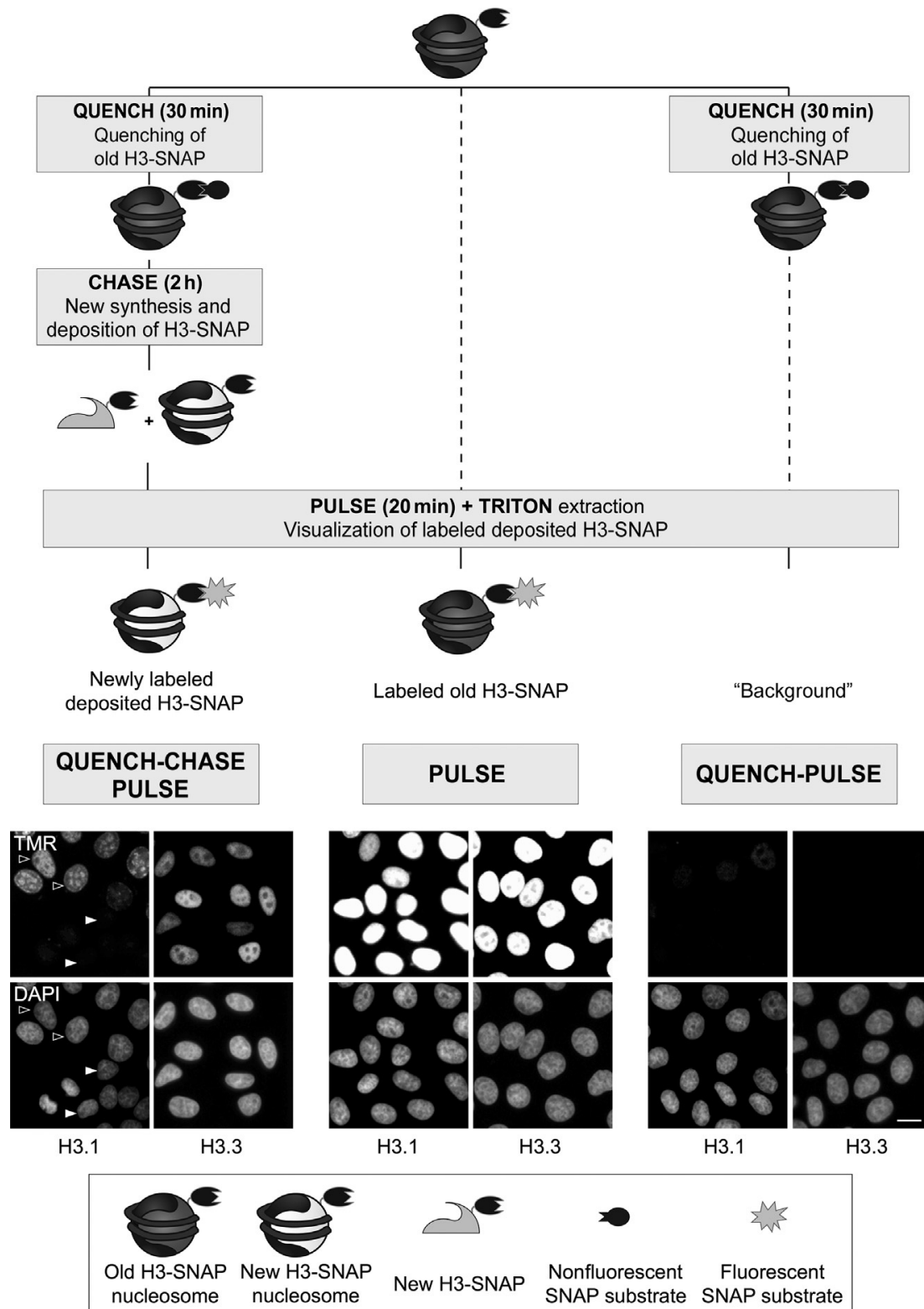


**Fig. 2** Validation of the de novo histone H3 deposition assay. Schemes and cell images for the de novo histone H3 deposition assay “quench-chase-pulse” and two control experiments “pulse” and “quench-pulse” in HeLa cell lines stably expressing H3.1- or H3.3-SNAP. The “quench-chase-pulse” assay visualizes the newly deposited histones H3-SNAP (TMR): while all the cells are labeled in the H3.3-SNAP cell line, only the cells that are in S phase are fluorescent in the H3.1-SNAP cell line (see *arrows* and [Fig. 3](#)).

- Wash cells with 1 mL of cytoskeleton (CSK) buffer (10 mM Pipes-KOH, pH 7.0, 100 mM NaCl, 300 mM sucrose, 3 mM MgCl<sub>2</sub>)
- Replace the buffer with 200  $\mu$ L of CSK with 0.5% Triton
- Incubate at room temperature for 5 min
- Wash cells twice gently with 1 mL of CSK (the second wash should be 5 min)
- Fix cells in 2% paraformaldehyde at room temperature for 20 min
- Wash cells three times with 1 mL of PBS

### 2.2.6 Cell Imaging

Prepare coverslips on slides with mounting medium containing DAPI (4',6-diaminido-2-phenylindole) or process for immunostaining beforehand. Visualize cells by microscopy and acquire images for SNAP-labeling quantification (see later).

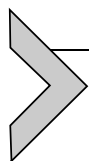
### 2.2.7 Controls in the “Quench-Chase-Pulse” Assay

Two other combinations of labeling are necessary along with the “quench-chase-pulse” (Fig. 2): a “pulse” to label all preexisting histones, and a “quench-pulse” with a “quench” immediately followed by a “pulse” to monitor the efficiency of the quenching under our experimental conditions. As expected, the amount of newly synthesized and deposited histones observed after a “quench-chase-pulse” is lower than the amount of all preexisting histones after a “pulse” (Fig. 2, bottom). The low signal in the “quench-pulse” condition confirms the efficiency of the “quench” step and thus defines a minimal background signal for our assays (Fig. 2, bottom). Therefore, with the SNAP-tag system, under our experimental conditions, we have at hand a useful tool to study new histone variant deposition. Using cell lines expressing H3.1- and H3.3-SNAP, described earlier, and combining the “quench-chase-pulse” assay with siRNA depletion of histone

---

Dark arrows indicate cells in S phase, white arrows indicate cells that are not in S phase). The “pulse” assay visualizes the old (preexisting) H3-SNAP (TMR): all the cells in both H3.1 and H3.3-SNAP cell lines are labeled and show a strong fluorescence signal. The “quench-pulse” assay with a “pulse” just after the “quench” step (without a chase period) allows to control the efficiency of the quenching: no cells should be labeled (TMR) as shown in the images for both H3.1- and H3.3-SNAP cell lines. Note that the image acquisition time is the same for the three assays, explaining the overexposed image for the TMR staining in the “pulse” as compared to the “quench-chase-pulse.” Scale bar, 10  $\mu$ m. Adapted from Ray-Gallet, D., Woolfe, A., Vassias, I., Pellentz, C., Lacoste, N., Puri, A., ... Almouzni, G. (2011). Dynamics of histone H3 deposition in vivo reveal a nucleosome gap-filling mechanism for H3.3 to maintain chromatin integrity. *Molecular Cell*, 44(6), 928–941.

chaperones, we investigated the role of several histone chaperones in the de novo deposition of these two variants (Ray-Gallet et al., 2011).



### 3. DE NOVO HISTONE DEPOSITION ASSAY COUPLED WITH HISTONE CHAPERONE DEPLETION AND LABELING OF REPLICATING CELLS

Based on previous work on the histone variants H3.1 and H3.3, we further investigated the role of the histone chaperone CAF-1 on histone H3 deposition in vivo. To assess how the depletion of CAF-1 p60 by siRNA would affect H3.1/H3.3 de novo deposition, we used a modified “quench-chase-pulse” experiment in H3.1- and H3.3-SNAP HeLa cells (Fig. 3A). We performed siRNA transfections using Lipofectamine RNaimax (13778-150, Invitrogen) 48 h prior to the “quench-chase-pulse.” To determine whether H3.1- and H3.3-SNAP de novo depositions are cell cycle-specific, S phase cells were labeled in the presence of 10  $\mu$ M of EdU (5-ethynyl-2'-deoxyuridine) in the medium during the “pulse” step. Colabeling of SNAP-tagged histones (with TMR for example) and EdU (with Click chemistry, for example (C10337, Invitrogen)) allows the visualization of new H3.1- and H3.3-SNAP in cells undergoing replication. In Fig. 3B, new H3.1 was only deposited in replicating cells (EdU positive), at replication sites as shown by the strong colocalization between the TMR signal and the EdU staining, while non replicating cells (EdU negative) showed no labeling. In contrast, all cells displayed TMR signal for H3.3 without any colocalization between H3.3 and replication foci, indicating that this variant is deposited throughout the whole cell cycle with a broad distribution. This may seem in contrast with data from ChIP experiments that show enrichment at gene bodies, promoters and regulatory elements (Goldberg et al., 2010; Ray-Gallet et al., 2011), but can be explained if one considers that incorporation of H3.3 is broad and random at sites of unexpected dynamics, while systematic at sites of transcription. Since ChIP data obtained on populations of cells provide an average, they will only reveal changes that occur at the same place in all cells. This highlights the complementary nature of the two techniques. Notably, upon depletion of CAF-1 p60, TMR signal for H3.1 was reduced by 50%, whereas TMR signal for H3.3 was not affected. These findings establish that de novo deposition of the variant H3.1, but not H3.3, occurs at replication sites in S phase and is mediated by the histone chaperone CAF-1 in vivo. We also showed that depletion of the histone chaperone HIRA—and not CAF-1—affects de

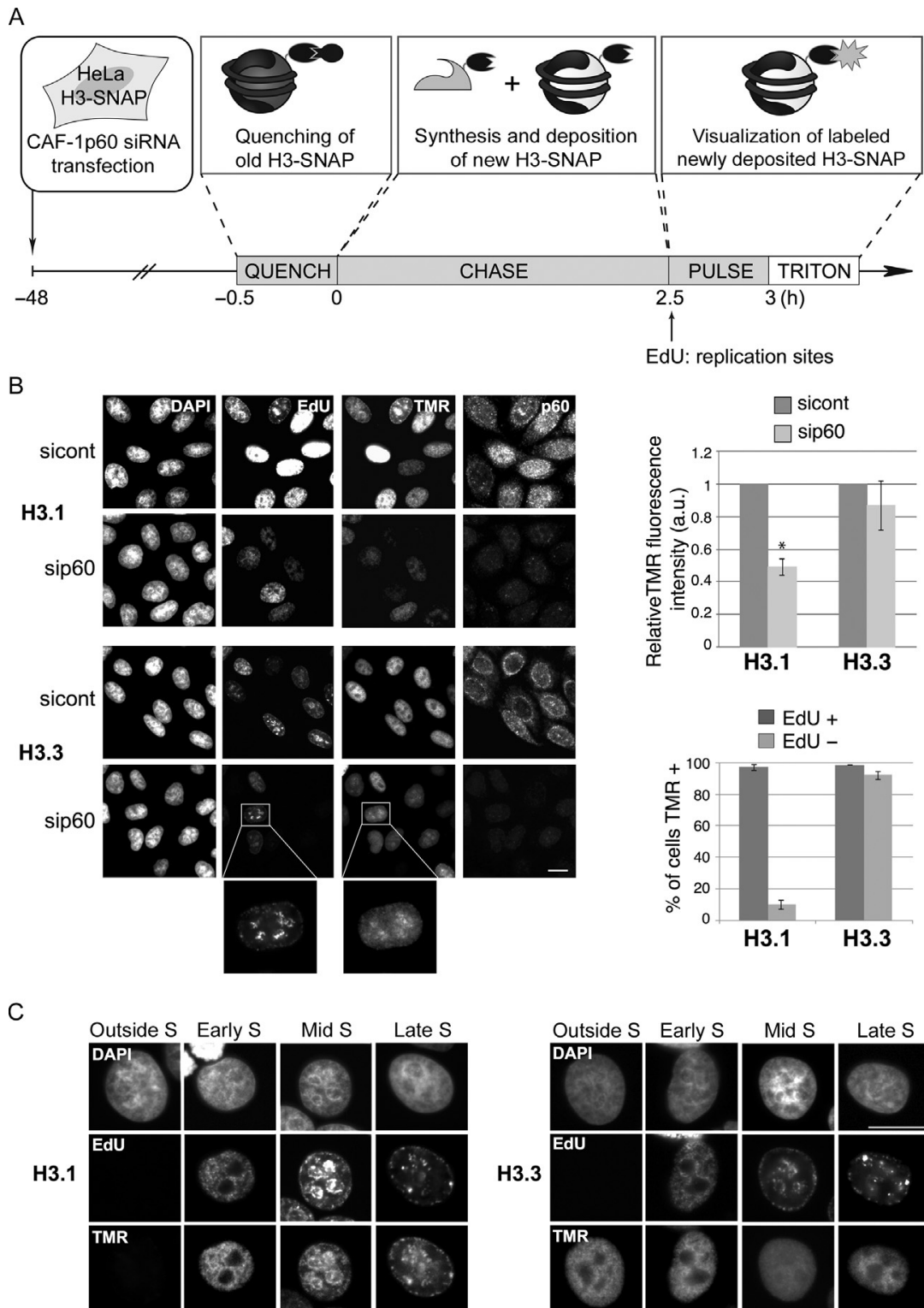
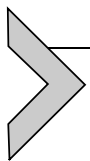


**Fig. 3** De novo histone H3 deposition assay coupled with histone chaperone CAF-1 depletion and EdU staining. (A) Scheme of the de novo histone H3 deposition assay coupled with histone chaperone depletion and replication sites labeling in H3.1- and H3.3-SNAP HeLa cells. The cells are transfected with CAF-1 p60 or control siRNA before labeling of new H3-SNAP with TMR (by the “quench-chase-pulse” experiment) and replication sites with EdU. (B) (Left) Fluorescent microscopy visualization of new deposited (Continued)

novo deposition of the variant H3.3 (Ray-Gallet et al., 2011). Importantly, the EdU staining reveals specific S phase patterns that can be analyzed individually (early, mid and late S phase are characteristic) (Fig. 3C). Thus, one can also refine the analysis at the level of individual nuclei by studying particular patterns. Furthermore, this assay revealed that, upon CAF-1 depletion, about 20% of cells displayed HIRA-dependent deposition of H3.3 at replication sites, suggesting a compensatory mechanism. This uncovers an alternative mode of HIRA-dependent H3.3 deposition at any region where nonnucleosomal/naked DNA is accessible, that could differ from one cell to the next and thus would not have been picked up in analyzing genome-wide H3.3 enrichment profiles. This alternative mode would function as a nucleosome gap-filling mechanism compensating for the decreased H3.1 deposition. This study advanced our understanding of the role of histone chaperones in the de novo deposition of specific histone variants in vivo during the cell cycle under normal conditions. We next wished to investigate histone dynamics after DNA damage and determine which histone chaperones could be involved and when.



#### 4. DE NOVO HISTONE DEPOSITION ASSAY COUPLED WITH HISTONE CHAPERONE DEPLETION IN RESPONSE TO UV-DNA DAMAGE

Repair of UV damage in DNA entails specific histone dynamics in the context of chromatin (Polo & Almouzni, 2015). These can be depicted in

**Fig. 3—Cont'd** H3.1- or H3.3-SNAP (TMR) and replication sites (EdU) after siRNA transfection against CAF-1 p60 or control. CAF-1 p60 is detected by immunofluorescence. The insets represent enlarged images of one selected cell. Scale bar, 10  $\mu$ m. (Right) The upper graph shows the sip60/sicont ratio corresponding to TMR fluorescence intensity for new deposited H3.1- and H3.3-SNAP. The lower graph represents the percentage of TMR-labeled H3.1- and H3.3-SNAP cells negative (EdU -) or positive (EdU +) for EdU staining. The statistical significance of the difference between siRNA and sicont—as represented by the "\*" when the difference is significant—was analyzed using a Mann and Whitney test. Error bars indicate standard deviation in at least three experiments. (C) Fluorescent microscopy visualization of the different patterns of replication sites (EdU) during early, mid, or late S phase and of new incorporated H3.1 or H3.3 (TMR) after in vivo labeling by a "quench-chase-pulse" experiment. Adapted from Ray-Gallet, D., Woolfe, A., Vassias, I., Pellentz, C., Lacoste, N., Puri, A., ... Almouzni, G. (2011). Dynamics of histone H3 deposition in vivo reveal a nucleosome gap-filling mechanism for H3.3 to maintain chromatin integrity. *Molecular Cell*, 44(6), 928–941.

the “prime-repair-restore” model whereby, first, very early and at the site of the lesion, particular chromatin dynamics are critical to mark where the repair process can take place. Then, rearrangements enable the repair machinery to gain access to DNA lesions. After removal of the damage, further histone deposition occurs to fully restore chromatin organization. We used the “quench-chase-pulse” assay with the H3.3-SNAP U2OS cell line to assess the dynamics of this variant when inflicting local UV damage with UVC (see later). This assay, coupled with histone chaperone depletion, enabled us to identify the HIRA-mediated deposition of H3.3 as an early step to prime chromatin (Adam et al., 2013). This is critical to enable transcription recovery after repair is complete.

The protocol is essentially as described earlier, with the exception of the addition of a local UVC irradiation after the “chase” period. We irradiate the cells through micropore filters to induce DNA damage at discrete regions in the nucleus. A schematic representation of this assay is presented in Fig. 4A. The UVC irradiation protocol, under conditions described later, produces predominantly pyrimidine dimers that are repaired by the NER pathway as verified in Adam et al. (2013).

#### **Protocol for UVC Irradiation**

- Use a UVC lamp at 254 nm and monitor the fluence rate with a VLX-3W dosimeter (both from Vilber Lourmat)
- After the “chase” step, transfer one coverslip to a 6-cm plate without medium
- Cover the coverslip by a microfilter (isopore membrane filter with 5 μm pores from Millipore)
- Irradiate the cells. We usually use a UV dose of 150 J/m<sup>2</sup>
- Remove the filter by adding PBS into the plate
- Transfer back the coverslip into the plate containing the complete culture medium
- Perform the “pulse,” triton extraction and fixation steps as described above
- Perform an immunodetection of the repair factor XPA (Xeroderma Pigmentosum, complementation group A) to visualize the sites of DNA damage when imaging cells on the microscope

For more details of the “quench-chase-pulse” assay coupled with local UV irradiation, see Adam, Dabin, Bai, and Polo (2015).

This assay combined with depletion of the HIRA and UBN1 subunits enabled us to assess the role of the HIRA complex in chromatin dynamics

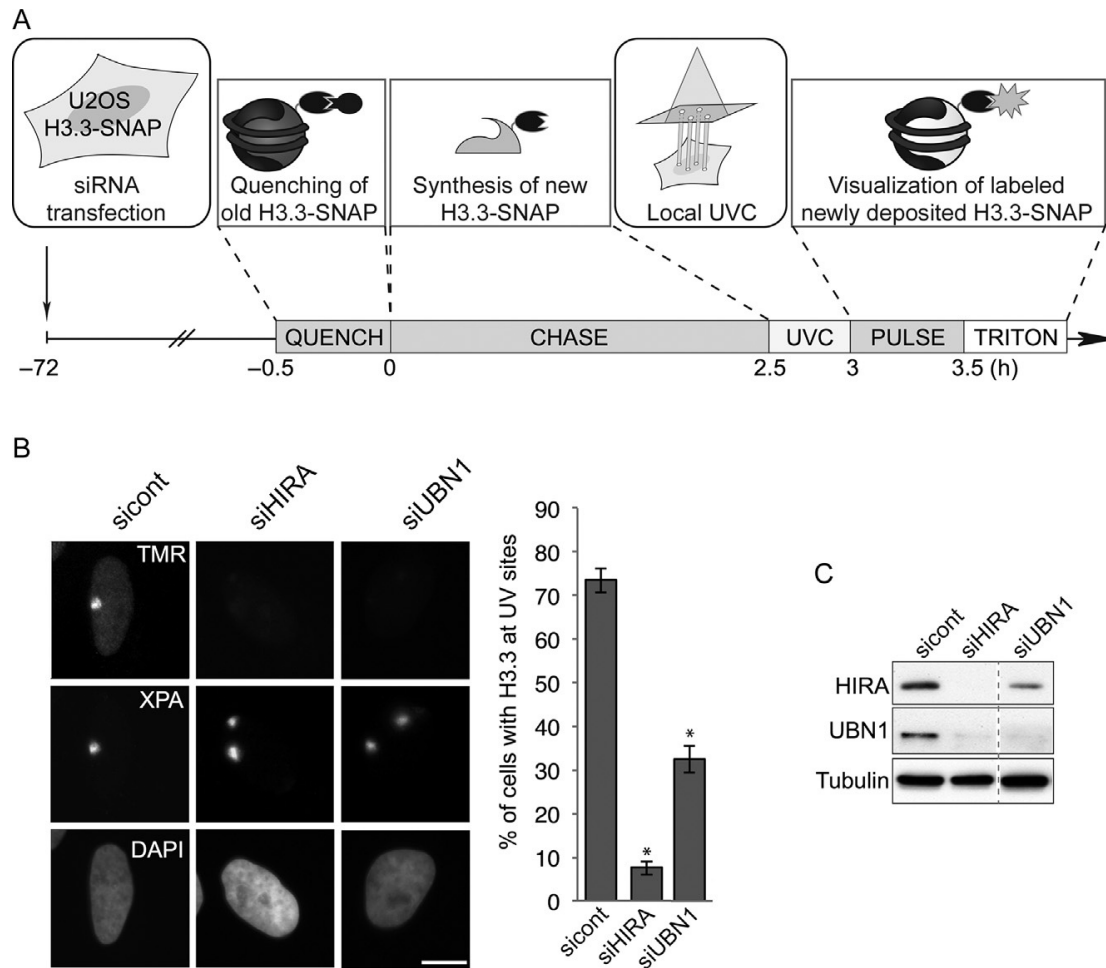
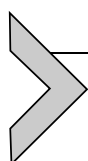


**Fig. 4** De novo histone H3.3 deposition assay coupled with histone chaperone depletion in response to DNA damage. (A) Scheme of the de novo histone deposition assay in response to UVC irradiation coupled with histone chaperone depletion for monitoring accumulation of newly synthesized H3.3-SNAP at damage sites in H3.3-SNAP U2OS cells. Cells are transfected with histone chaperone or control siRNA before local UV irradiation and labeling of new H3.3-SNAP with TMR (by the “quench-chase-pulse” experiment). (B) (Left) Fluorescent microscopy visualization of newly deposited H3.3-SNAP (TMR) accumulating at UV-damaged sites after siRNA transfection against HIRA, UBN1, or control. Immunofluorescence labeling of XPA repair protein allows the visualization of damaged sites. Scale bar, 10  $\mu$ m. (Right) The graph represents the percentage of cells with accumulation of new deposited H3.3-SNAP (TMR) at UV sites. The statistical significance of the difference between siRNA and sicont—as represented by the “\*” when the difference is significant—was analyzed using *t*-test or one-way ANOVA followed by Tukey posttests performed with Prism 5 software. Error bars indicate standard deviation in at least three experiments. (C) SiRNA efficiencies are controlled on the Western blots. Adapted from Adam, S., Polo, S. E., & Almouzni, G. (2013). Transcription recovery after DNA damage requires chromatin priming by the H3.3 histone chaperone HIRA. *Cell*, 155(1), 94–106.

following DNA damage. We carried out the experiments in U2OS cells stably expressing the histone variant H3.3-SNAP. In control cells, H3.3 accumulated at the site of local DNA damage, as defined by the early repair factor XPA immunodetection. In contrast, in cells treated with HIRA and UBN1 siRNA, H3.3 failed to accumulate at XPA-positive sites (Fig. 4B). The depletion efficiencies verified by Western blot for both the HIRA and UBN1 subunits showed that the siRNA had effectively functioned (Fig. 4C). To quantify the defects in histone deposition, we determined the percentage of cells with new H3.3 at UV damage sites in control, HIRA, or UBN1 siRNA treated cells. This percentage decreased in a statistically significant manner (see later for the statistical analysis) for both HIRA and UBN1 siRNA treated cells. The most dramatic effect occurred upon depletion of the HIRA subunit (Fig. 4B). This is consistent with the central role of the HIRA subunit in maintaining the stability of the complex, as shown by the reduced level of UBN1 in HIRA-depleted cells. From the data obtained in this assay, we could conclude that the histone chaperone HIRA was essential for the deposition of the H3.3 histone variant in response to UVC irradiation (Adam et al., 2013).



## 5. IMAGING AND QUANTIFYING SNAP LABELING

For fluorescence image acquisition, we recommend using an epifluorescence microscope equipped with a  $63\times$  objective (we currently use a AxiImager Zeiss Z1 microscope). For consistency, it is essential to carry out image acquisition with identical parameters for all different experimental conditions and to set exposure times carefully for the entire duration of the experiment to avoid camera sensor saturation. For a first approach, 2D images are usually sufficient and recommended to help avoid bleaching. Adaptations are however possible for 3D, but would require specific settings, not detailed here.

Since TMR labeling usually gives rise to higher fluorescence background compared to classical antibody detection, we recommend extensive washing of the fluorescent substrate after the “pulse” step as mentioned above (after two quick washes, an extended wash for 30 min at  $37^{\circ}\text{C}$  5%  $\text{CO}_2$  is followed by two additional quick washes). TMR background level is calculated for all experiments and subtracted from all acquisitions to properly quantify specific

fluorescent labeling. For each TMR image, this is achieved using the ImageJ software, by measuring the mean gray value from an area containing no nucleus in the field. We define this value as the background and subtract it from the entire image. We then perform our quantitative analysis with these background-subtracted images.

To quantify TMR fluorescence intensity in the acquired images, first, the DAPI staining allows the detection of all nuclei and the generation of a mask corresponding to the nuclei. This mask is applied to the TMR fluorescent images, enabling the evaluation of the average TMR fluorescence intensity—represented by the mean gray value (gray value to area ratio)—in each nucleus. This method can easily be automated in ImageJ by a macro allowing quantification of hundreds of nuclei in a fast and effective way. For each condition, we analyze at least a hundred nuclei. We calculate the average TMR fluorescence intensity for each condition and normalize to the control condition. We perform at least three independent experiments for each condition and standard statistical tests (Mann and Whitney test, t.test, or one-way ANOVA followed by Tukey posttests performed with Prism 5 software) are applied to the data.

For H3.3-SNAP labeling, we evaluate the mean gray value in all nuclei, as more than 95% of cells are TMR positive in “quench-chase-pulse” experiments (Ray-Gallet et al., 2011). Moreover, the pattern of labeling is rather homogenous all over the nuclei, with the exception of nucleoli, which display lower signal. In contrast, for H3.1-SNAP labeling, only replicating cells are labeled with newly incorporated H3.1 (Ray-Gallet et al., 2011). Therefore, we costain cells with EdU to detect cells in S phase. After quantification of TMR and EdU fluorescence, we select EdU positive cells and determine TMR fluorescence levels only in these cells. Thus, more cells are needed initially to reach the threshold of a hundred positive cells. Other cell cycle markers can be used effectively (Boyarchuk, Filipescu, Vassias, Cantaloube, & Almouzni, 2014).

To quantify variation in de novo histone deposition in response to local UVC damage, we use a different approach. Instead of exploring the impact of the chaperone depletion on normal incorporation, we count the number of cells with an accumulation of H3.3-SNAP labeling at damaged sites (assessed by XPA immunodetection) (Fig. 4B). Fluorescence quantification is also possible in this case, using XPA staining as a mask instead of the DAPI staining. For example, this can be done to evaluate more subtle impact on the de novo histone deposition coupled with DNA repair.



## 6. INTERPRETING THE DE NOVO HISTONE DEPOSITION ASSAY COUPLED WITH HISTONE CHAPERONE DEPLETION

Drawing conclusions based on this approach requires careful evaluation of the following points, especially to ascertain at which level the impact occurred. It is critical to assess whether any effect occurred at the expression level of the SNAP-tagged histone variant. Indeed, a decrease or an increase of the soluble pool of the SNAP-tagged histone variant, by mass action, could ultimately impinge on the efficiency of its de novo deposition. Thus, we systematically monitor variations in histone pools in soluble, cytosolic, and nuclear extracts from both control and chaperone-depleted cells (Martini, Roche, Marheineke, Verreault, & Almouzni, 1998). By Western blot, we carefully evaluate if any significant changes in the soluble pool of SNAP-tagged histones have occurred. It is also important to assess whether the cell cycle or a chromatin-dependent process such as transcription or replication have been affected. Indeed, changes in these processes could potentially impact histone deposition without interfering directly with the incorporation mechanism. Thus, it is essential, when interpreting the results of the “quench–chase–pulse” assay, to consider not only the deposition event in itself, but the whole assembly line from histone synthesis, to incorporation into chromatin, eviction, and degradation, since all these aspects could potentially influence the results.

In addition to the global fluorescence quantification, analysis of the specific labeling pattern of the newly deposited histone variants is also very informative. In particular, the depletion may affect the site of the histone variant deposition, or the time, without necessarily affecting significantly its efficiency. The method can be further extended to investigate the de novo deposition of a histone variant in specific genomic regions. In this case, specific markers (using antibody recognizing a protein specific to the regions, or DNA FISH, or TALEN, etc.) to covisualize the regions of interest will be needed along with the visualization of new histones.



## 7. CONCLUSION AND PERSPECTIVES

The approach using the SNAP-tag system, pioneered for centromeric variant CENP-A incorporation in late mitosis (Jansen et al., 2007), proved to be instrumental to define the role of the CENP-A dedicated chaperone

HJURP (Dunleavy et al., 2009; Foltz et al., 2009) at this particular time of the cell cycle (Muller et al., 2014; Tachiwana et al., 2015). Here, we describe how it can be extended as a powerful assay to systematically test the contribution of histone chaperones to the de novo deposition of histone variants throughout the different phases of the cell cycle. This can also be achieved after inducing a specific local perturbation in the genome such as DNA damage. We illustrated the two cases with the dynamics of the histone variants H3.1 and H3.3. Importantly, beyond H3.1 and H3.3, we have also used this system effectively for the variants H2A and H2A.Z to explore their distinct dynamics, at euchromatic and heterochromatic loci such as pericentric heterochromatin (Boyarchuk et al., 2014). While these studies used the SNAP-tag system, the CLIP-tag—a modified version of the SNAP-tag—offers an interesting alternative and can be combined with the SNAP-tag system to allow the labeling of two different SNAP and CLIP fusion proteins simultaneously (Gautier et al., 2008). This can be most useful to compare the behavior of distinct tagged proteins and the relative impact of interference with one chaperone or another.

To date, most studies have focused on de novo deposition of histone variants. The system offers interesting avenues to explore the fate of old histones and their recycling during genomic transactions such as DNA replication, repair, or transcription, in order to elucidate, in each case, the exact role of histone chaperones in vivo (Probst, Dunleavy, & Almouzni, 2009). These approaches could help to follow both new and old material, which can be critical to determine how parental information is passed during replication or cell division. How these events function within a given cell lineage to ensure propagation of a given state, and how they may be altered during asymmetric division during a planned differentiation program (Filipescu et al., 2014) is a fascinating question. Considering the recent data highlighting the importance of CAF-1 and its role as a barrier to cell reprogramming (Cheloufi et al., 2015; Hatanaka et al., 2015; Ishiuchi et al., 2015), it is tempting to further explore how this relates to changes in histone variant dynamics. Perturbing histone chaperones—and through them the tight coordination of histone recycling and de novo deposition—provides a unique perspective to address it. In vivo monitoring of old and new histones using the SNAP-tag system, combined with advances in microscopy, along with new genome editing techniques to knockout the chaperones, should further our knowledge of the mechanisms by which the histone chaperone network mediates chromatin assembly at different stages of cellular life.

## ACKNOWLEDGMENTS

We are grateful to Jean Gautier and Lisa Prendergast for critical reading of the manuscript. This work was supported by la Ligue Nationale contre le Cancer (Equipe labellisée Ligue), the European Commission Network of Excellence EpiGeneSys (HEALTH-F4-2010-257082), ERC Advanced Grant 2009-AdG\_20090506 “Eccentric,” the European Commission large-scale integrating project FP7\_HEALTH-2010-259743 “MODHEP,” ANR-11-LABX-0044\_DEEP and ANR-10-IDEX-0001-02 PSL, ANR “CHAPINHIB” ANR-12-BSV5-0022-02, ANR “Epicure” ANR-14-CE16-0009, ANR “CELLECTCHIP” ANR-14-CE10-0013, and Aviesan-ITMO cancer project “Epigenomics of breast cancer.”

## REFERENCES

- Adam, S., Dabin, J., Bai, S. K., & Polo, S. E. (2015). Imaging local deposition of newly synthesized histones in UVC-damaged chromatin. *Methods in Molecular Biology*, 1288, 337–347.
- Adam, S., Polo, S. E., & Almouzni, G. (2013). Transcription recovery after DNA damage requires chromatin priming by the H3.3 histone chaperone HIRA. *Cell*, 155(1), 94–106.
- Bodor, D. L., Rodriguez, M. G., Moreno, N., & Jansen, L. E. (2012). Analysis of protein turnover by quantitative SNAP-based pulse-chase imaging. *Current Protocols in Cell Biology*. Chapter 8, Unit 8.8.
- Boyarchuk, E., Filipescu, D., Vassias, I., Cantaloube, S., & Almouzni, G. (2014). The histone variant composition of centromeres is controlled by the pericentric heterochromatin state during the cell cycle. *Journal of Cell Science*, 127(Pt. 15), 3347–3359.
- Cheloufi, S., Elling, U., Hopfgartner, B., Jung, Y. L., Murn, J., Ninova, M., ... Hochedlinger, K. (2015). The histone chaperone CAF-1 safeguards somatic cell identity. *Nature*, 528, 218–224.
- De Koning, L., Corpet, A., Haber, J. E., & Almouzni, G. (2007). Histone chaperones: An escort network regulating histone traffic. *Nature Structural & Molecular Biology*, 14(11), 997–1007.
- Dunleavy, E. M., Almouzni, G., & Karpen, G. H. (2011). H3.3 is deposited at centromeres in S phase as a placeholder for newly assembled CENP-A in G(1) phase. *Nucleus*, 2(2), 146–157.
- Dunleavy, E. M., Roche, D., Tagami, H., Lacoste, N., Ray-Gallet, D., Nakamura, Y., ... Almouzni-Pettinotti, G. (2009). HJURP is a cell-cycle-dependent maintenance and deposition factor of CENP-A at centromeres. *Cell*, 137(3), 485–497.
- Filipescu, D., Muller, S., & Almouzni, G. (2014). Histone H3 variants and their chaperones during development and disease: Contributing to epigenetic control. *Annual Review of Cell and Developmental Biology*, 30, 615–646.
- Foltz, D. R., Jansen, L. E., Bailey, A. O., Yates, J. R., 3rd., Bassett, E. A., Wood, S., ... Cleveland, D. W. (2009). Centromere-specific assembly of CENP-A nucleosomes is mediated by HJURP. *Cell*, 137(3), 472–484.
- Gaillard, P. H., Martini, E. M., Kaufman, P. D., Stillman, B., Moustacchi, E., & Almouzni, G. (1996). Chromatin assembly coupled to DNA repair: A new role for chromatin assembly factor I. *Cell*, 86(6), 887–896.
- Gaillard, P. H., Roche, D., & Almouzni, G. (1999). Nucleotide excision repair coupled to chromatin assembly. *Methods in Molecular Biology*, 119, 231–243.
- Gautier, A., Juillerat, A., Heinis, C., Correa, I. R., Jr., Kindermann, M., Beaufils, F., & Johnsson, K. (2008). An engineered protein tag for multiprotein labeling in living cells. *Chemistry & Biology*, 15(2), 128–136.

- Goldberg, A. D., Banaszynski, L. A., Noh, K. M., Lewis, P. W., Elsaesser, S. J., Stadler, S., ... Allis, C. D. (2010). Distinct factors control histone variant H3.3 localization at specific genomic regions. *Cell*, *140*(5), 678–691.
- Gurard-Levin, Z. A., Quivy, J. P., & Almouzni, G. (2014). Histone chaperones: Assisting histone traffic and nucleosome dynamics. *Annual Review of Biochemistry*, *83*, 487–517.
- Hatanaka, Y., Inoue, K., Oikawa, M., Kamimura, S., Ogonuki, N., Kodama, E. N., ... Ogura, A. (2015). Histone chaperone CAF-1 mediates repressive histone modifications to protect preimplantation mouse embryos from endogenous retrotransposons. *Proceedings of the National Academy of Sciences of the United States of America*, *112*(47), 14641–14646.
- Ishiuchi, T., Enriquez-Gasca, R., Mizutani, E., Boskovic, A., Ziegler-Birling, C., Rodriguez-Terrones, D., ... Torres-Padilla, M. E. (2015). Early embryonic-like cells are induced by downregulating replication-dependent chromatin assembly. *Nature Structural & Molecular Biology*, *22*, 662–671.
- Jansen, L. E., Black, B. E., Foltz, D. R., & Cleveland, D. W. (2007). Propagation of centromeric chromatin requires exit from mitosis. *The Journal of Cell Biology*, *176*(6), 795–805.
- Kaufman, P. D., & Almouzni, G. (2006). Chromatin assembly. In M. L. De Pamphilis (Ed.), *DNA replication in eucaryotic cells* (pp. 121–140): Cold Spring Harbor: Cold Spring Harbor Press.
- Keppler, A., Gendreizig, S., Gronemeyer, T., Pick, H., Vogel, H., & Johnsson, K. (2003). A general method for the covalent labeling of fusion proteins with small molecules in vivo. *Nature Biotechnology*, *21*(1), 86–89.
- Laskey, R. A., Honda, B. M., Mills, A. D., & Finch, J. T. (1978). Nucleosomes are assembled by an acidic protein which binds histones and transfers them to DNA. *Nature*, *275*(5679), 416–420.
- Martini, E., Roche, D. M., Marheineke, K., Verreault, A., & Almouzni, G. (1998). Recruitment of phosphorylated chromatin assembly factor 1 to chromatin after UV irradiation of human cells. *The Journal of Cell Biology*, *143*(3), 563–575.
- Muller, S., Montes de Oca, R., Lacoste, N., Dingli, F., Loew, D., & Almouzni, G. (2014). Phosphorylation and DNA binding of HJURP determine its centromeric recruitment and function in CenH3(CENP-A) loading. *Cell Reports*, *8*(1), 190–203.
- Polo, S. E., & Almouzni, G. (2015). Chromatin dynamics after DNA damage: The legacy of the access-repair-restore model. *DNA Repair (Amst)*, *36*, 114–121.
- Probst, A. V., Dunleavy, E., & Almouzni, G. (2009). Epigenetic inheritance during the cell cycle. *Nature Reviews. Molecular Cell Biology*, *10*(3), 192–206.
- Ray-Gallet, D., & Almouzni, G. (2004). DNA synthesis-dependent and -independent chromatin assembly pathways in *Xenopus* egg extracts. *Methods in Enzymology*, *375*, 117–131.
- Ray-Gallet, D., Quivy, J. P., Scamps, C., Martini, E. M., Lipinski, M., & Almouzni, G. (2002). HIRA is critical for a nucleosome assembly pathway independent of DNA synthesis. *Molecular Cell*, *9*(5), 1091–1100.
- Ray-Gallet, D., Woolfe, A., Vassias, I., Pellentz, C., Lacoste, N., Puri, A., ... Almouzni, G. (2011). Dynamics of histone H3 deposition in vivo reveal a nucleosome gap-filling mechanism for H3.3 to maintain chromatin integrity. *Molecular Cell*, *44*(6), 928–941.
- Santoro, S. W., & Dulac, C. (2015). Histone variants and cellular plasticity. *Trends in Genetics*, *31*(9), 516–527.
- Shah, J. V., Botvinick, E., Bonday, Z., Furnari, F., Berns, M., & Cleveland, D. W. (2004). Dynamics of centromere and kinetochore proteins: Implications for checkpoint signaling and silencing. *Current Biology*, *14*(11), 942–952.
- Smith, S., & Stillman, B. (1989). Purification and characterization of CAF-I, a human cell factor required for chromatin assembly during DNA replication in vitro. *Cell*, *58*(1), 15–25.

- Stillman, B. (1986). Chromatin assembly during SV40 DNA replication in vitro. *Cell*, 45(4), 555–565.
- Szenker, E., Lacoste, N., & Almouzni, G. (2012). A developmental requirement for HIRA-dependent H3.3 deposition revealed at gastrulation in *Xenopus*. *Cell Reports*, 1(6), 730–740.
- Szenker, E., Ray-Gallet, D., & Almouzni, G. (2011). The double face of the histone variant H3.3. *Cell Research*, 21(3), 421–434.
- Tachiwana, H., Muller, S., Blumer, J., Klare, K., Musacchio, A., & Almouzni, G. (2015). HJURP involvement in de novo CenH3(CENP-A) and CENP-C recruitment. *Cell Reports*, 11(1), 22–32.
- Tagami, H., Ray-Gallet, D., Almouzni, G., & Nakatani, Y. (2004). Histone H3.1 and H3.3 complexes mediate nucleosome assembly pathways dependent or independent of DNA synthesis. *Cell*, 116(1), 51–61.
- Talbert, P. B., & Henikoff, S. (2010). Histone variants—Ancient wrap artists of the epigenome. *Nature Reviews. Molecular Cell Biology*, 11(4), 264–275.



# References

---



- Abascal, F., A. Corpet, Z. A. Gurard-Levin, D. Juan, F. Ochsenbein, D. Rico, A. Valencia and G. Almouzni (2013). "Subfunctionalization via adaptive evolution influenced by genomic context: the case of histone chaperones ASF1a and ASF1b." Mol Biol Evol **30**(8): 1853-1866.
- Adam, S., S. E. Polo and G. Almouzni (2013). "Transcription recovery after DNA damage requires chromatin priming by the H3.3 histone chaperone HIRA." Cell **155**(1): 94-106.
- Adams, P. D. (2009). "Healing and hurting: molecular mechanisms, functions, and pathologies of cellular senescence." Mol Cell **36**(1): 2-14.
- Adkins, M. W., S. R. Howar and J. K. Tyler (2004). "Chromatin disassembly mediated by the histone chaperone Asf1 is essential for transcriptional activation of the yeast PHO5 and PHO8 genes." Molecular cell **14**(5): 657-666.
- Adkins, M. W. and J. K. Tyler (2004). "The histone chaperone Asf1p mediates global chromatin disassembly in vivo." The Journal of biological chemistry **279**(50): 52069-52074.
- Adkins, M. W. and J. K. Tyler (2006). "Transcriptional activators are dispensable for transcription in the absence of Spt6-mediated chromatin reassembly of promoter regions." Mol Cell **21**(3): 405-416.
- Agez, M., J. Chen, R. Guerois, C. van Heijenoort, J. Y. Thuret, C. Mann and F. Ochsenbein (2007). "Structure of the histone chaperone ASF1 bound to the histone H3 C-terminal helix and functional insights." Structure **15**(2): 191-199.
- Ahmad, K. and S. Henikoff (2002). "Histone H3 variants specify modes of chromatin assembly." Proc Natl Acad Sci U S A **99 Suppl 4**: 16477-16484.
- Ahmad, K. and S. Henikoff (2002). "The histone variant H3.3 marks active chromatin by replication-independent nucleosome assembly." Mol Cell **9**(6): 1191-1200.
- Akai, Y., N. Adachi, Y. Hayashi, M. Eitoku, N. Sano, R. Natsume, N. Kudo, M. Tanokura, T. Senda and M. Horikoshi (2010). "Structure of the histone chaperone CIA/ASF1-double bromodomain complex linking histone modifications and site-specific histone eviction." Proc Natl Acad Sci U S A **107**(18): 8153-8158.
- Akiyama, T., O. Suzuki, J. Matsuda and F. Aoki (2011). "Dynamic replacement of histone H3 variants reprograms epigenetic marks in early mouse embryos." PLoS Genet **7**(10): e1002279.

Alabert, C., T. K. Barth, N. Reveron-Gomez, S. Sidoli, A. Schmidt, O. N. Jensen, A. Imhof and A. Groth (2015). "Two distinct modes for propagation of histone PTMs across the cell cycle." Genes & development **29**(6): 585-590.

Alabert, C., J. C. Bukowski-Wills, S. B. Lee, G. Kustatscher, K. Nakamura, F. de Lima Alves, P. Menard, J. Mejlvang, J. Rappsilber and A. Groth (2014). "Nascent chromatin capture proteomics determines chromatin dynamics during DNA replication and identifies unknown fork components." Nature cell biology **16**(3): 281-293.

Allfrey, V. G., R. Faulkner and A. E. Mirsky (1964). "Acetylation and Methylation of Histones and Their Possible Role in the Regulation of Rna Synthesis." Proc Natl Acad Sci U S A **51**: 786-794.

Allfrey, V. G. and A. E. Mirsky (1964). "Structural Modifications of Histones and their Possible Role in the Regulation of RNA Synthesis." Science **144**(3618): 559.

Allshire, R. C. and G. H. Karpen (2008). "Epigenetic regulation of centromeric chromatin: old dogs, new tricks?" Nat Rev Genet **9**(12): 923-937.

Almouzni, G. and H. Cedar (2016). "Maintenance of Epigenetic Information." Cold Spring Harbor Perspectives in Biology **8**(5): a019372.

Antczak, A. J., T. Tsubota, P. D. Kaufman and J. M. Berger (2006). "Structure of the yeast histone H3-ASF1 interaction: implications for chaperone mechanism, species-specific interactions, and epigenetics." BMC Struct Biol **6**: 26.

Arents, G., R. W. Burlingame, B. C. Wang, W. E. Love and E. N. Moudrianakis (1991). "The nucleosomal core histone octamer at 3.1 A resolution: a tripartite protein assembly and a left-handed superhelix." Proc Natl Acad Sci U S A **88**(22): 10148-10152.

Arents, G. and E. N. Moudrianakis (1995). "The histone fold: a ubiquitous architectural motif utilized in DNA compaction and protein dimerization." Proc Natl Acad Sci U S A **92**(24): 11170-11174.

Arlt, M. F., J. G. Mülle, V. M. Schaibley, R. L. Ragland, S. G. Durkin, S. T. Warren and T. W. Glover (2009). "Replication stress induces genome-wide copy number changes in human cells that resemble polymorphic and pathogenic variants." Am J Hum Genet **84**(3): 339-350.

Arlt, M. F., A. C. Ozdemir, S. R. Birkeland, T. E. Wilson and T. W. Glover (2011). "Hydroxyurea induces de novo copy number variants in human cells." Proc Natl Acad Sci U S A **108**(42): 17360-17365.

- Ask, K., Z. Jasencakova, P. Menard, Y. Feng, G. Almouzni and A. Groth (2012). "Codanin-1, mutated in the anaemic disease CDAI, regulates Asf1 function in S-phase histone supply." The EMBO journal **31**(8): 2013-2023.
- Balhorn, R. (2007). "The protamine family of sperm nuclear proteins." Genome Biol **8**(9): 227.
- Banaszynski, L. A., D. Wen, S. Dewell, S. J. Whitcomb, M. Lin, N. Diaz, S. J. Elsassner, A. Chapgier, A. D. Goldberg, E. Canaani, S. Rafii, D. Zheng and C. D. Allis (2013). "Hira-dependent histone H3.3 deposition facilitates PRC2 recruitment at developmental loci in ES cells." Cell **155**(1): 107-120.
- Bannister, A. J., P. Zegerman, J. F. Partridge, E. A. Miska, J. O. Thomas, R. C. Allshire and T. Kouzarides (2001). "Selective recognition of methylated lysine 9 on histone H3 by the HP1 chromo domain." Nature **410**(6824): 120-124.
- Bantignies, F., V. Roure, I. Comet, B. Leblanc, B. Schuettengruber, J. Bonnet, V. Tixier, A. Mas and G. Cavalli (2011). "Polycomb-dependent regulatory contacts between distant Hox loci in Drosophila." Cell **144**(2): 214-226.
- Barski, A., S. Cuddapah, K. Cui, T. Y. Roh, D. E. Schones, Z. Wang, G. Wei, I. Chepelev and K. Zhao (2007). "High-resolution profiling of histone methylations in the human genome." Cell **129**(4): 823-837.
- Bartkova, J., Z. Horejsi, K. Koed, A. Kramer, F. Tort, K. Zieger, P. Guldborg, M. Sehested, J. M. Nesland, C. Lukas, T. Orntoft, J. Lukas and J. Bartek (2005). "DNA damage response as a candidate anti-cancer barrier in early human tumorigenesis." Nature **434**(7035): 864-870.
- Bartkova, J., N. Rezaei, M. Lontos, P. Karakaidos, D. Kletsas, N. Issaeva, L. V. Vassiliou, E. Kolettas, K. Niforou, V. C. Zoumpourlis, M. Takaoka, H. Nakagawa, F. Tort, K. Fugger, F. Johansson, M. Sehested, C. L. Andersen, L. Dyrskjot, T. Orntoft, J. Lukas, C. Kittas, T. Helleday, T. D. Halazonetis, J. Bartek and V. G. Gorgoulis (2006). "Oncogene-induced senescence is part of the tumorigenesis barrier imposed by DNA damage checkpoints." Nature **444**(7119): 633-637.
- Beliveau, B. J., A. N. Boettiger, M. S. Avendano, R. Jungmann, R. B. McCole, E. F. Joyce, C. Kim-Kiselak, F. Bantignies, C. Y. Fonseka, J. Erceg, M. A. Hannan, H. G. Hoang, D. Colognori, J. T. Lee, W. M. Shih, P. Yin, X. Zhuang and C. T. Wu (2015). "Single-molecule super-resolution imaging of chromosomes and in situ haplotype visualization using Oligopaint FISH probes." Nat Commun **6**: 7147.
- Beliveau, B. J., E. F. Joyce, N. Apostolopoulos, F. Yilmaz, C. Y. Fonseka, R. B. McCole, Y. Chang, J. B. Li, T. N. Senaratne, B. R. Williams, J. M. Rouillard and C. T. Wu (2012). "Versatile design and synthesis platform for visualizing genomes with Oligopaint FISH probes." Proc Natl Acad Sci U S A **109**(52): 21301-21306.

- Belotserkovskaya, R., S. Oh, V. A. Bondarenko, G. Orphanides, V. M. Studitsky and D. Reinberg (2003). "FACT facilitates transcription-dependent nucleosome alteration." Science **301**(5636): 1090-1093.
- Bensimon, A., A. Simon, A. Chiffaudel, V. Croquette, F. Heslot and D. Bensimon (1994). "Alignment and sensitive detection of DNA by a moving interface." Science **265**(5181): 2096-2098.
- Bernstein, B. E., M. Kamal, K. Lindblad-Toh, S. Bekiranov, D. K. Bailey, D. J. Huebert, S. McMahon, E. K. Karlsson, E. J. Kulbokas, 3rd, T. R. Gingeras, S. L. Schreiber and E. S. Lander (2005). "Genomic maps and comparative analysis of histone modifications in human and mouse." Cell **120**(2): 169-181.
- Bernstein, E., E. M. Duncan, O. Masui, J. Gil, E. Heard and C. D. Allis (2006). "Mouse polycomb proteins bind differentially to methylated histone H3 and RNA and are enriched in facultative heterochromatin." Mol Cell Biol **26**(7): 2560-2569.
- Bester, A. C., M. Roniger, Y. S. Oren, M. M. Im, D. Sarni, M. Chaoat, A. Bensimon, G. Zamir, D. S. Shewach and B. Kerem (2011). "Nucleotide deficiency promotes genomic instability in early stages of cancer development." Cell **145**(3): 435-446.
- Billing, R. J. and J. Bonner (1972). "The structure of chromatin as revealed by deoxyribonuclease digestion studies." Biochim Biophys Acta **281**(3): 453-462.
- Bird, A. (2007). "Perceptions of epigenetics." Nature **447**(7143): 396-398.
- Bird, A., M. Taggart, M. Frommer, O. J. Miller and D. Macleod (1985). "A fraction of the mouse genome that is derived from islands of nonmethylated, CpG-rich DNA." Cell **40**(1): 91-99.
- Bird, A. P. (1986). "CpG-rich islands and the function of DNA methylation." Nature **321**(6067): 209-213.
- Black, B. E. and E. A. Bassett (2008). "The histone variant CENP-A and centromere specification." Curr Opin Cell Biol **20**(1): 91-100.
- Black, B. E., D. R. Foltz, S. Chakravarthy, K. Luger, V. L. Woods, Jr. and D. W. Cleveland (2004). "Structural determinants for generating centromeric chromatin." Nature **430**(6999): 578-582.
- Blackwell, J. S., Jr., S. T. Wilkinson, N. Mosammamaparast and L. F. Pemberton (2007). "Mutational analysis of H3 and H4 N termini reveals distinct roles in nuclear import." J Biol Chem **282**(28): 20142-20150.
- Bode, J., M. M. Gomez-Lira and H. Schroter (1983). "Nucleosomal particles open as the histone core becomes hyperacetylated." Eur J Biochem **130**(3): 437-445.

Bolzer, A., G. Kreth, I. Solovei, D. Koehler, K. Saracoglu, C. Fauth, S. Muller, R. Eils, C. Cremer, M. R. Speicher and T. Cremer (2005). "Three-dimensional maps of all chromosomes in human male fibroblast nuclei and prometaphase rosettes." PLoS Biol **3**(5): e157.

Bonne-Andrea, C., M. L. Wong and B. M. Alberts (1990). "In vitro replication through nucleosomes without histone displacement." Nature **343**(6260): 719-726.

Boyarchuk, E., R. Montes de Oca and G. Almouzni (2011). "Cell cycle dynamics of histone variants at the centromere, a model for chromosomal landmarks." Curr Opin Cell Biol **23**(3): 266-276.

Boyes, J. and A. Bird (1991). "DNA methylation inhibits transcription indirectly via a methyl-CpG binding protein." Cell **64**(6): 1123-1134.

Bush, K. M., B. T. Yuen, B. L. Barrilleaux, J. W. Riggs, H. O'Geen, R. F. Cotterman and P. S. Knoepfler (2013). "Endogenous mammalian histone H3.3 exhibits chromatin-related functions during development." Epigenetics Chromatin **6**(1): 7.

Cairns, B. R. (2009). "The logic of chromatin architecture and remodelling at promoters." Nature **461**(7261): 193-198.

Camozzi, D., C. Capanni, V. Cenni, E. Mattioli, M. Columbaro, S. Squarzone and G. Lattanzi (2014). "Diverse lamin-dependent mechanisms interact to control chromatin dynamics." Nucleus **5**(5): 427-440.

Campos, E. I., A. H. Smits, Y. H. Kang, S. Landry, T. M. Escobar, S. Nayak, B. M. Ueberheide, D. Durocher, M. Vermeulen, J. Hurwitz and D. Reinberg (2015). "Analysis of the Histone H3.1 Interactome: A Suitable Chaperone for the Right Event." Mol Cell.

Cattoni, D. I., A. M. Cardozo Gizzi, M. Georgieva, M. Di Stefano, A. Valeri, D. Chamousset, C. Houbron, S. Dejardin, J. B. Fiche, I. Gonzalez, J. M. Chang, T. Sexton, M. A. Marti-Renom, F. Bantignies, G. Cavalli and M. Nollmann (2017). "Single-cell absolute contact probability detection reveals chromosomes are organized by multiple low-frequency yet specific interactions." Nat Commun **8**(1): 1753.

Cheloufi, S., U. Elling, B. Hopfgartner, Y. L. Jung, J. Murn, M. Ninova, M. Hubmann, A. I. Badeaux, C. E. Ang, D. Tenen, D. J. Wesche, N. Abazova, M. Hogue, N. Tasdemir, J. Brumbaugh, P. Rathert, J. Jude, F. Ferrari, A. Blanco, M. Fellner, D. Wenzel, M. Zinner, S. E. Vidal, O. Bell, M. Stadtfeld, H. Y. Chang, G. Almouzni, J. Rinn, M. Wernig, A. Aravin, Y. Shi, J. M. Penninger, J. Zuber and K. Hochedlinger (2015). "The histone chaperone CAF-1 safeguards somatic cell identity." Nature(in press).

Chimura, T., T. Kuzuhara and M. Horikoshi (2002). "Identification and characterization of CIA/ASF1 as an interactor of bromodomains associated with TFIID." Proc Natl Acad Sci U S A **99**(14): 9334-9339.

Cimprich, K. A. and D. Cortez (2008). "ATR: an essential regulator of genome integrity." Nat Rev Mol Cell Biol **9**(8): 616-627.

Coleman, R. T. and G. Struhl (2017). "Causal role for inheritance of H3K27me3 in maintaining the OFF state of a Drosophila HOX gene." Science **356**(6333).

Cook, A. J., Z. A. Gurard-Levin, I. Vassias and G. Almouzni (2011). "A specific function for the histone chaperone NASP to fine-tune a reservoir of soluble H3-H4 in the histone supply chain." Molecular cell **44**(6): 918-927.

Corpet, A. and G. Almouzni (2009). "Making copies of chromatin: the challenge of nucleosomal organization and epigenetic information." Trends in cell biology **19**(1): 29-41.

Corpet, A., L. De Koning, J. Toedling, A. Savignoni, F. Berger, C. Lemaitre, R. J. O'Sullivan, J. Karlseder, E. Barillot, B. Asselain, X. Sastre-Garau and G. Almouzni (2011). "Asf1b, the necessary Asf1 isoform for proliferation, is predictive of outcome in breast cancer." The EMBO journal **30**(3): 480-493.

Costantino, L., S. K. Sotiriou, J. K. Rantala, S. Magin, E. Mladenov, T. Helleday, J. E. Haber, G. Iliakis, O. P. Kallioniemi and T. D. Halazonetis (2014). "Break-induced replication repair of damaged forks induces genomic duplications in human cells." Science **343**(6166): 88-91.

Couldrey, C., M. B. Carlton, P. M. Nolan, W. H. Colledge and M. J. Evans (1999). "A retroviral gene trap insertion into the histone 3.3A gene causes partial neonatal lethality, stunted growth, neuromuscular deficits and male sub-fertility in transgenic mice." Hum Mol Genet **8**(13): 2489-2495.

Creyghton, M. P., A. W. Cheng, G. G. Welstead, T. Kooistra, B. W. Carey, E. J. Steine, J. Hanna, M. A. Lodato, G. M. Frampton, P. A. Sharp, L. A. Boyer, R. A. Young and R. Jaenisch (2010). "Histone H3K27ac separates active from poised enhancers and predicts developmental state." Proc Natl Acad Sci U S A **107**(50): 21931-21936.

Cusick, M. E., M. L. DePamphilis and P. M. Wassarman (1984). "Dispersive segregation of nucleosomes during replication of simian virus 40 chromosomes." J Mol Biol **178**(2): 249-271.

Daganzo, S. M., J. P. Erzberger, W. M. Lam, E. Skordalakes, R. Zhang, A. A. Franco, S. J. Brill, P. D. Adams, J. M. Berger and P. D. Kaufman (2003). "Structure and function of the conserved core of histone deposition protein Asf1." Curr Biol **13**(24): 2148-2158.

- Dalal, Y., T. Furuyama, D. Vermaak and S. Henikoff (2007). "Structure, dynamics, and evolution of centromeric nucleosomes." Proc Natl Acad Sci U S A **104**(41): 15974-15981.
- Daujat, S., U. Zeissler, T. Waldmann, N. Happel and R. Schneider (2005). "HP1 binds specifically to Lys26-methylated histone H1.4, whereas simultaneous Ser27 phosphorylation blocks HP1 binding." J Biol Chem **280**(45): 38090-38095.
- Davey, C. A. and T. J. Richmond (2002). "DNA-dependent divalent cation binding in the nucleosome core particle." Proc Natl Acad Sci U S A **99**(17): 11169-11174.
- Davey, C. A., D. F. Sargent, K. Luger, A. W. Maeder and T. J. Richmond (2002). "Solvent mediated interactions in the structure of the nucleosome core particle at 1.9 a resolution." J Mol Biol **319**(5): 1097-1113.
- Dawson, S. C., M. S. Sagolla and W. Z. Cande (2007). "The cenH3 histone variant defines centromeres in *Giardia intestinalis*." Chromosoma **116**(2): 175-184.
- De Koning, L., A. Corpet, J. E. Haber and G. Almouzni (2007). "Histone chaperones: an escort network regulating histone traffic." Nature structural & molecular biology **14**(11): 997-1007.
- Dhalluin, C., J. E. Carlson, L. Zeng, C. He, A. K. Aggarwal and M. M. Zhou (1999). "Structure and ligand of a histone acetyltransferase bromodomain." Nature **399**(6735): 491-496.
- Di Micco, R., M. Fumagalli, A. Cicalese, S. Piccinin, P. Gasparini, C. Luise, C. Schurra, M. Garre, P. G. Nuciforo, A. Bensimon, R. Maestro, P. G. Pelicci and F. d'Adda di Fagagna (2006). "Oncogene-induced senescence is a DNA damage response triggered by DNA hyper-replication." Nature **444**(7119): 638-642.
- Dileep, V., F. Ay, J. Sima, D. L. Vera, W. S. Noble and D. M. Gilbert (2015). "Topologically associating domains and their long-range contacts are established during early G1 coincident with the establishment of the replication-timing program." Genome Res **25**(8): 1104-1113.
- Dimitriadis, E. K., C. Weber, R. K. Gill, S. Diekmann and Y. Dalal (2010). "Tetrameric organization of vertebrate centromeric nucleosomes." Proc Natl Acad Sci U S A **107**(47): 20317-20322.
- Dittmer, T. A. and T. Misteli (2011). "The lamin protein family." Genome biology **12**(5): 222.
- Dixon, J. R., S. Selvaraj, F. Yue, A. Kim, Y. Li, Y. Shen, M. Hu, J. S. Liu and B. Ren (2012). "Topological domains in mammalian genomes identified by analysis of chromatin interactions." Nature **485**(7398): 376-380.

- Dodd, I. B., M. A. Micheelsen, K. Sneppen and G. Thon (2007). "Theoretical analysis of epigenetic cell memory by nucleosome modification." Cell **129**(4): 813-822.
- Dorigo, B., T. Schalch, A. Kulangara, S. Duda, R. R. Schroeder and T. J. Richmond (2004). "Nucleosome arrays reveal the two-start organization of the chromatin fiber." Science **306**(5701): 1571-1573.
- Drane, P., K. Ouararhni, A. Depaux, M. Shuaib and A. Hamiche (2010). "The death-associated protein DAXX is a novel histone chaperone involved in the replication-independent deposition of H3.3." Genes Dev **24**(12): 1253-1265.
- Dunleavy, E. M., G. Almouzni and G. H. Karpen (2011). "H3.3 is deposited at centromeres in S phase as a placeholder for newly assembled CENP-A in G(1) phase." Nucleus **2**(2): 146-157.
- Dunleavy, E. M., D. Roche, H. Tagami, N. Lacoste, D. Ray-Gallet, Y. Nakamura, Y. Daigo, Y. Nakatani and G. Almouzni-Pettinotti (2009). "HJURP is a cell-cycle-dependent maintenance and deposition factor of CENP-A at centromeres." Cell **137**(3): 485-497.
- Duro, E., C. Lundin, K. Ask, L. Sanchez-Pulido, T. J. MacArtney, R. Toth, C. P. Ponting, A. Groth, T. Helleday and J. Rouse (2010). "Identification of the MMS22L-TONSL complex that promotes homologous recombination." Mol Cell **40**(4): 632-644.
- Earnshaw, W. C., B. M. Honda, R. A. Laskey and J. O. Thomas (1980). "Assembly of nucleosomes: the reaction involving *X. laevis* nucleoplasmin." Cell **21**(2): 373-383.
- Earnshaw, W. C. and N. Rothfield (1985). "Identification of a family of human centromere proteins using autoimmune sera from patients with scleroderma." Chromosoma **91**(3-4): 313-321.
- Edmunds, C. E., L. J. Simpson and J. E. Sale (2008). "PCNA ubiquitination and REV1 define temporally distinct mechanisms for controlling translesion synthesis in the avian cell line DT40." Mol Cell **30**(4): 519-529.
- Eissenberg, J. C. and S. C. Elgin (2000). "The HP1 protein family: getting a grip on chromatin." Curr Opin Genet Dev **10**(2): 204-210.
- Ekwall, K., T. Olsson, B. M. Turner, G. Cranston and R. C. Allshire (1997). "Transient inhibition of histone deacetylation alters the structural and functional imprint at fission yeast centromeres." Cell **91**(7): 1021-1032.

- Elgin, S. C. and H. Weintraub (1975). "Chromosomal proteins and chromatin structure." Annu Rev Biochem **44**: 725-774.
- Elliott, S. G. and C. S. McLaughlin (1978). "Rate of macromolecular synthesis through the cell cycle of the yeast *Saccharomyces cerevisiae*." Proc Natl Acad Sci U S A **75**(9): 4384-4388.
- Eltsov, M., K. M. Maclellan, K. Maeshima, A. S. Frangakis and J. Dubochet (2008). "Analysis of cryo-electron microscopy images does not support the existence of 30-nm chromatin fibers in mitotic chromosomes in situ." Proc Natl Acad Sci U S A **105**(50): 19732-19737.
- Emili, A., D. M. Schieltz, J. R. Yates, 3rd and L. H. Hartwell (2001). "Dynamic interaction of DNA damage checkpoint protein Rad53 with chromatin assembly factor Asf1." Molecular cell **7**(1): 13-20.
- English, C. M., M. W. Adkins, J. J. Carson, M. E. Churchill and J. K. Tyler (2006). "Structural basis for the histone chaperone activity of Asf1." Cell **127**(3): 495-508.
- Filion, G. J., J. G. van Bommel, U. Braunschweig, W. Talhout, J. Kind, L. D. Ward, W. Brugman, I. J. de Castro, R. M. Kerkhoven, H. J. Bussemaker and B. van Steensel (2010). "Systematic protein location mapping reveals five principal chromatin types in *Drosophila* cells." Cell **143**(2): 212-224.
- Fillingham, J., P. Kainth, J. P. Lambert, H. van Bakel, K. Tsui, L. Pena-Castillo, C. Nislow, D. Figeys, T. R. Hughes, J. Greenblatt and B. J. Andrews (2009). "Two-color cell array screen reveals interdependent roles for histone chaperones and a chromatin boundary regulator in histone gene repression." Mol Cell **35**(3): 340-351.
- Finch, J. T. and A. Klug (1976). "Solenoidal model for superstructure in chromatin." Proc Natl Acad Sci U S A **73**(6): 1897-1901.
- Flemming, J. (1882). "Zellsubstanz, Kern und Zelltheilung."
- Foltz, D. R., L. E. Jansen, A. O. Bailey, J. R. Yates, 3rd, E. A. Bassett, S. Wood, B. E. Black and D. W. Cleveland (2009). "Centromere-specific assembly of CENP-a nucleosomes is mediated by HJURP." Cell **137**(3): 472-484.
- Fragkos, M., O. Ganier, P. Coulombe and M. Mechali (2015). "DNA replication origin activation in space and time." Nat Rev Mol Cell Biol **16**(6): 360-374.
- Franklin, S. G. and A. Zweidler (1977). "Non-allelic variants of histones 2a, 2b and 3 in mammals." Nature **266**(5599): 273-275.

- Fromental-Ramain, C., P. Ramain and A. Hamiche (2017). "The Drosophila DAXX like protein (DLP) cooperates with ASF1 for H3.3 deposition and heterochromatin formation." Mol Cell Biol.
- Fuller, M. T. and A. C. Spradling (2007). "Male and female Drosophila germline stem cells: two versions of immortality." Science **316**(5823): 402-404.
- Furuyama, T. and S. Henikoff (2009). "Centromeric nucleosomes induce positive DNA supercoils." Cell **138**(1): 104-113.
- Fussner, E., M. Strauss, U. Djuric, R. Li, K. Ahmed, M. Hart, J. Ellis and D. P. Bazett-Jones (2012). "Open and closed domains in the mouse genome are configured as 10-nm chromatin fibres." EMBO Rep **13**(11): 992-996.
- Gaillard, P. H., E. M. Martini, P. D. Kaufman, B. Stillman, E. Moustacchi and G. Almouzni (1996). "Chromatin assembly coupled to DNA repair: a new role for chromatin assembly factor I." Cell **86**(6): 887-896.
- Galili, G., A. Levy and K. M. Jakob (1981). "Changes in chromatin structure at the replication fork. II The DNPs containing nascent DNA and a transient chromatin modification detected by DNAase I." Nucleic Acids Res **9**(16): 3991-4005.
- Garcia-Ramirez, M., F. Dong and J. Ausio (1992). "Role of the histone "tails" in the folding of oligonucleosomes depleted of histone H1." J Biol Chem **267**(27): 19587-19595.
- Garcia-Ramirez, M., C. Rocchini and J. Ausio (1995). "Modulation of chromatin folding by histone acetylation." J Biol Chem **270**(30): 17923-17928.
- Gasser, R., T. Koller and J. M. Sogo (1996). "The stability of nucleosomes at the replication fork." Journal of molecular biology **258**(2): 224-239.
- Gaydos, L. J., W. Wang and S. Strome (2014). "Gene repression. H3K27me and PRC2 transmit a memory of repression across generations and during development." Science **345**(6203): 1515-1518.
- Gazin, C., N. Wajapeyee, S. Gobeil, C. M. Virbasius and M. R. Green (2007). "An elaborate pathway required for Ras-mediated epigenetic silencing." Nature **449**(7165): 1073-1077.
- Gellert, M., M. N. Lipsett and D. R. Davies (1962). "Helix formation by guanylic acid." Proc Natl Acad Sci U S A **48**: 2013-2018.
- Goldberg, A. D., L. A. Banaszynski, K. M. Noh, P. W. Lewis, S. J. Elsaesser, S. Stadler, S. Dewell, M. Law, X. Guo, X. Li, D. Wen, A. Chapgier, R. C. DeKever, J. C. Miller, Y. L. Lee, E. A. Boydston, M. C. Holmes, P. D. Gregory, J. M. Greally, S. Rafii, C. Yang, P.

- J. Scambler, D. Garrick, R. J. Gibbons, D. R. Higgs, I. M. Cristea, F. D. Urnov, D. Zheng and C. D. Allis (2010). "Distinct factors control histone variant H3.3 localization at specific genomic regions." Cell **140**(5): 678-691.
- Gonzalez-Munoz, E., Y. Arboleda-Estudillo, H. H. Otu and J. B. Cibelli (2014). "Cell reprogramming. Histone chaperone ASF1A is required for maintenance of pluripotency and cellular reprogramming." Science **345**(6198): 822-825.
- Goodfellow, H., A. Krejci, Y. Moshkin, C. P. Verrijzer, F. Karch and S. J. Bray (2007). "Gene-specific targeting of the histone chaperone asf1 to mediate silencing." Dev Cell **13**(4): 593-600.
- Gorgoulis, V. G., L. V. Vassiliou, P. Karakaidos, P. Zacharatos, A. Kotsinas, T. Liloglou, M. Venere, R. A. Ditullio, Jr., N. G. Kastrinakis, B. Levy, D. Kletsas, A. Yoneta, M. Herlyn, C. Kittas and T. D. Halazonetis (2005). "Activation of the DNA damage checkpoint and genomic instability in human precancerous lesions." Nature **434**(7035): 907-913.
- Govin, J., C. Caron, S. Rousseaux and S. Khochbin (2005). "Testis-specific histone H3 expression in somatic cells." Trends Biochem Sci **30**(7): 357-359.
- Green, E. M., A. J. Antczak, A. O. Bailey, A. A. Franco, K. J. Wu, J. R. Yates, 3rd and P. D. Kaufman (2005). "Replication-independent histone deposition by the HIR complex and Asf1." Current biology : CB **15**(22): 2044-2049.
- Groth, A., A. Corpet, A. J. Cook, D. Roche, J. Bartek, J. Lukas and G. Almouzni (2007). "Regulation of replication fork progression through histone supply and demand." Science **318**(5858): 1928-1931.
- Groth, A., D. Ray-Gallet, J. P. Quivy, J. Lukas, J. Bartek and G. Almouzni (2005). "Human Asf1 regulates the flow of S phase histones during replicational stress." Molecular cell **17**(2): 301-311.
- Gruss, C., J. Wu, T. Koller and J. M. Sogo (1993). "Disruption of the nucleosomes at the replication fork." EMBO J **12**(12): 4533-4545.
- Guilbaud, G., A. Rappailles, A. Baker, C. L. Chen, A. Arneodo, A. Goldar, Y. d'Aubenton-Carafa, C. Thermes, B. Audit and O. Hyrien (2011). "Evidence for sequential and increasing activation of replication origins along replication timing gradients in the human genome." PLoS Comput Biol **7**(12): e1002322.
- Hake, S. B., B. A. Garcia, E. M. Duncan, M. Kauer, G. Dellaire, J. Shabanowitz, D. P. Bazett-Jones, C. D. Allis and D. F. Hunt (2006). "Expression patterns and post-translational modifications associated with mammalian histone H3 variants." J Biol Chem **281**(1): 559-568.

Hake, S. B., B. A. Garcia, M. Kauer, S. P. Baker, J. Shabanowitz, D. F. Hunt and C. D. Allis (2005). "Serine 31 phosphorylation of histone variant H3.3 is specific to regions bordering centromeres in metaphase chromosomes." Proc Natl Acad Sci U S A **102**(18): 6344-6349.

Halazonetis, T. D., V. G. Gorgoulis and J. Bartek (2008). "An oncogene-induced DNA damage model for cancer development." Science **319**(5868): 1352-1355.

Hall, M. A., A. Shundrovsky, L. Bai, R. M. Fulbright, J. T. Lis and M. D. Wang (2009). "High-resolution dynamic mapping of histone-DNA interactions in a nucleosome." Nat Struct Mol Biol **16**(2): 124-129.

Hartford, S. A., Y. Luo, T. L. Southard, I. M. Min, J. T. Lis and J. C. Schimenti (2011). "Minichromosome maintenance helicase paralog MCM9 is dispensible for DNA replication but functions in germ-line stem cells and tumor suppression." Proceedings of the National Academy of Sciences of the United States of America **108**(43): 17702-17707.

Hathaway, N. A., O. Bell, C. Hodges, E. L. Miller, D. S. Neel and G. R. Crabtree (2012). "Dynamics and memory of heterochromatin in living cells." Cell **149**(7): 1447-1460.

He, Y. F., B. Z. Li, Z. Li, P. Liu, Y. Wang, Q. Tang, J. Ding, Y. Jia, Z. Chen, L. Li, Y. Sun, X. Li, Q. Dai, C. X. Song, K. Zhang, C. He and G. L. Xu (2011). "Tet-mediated formation of 5-carboxylcytosine and its excision by TDG in mammalian DNA." Science **333**(6047): 1303-1307.

Heintzman, N. D., G. C. Hon, R. D. Hawkins, P. Kheradpour, A. Stark, L. F. Harp, Z. Ye, L. K. Lee, R. K. Stuart, C. W. Ching, K. A. Ching, J. E. Antosiewicz-Bourget, H. Liu, X. Zhang, R. D. Green, V. V. Lobanenko, R. Stewart, J. A. Thomson, G. E. Crawford, M. Kellis and B. Ren (2009). "Histone modifications at human enhancers reflect global cell-type-specific gene expression." Nature **459**(7243): 108-112.

Heitz, E. (1928). "Das heterochromatin der Moose." Jb Wiss Bot **69**:728.

Hendrich, B. and A. Bird (1998). "Identification and characterization of a family of mammalian methyl-CpG binding proteins." Mol Cell Biol **18**(11): 6538-6547.

Hewish, D. R. and L. A. Burgoyne (1973). "Chromatin sub-structure. The digestion of chromatin DNA at regularly spaced sites by a nuclear deoxyribonuclease." Biochem Biophys Res Commun **52**(2): 504-510.

Hirano, Y., K. Hizume, H. Kimura, K. Takeyasu, T. Haraguchi and Y. Hiraoka (2012). "Lamin B receptor recognizes specific modifications of histone H4 in heterochromatin formation." The Journal of biological chemistry **287**(51): 42654-42663.

- Hiratani, I. and D. M. Gilbert (2009). "Replication timing as an epigenetic mark." Epigenetics **4**(2): 93-97.
- Hiratani, I., S. Takebayashi, J. Lu and D. M. Gilbert (2009). "Replication timing and transcriptional control: beyond cause and effect--part II." Curr Opin Genet Dev **19**(2): 142-149.
- Hodl, M. and K. Basler (2009). "Transcription in the absence of histone H3.3." Curr Biol **19**(14): 1221-1226.
- Hodl, M. and K. Basler (2012). "Transcription in the absence of histone H3.2 and H3K4 methylation." Curr Biol **22**(23): 2253-2257.
- Hojfeldt, J. W., A. Laugesen, B. M. Willumsen, H. Damhofer, L. Hedehus, A. Tvardovskiy, F. Mohammad, O. N. Jensen and K. Helin (2018). "Accurate H3K27 methylation can be established de novo by SUZ12-directed PRC2." Nat Struct Mol Biol **25**(3): 225-232.
- Holliday, R. (1994). "Epigenetics: an overview." Dev Genet **15**(6): 453-457.
- Hu, F., A. A. Alcasabas and S. J. Elledge (2001). "Asf1 links Rad53 to control of chromatin assembly." Genes & development **15**(9): 1061-1066.
- Huang, C., Z. Zhang, M. Xu, Y. Li, Z. Li, Y. Ma, T. Cai and B. Zhu (2013). "H3.3-H4 tetramer splitting events feature cell-type specific enhancers." PLoS genetics **9**(6): e1003558.
- Huang, H., C. B. Strømme, G. Saredi, M. Hödl, A. Strandsby, C. González-Aguilera, S. Chen, A. Groth and D. J. Patel (2015). "A unique binding mode enables MCM2 to chaperone histones H3-H4 at replication forks." Nature structural & molecular biology(this issue).
- Ishiuchi, T., R. Enriquez-Gasca, E. Mizutani, A. Boskovic, C. Ziegler-Birling, D. Rodriguez-Terrones, T. Wakayama, J. M. Vaquerizas and M. E. Torres-Padilla (2015). "Early embryonic-like cells are induced by downregulating replication-dependent chromatin assembly." Nat Struct Mol Biol.
- Ito, S., A. C. D'Alessio, O. V. Taranova, K. Hong, L. C. Sowers and Y. Zhang (2010). "Role of Tet proteins in 5mC to 5hmC conversion, ES-cell self-renewal and inner cell mass specification." Nature **466**(7310): 1129-1133.
- Ito, S., L. Shen, Q. Dai, S. C. Wu, L. B. Collins, J. A. Swenberg, C. He and Y. Zhang (2011). "Tet proteins can convert 5-methylcytosine to 5-formylcytosine and 5-carboxylcytosine." Science **333**(6047): 1300-1303.

Jackson, V. and R. Chalkley (1981). "A new method for the isolation of replicative chromatin: selective deposition of histone on both new and old DNA." Cell **23**(1): 121-134.

Jackson, V. and R. Chalkley (1985). "Histone segregation on replicating chromatin." Biochemistry **24**(24): 6930-6938.

Jansen, J. G., A. Tsaalbi-Shtylik, G. Hendriks, H. Gali, A. Hendel, F. Johansson, K. Erixon, Z. Livneh, L. H. Mullenders, L. Haracska and N. de Wind (2009). "Separate domains of Rev1 mediate two modes of DNA damage bypass in mammalian cells." Mol Cell Biol **29**(11): 3113-3123.

Jansen, L. E., B. E. Black, D. R. Foltz and D. W. Cleveland (2007). "Propagation of centromeric chromatin requires exit from mitosis." The Journal of cell biology **176**(6): 795-805.

Jasencakova, Z. and A. Groth (2010). "Restoring chromatin after replication: how new and old histone marks come together." Seminars in cell & developmental biology **21**(2): 231-237.

Jasencakova, Z., A. N. Scharf, K. Ask, A. Corpet, A. Imhof, G. Almouzni and A. Groth (2010). "Replication stress interferes with histone recycling and predeposition marking of new histones." Molecular cell **37**(5): 736-743.

Jenuwein, T. and C. D. Allis (2001). "Translating the histone code." Science **293**(5532): 1074-1080.

Jiao, Y., K. Seeger, A. Lautrette, A. Gaubert, F. Mousson, R. Guerois, C. Mann and F. Ochsenbein (2012). "Surprising complexity of the Asf1 histone chaperone-Rad53 kinase interaction." Proc Natl Acad Sci U S A **109**(8): 2866-2871.

Jin, C. and G. Felsenfeld (2007). "Nucleosome stability mediated by histone variants H3.3 and H2A.Z." Genes Dev **21**(12): 1519-1529.

Johnson, L. M., P. S. Kayne, E. S. Kahn and M. Grunstein (1990). "Genetic evidence for an interaction between SIR3 and histone H4 in the repression of the silent mating loci in *Saccharomyces cerevisiae*." Proc Natl Acad Sci U S A **87**(16): 6286-6290.

Jones, R. M., O. Mortusewicz, I. Afzal, M. Lorvellec, P. Garcia, T. Helleday and E. Petermann (2013). "Increased replication initiation and conflicts with transcription underlie Cyclin E-induced replication stress." Oncogene **32**(32): 3744-3753.

- Kaplan, C. D., L. Laprade and F. Winston (2003). "Transcription elongation factors repress transcription initiation from cryptic sites." Science **301**(5636): 1096-1099.
- Kaufman, P. D., R. Kobayashi, N. Kessler and B. Stillman (1995). "The p150 and p60 subunits of chromatin assembly factor I: a molecular link between newly synthesized histones and DNA replication." Cell **81**(7): 1105-1114.
- Kemble, D. J., F. G. Whitby, H. Robinson, L. L. McCullough, T. Formosa and C. P. Hill (2013). "Structure of the Spt16 middle domain reveals functional features of the histone chaperone FACT." J Biol Chem **288**(15): 10188-10194.
- Keppler, A., S. Gendreizig, T. Gronemeyer, H. Pick, H. Vogel and K. Johnsson (2003). "A general method for the covalent labeling of fusion proteins with small molecules in vivo." Nat Biotechnol **21**(1): 86-89.
- Killander, D. and A. Zetterberg (1965). "Quantitative Cytochemical Studies on Interphase Growth. I. Determination of DNA, Rna and Mass Content of Age Determined Mouse Fibroblasts in Vitro and of Intercellular Variation in Generation Time." Exp Cell Res **38**: 272-284.
- Kind, J., L. Pagie, H. Ortabozkoyun, S. Boyle, S. S. de Vries, H. Janssen, M. Amendola, L. D. Nolen, W. A. Bickmore and B. van Steensel (2013). "Single-cell dynamics of genome-nuclear lamina interactions." Cell **153**(1): 178-192.
- Klempnauer, K. H., E. Fanning, B. Otto and R. Knippers (1980). "Maturation of newly replicated chromatin of simian virus 40 and its host cell." J Mol Biol **136**(4): 359-374.
- Korber, P., S. Barbaric, T. Luckenbach, A. Schmid, U. J. Schermer, D. Blaschke and W. Horz (2006). "The histone chaperone Asf1 increases the rate of histone eviction at the yeast PHO5 and PHO8 promoters." J Biol Chem **281**(9): 5539-5545.
- Kornberg, R. D. (1974). "Chromatin structure: a repeating unit of histones and DNA." Science **184**(4139): 868-871.
- Kouzarides, T. (2007). "Chromatin modifications and their function." Cell **128**(4): 693-705.
- Krawitz, D. C., T. Kama and P. D. Kaufman (2002). "Chromatin Assembly Factor I Mutants Defective for PCNA Binding Require Asf1/Hir Proteins for Silencing." Molecular and Cellular Biology **22**(2): 614-625.

- Kriaucionis, S. and N. Heintz (2009). "The nuclear DNA base 5-hydroxymethylcytosine is present in Purkinje neurons and the brain." Science **324**(5929): 929-930.
- Krude, T. and R. Knippers (1991). "Transfer of nucleosomes from parental to replicated chromatin." Mol Cell Biol **11**(12): 6257-6267.
- Krude, T. and R. Knippers (1993). "Nucleosome assembly during complementary DNA strand synthesis in extracts from mammalian cells." J Biol Chem **268**(19): 14432-14442.
- Lachner, M., D. O'Carroll, S. Rea, K. Mechtler and T. Jenuwein (2001). "Methylation of histone H3 lysine 9 creates a binding site for HP1 proteins." Nature **410**(6824): 116-120.
- Lamour, V., Y. Lecluse, C. Desmaze, M. Spector, M. Bodescot, A. Aurias, M. A. Osley and M. Lipinski (1995). "A human homolog of the *S. cerevisiae* HIR1 and HIR2 transcriptional repressors cloned from the DiGeorge syndrome critical region." Hum Mol Genet **4**(5): 791-799.
- Laprell, F., K. Finkl and J. Muller (2017). "Propagation of Polycomb-repressed chromatin requires sequence-specific recruitment to DNA." Science **356**(6333): 85-88.
- Larson, A. G., D. Elnatan, M. M. Keenen, M. J. Trnka, J. B. Johnston, A. L. Burlingame, D. A. Agard, S. Redding and G. J. Narlikar (2017). "Liquid droplet formation by HP1alpha suggests a role for phase separation in heterochromatin." Nature **547**(7662): 236-240.
- Laskey, R. A., B. M. Honda, A. D. Mills and J. T. Finch (1978). "Nucleosomes are assembled by an acidic protein which binds histones and transfers them to DNA." Nature **275**(5679): 416-420.
- Laskey, R. A., A. D. Mills and N. R. Morris (1977). "Assembly of SV40 chromatin in a cell-free system from *Xenopus* eggs." Cell **10**(2): 237-243.
- Latreille, D., L. Bluy, M. Benkirane and R. E. Kiernan (2014). "Identification of histone 3 variant 2 interacting factors." Nucleic Acids Res **42**(6): 3542-3550.
- Le, S., C. Davis, J. B. Konopka and R. Sternglanz (1997). "Two new S-phase-specific genes from *Saccharomyces cerevisiae*." Yeast **13**(11): 1029-1042.
- Lee, T. I., R. G. Jenner, L. A. Boyer, M. G. Guenther, S. S. Levine, R. M. Kumar, B. Chevalier, S. E. Johnstone, M. F. Cole, K. Isono, H. Koseki, T. Fuchikami, K. Abe, H. L. Murray, J. P. Zucker, B. Yuan, G. W. Bell, E. Herbolsheimer, N. M. Hannett, K. Sun, D. T. Odom, A. P. Otte, T. L. Volkert, D. P. Bartel, D. A. Melton, D. K. Gifford, R.

- Jaenisch and R. A. Young (2006). "Control of developmental regulators by Polycomb in human embryonic stem cells." *Cell* **125**(2): 301-313.
- Lehnertz, B., Y. Ueda, A. A. Derijck, U. Braunschweig, L. Perez-Burgos, S. Kubicek, T. Chen, E. Li, T. Jenuwein and A. H. Peters (2003). "Suv39h-mediated histone H3 lysine 9 methylation directs DNA methylation to major satellite repeats at pericentric heterochromatin." *Curr Biol* **13**(14): 1192-1200.
- Li, E. and Y. Zhang (2014). "DNA methylation in mammals." *Cold Spring Harb Perspect Biol* **6**(5): a019133.
- Li, Y., Z. F. Pursell and S. Linn (2000). "Identification and cloning of two histone fold motif-containing subunits of HeLa DNA polymerase epsilon." *J Biol Chem* **275**(30): 23247-23252.
- Lieberman-Aiden, E., N. L. van Berkum, L. Williams, M. Imakaev, T. Ragozy, A. Telling, I. Amit, B. R. Lajoie, P. J. Sabo, M. O. Dorschner, R. Sandstrom, B. Bernstein, M. A. Bender, M. Groudine, A. Gnirke, J. Stamatoyannopoulos, L. A. Mirny, E. S. Lander and J. Dekker (2009). "Comprehensive mapping of long-range interactions reveals folding principles of the human genome." *Science* **326**(5950): 289-293.
- Liu, S., Z. Xu, H. Leng, P. Zheng, J. Yang, K. Chen, J. Feng and Q. Li (2017). "RPA binds histone H3-H4 and functions in DNA replication-coupled nucleosome assembly." *Science* **355**(6323): 415-420.
- Loppin, B., E. Bonnefoy, C. Anselme, A. Laurencon, T. L. Karr and P. Couble (2005). "The histone H3.3 chaperone HIRA is essential for chromatin assembly in the male pronucleus." *Nature* **437**(7063): 1386-1390.
- Lorain, S., J. P. Quivy, F. Monier-Gavelle, C. Scamps, Y. Lecluse, G. Almouzni and M. Lipinski (1998). "Core histones and HIRIP3, a novel histone-binding protein, directly interact with WD repeat protein HIRA." *Mol Cell Biol* **18**(9): 5546-5556.
- Loyola, A., T. Bonaldi, D. Roche, A. Imhof and G. Almouzni (2006). "PTMs on H3 variants before chromatin assembly potentiate their final epigenetic state." *Molecular cell* **24**(2): 309-316.
- Loyola, A., H. Tagami, T. Bonaldi, D. Roche, J. P. Quivy, A. Imhof, Y. Nakatani, S. Y. Dent and G. Almouzni (2009). "The HP1alpha-CAF1-SetDB1-containing complex provides H3K9me1 for Suv39-mediated K9me3 in pericentric heterochromatin." *EMBO reports* **10**(7): 769-775.
- Lucchini, R. and J. M. Sogo (1995). "Replication of transcriptionally active chromatin." *Nature* **374**(6519): 276-280.

- Luger, K., A. W. Mader, R. K. Richmond, D. F. Sargent and T. J. Richmond (1997). "Crystal structure of the nucleosome core particle at 2.8 Å resolution." Nature **389**(6648): 251-260.
- Macheret, M. and T. D. Halazonetis (2015). "DNA replication stress as a hallmark of cancer." Annu Rev Pathol **10**: 425-448.
- Macheret, M. and T. D. Halazonetis (2018). "Intragenic origins due to short G1 phases underlie oncogene-induced DNA replication stress." Nature **555**(7694): 112-116.
- Machida, S., Y. Takizawa, M. Ishimaru, Y. Sugita, S. Sekine, J. I. Nakayama, M. Wolf and H. Kurumizaka (2018). "Structural Basis of Heterochromatin Formation by Human HP1." Mol Cell **69**(3): 385-397 e388.
- Maison, C. and G. Almouzni (2004). "HP1 and the dynamics of heterochromatin maintenance." Nature reviews. Molecular cell biology **5**(4): 296-304.
- Maison, C., D. Bailly, D. Roche, R. Montes de Oca, A. V. Probst, I. Vassias, F. Dingli, B. Lombard, D. Loew, J. P. Quivy and G. Almouzni (2011). "SUMOylation promotes de novo targeting of HP1 $\alpha$  to pericentric heterochromatin." Nature genetics **43**(3): 220-227.
- Majka, J. and P. M. Burgers (2004). "The PCNA-RFC families of DNA clamps and clamp loaders." Prog Nucleic Acid Res Mol Biol **78**: 227-260.
- Malay, A. D., T. Umehara, K. Matsubara-Malay, B. Padmanabhan and S. Yokoyama (2008). "Crystal structures of fission yeast histone chaperone Asf1 complexed with the Hip1 B-domain or the Cac2 C terminus." J Biol Chem **283**(20): 14022-14031.
- Malik, H. S. and S. Henikoff (2003). "Phylogenomics of the nucleosome." Nat Struct Biol **10**(11): 882-891.
- Margueron, R., N. Justin, K. Ohno, M. L. Sharpe, J. Son, W. J. Drury, 3rd, P. Voigt, S. R. Martin, W. R. Taylor, V. De Marco, V. Pirrotta, D. Reinberg and S. J. Gambelin (2009). "Role of the polycomb protein EED in the propagation of repressive histone marks." Nature **461**(7265): 762-767.
- Margueron, R. and D. Reinberg (2010). "Chromatin structure and the inheritance of epigenetic information." Nat Rev Genet **11**(4): 285-296.
- Masai, H., S. Matsumoto, Z. You, N. Yoshizawa-Sugata and M. Oda (2010). "Eukaryotic chromosome DNA replication: where, when, and how?" Annu Rev Biochem **79**: 89-130.

Masumoto, H., D. Hawke, R. Kobayashi and A. Verreault (2005). "A role for cell-cycle-regulated histone H3 lysine 56 acetylation in the DNA damage response." Nature **436**(7048): 294-298.

Mattiroli, F., Y. Gu, T. Yadav, J. L. Balsbaugh, M. R. Harris, E. S. Findlay, Y. Liu, C. A. Radebaugh, L. A. Stargell, N. G. Ahn, I. Whitehouse and K. Luger (2017). "DNA-mediated association of two histone-bound CAF-1 complexes drives tetrasome assembly in the wake of DNA replication." Elife **6**.

McDowall, A. W., J. M. Smith and J. Dubochet (1986). "Cryo-electron microscopy of vitrified chromosomes in situ." EMBO J **5**(6): 1395-1402.

Melcher, M., M. Schmid, L. Aagaard, P. Selenko, G. Laible and T. Jenuwein (2000). "Structure-function analysis of SUV39H1 reveals a dominant role in heterochromatin organization, chromosome segregation, and mitotic progression." Molecular and Cellular Biology **20**(10): 3728-3741.

Mello, J. A., H. H. Sillje, D. M. Roche, D. B. Kirschner, E. A. Nigg and G. Almouzni (2002). "Human Asf1 and CAF-1 interact and synergize in a repair-coupled nucleosome assembly pathway." EMBO reports **3**(4): 329-334.

Messiaen, S., J. Guiard, C. Aigueperse, I. Fliniaux, S. Tourpin, V. Barroca, I. Allemand, P. Fouchet, G. Livera and M. Vernet (2016). "Loss of the histone chaperone ASF1B reduces female reproductive capacity in mice." Reproduction **151**(5): 477-489.

Mikkelsen, T. S., M. Ku, D. B. Jaffe, B. Issac, E. Lieberman, G. Giannoukos, P. Alvarez, W. Brockman, T. K. Kim, R. P. Koche, W. Lee, E. Mendenhall, A. O'Donovan, A. Presser, C. Russ, X. Xie, A. Meissner, M. Wernig, R. Jaenisch, C. Nusbaum, E. S. Lander and B. E. Bernstein (2007). "Genome-wide maps of chromatin state in pluripotent and lineage-committed cells." Nature **448**(7153): 553-560.

Mirsky, A. E., B. Silverman and N. C. Panda (1972). "Blocking by histones of accessibility to DNA in chromatin: addition of histones." Proc Natl Acad Sci U S A **69**(11): 3243-3246.

Mito, Y., J. G. Henikoff and S. Henikoff (2005). "Genome-scale profiling of histone H3.3 replacement patterns." Nat Genet **37**(10): 1090-1097.

Mohandas, T., R. S. Sparkes and L. J. Shapiro (1981). "Reactivation of an inactive human X chromosome: evidence for X inactivation by DNA methylation." Science **211**(4480): 393-396.

Montes de Oca, R., P. R. Andreassen and K. L. Wilson (2011). "Barrier-to-Autointegration Factor influences specific histone modifications." Nucleus **2**(6): 580-590.

Montes de Oca, R., Z. A. Gurard-Levin, F. Berger, H. Rehman, E. Martel, A. Corpet, L. de Koning, I. Vassias, L. O. Wilson, D. Meseure, F. Reyat, A. Savignoni, B. Asselain, X. Sastre-Garau and G. Almouzni (2015). "The histone chaperone HJURP is a new independent prognostic marker for luminal A breast carcinoma." Mol Oncol **9**(3): 657-674.

Moshkin, Y. M., J. A. Armstrong, R. K. Maeda, J. W. Tamkun, P. Verrijzer, J. A. Kennison and F. Karch (2002). "Histone chaperone ASF1 cooperates with the Brahma chromatin-remodelling machinery." Genes Dev **16**(20): 2621-2626.

Moshkin, Y. M., T. W. Kan, H. Goodfellow, K. Bezstarosti, R. K. Maeda, M. Pilyugin, F. Karch, S. J. Bray, J. A. Demmers and C. P. Verrijzer (2009). "Histone chaperones ASF1 and NAP1 differentially modulate removal of active histone marks by LID-RPD3 complexes during NOTCH silencing." Mol Cell **35**(6): 782-793.

Mousson, F., A. Lautrette, J. Y. Thuret, M. Agez, R. Courbeyrette, B. Amigues, E. Becker, J. M. Neumann, R. Guerois, C. Mann and F. Ochsenbein (2005). "Structural basis for the interaction of Asf1 with histone H3 and its functional implications." Proceedings of the National Academy of Sciences of the United States of America **102**(17): 5975-5980.

Mousson, F., F. Ochsenbein and C. Mann (2007). "The histone chaperone Asf1 at the crossroads of chromatin and DNA checkpoint pathways." Chromosoma **116**(2): 79-93.

Mozzetta, C., E. Boyarchuk, J. Pontis and S. Ait-Si-Ali (2015). "Sound of silence: the properties and functions of repressive Lys methyltransferases." Nat Rev Mol Cell Biol **16**(8): 499-513.

Munakata, T., N. Adachi, N. Yokoyama, T. Kuzuhara and M. Horikoshi (2000). "A human homologue of yeast anti-silencing factor has histone chaperone activity." Genes Cells **5**(3): 221-233.

Murray, K. (1964). "The Occurrence of Epsilon-N-Methyl Lysine in Histones." Biochemistry **3**: 10-15.

Murzina, N., A. Verreault, E. Laue and B. Stillman (1999). "Heterochromatin dynamics in mouse cells: interaction between chromatin assembly factor 1 and HP1 proteins." Mol Cell **4**(4): 529-540.

- Natsume, R., M. Eitoku, Y. Akai, N. Sano, M. Horikoshi and T. Senda (2007). "Structure and function of the histone chaperone CIA/ASF1 complexed with histones H3 and H4." Nature **446**(7133): 338-341.
- Neelsen, K. J., I. M. Zanini, R. Herrador and M. Lopes (2013). "Oncogenes induce genotoxic stress by mitotic processing of unusual replication intermediates." J Cell Biol **200**(6): 699-708.
- Ng, R. K. and J. B. Gurdon (2008). "Epigenetic memory of an active gene state depends on histone H3.3 incorporation into chromatin in the absence of transcription." Nat Cell Biol **10**(1): 102-109.
- Nishino, Y., M. Eltsov, Y. Joti, K. Ito, H. Takata, Y. Takahashi, S. Hihara, A. S. Frangakis, N. Imamoto, T. Ishikawa and K. Maeshima (2012). "Human mitotic chromosomes consist predominantly of irregularly folded nucleosome fibres without a 30-nm chromatin structure." EMBO J **31**(7): 1644-1653.
- O'Connell, B. C., B. Adamson, J. R. Lydeard, M. E. Sowa, A. Ciccio, A. L. Bredemeyer, M. Schlabach, S. P. Gygi, S. J. Elledge and J. W. Harper (2010). "A genome-wide camptothecin sensitivity screen identifies a mammalian MMS22L-NFKBIL2 complex required for genomic stability." Mol Cell **40**(4): 645-657.
- O'Donnell, L., S. Panier, J. Wildenhain, J. M. Tkach, A. Al-Hakim, M. C. Landry, C. Escribano-Diaz, R. K. Szilard, J. T. Young, M. Munro, M. D. Canny, N. K. Kolas, W. Zhang, S. M. Harding, J. Ylanko, M. Mendez, M. Mullin, T. Sun, B. Habermann, A. Datti, R. G. Bristow, A. C. Gingras, M. D. Tyers, G. W. Brown and D. Durocher (2010). "The MMS22L-TONSL complex mediates recovery from replication stress and homologous recombination." Mol Cell **40**(4): 619-631.
- O'Sullivan, R. J. and G. Almouzni (2014). "Assembly of telomeric chromatin to create ALternative endings." Trends in cell biology **24**(11): 675-685.
- O'Sullivan, R. J., N. Arnoult, D. H. Lackner, L. Oganessian, C. Haggblom, A. Corpet, G. Almouzni and J. Karlseder (2014). "Rapid induction of alternative lengthening of telomeres by depletion of the histone chaperone ASF1." Nature structural & molecular biology **21**(2): 167-174.
- Olins, A. L. and D. E. Olins (1974). "Spheroid chromatin units (v bodies)." Science **183**(4122): 330-332.
- Olins, A. L., G. Rhodes, D. B. Welch, M. Zwerger and D. E. Olins (2010). "Lamin B receptor: multi-tasking at the nuclear envelope." Nucleus **1**(1): 53-70.
- Orphanides, G., W. H. Wu, W. S. Lane, M. Hampsey and D. Reinberg (1999). "The chromatin-specific transcription elongation factor FACT comprises human SPT16 and SSRP1 proteins." Nature **400**(6741): 284-288.

- Orsi, G. A., P. Couble and B. Loppin (2009). "Epigenetic and replacement roles of histone variant H3.3 in reproduction and development." Int J Dev Biol **53**(2-3): 231-243.
- Osada, S., A. Sutton, N. Muster, C. E. Brown, J. R. Yates, 3rd, R. Sternglanz and J. L. Workman (2001). "The yeast SAS (something about silencing) protein complex contains a MYST-type putative acetyltransferase and functions with chromatin assembly factor ASF1." Genes Dev **15**(23): 3155-3168.
- Ou, H. D., S. Phan, T. J. Deerinck, A. Thor, M. H. Ellisman and C. C. O'Shea (2017). "ChromEMT: Visualizing 3D chromatin structure and compaction in interphase and mitotic cells." Science **357**(6349).
- Oudet, P., M. Gross-Bellard and P. Chambon (1975). "Electron microscopic and biochemical evidence that chromatin structure is a repeating unit." Cell **4**(4): 281-300.
- Owen, D. J., P. Ornaghi, J. C. Yang, N. Lowe, P. R. Evans, P. Ballario, D. Neuhaus, P. Filetici and A. A. Travers (2000). "The structural basis for the recognition of acetylated histone H4 by the bromodomain of histone acetyltransferase gcn5p." EMBO J **19**(22): 6141-6149.
- Pace, L., C. Goudot, E. Zueva, P. Gueguen, N. Burgdorf, J. J. Waterfall, J. P. Quivy, G. Almouzni and S. Amigorena (2018). "The epigenetic control of stemness in CD8(+) T cell fate commitment." Science **359**(6372): 177-186.
- Pederson, T. (1972). "Chromatin structure and the cell cycle." Proc Natl Acad Sci U S A **69**(8): 2224-2228.
- Pengelly, A. R., O. Copur, H. Jackle, A. Herzig and J. Muller (2013). "A histone mutant reproduces the phenotype caused by loss of histone-modifying factor Polycomb." Science **339**(6120): 698-699.
- Peters, A. H., S. Kubicek, K. Mechtler, R. J. O'Sullivan, A. A. Derijck, L. Perez-Burgos, A. Kohlmaier, S. Opravil, M. Tachibana, Y. Shinkai, J. H. Martens and T. Jenuwein (2003). "Partitioning and plasticity of repressive histone methylation states in mammalian chromatin." Molecular cell **12**(6): 1577-1589.
- Peters, A. H., D. O'Carroll, H. Scherthan, K. Mechtler, S. Sauer, C. Schofer, K. Weipoltshammer, M. Pagani, M. Lachner, A. Kohlmaier, S. Opravil, M. Doyle, M. Sibilia and T. Jenuwein (2001). "Loss of the Suv39h histone methyltransferases impairs mammalian heterochromatin and genome stability." Cell **107**(3): 323-337.

Petruk, S., K. L. Black, S. K. Kovermann, H. W. Brock and A. Mazo (2013). "Stepwise histone modifications are mediated by multiple enzymes that rapidly associate with nascent DNA during replication." Nat Commun **4**: 2841.

Petruk, S., Y. Sedkov, D. M. Johnston, J. W. Hodgson, K. L. Black, S. K. Kovermann, S. Beck, E. Canaani, H. W. Brock and A. Mazo (2012). "TrxG and PcG proteins but not methylated histones remain associated with DNA through replication." Cell **150**(5): 922-933.

Pfeiffer, S. E. (1968). "RNA synthesis in synchronously growing populations of HeLa S3 cells. II. Rate of synthesis of individual RNA fractions." J Cell Physiol **71**(1): 95-104.

Piwko, W., M. H. Olma, M. Held, J. N. Bianco, P. G. Pedrioli, K. Hofmann, P. Pasero, D. W. Gerlich and M. Peter (2010). "RNAi-based screening identifies the Mms22L-Nfkbil2 complex as a novel regulator of DNA replication in human cells." EMBO J **29**(24): 4210-4222.

Platero, J. S., T. Hartnett and J. C. Eissenberg (1995). "Functional analysis of the chromo domain of HP1." EMBO J **14**(16): 3977-3986.

Pokholok, D. K., C. T. Harbison, S. Levine, M. Cole, N. M. Hannett, T. I. Lee, G. W. Bell, K. Walker, P. A. Rolfe, E. Herbolzheimer, J. Zeitlinger, F. Lewitter, D. K. Gifford and R. A. Young (2005). "Genome-wide map of nucleosome acetylation and methylation in yeast." Cell **122**(4): 517-527.

Poleshko, A., K. M. Mansfield, C. C. Burlingame, M. D. Andrade, N. R. Shah and R. A. Katz (2013). "The human protein PRR14 tethers heterochromatin to the nuclear lamina during interphase and mitotic exit." Cell reports **5**(2): 292-301.

Polo, S. E., D. Roche and G. Almouzni (2006). "New histone incorporation marks sites of UV repair in human cells." Cell **127**(3): 481-493.

Poot, R. A., L. Bozhenok, D. L. van den Berg, S. Steffensen, F. Ferreira, M. Grimaldi, N. Gilbert, J. Ferreira and P. D. Varga-Weisz (2004). "The Williams syndrome transcription factor interacts with PCNA to target chromatin remodelling by ISWI to replication foci." Nat Cell Biol **6**(12): 1236-1244.

Prado, F., F. Cortes-Ledesma and A. Aguilera (2004). "The absence of the yeast chromatin assembly factor Asf1 increases genomic instability and sister chromatid exchange." EMBO Rep **5**(5): 497-502.

Prescott, D. M. (1966). "The syntheses of total macronuclear protein, histone, and DNA during the cell cycle in *Euplotes eurystomus*." J Cell Biol **31**(1): 1-9.

- Probst, A. V. and G. Almouzni (2011). "Heterochromatin establishment in the context of genome-wide epigenetic reprogramming." Trends in genetics : TIG **27**(5): 177-185.
- Probst, A. V., E. Dunleavy and G. Almouzni (2009). "Epigenetic inheritance during the cell cycle." Nature reviews. Molecular cell biology **10**(3): 192-206.
- Pueschel, R., F. Coraggio and P. Meister (2016). "From single genes to entire genomes: the search for a function of nuclear organization." Development **143**(6): 910-923.
- Quivy, J. P., P. Grandi and G. Almouzni (2001). "Dimerization of the largest subunit of chromatin assembly factor 1: importance in vitro and during *Xenopus* early development." The EMBO journal **20**(8): 2015-2027.
- Quivy, J. P., D. Roche, D. Kirschner, H. Tagami, Y. Nakatani and G. Almouzni (2004). "A CAF-1 dependent pool of HP1 during heterochromatin duplication." EMBO J **23**(17): 3516-3526.
- Rada-Iglesias, A., R. Bajpai, T. Swigut, S. A. Brugmann, R. A. Flynn and J. Wysocka (2011). "A unique chromatin signature uncovers early developmental enhancers in humans." Nature **470**(7333): 279-283.
- Radman-Livaja, M., K. F. Verzijlbergen, A. Weiner, T. van Welsem, N. Friedman, O. J. Rando and F. van Leeuwen (2011). "Patterns and mechanisms of ancestral histone protein inheritance in budding yeast." PLoS biology **9**(6): e1001075.
- Ramachandran, S., K. Ahmad and S. Henikoff (2017). "Capitalizing on disaster: Establishing chromatin specificity behind the replication fork." Bioessays **39**(4).
- Ramachandran, S. and S. Henikoff (2015). "Replicating Nucleosomes." Sci Adv **1**(7).
- Ramachandran, S. and S. Henikoff (2016). "Transcriptional Regulators Compete with Nucleosomes Post-replication." Cell **165**(3): 580-592.
- Ramey, C. J., S. Howar, M. Adkins, J. Linger, J. Spicer and J. K. Tyler (2004). "Activation of the DNA damage checkpoint in yeast lacking the histone chaperone anti-silencing function 1." Mol Cell Biol **24**(23): 10313-10327.
- Randall, S. K. and T. J. Kelly (1992). "The fate of parental nucleosomes during SV40 DNA replication." J Biol Chem **267**(20): 14259-14265.
- Rao, S. S. P., S. C. Huang, B. Glenn St Hilaire, J. M. Engreitz, E. M. Perez, K. R. Kieffer-Kwon, A. L. Sanborn, S. E. Johnstone, G. D. Bascom, I. D. Bochkov, X. Huang, M. S. Shamim, J. Shin, D. Turner, Z. Ye, A. D. Omer, J. T. Robinson, T.

- Schlick, B. E. Bernstein, R. Casellas, E. S. Lander and E. L. Aiden (2017). "Cohesin Loss Eliminates All Loop Domains." Cell **171**(2): 305-320 e324.
- Ray-Gallet, D. and G. Almouzni (2004). "DNA synthesis-dependent and -independent chromatin assembly pathways in *Xenopus* egg extracts." Methods Enzymol **375**: 117-131.
- Ray-Gallet, D. and G. Almouzni (2010). "Molecular biology. Mixing or not mixing." Science **328**(5974): 56-57.
- Ray-Gallet, D., J. P. Quivy, C. Scamps, E. M. Martini, M. Lipinski and G. Almouzni (2002). "HIRA is critical for a nucleosome assembly pathway independent of DNA synthesis." Molecular cell **9**(5): 1091-1100.
- Ray-Gallet, D., J. P. Quivy, H. W. Sillje, E. A. Nigg and G. Almouzni (2007). "The histone chaperone Asf1 is dispensable for direct de novo histone deposition in *Xenopus* egg extracts." Chromosoma **116**(5): 487-496.
- Ray-Gallet, D., A. Woolfe, I. Vassias, C. Pellentz, N. Lacoste, A. Puri, D. C. Schultz, N. A. Pchelintsev, P. D. Adams, L. E. Jansen and G. Almouzni (2011). "Dynamics of histone H3 deposition in vivo reveal a nucleosome gap-filling mechanism for H3.3 to maintain chromatin integrity." Molecular cell **44**(6): 928-941.
- Recht, J., T. Tsubota, J. C. Tanny, R. L. Diaz, J. M. Berger, X. Zhang, B. A. Garcia, J. Shabanowitz, A. L. Burlingame, D. F. Hunt, P. D. Kaufman and C. D. Allis (2006). "Histone chaperone Asf1 is required for histone H3 lysine 56 acetylation, a modification associated with S phase in mitosis and meiosis." Proc Natl Acad Sci U S A **103**(18): 6988-6993.
- Rhind, N. and D. M. Gilbert (2013). "DNA replication timing." Cold Spring Harb Perspect Biol **5**(8): a010132.
- Richet, N., D. Liu, P. Legrand, C. Velours, A. Corpet, A. Gaubert, M. Bakail, G. Moal-Raisin, R. Guerois, C. Compper, A. Besle, B. Guichard, G. Almouzni and F. Ochsenbein (2015). "Structural insight into how the human helicase subunit MCM2 may act as a histone chaperone together with ASF1 at the replication fork." Nucleic acids research.
- Richmond, T. J., M. A. Searles and R. T. Simpson (1988). "Crystals of a nucleosome core particle containing defined sequence DNA." J Mol Biol **199**(1): 161-170.
- Rivera, C. M. and B. Ren (2013). "Mapping human epigenomes." Cell **155**(1): 39-55.

- Robbins, E. and T. W. Borun (1967). "The cytoplasmic synthesis of histones in hela cells and its temporal relationship to DNA replication." Proc Natl Acad Sci U S A **57**(2): 409-416.
- Robinson, K. M. and M. C. Schultz (2003). "Replication-Independent Assembly of Nucleosome Arrays in a Novel Yeast Chromatin Reconstitution System Involves Antisilencing Factor Asf1p and Chromodomain Protein Chd1p." Molecular and Cellular Biology **23**(22): 7937-7946.
- Robinson, P. J., L. Fairall, V. A. Huynh and D. Rhodes (2006). "EM measurements define the dimensions of the "30-nm" chromatin fiber: evidence for a compact, interdigitated structure." Proc Natl Acad Sci U S A **103**(17): 6506-6511.
- Rocheteau, P., B. Gayraud-Morel, I. Siegl-Cachedenier, M. A. Blasco and S. Tajbakhsh (2012). "A subpopulation of adult skeletal muscle stem cells retains all template DNA strands after cell division." Cell **148**(1-2): 112-125.
- Sadgopal, A. and J. Bonner (1969). "The relationship between histone and DNA synthesis in HeLa cells." Biochim Biophys Acta **186**(2): 349-357.
- Sakai, A., B. E. Schwartz, S. Goldstein and K. Ahmad (2009). "Transcriptional and developmental functions of the H3.3 histone variant in Drosophila." Curr Biol **19**(21): 1816-1820.
- Sanematsu, F., Y. Takami, H. K. Barman, T. Fukagawa, T. Ono, K. Shibahara and T. Nakayama (2006). "Asf1 is required for viability and chromatin assembly during DNA replication in vertebrate cells." The Journal of biological chemistry **281**(19): 13817-13827.
- Santenard, A., C. Ziegler-Birling, M. Koch, L. Tora, A. J. Bannister and M. E. Torres-Padilla (2010). "Heterochromatin formation in the mouse embryo requires critical residues of the histone variant H3.3." Nat Cell Biol **12**(9): 853-862.
- Saredi, G., H. Huang, C. M. Hammond, C. Alabert, S. Bekker-Jensen, I. Forne, N. Reveron-Gomez, B. M. Foster, L. Mlejnkova, T. Bartke, P. Cejka, N. Mailand, A. Imhof, D. J. Patel and A. Groth (2016). "H4K20me0 marks post-replicative chromatin and recruits the TONSL-MMS22L DNA repair complex." Nature **534**(7609): 714-718.
- Sarkies, P., P. Murat, L. G. Phillips, K. J. Patel, S. Balasubramanian and J. E. Sale (2012). "FANCD1 coordinates two pathways that maintain epigenetic stability at G-quadruplex DNA." Nucleic Acids Res **40**(4): 1485-1498.
- Sarkies, P., C. Reams, L. J. Simpson and J. E. Sale (2010). "Epigenetic instability due to defective replication of structured DNA." Mol Cell **40**(5): 703-713.

- Schalch, T., S. Duda, D. F. Sargent and T. J. Richmond (2005). "X-ray structure of a tetranucleosome and its implications for the chromatin fibre." Nature **436**(7047): 138-141.
- Schiavone, D., G. Guilbaud, P. Murat, C. Papadopoulou, P. Sarkies, M. N. Prioleau, S. Balasubramanian and J. E. Sale (2014). "Determinants of G quadruplex-induced epigenetic instability in REV1-deficient cells." EMBO J **33**(21): 2507-2520.
- Schleif, R. (1992). "DNA looping." Annu Rev Biochem **61**: 199-223.
- Schulz, L. L. and J. K. Tyler (2006). "The histone chaperone ASF1 localizes to active DNA replication forks to mediate efficient DNA replication." FASEB journal : official publication of the Federation of American Societies for Experimental Biology **20**(3): 488-490.
- Schwabish, M. A. and K. Struhl (2006). "Asf1 mediates histone eviction and deposition during elongation by RNA polymerase II." Molecular cell **22**(3): 415-422.
- Schwartz, B. E. and K. Ahmad (2005). "Transcriptional activation triggers deposition and removal of the histone variant H3.3." Genes Dev **19**(7): 804-814.
- Sexton, T., E. Yaffe, E. Kenigsberg, F. Bantignies, B. Leblanc, M. Hoichman, H. Parrinello, A. Tanay and G. Cavalli (2012). "Three-dimensional folding and functional organization principles of the Drosophila genome." Cell **148**(3): 458-472.
- Sharp, J. A., E. T. Fouts, D. C. Krawitz and P. D. Kaufman (2001). "Yeast histone deposition protein Asf1p requires Hir proteins and PCNA for heterochromatic silencing." Curr Biol **11**(7): 463-473.
- Sherwood, P. W. and M. A. Osley (1991). "Histone regulatory (hir) mutations suppress delta insertion alleles in Saccharomyces cerevisiae." Genetics **128**(4): 729-738.
- Shibahara, K. and B. Stillman (1999). "Replication-dependent marking of DNA by PCNA facilitates CAF-1-coupled inheritance of chromatin." Cell **96**(4): 575-585.
- Shibahara, K., A. Verreault and B. Stillman (2000). "The N-terminal domains of histones H3 and H4 are not necessary for chromatin assembly factor-1-mediated nucleosome assembly onto replicated DNA in vitro." Proc Natl Acad Sci U S A **97**(14): 7766-7771.

- Shinin, V., B. Gayraud-Morel, D. Gomes and S. Tajbakhsh (2006). "Asymmetric division and cosegregation of template DNA strands in adult muscle satellite cells." Nat Cell Biol **8**(7): 677-687.
- Shogren-Knaak, M., H. Ishii, J. M. Sun, M. J. Pazin, J. R. Davie and C. L. Peterson (2006). "Histone H4-K16 acetylation controls chromatin structure and protein interactions." Science **311**(5762): 844-847.
- Sillje, H. H. and E. A. Nigg (2001). "Identification of human Asf1 chromatin assembly factors as substrates of Tousled-like kinases." Current biology : CB **11**(13): 1068-1073.
- Singer, M. S., A. Kahana, A. J. Wolf, L. L. Meisinger, S. E. Peterson, C. Goggin, M. Mahowald and D. E. Gottschling (1998). "Identification of high-copy disruptors of telomeric silencing in *Saccharomyces cerevisiae*." Genetics **150**(2): 613-632.
- Smith, D. J. and I. Whitehouse (2012). "Intrinsic coupling of lagging-strand synthesis to chromatin assembly." Nature **483**(7390): 434-438.
- Smith, S. and B. Stillman (1989). "Purification and characterization of CAF-I, a human cell factor required for chromatin assembly during DNA replication in vitro." Cell **58**(1): 15-25.
- Sobel, R. E., R. G. Cook, C. A. Perry, A. T. Annunziato and C. D. Allis (1995). "Conservation of deposition-related acetylation sites in newly synthesized histones H3 and H4." Proc Natl Acad Sci U S A **92**(4): 1237-1241.
- Sogo, J. M., H. Stahl, T. Koller and R. Knippers (1986). "Structure of replicating simian virus 40 minichromosomes. The replication fork, core histone segregation and terminal structures." J Mol Biol **189**(1): 189-204.
- Solovei, I., A. S. Wang, K. Thanisch, C. S. Schmidt, S. Krebs, M. Zwerger, T. V. Cohen, D. Devys, R. Foisner, L. Peichl, H. Herrmann, H. Blum, D. Engelkamp, C. L. Stewart, H. Leonhardt and B. Joffe (2013). "LBR and lamin A/C sequentially tether peripheral heterochromatin and inversely regulate differentiation." Cell **152**(3): 584-598.
- Song, F., P. Chen, D. Sun, M. Wang, L. Dong, D. Liang, R. M. Xu, P. Zhu and G. Li (2014). "Cryo-EM study of the chromatin fiber reveals a double helix twisted by tetranucleosomal units." Science **344**(6182): 376-380.
- Srinivasan, S. V., D. Dominguez-Sola, L. C. Wang, O. Hyrien and J. Gautier (2013). "Cdc45 is a critical effector of myc-dependent DNA replication stress." Cell Rep **3**(5): 1629-1639.

- Stein, A. (1989). "Reconstitution of chromatin from purified components." Methods Enzymol **170**: 585-603.
- Stein, A., J. P. Whitlock, Jr. and M. Bina (1979). "Acidic polypeptides can assemble both histones and chromatin in vitro at physiological ionic strength." Proc Natl Acad Sci U S A **76**(10): 5000-5004.
- Stevely, W. S. and L. A. Stocken (1966). "Phosphorylation of rat-thymus histone." Biochem J **100**(2): 20C-21C.
- Stillman, B. (1986). "Chromatin assembly during SV40 DNA replication in vitro." Cell **45**(4): 555-565.
- Strom, A. R., A. V. Emelyanov, M. Mir, D. V. Fyodorov, X. Darzacq and G. H. Karpen (2017). "Phase separation drives heterochromatin domain formation." Nature **547**(7662): 241-245.
- Sugasawa, K., Y. Ishimi, T. Eki, J. Hurwitz, A. Kikuchi and F. Hanaoka (1992). "Nonconservative segregation of parental nucleosomes during simian virus 40 chromosome replication in vitro." Proc Natl Acad Sci U S A **89**(3): 1055-1059.
- Sutton, A., J. Bucaria, M. A. Osley and R. Sternglanz (2001). "Yeast ASF1 protein is required for cell cycle regulation of histone gene transcription." Genetics **158**(2): 587-596.
- Svikovic, S. and J. E. Sale (2017). "The Effects of Replication Stress on S Phase Histone Management and Epigenetic Memory." J Mol Biol **429**(13): 2011-2029.
- Szabo, Q., D. Jost, J. M. Chang, D. I. Cattoni, G. L. Papadopoulos, B. Bonev, T. Sexton, J. Gurgo, C. Jacquier, M. Nollmann, F. Bantignies and G. Cavalli (2018). "TADs are 3D structural units of higher-order chromosome organization in Drosophila." Sci Adv **4**(2): eaar8082.
- Szenker, E., N. Lacoste and G. Almouzni (2012). "A developmental requirement for HIRA-dependent H3.3 deposition revealed at gastrulation in Xenopus." Cell Rep **1**(6): 730-740.
- Tagami, H., D. Ray-Gallet, G. Almouzni and Y. Nakatani (2004). "Histone H3.1 and H3.3 complexes mediate nucleosome assembly pathways dependent or independent of DNA synthesis." Cell **116**(1): 51-61.
- Tahiliani, M., K. P. Koh, Y. Shen, W. A. Pastor, H. Bandukwala, Y. Brudno, S. Agarwal, L. M. Iyer, D. R. Liu, L. Aravind and A. Rao (2009). "Conversion of 5-methylcytosine to 5-hydroxymethylcytosine in mammalian DNA by MLL partner TET1." Science **324**(5929): 930-935.

Takahata, S., Y. Yu and D. J. Stillman (2009). "FACT and Asf1 regulate nucleosome dynamics and coactivator binding at the HO promoter." *Mol Cell* **34**(4): 405-415.

Takai, S., T. W. Borun, J. Muchmore and I. Lieberman (1968). "Concurrent synthesis of histone and deoxyribonucleic acid in liver after partial hepatectomy." *Nature* **219**(5156): 860-861.

Talbert, P. B. (2002). "Centromeric Localization and Adaptive Evolution of an Arabidopsis Histone H3 Variant." *The Plant Cell Online* **14**(5): 1053-1066.

Tamburini, B. A., J. J. Carson, M. W. Adkins and J. K. Tyler (2005). "Functional conservation and specialization among eukaryotic anti-silencing function 1 histone chaperones." *Eukaryotic cell* **4**(9): 1583-1590.

Tan, B. C., C. T. Chien, S. Hirose and S. C. Lee (2006). "Functional cooperation between FACT and MCM helicase facilitates initiation of chromatin DNA replication." *EMBO J* **25**(17): 3975-3985.

Tang, Y., M. V. Poustovoitov, K. Zhao, M. Garfinkel, A. Canutescu, R. Dunbrack, P. D. Adams and R. Marmorstein (2006). "Structure of a human ASF1a-HIRA complex and insights into specificity of histone chaperone complex assembly." *Nature structural & molecular biology* **13**(10): 921-929.

Thoma, F., T. Koller and A. Klug (1979). "Involvement of histone H1 in the organization of the nucleosome and of the salt-dependent superstructures of chromatin." *J Cell Biol* **83**(2 Pt 1): 403-427.

Torres-Padilla, M. E., A. J. Bannister, P. J. Hurd, T. Kouzarides and M. Zernicka-Goetz (2006). "Dynamic distribution of the replacement histone variant H3.3 in the mouse oocyte and preimplantation embryos." *Int J Dev Biol* **50**(5): 455-461.

Towbin, B. D., C. Gonzalez-Aguilera, R. Sack, D. Gaidatzis, V. Kalck, P. Meister, P. Askjaer and S. M. Gasser (2012). "Step-wise methylation of histone H3K9 positions heterochromatin at the nuclear periphery." *Cell* **150**(5): 934-947.

Tran, V., L. Feng and X. Chen (2013). "Asymmetric distribution of histones during Drosophila male germline stem cell asymmetric divisions." *Chromosome Res* **21**(3): 255-269.

Tran, V., C. Lim, J. Xie and X. Chen (2012). "Asymmetric division of Drosophila male germline stem cell shows asymmetric histone distribution." *Science* **338**(6107): 679-682.

Trojer, P. and D. Reinberg (2007). "Facultative heterochromatin: is there a distinctive molecular signature?" *Mol Cell* **28**(1): 1-13.

- Tsantoulis, P. K. and V. G. Gorgoulis (2005). "Involvement of E2F transcription factor family in cancer." Eur J Cancer **41**(16): 2403-2414.
- Tse, C., T. Sera, A. P. Wolffe and J. C. Hansen (1998). "Disruption of higher-order folding by core histone acetylation dramatically enhances transcription of nucleosomal arrays by RNA polymerase III." Mol Cell Biol **18**(8): 4629-4638.
- Turner, B. M., A. J. Birley and J. Lavender (1992). "Histone H4 isoforms acetylated at specific lysine residues define individual chromosomes and chromatin domains in *Drosophila* polytene nuclei." Cell **69**(2): 375-384.
- Tyler, J. K., C. R. Adams, S. R. Chen, R. Kobayashi, R. T. Kamakaka and J. T. Kadonaga (1999). "The RCAF complex mediates chromatin assembly during DNA replication and repair." Nature **402**(6761): 555-560.
- Tyler, J. K., K. A. Collins, J. Prasad-Sinha, E. Amriott, M. Bulger, P. J. Harte, R. Kobayashi and J. T. Kadonaga (2001). "Interaction between the *Drosophila* CAF-1 and ASF1 Chromatin Assembly Factors." Molecular and Cellular Biology **21**(19): 6574-6584.
- Umehara, T. and M. Horikoshi (2003). "Transcription initiation factor IID-interactive histone chaperone CIA-II implicated in mammalian spermatogenesis." The Journal of biological chemistry **278**(37): 35660-35667.
- Urahama, T., A. Harada, K. Maehara, N. Horikoshi, K. Sato, Y. Sato, K. Shiraishi, N. Sugino, A. Osakabe, H. Tachiwana, W. Kagawa, H. Kimura, Y. Ohkawa and H. Kurumizaka (2016). "Histone H3.5 forms an unstable nucleosome and accumulates around transcription start sites in human testis." Epigenetics Chromatin **9**: 2.
- van der Heijden, G. W., J. W. Dieker, A. A. Derijck, S. Muller, J. H. Berden, D. D. Braat, J. van der Vlag and P. de Boer (2005). "Asymmetry in histone H3 variants and lysine methylation between paternal and maternal chromatin of the early mouse zygote." Mech Dev **122**(9): 1008-1022.
- VanDemark, A. P., M. Blanksma, E. Ferris, A. Heroux, C. P. Hill and T. Formosa (2006). "The structure of the yFACT Pob3-M domain, its interaction with the DNA replication factor RPA, and a potential role in nucleosome deposition." Mol Cell **22**(3): 363-374.
- VerMilyea, M. D., L. P. O'Neill and B. M. Turner (2009). "Transcription-independent heritability of induced histone modifications in the mouse preimplantation embryo." PLoS One **4**(6): e6086.

- Verreault, A., P. D. Kaufman, R. Kobayashi and B. Stillman (1996). "Nucleosome assembly by a complex of CAF-1 and acetylated histones H3/H4." Cell **87**(1): 95-104.
- Vestner, B., T. Waldmann and C. Gruss (2000). "Histone octamer dissociation is not required for in vitro replication of simian virus 40 minichromosomes." J Biol Chem **275**(11): 8190-8195.
- Voichek, Y., R. Bar-Ziv and N. Barkai (2016). "Expression homeostasis during DNA replication." Science **351**(6277): 1087-1090.
- Wang, S., J. H. Su, B. J. Beliveau, B. Bintu, J. R. Moffitt, C. T. Wu and X. Zhuang (2016). "Spatial organization of chromatin domains and compartments in single chromosomes." Science **353**(6299): 598-602.
- Watt, F. and P. L. Molloy (1988). "Cytosine methylation prevents binding to DNA of a HeLa cell transcription factor required for optimal expression of the adenovirus major late promoter." Genes Dev **2**(9): 1136-1143.
- Wiedemann, S. M., S. N. Mildner, C. Bonisch, L. Israel, A. Maiser, S. Matheisl, T. Straub, R. Merkl, H. Leonhardt, E. Kremmer, L. Schermelleh and S. B. Hake (2010). "Identification and characterization of two novel primate-specific histone H3 variants, H3.X and H3.Y." J Cell Biol **190**(5): 777-791.
- Williamson, I., S. Berlivet, R. Eskeland, S. Boyle, R. S. Illingworth, D. Paquette, J. Dostie and W. A. Bickmore (2014). "Spatial genome organization: contrasting views from chromosome conformation capture and fluorescence in situ hybridization." Genes Dev **28**(24): 2778-2791.
- Winston, F. and C. D. Allis (1999). "The bromodomain: a chromatin-targeting module?" Nat Struct Biol **6**(7): 601-604.
- Witt, O., W. Albig and D. Doenecke (1996). "Testis-specific expression of a novel human H3 histone gene." Exp Cell Res **229**(2): 301-306.
- Wong, L. H., H. Ren, E. Williams, J. McGhie, S. Ahn, M. Sim, A. Tam, E. Earle, M. A. Anderson, J. Mann and K. H. Choo (2009). "Histone H3.3 incorporation provides a unique and functionally essential telomeric chromatin in embryonic stem cells." Genome Res **19**(3): 404-414.
- Wu, M. Y., C. Y. Lin, H. Y. Tseng, F. M. Hsu, P. Y. Chen and C. F. Kao (2017). "H2B ubiquitylation and the histone chaperone Asf1 cooperatively mediate the formation and maintenance of heterochromatin silencing." Nucleic Acids Res **45**(14): 8225-8238.

- Wu, R. S. and W. M. Bonner (1981). "Separation of basal histone synthesis from S-phase histone synthesis in dividing cells." *Cell* **27**(2 Pt 1): 321-330.
- Wu, S. C. and Y. Zhang (2010). "Active DNA demethylation: many roads lead to Rome." *Nat Rev Mol Cell Biol* **11**(9): 607-620.
- Xie, J., M. Wooten, V. Tran, B. C. Chen, C. Pozmanter, C. Simbolon, E. Betzig and X. Chen (2015). "Histone H3 Threonine Phosphorylation Regulates Asymmetric Histone Inheritance in the Drosophila Male Germline." *Cell* **163**(4): 920-933.
- Xu, M., C. Long, X. Chen, C. Huang, S. Chen and B. Zhu (2010). "Partitioning of histone H3-H4 tetramers during DNA replication-dependent chromatin assembly." *Science* **328**(5974): 94-98.
- Yadav, T. and I. Whitehouse (2016). "Replication-Coupled Nucleosome Assembly and Positioning by ATP-Dependent Chromatin-Remodeling Enzymes." *Cell Rep* **15**(4): 715-723.
- Yang, J., X. Zhang, J. Feng, H. Leng, S. Li, J. Xiao, S. Liu, Z. Xu, J. Xu, D. Li, Z. Wang, J. Wang and Q. Li (2016). "The Histone Chaperone FACT Contributes to DNA Replication-Coupled Nucleosome Assembly." *Cell Rep*.
- Zabaronick, S. R. and J. K. Tyler (2005). "The histone chaperone anti-silencing function 1 is a global regulator of transcription independent of passage through S phase." *Mol Cell Biol* **25**(2): 652-660.
- Zhang, H., H. Gan, Z. Wang, J. H. Lee, H. Zhou, T. Ordog, M. S. Wold, M. Ljungman and Z. Zhang (2017). "RPA Interacts with HIRA and Regulates H3.3 Deposition at Gene Regulatory Elements in Mammalian Cells." *Mol Cell* **65**(2): 272-284.
- Zhang, R., M. V. Poustovoitov, X. Ye, H. A. Santos, W. Chen, S. M. Daganzo, J. P. Erzberger, I. G. Serebriiskii, A. A. Canutescu, R. L. Dunbrack, J. R. Pehrson, J. M. Berger, P. D. Kaufman and P. D. Adams (2005). "Formation of MacroH2A-containing senescence-associated heterochromatin foci and senescence driven by ASF1a and HIRA." *Developmental cell* **8**(1): 19-30.
- Zhu, J. Q., J. H. Liu, X. W. Liang, B. Z. Xu, Y. Hou, X. X. Zhao and Q. Y. Sun (2008). "Heat stress causes aberrant DNA methylation of H19 and Igf-2r in mouse blastocysts." *Mol Cells* **25**(2): 211-215.
- Zorn, C., C. Cremer, T. Cremer and J. Zimmer (1979). "Unscheduled DNA synthesis after partial UV irradiation of the cell nucleus. Distribution in interphase and metaphase." *Exp Cell Res* **124**(1): 111-119.



# Résumé

## Introduction

Chez les eucaryotes, le génome est compacté en une structure appelée chromatine. L'unité de base de la chromatine est le nucléosome, composé d'ADN entouré de protéines nommées histones. Ces histones peuvent exister sous différentes formes, les variants d'histones, ou porter des modifications post-traductionnelles. Ainsi, le nucléosome est un module porteur d'informations dites épigénétiques, et la présence de variants d'histones ou de modifications particulières peut délimiter différentes zones fonctionnelles du génome et réguler son expression, déterminant de cette manière l'identité cellulaire.

La réplication de l'ADN représente un défi pour la cellule, qui doit d'une part dupliquer son matériel génétique, mais également reconstituer son paysage épigénétique. La transmission fidèle des caractéristiques épigénétiques, comme les variants d'histones et leurs modifications, permet de dupliquer l'identité parentale et donc garantit le maintien de l'identité cellulaire. En revanche, la réplication offre aussi une opportunité pour changer le paysage épigénétique, apportant des modifications parfois planifiées - comme dans un contexte de différenciation -, parfois inattendues - comme dans le cas de certaines pathologies. Pendant ma thèse, je me suis plus particulièrement intéressée aux mécanismes qui permettent de dupliquer l'identité parentale.

Au cours de la réplication, afin de permettre le passage de la machinerie de réplication, les histones parentales, présentes sur le brin d'ADN parental, sont évincées puis recyclées de l'autre côté de la fourche sur le brin d'ADN nouvellement synthétisé. En parallèle de nouvelles histones sont déposées afin de maintenir la densité nucléosomale. Si les mécanismes qui permettent de déposer de nouvelles histones sont bien connus, il reste de nombreuses questions concernant le recyclage des histones parentales. Pourtant, le recyclage est essentiel pour garantir la transmission de l'information parentale sous la forme de variants d'histones et de modifications.

Au sein du nucléosome se trouvent huit histones: deux copies de H2A, H2B, H3 et H4. Pour l'histone H3, une première catégorie de variants est constituée de H3.1 et H3.2, aussi nommés variants

réplicatifs. Leur expression connaît un pic en phase S, permettant de fournir un stock d'histones disponibles pour la réplication. Le variant d'histone H3.3, aussi appelé histone de remplacement, en revanche, est exprimé tout au long du cycle cellulaire et est déposé indépendamment de la synthèse d'ADN lors de situations qui nécessitent un apport en histones. Par exemple, H3.3 est enrichi aux gènes actifs, promoteurs et éléments de régulation - et est ainsi souvent associé à la transcription - ou encore aux télomères. Les histones sont déposées par des protéines appelées chaperons d'histones. Les chaperons peuvent être plus ou moins dédiés à des variants particuliers. Le chaperon d'histone Chromatin Assembly Factor 1 (CAF-1) est dédié au variant H3.1 et le dépose de manière couplée à la synthèse d'ADN, par exemple au cours de la réplication ou de la réparation de l'ADN. Le variant d'histone H3.3 est déposé de manière indépendante de la synthèse d'ADN par le complexe Histone Regulator A (HIRA) ou encore par Death Domain-Associated protein (DAXX). D'autres chaperons, en revanche, peuvent s'associer à plusieurs variants. C'est le cas du chaperon d'H3-H4 Anti-Silencing Function 1 (ASF1), qui s'associe à la fois à H3.1 et à H3.3.

ASF1 a deux paralogues chez l'homme, ASF1a et ASF1b, impliqués dans de nombreuses voies de gestion des histones. En effet, ASF1a et ASF1b ont été impliqués dans le stockage des histones solubles, ou encore dans la déposition *de novo* des histones en partenariat avec CAF-1 et HIRA. ASF1 semble avoir un rôle particulièrement important lors de la réplication, et notamment pour le recyclage des histones parentales. La déplétion d'ASF1 ralentit la progression de la phase S. Par ailleurs, ASF1 forme un complexe avec la sous-unité MCM2 de l'hélicase répllicative MCM via H3-H4 et est donc idéalement situé pour transférer les histones parentales. Après traitement avec de l'hydroxyurée, qui empêche la synthèse d'ADN, des complexes ASF1 contenant des histones portant des modifications typiques d'histones parentales s'accumulent. Ainsi, un modèle attractif proposait qu'ASF1 recyclait les histones parentales en partenariat avec MCM2 au cours de la réplication. En revanche, quand j'ai commencé ma thèse, un certain nombre de questions demeurait: (i) ce modèle est-il valable dans des cellules? (ii) comment sont recyclés les deux variants H3.1 et H3.3? (iii) quel est le rôle exact d'ASF1 dans le recyclage des variants? (iv) quel est l'impact de défauts de recyclage des variants pour l'épigénome?

## Question

Au cours de ma thèse, j'ai donc tenté de répondre à la question:

Comment les variants d'histone H3.1 et H3.3 parentaux sont-ils recyclés au cours de la réplication de l'ADN?

## Approche

Pour répondre à cette question, j'avais besoin: (i) de pouvoir distinguer les variants d'histone H3.1 et H3.3, (ii) de pouvoir marquer spécifiquement les histones parentales, et (iii) d'avoir une résolution suffisante pour suivre avec précision les histones aux sites de réplication.

J'ai choisi d'utiliser le système SNAP pour suivre les variants d'histones parentaux. Le SNAP-tag peut réagir de manière covalente avec la benzylguanine, et donc notamment avec des dérivés où la benzylguanine est couplée à un fluorophore. Ainsi, en fusionnant une protéine d'intérêt avec le SNAP-tag, on peut en observer des sous-populations spécifiques: nouvelles ou parentales. Dans mon cas, j'ai utilisé des lignées cellulaires exprimant soit H3.1-SNAP, soit H3.3-SNAP, me permettant par ailleurs de distinguer les variants. Pour observer les histones parentales, j'ai effectué des expériences de pulse-chase: le pulse permet de marquer toutes les histones SNAP disponibles avec un fluorophore; ensuite, un chase de 48h permet la synthèse de nouvelles histones SNAP non marquées; à la fin de l'expérience, on observe par microscopie uniquement les histones marquées, c'est-à-dire les histones parentales. Il est également possible d'effectuer uniquement un pulse: dans ce cas, on observe les histones globales.

Le système SNAP permet donc de visualiser en microscopie les variants d'histone parentaux. Cependant, pour étudier leur recyclage aux sites de réplication, j'avais besoin d'une résolution élevée pour observer avec précision, en deux couleurs, les histones et les sites de réplication. J'ai choisi d'utiliser une technique de super-résolution: le STORM (STochastic Optical Reconstruction Microscopy). Le STORM repose sur le fait que certains fluorophores, dans des conditions particulières, alternent entre un état excité et non excité et, ainsi, clignotent. Ce phénomène étant stochastique, les fluorophores de l'échantillon s'allument à des moments distincts; ainsi, en filmant l'échantillon, on peut localiser individuellement les molécules avec une grande précision. Deux fluorophore très proches, qu'on ne pourrait habituellement pas résoudre, s'allument alors à des

moment différents, et peuvent donc être résolus. Cette technologie permet d'obtenir une résolution de l'ordre de 10-40 nm, au lieu de 250-300 nm avec une technique de microscopie classique. J'ai donc utilisé le STORM pour observer d'une part, les histones, d'autre part, les sites de réplication (identifiés grâce à l'EdU).

Mon projet, combinant le SNAP et le STORM pour étudier le recyclage des variants d'histones parentaux au cours de la réplication, a donné lieu à une publication intitulée: "High resolution visualization of H3 variants during replication reveals their controlled recycling". Les résultats biologiques de cette étude sont résumés ci-dessous.

## **Résultats**

Afin d'étudier le recyclage des variants d'histone au cours de la réplication, j'ai procédé en deux temps: (i) j'ai tout d'abord étudié la distributions des variants d'histones globaux, à la fois dans le génome et en 3D dans le noyau par rapport au timing de réplication, et (ii) je me suis ensuite concentrée sur les variants d'histone parentaux pour comprendre leur recyclage.

Pour déterminer la distribution génomique de H3.1 et H3.3, j'ai collaboré avec des membres de mon équipe pour effectuer une expérience de ChIP-seq. Nous avons pu observer que le variant d'histone H3.3 était enrichi dans les régions qui se répliquent en début de phase S (que nous appellerons par la suite "early" et qui, de manière générale, correspondent à l'euchromatine), alors que H3.1 était au contraire enrichi dans les régions qui se répliquent en fin de phase S (que nous appellerons par la suite "late" et qui, de manière générale, correspondent à l'hétérochromatine). Nous avons voulu déterminer si la transcription était seule responsable de l'association de H3.3 avec les régions early. Pour cela, nous avons utilisé des données d'activité transcriptionnelle (nascent RNA-seq). De manière intéressante, nous avons observé que, si H3.3 était en effet associé à la transcription, la corrélation entre H3.3 et le timing de réplication est vraie indépendamment de l'activité transcriptionnelle. En d'autres termes, la transcription seule ne suffit pas à expliquer l'association de H3.3 avec les régions early.

Si l'analyse génomique est très informative, elle ne permet pas de connaître la distribution en 3D des variants. J'ai donc utilisé la technologie STORM pour observer H3.1 global et H3.3 global dans le noyau. J'ai observé que ces deux variants formaient des clusters, et j'ai décidé d'étudier le volume et

la densité de ces clusters dans des cellules en début de phase S et des cellules en fin de phase S. J'ai constaté des comportements opposés pour H3.3 et H3.1. J'ai tout d'abord observé que les clusters H3.3 étaient plus denses dans les régions early du génome par rapport aux régions late, alors que les clusters H3.1 étaient plus denses dans les régions late du génome par rapport aux régions early. Ce résultat est en accord avec les résultats de l'analyse génomique. Par ailleurs, le volume des clusters H3.3 est indépendant du cycle et notamment de la phase S. En revanche, la densité de ces clusters diminue au cours de la phase S. De manière opposée, le volume des clusters H3.1 dépend du cycle cellulaire, et plus particulièrement de la phase S, et leur densité augmente au cours de la phase S. Une interprétation possible de ces observations est liée au caractère répliatif du variant H3.1, et non H3.3: H3.1 étant déposé pendant la réplication, il est enrichi au cours de la phase S, et H3.3 est ainsi dilué.

J'ai ensuite voulu suivre spécifiquement les histones parentales en utilisant le système SNAP. Je me suis d'abord placée dans un contexte censé, a priori, perturber leur recyclage pour déterminer si je pouvais détecter un défaut de recyclage avec mon système. Pour cela, j'ai traité les cellules avec de l'hydroxyurée pour infliger un stress répliatif. Après ce traitement, j'ai mesuré moins d'histones parentales aux sites répliqués par rapport au contrôle, ce qui suggère un défaut de recyclage. J'ai ensuite voulu tester le rôle du chaperon d'histone ASF1 dans le recyclage de H3.3 et H3.1 en déplaçant ASF1 par siRNA. En l'absence d'ASF1, j'ai mesuré une baisse du nombre d'histones parentales aux sites répliqués à la fois pour H3.1 et H3.3. Cette observation suggère qu'ASF1 est impliqué dans le recyclage des deux variants H3.1 et H3.3. J'ai ensuite voulu déterminer si ce défaut de recyclage avait un impact sur la distribution spatiale des variants autour des sites de réplication. De manière intéressante, j'ai observé que la distribution spatiale de H3.1, mais pas H3.3, était perturbée en l'absence d'ASF1 dans les régions early. Dans les régions late en revanche, la distribution des deux variants H3.1 et H3.3 est affectée.

## **Conclusion**

Mon projet utilisant la microscopie STORM a permis de montrer que les deux variants d'histone H3.1 et H3.3 sont recyclés pendant la réplication par un mécanisme impliquant le chaperon d'histone ASF1. Un défaut de recyclage des histones parentales déséquilibre le paysage des variants. Mon travail permet ainsi de montrer l'importance du recyclage contrôlé des variants d'histone pour le maintien de l'épigénome, et ouvre la question de l'impact pour l'identité cellulaire.





## Résumé

Chez les eucaryotes, l'ADN s'enroule autour de protéines appelées histones pour former la chromatine. Cette structure permet, d'une part, de compacter le génome dans le noyau, mais également de réguler son expression. En effet, les histones sont porteuses d'information dite « épigénétique » : elles existent sous différentes formes, les variants d'histone, et peuvent porter des modifications post-traductionnelles. La présence de tels variants et modifications organise le génome en domaines au statut transcriptionnel différent.

La réplication de l'ADN déstabilise la structure chromatiniennne, et représente ainsi un défi pour la cellule qui doit à la fois dupliquer son matériel génétique et transmettre son paysage épigénétique pour garantir le maintien de son identité. Ceci passe par le recyclage des histones parentales, processus essentiel pour transmettre de manière fidèle les variants d'histone et leurs modifications.

Au cours de ma thèse, j'ai tenté de répondre à la question : **comment les variants d'histone H3.1 et H3.3 sont-ils recyclés au cours de la réplication de l'ADN ?** En particulier, je me suis intéressée au rôle du chaperon d'histone Anti-Silencing Function 1 (ASF1) dans ce processus.

Mon approche a été de développer une technique de microscopie de super-résolution (STORM) pour visualiser les variants d'histone parentaux précisément aux sites de réplication. Grâce à cette technologie, j'ai pu étudier l'impact de la déplétion d'ASF1 sur le recyclage des histones parentales, apportant ainsi des éléments de compréhension sur les mécanismes fondamentaux qui transmettent l'information épigénétique.

## Mots Clés

Chromatine, variant d'histone, chaperon d'histone, réplication de l'ADN, microscopie de super-résolution

## Abstract

In eukaryotes, DNA wraps around proteins called histones to form chromatin. This structure allows, first, the compaction of the genome in the nucleus, but also the regulation of its expression. Indeed, histones can be a source of information referred to as "epigenetic": they exist under different forms, histone variants, and can have post-translational modifications. The presence of these variants and modifications organizes the genome into domains with different transcriptional status.

DNA replication destabilizes chromatin structure and, therefore, represents a challenge for the cell, which must duplicate its genetic material while also transmitting its epigenetic landscape in order to maintain its identity. In this context, recycling parental histones is essential to faithfully transmit histone variants and their modifications.

During my PhD, I tried to address the question: **how are the histone variants H3.1 and H3.3 recycled during DNA replication?** In particular, I investigated the role of the histone chaperone Anti-Silencing Function 1 (ASF1) in this process.

My approach was to develop a super-resolution microscopy technique (STORM) to visualize parental histone variants precisely at replication sites. Using this technology, I could study the impact of ASF1 depletion on the recycling of parental histones, and further our understanding of fundamental mechanisms that transmit epigenetic information.

## Keywords

Chromatin, histone variant, histone chaperone, DNA replication, super-resolution microscopy